NASA CR 135244

NASA

THERMAL ENERGY STORAGE HEAT EXCHANGER

(NASA-CR-135244) THERMAL ENERGY STORAGE HEAT EXCHANGER: MOLTEN SALT HEAT EXCHANGER DESIGN FOR UTILITY POWER PLANTS Final Report, Jul. 1976 - Jul. 1977 (Grumman Aerospace Corp.) 207 p HC A10/MF A01
N78-14632
Unclas
G3/44 59481

By Angelo Ferrara, George Yenetchi,
Robert Haslett, Robert Kosson

GRUMMAN AEROSPACE CORPORATION

Prepared for
NATIONAL AERONAUTICS AND SPACE ADMINISTRATION

NASA Lewis Research Center
Contract NAS 3-20117

1. Report No. NASA CR 135244	2. Government Accession No.	3. Recipient's Catalog No.

4. Title and Subtitle THERMAL ENERGY STORAGE HEAT EXCHANGER (Molten Salt Heat Exchanger Design for Utility Power Plants)	5. Report Date October, 1977
	6. Performing Organization Code
7. Author(s) Angelo Ferarra, George Yenetchi, Robert Haslett and Robert Kosson	8. Performing Organization Report No.
	10. Work Unit No.
9. Performing Organization Name and Address Grumman Aerospace Corporation Bethpage, New York	11. Contract or Grant No. NAS 3-20117
	13. Type of Report and Period Covered Final, July 1976 – July 1977
12. Sponsoring Agency Name and Address National Aeronautics and Space Administration Washington, D.C. 20546	14. Sponsoring Agency Code

15. Supplementary Notes

16. Abstract

This study is a comprehensive evaluation of the use of thermal energy storage (TES) in the latent heat of molten salts as a means of conserving fossil fuels and lowering the cost of electric power. Public utility systems provide electric power on demand. This demand is generally maximum during late weekday afternoons, with considerably lower overnight and weekend loads. Typically, the average demand is only 60% to 80% of peak load. As peak load increases, the present method is to purchase power from other grid facilities or to bring older less efficient fossil-fuel plants on line which increases the cost of electric power. The widespread use of oil-fired boilers, gas turbine and diesel equipment to meet peaking loads depletes our oil-based energy resources. Heat exchangers utilizing molten salts can be used to level the energy consumption curve. The study begins with a demand analysis and the consideration of several existing modern fossil-fuel and nuclear power plants for use as models. Salts are evaluated for thermodynamic, economic, corrosive, and safety characteristics. Heat exchanger concepts are explored and heat exchanger designs are conceived. Finally, the economics of TES conversions in existing plants and new construction is analyzed. The study concluded that TES is feasible in electric power generation. Substantial data is presented for TES design and reference material for further investigation of techniques is included.

17. Key Words (Suggested by Author(s)) Power Plant, Thermal Energy Storage, Molten Salt Heat Exchanger	18. Distribution Statement

19. Security Classif. (of this report) Unclassified	20. Security Classif. (of this page) Unclassified	21. No. of Pages 216	22. Price*

* For sale by the National Technical Information Service, Springfield, Virginia 22161

TABLE OF CONTENTS

TABLE OF CONTENTS (Cont)

TABLE OF CONTENTS (Cont)

LIST OF ILLUSTRATIONS

LIST OF ILLUSTRATIONS (Cont)

LIST OF ILLUSTRATIONS (Cont)

LIST OF ILLUSTRATIONS (Cont)

FORWORD

The material in this report was prepared by the Grumman Aerospace Corporation with main subcontract support from the electric utility engineering and architectural firm, Burns and Roe, Inc.: Messres Robert Vondrasek and Chris Mallner of Burns and Roe, Inc., performed the plant thermodynamic analysis and prepared the installation layouts and cost summaries. Drs. Alina Borucka and George Janz provided consulting on the properties of salts and aided in the selection of specific salt eutectics for this application. The Contract Technical Manager at NASA Lewis Research Center was Mr. Joseph Joyce. The authors wish to extend our appreciation to the above personnel for their valuable contributions.

Section 1

INTRODUCTION AND SUMMARY

Electric utilities provide electricity on demand, which is generally maximum during the late afternoon, with considerably less power required overnight and on weekends. The integrated average system demand is typically 60% to 80% of the peak load. Excluding those utilities producing hydroelectric power, the industry approach is to consider the load curve composed of base load, intermediate load and peaking load with the optimum equipment selected to match demand. Base load is the "round the clock" load that the utility meets with its most fuel efficient equipment, i.e., coal or nuclear power plants. As the daily load increases, the utility incrementally brings the next least costly equipment on line. Short term peaks are usually met with small older oil-fired plants, gas turbine or diesel equipment. This is of course an over-simplification of a complex procedure which must include consideration of plant size, part load capability, start-up constraints, transmission dispatch considerations, and the purchase and sale of power to neighboring utilities. However, it does illustrate an essential fact; that peaking loads are generally met with the least fuel efficient equipment, and this equipment uses oil.

In his energy message, President Carter emphasized that the U.S. dependence on oil must be greatly reduced. In the near term, new utility plants will probably be coal or nuclear fueled and some existing plants will be switched from oil to coal. The dependence on oil-fired equipment to provide intermediate and peaking loads can be reduced in one of two ways: (1) by cycling coal or nuclear plants to follow the load curve, or (2) by baseloading coal or nuclear plants and storing excess off-peak energy for later use in meeting peak demands. Many methods of energy storage, e.g., batteries, compressed gas, fly wheels, and super-conducting magnets have been suggested. Currently, the only method in use is pumped hydro storage and this relies on suitable site geography. This study was to evaluate the potential for thermal energy storage (TES) to meet peaking power demands. Specifically, the use of the latent heat capacity of salts that melt at the high temperatures required for energy storage in conventional utilities was to be explored and a suitable heat exchanger defined. The heat absorbed in melting a material can be double or triple the sensible heat stored by heating the material to a higher temperature. Latent heat storage thus offers the possibility of designing much smaller TES systems, but also introduces many technical concerns since salts are typically corrosive, have low thermal conductivity, and may be hazardous.

This report documents a ten month study performed for the NASA Lewis Research Center to assess the technical and economic acceptability of a latent heat TES heat exchanger system for application in conventional utilities. The study was divided into five tasks that progressed according to the work plan presented in Figure 1-1 and the schedule shown in Figure 1-2. The goal of our program was to determine whether a coal or nuclear generating plant with a TES system is cost effective (considering both investment and operating costs), compared to a similar sized plant cycled to follow the load curve. Since both plants must meet the electrical demand, turbine/generator requirements are the same. Investment cost comparison is thus the cost of the TES system versus the cost of the larger steam capacity (boiler or nuclear island), which is (in 1977 prices) approximately \$450 per KW_e. Based on the latent heat capacity of suitable salts and typical plant load curves which determine the total energy to be stored, we showed that the TES system must cost less than about \$1 per pound of salt for a system providing significant peaking capability ($\approx$7% increase in capacity). A typical 1000 megawatt electrical plant requires approximately 14 million pounds of salt to store the required 900 megawatt-hours of thermal energy to provide 6 hours of peaking capability.

Operating costs with the TES system must consider two thermal inefficiencies; one is heat loss from the storage unit and the second is the thermodynamic necessity that heat must be returned to the power plant cycle at a lower temperature than it is extracted due to temperature differences required to transfer heat into and out of storage. The latter is not a heat loss but a loss in energy availability. The alternate approach of cycling a (larger) plant to follow the load curve, however, also introduces an inefficiency (operating the boiler at less than 100% load). Detailed heat balances based on specific energy storage and usage conditions and plant duty cycles are required to determine which system, in fact, has the lower fuel cost.

To maximize the realism of our plant cycle analysis, five existing nuclear and fossil electric utility plants were chosen to represent present day technology (see Fig. 1-3) and their current operating data were obtained (see Fig. 1-4). TES concepts can be considered as possible retrofits to these plants or as new plant construction of that generic type. Ten (10) locations for the TES in the plant cycle were identified, which resulted in 35 feasible plant/location combinations. Since the study was to emphasize heat exchanger concepts and not differences between plants, the choice was narrowed to one plant; the coal fired Ft. Martin unit in West Virginia and two locations (or cases) of thermal energy storage. Both cycle locations use main steam as the heat source. Usage in one case was for feedwater heating which decreased turbine steam extraction and hence increased turbine output. A second case

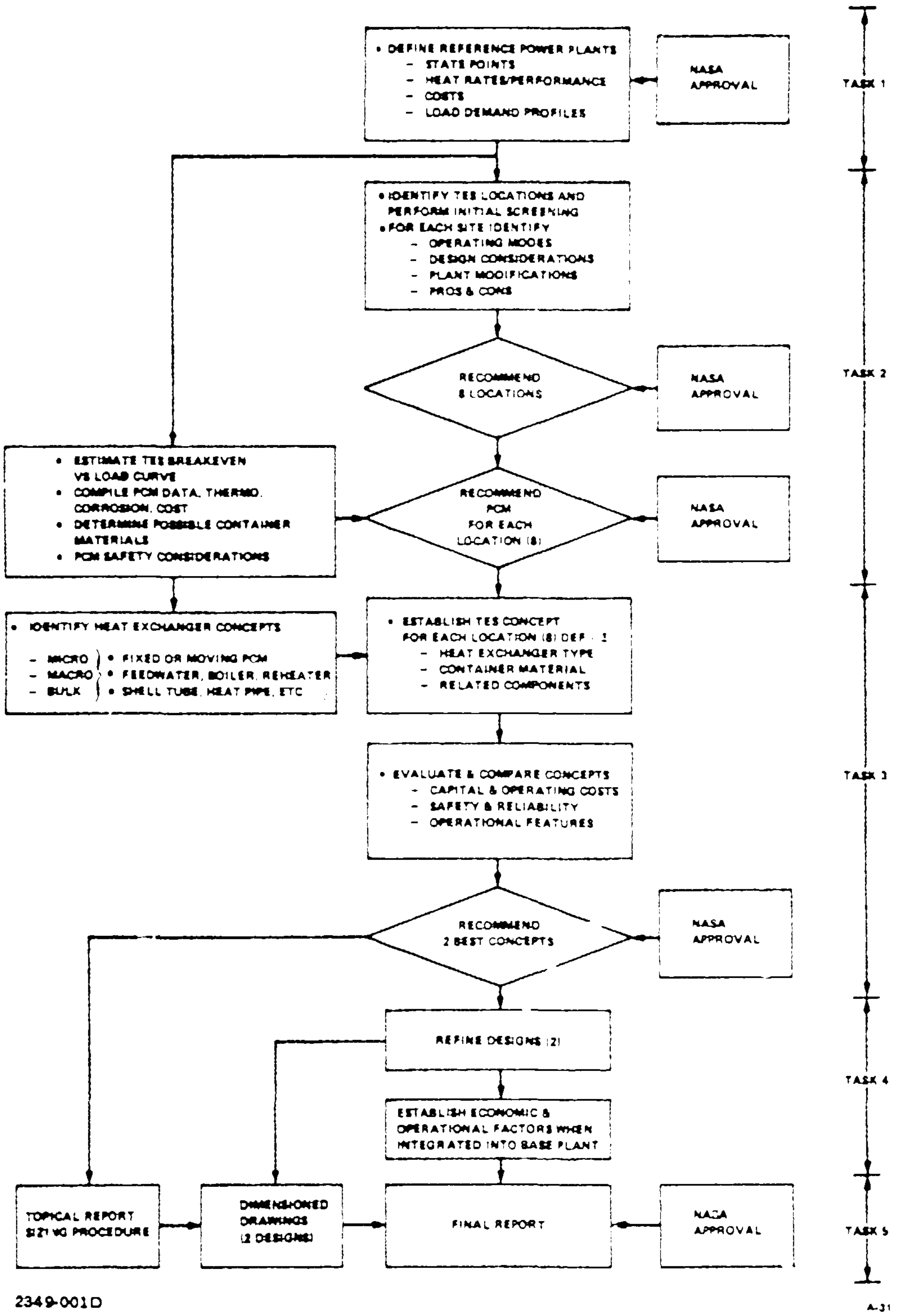

Fig. 1-1 Work Flow Plan

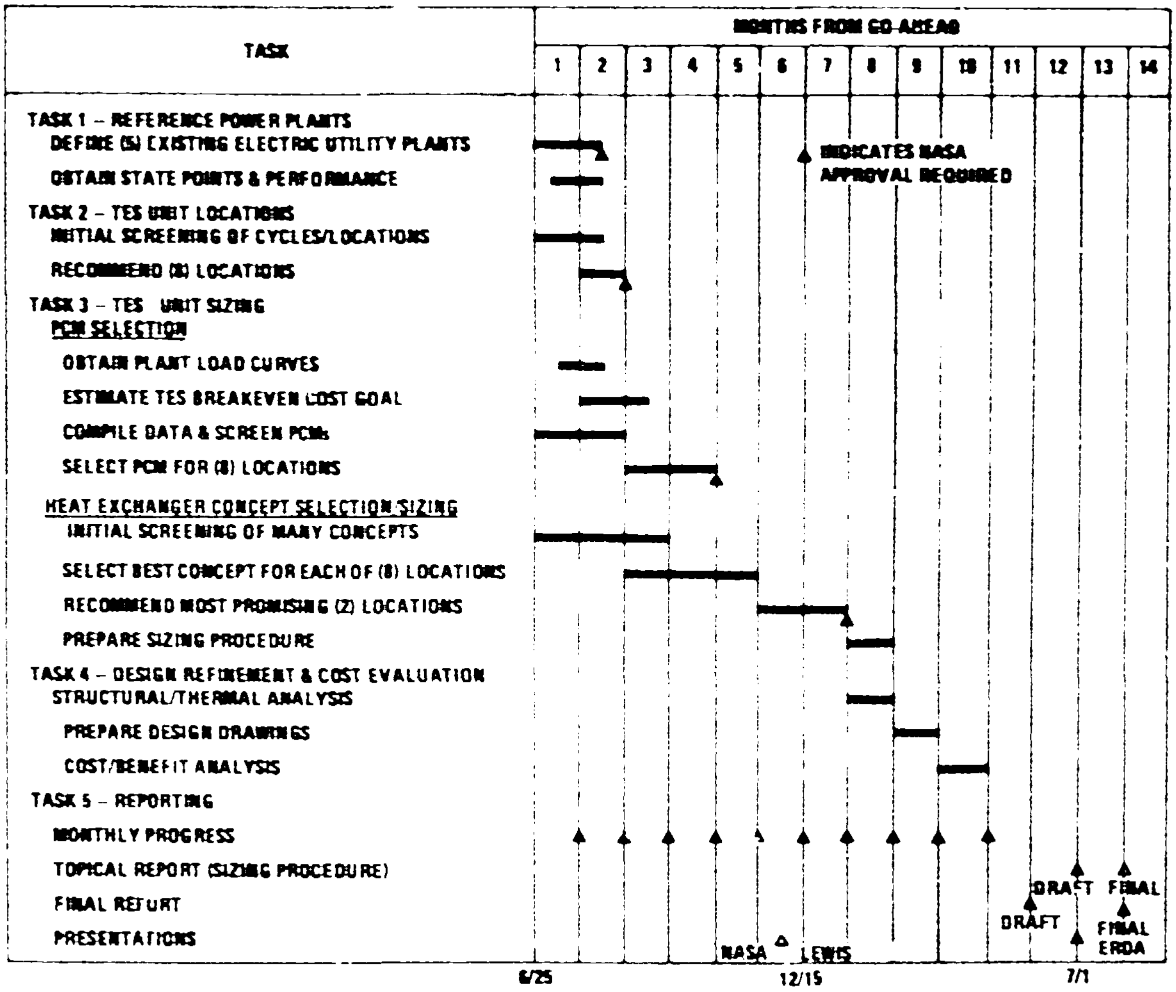

2349-002D

Fig. 1-2 Program Schedule

Generic Type	Operating Station	Location	Net MW Output	Throttle Press, Psig	Throttle Temp., °F	Reheat, °F
1. Boiling Water Reactor	Copper Nuclear Station Unit #1	Nebraska	835	970	541	---
2. Pressurized Water Reactor	Three Mile Island Unit #1	Pennsylvania	870	900	565	---
3. Supercritical Fossil Fueled Boiler	Fort Martin Unit #1	W. Virginia	540	3500	1000	1000
4. High Temperature Gas-Cooled Reactor	Fort. St. Vrain Unit #1	Colorado	355	2400	1000	1000
5. High Pressure Fossil Fueled Boiler	Roseton Unit #1	New York	600	2400	1000	1000

2349-003D

Fig. 1-3 Reference Utility Power Plants

GENERATING STATION	COOPER	THREE MILE ISLAND NO. 1	FORT MARTIN NO. 1	FORT ST. VRAIN	ROSETON NO. 1
GENERIC TYPE	BWR	PWR	SUPERCRITICAL FOSSIL (COAL)	HTGR	HIGH PRESSURE FOSSIL (OIL)
DATE OF INITIAL OPERATION	1974	1974	1967	1974	1974
INSTALLED CAPACITY (MW)	835	870	540	355	600
COST OF PLANT ($1000)	306,648	400, 929	71,410	102,000	160,885
COST/KW OF INSTALLED CAP.	$367.24	$460.84	$132.41	$287.33	$268.14
PRODUCTION EXPENSES					
a) FUEL, $1000 (MILLS/KWHR)	2,986(1.54)	19,933(2.45)	27,041(4.44)	N/A	41,624(9.56)
b) O&M, $1000 (MILLS/KWHR)	4,490(0.77)	11,235(1.84)	2,077(0.34)		1,239(0.28)
c) MISC., $1000 (MILLS/KWHR)	459(0.08)	2,991(0.49)	359(0.06)		1,241(0.29)
d) TOTAL, $1000	13,935	29,159	29,477		44,104
e) MILLS/NET KW-HR	2.38	4.78	7.30		10.13
FIXED CHARGES					
BASED ON FCR = 15%, $1000	45,997	60,139	10,712	15,300	24,133
HEAT RATES (BTU/KWHR)					
NET TURBINE	10,151	9,976	7,612	8,508	7,763
NET PLANT	10,685	10,501	8,836	8,956	8,936

2343-004D

Fig. 1-4 Plant Heat Rates and Generating Costs

used storage energy to generate steam for a separate turbine/generator (see Figure 1-5). In parallel to the plant cycle analysis we identified candidate salts for use as the storage media. Selection was based on cost, compatibility with steel container materials, thermal performance and safety. The recommended salt eutectics are in the chloride, nitrate/nitrite and hydroxide families. Figure 1-6 summarizes the 16 salts selected, which cover the temperature range of interest (~ 300 to 900°F), in about 100°F increments.

Final screening was to select two promising TES systems for detailed performance and economic evaluation. Alternate heat exchanger concepts were assessed, including standard technology such as a tube/shell heat exchanger with the salt on the shell side, and variations using heat pipes or an intermediate loop to transfer heat from the utility fluid to the salt. These are examples of passive systems where the salt phase change material (PCM) is used in bulk and is static. Alternately, macroencapsulated PCM (bricks) can be configured into a checkerboard heat exchanger, or microencapsulated PCM can be fluidized and heat-transferred to and from the flowing stream. Moving bulk PCM systems can also be devised using molten salt pumps, solid conveyors and scrapers. The reason for moving or fluidized systems is to eliminate the large thermal resistance resulting from any significant thickness of static salt. All static systems require a large heat exchanger area to overcome this resistance.

Advantages and disadvantages of these heat exchanger concepts were reviewed and it was decided that macroencapsulated systems did not offer significant advantages over the tube shell unit and that microencapsulation costs are likely to be extremely high. The heat

LOCATION 2 SINGLE LOOP REGENERATIVE HEATING AUGMENTATION

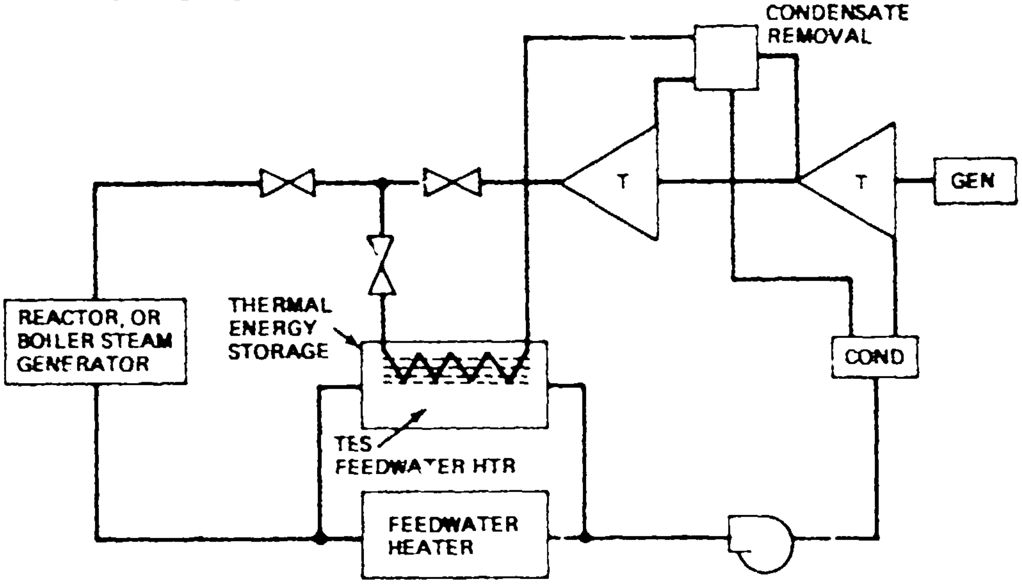

LOCATION 8 SINGLE LOOP SEPARATE POWER CONVERSION LOOP

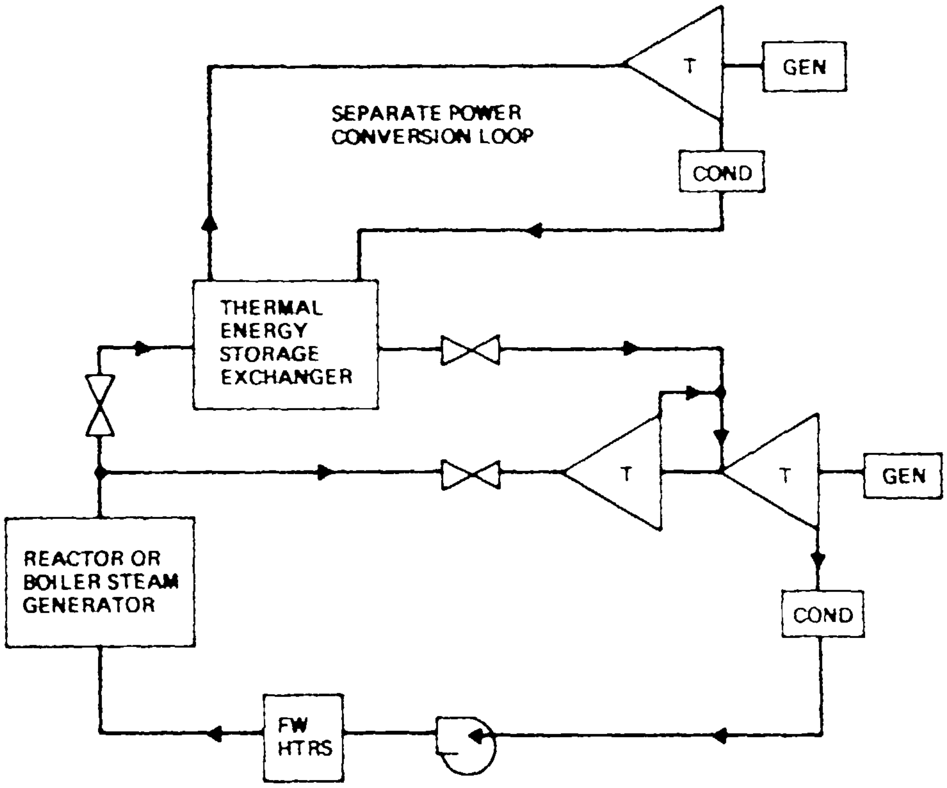

Fig. 1 5 Selected TES Locations in Power Plant Cycles

Salt Element A – B – C	Melt Point^{a} °C (°F)		Composition^{a} Weight %			Heat of Fusion, ΔH_{fs} Cal/gm (BTU/lb)	Specific Heat Cal/gm °C		Thermal Conductivity 10^3 x cal/sec °C cm (BTU/hr ft °F)		Density gm/cc (lb/ft^3)	
			A	B	C		Solid ($c_{p,s}$)	Liquid (c_{p1})	Solid (K_s)	Liquid (K_1)	Solid (ρs)	Liquid ($\rho \ell$)
$KNO_3 \bullet NaNO_3 \bullet NaKO_2$	142	(287)	53	7	40	19.8^{m} (36)	.28^{n}	.32^{m}	1.36^{c} (.33)	1.36^{m} (.33)	1.97^{c} (123)	1.97^{m} (123)
$KNO_3 \bullet NaNO_3 \bullet NaNO_2$	179	(354)	Partherm		350^{b}	19.8 (36)^{d}	.29^{d,n}	.32^{d}	1.36^{c,d} (.33)	1.36^{d} (.33)	1.97^{c,d} (123)	1.97^{d} (123)
$Ca(NO_3)_2 \bullet NaNO_2$	204	(399)	48.3	51.7	---	31.2^{c} (56)	.33^{n}	.36^{e}	1.70^{c,e} (.411)	1.70^{e} (.411)	2.34^{c} (146)	2.34^{f} (146)
$NaNO_3 \bullet KNO_3$	220	(428)	45.7	54.3	---	32.8 (58.8)^{f}	.36^{f}	.36^{f}	1.17^{f} (.28)	1.368^{f} (.33)	2.18^{g} (136)	1.88^{g} (117)
$NaNO_3 \bullet NaOH$	246	(475)	84.5	15.5		42.5^{f} (76.5)	.46^{f}	.46^{f}	1.56^{c,f} (.377)	1.56^{f} (.377)	2.24^{f} (140)	1.933^{f} (120.7)
$NaCl \bullet NaNO_3$	297	(567)	4.6	95.4	---	46.8^{f} (84)	.44^{f}	.43^{f}	1.46^{f} (.35)	1.46^{f,h} (.35)	2.26^{f} (141)	1.88^{f} (117)
$NaNO_3$	307	(585)	100		–	43.5^{m} (78.1)	.46^{m}	.44^{m}	1.36^{m} (.33)	1.45^{m} (.35)	2.26^{m} (141)	1.90^{m} (119)
$NaOH$	318	(605)	100	---	---	76^{g} (136)^{g}	.48^{m}	.50^{m}	2.2^{m,c}	2.2^{m}	2.73 (170)	1.74 (109)
$KCl \bullet KNO_3$	320	(608)	4.5	95.5	---	26.21^{f} (47)	.28^{f}	.29^{f}	1.15^{f} (.278)	1.15^{f,h} (.278)	2.11^{f} (132)	1.86^{f} (116)
KOH	360	(680)	100	--		32.1^{m} (57.8)	.32^{g}	.36^{m}	2.20^{c,d} (.53)	2.20^{d} (.53)	2.04^{m} (127)	1.73^{m} (108)
$KCl \bullet NaCl \bullet MgCl_2$	385	(725)	14.6^{g}	22.3^{g}	63.2^{g}	110^{g} (197)	.23^{f}	.248^{f}	3.6-3.8^{i} (.87-.92)	1.9-2.4^{j} (.47-.58)	2.25^{g} (140)	1.63^{g} (102)
$NaCl \bullet BaCl \bullet MgCl_2$	418	(784)	28.4^{g}	31.8^{g}	39.8^{g}	81.6^{g} (146)	.19^{f}	.21^{f}	3.6-3.8^{i} (.87-.92)	1.9-2.4^{j} (.47-.58)	2.76^{g} (172)	2.12^{g} (132)
$NaCl \bullet MgCl_2$	450	(842)	60	40	---	111^{g} (199)	.22^{k}	.24^{k}	3.6-3.8^{i} (.87-.92)	2.27^{k} (.55)	2.23^{k} (139.1)	1.61^{g} (100)
$CaCl_2 \bullet KCl \bullet NaCl$	465	(869)	64.5	6.5	29	77.8^{f} (139)	.21^{f}	.23^{f}	3.6-3.8^{i} (.87-.92)	1.9-2.4^{j} (.47-.58)	2.15^{f} (134)	1.85^{f} (115)
$NaCl \bullet CaCl_2$	500	(928)	33	67		67^{k,l} (121)	.20^{k}	.24^{k}	3.6-3.8^{i} (.87-.92)	2.44^{k} (.59)	2.15^{k} (134)	1.89^{g} (118)
$KCl \bullet NaCl \bullet CaCl_2$	504	(939)	5^{g}	29^{g}	66^{g}	67^{k,l} (120)	.28^{k}	.24^{k}	3.6-3.8^{i} (.87-.92)	2.39^{k} (.58)	2.15^{k} (134)	1.90^{g} (119)

Footnotes - Table 1.

(a) Values for melting point and composition are experimental data provided by Drs. Janz and Borucka

(b) Partherm salts are proprietary products of the Park Chemical Co and the composition is unavailable

(c) Due to a lack of information, value listed for solid is that of liquid phase of same salt.

(d) Value given is that of a different eutectic having the same or similar constituents (similar anions)

(e) Value given is for one of the eutectics constituent salts as values for the other(s) have not been found.

(f) Value determined by ratioing values for constituent salts by weight.

(g) Source (Ref. 8) states: "Not Accurate. Calculation based on assumed ideality, not true in most cases."

(h) Due to a lack of information, value given for liquid is the same as for solid phase.

(i) Values given are for KCl and NaCl

(j) Values given bracket range for Cl salts listed in Ref. 15 which are referred to as estimates.

(k) Values given in Ref. 15 are referred to as estimates.

(l) ΔH_{f_s} data sources disagree for this salt. Ref. 13 lists value as 77.8 cal/gm, but since Ref. 15 lists 67 cal/gm this figure was (conservatively) used

(m) Experimental data.

(n) Value of $c_p(s)$ determined from c_{p1}/c_{ps} = 1.10, as per Ref. 13

(o) Solid densities at 25°C.

(p) Liquid densities at melt point.

(q) Includes solid solid transformation at 565°F (296°C)

2349-006D

Fig. 1-6 Thermophysical Property Data of Selected Salts pipe unit, while exhibiting desirable features, was not feasible at the Ft. Martin plant temperature level since no suitable heat pipe working fluid is available. Heat pipe units are reasonable for the lower temperature steam conditions typical of nuclear plants, but we felt that the first applications of a new technology (TES) would not be in a nuclear plant.

Near term recommendations are therefore the standard tube/shell and the tube/shell with intermediate (liquid metal) fluid loop. The latter offers the advantage of isolating the salt from the utility steam and has certain control advantages, but does add the complexity of a liquid metal loop. For the longer term a moving PCM system has promise. In this system, molten salt is pumped to a rotating drum where it is scraped off. The solid is collected in a storage tank. Melting is by heating coils in the bottom of the tank and the liquid is drawn off for transfer to a separate tank. Total storage volume is twice as large as the tube/shell, but the required heat exchanger surface area is much less. Equipment needed for the system is non-standard so that estimated costs would not be nearly as reliable as those for the tube/shell unit. Based on this evaluation, we chose the tube/shell and the intermediate loop tube/shell as the two concepts for design refinement and cost analysis. Each was applied to both feedwater heating and separate cycle usage locations in the Ft. Martin plant cycle and plant heat balances were computed for comparison with the base plant.

Incorporating a TES in the cycle to supply feedwater heating results in an improvement in net plant heat rate with fuel (coal) saving of \$183,000 per year compared to cycling the plant. No change in net plant heat rate results in the separate power cycle case.

We suggest a stayed structural arrangement for the upper and lower domes of the tube and shell unit which greatly reduces unit weight and cost. Although not optimized, this approach results in a TES capital cost of ~ \$22.5 million which is somewhat less than the cost of enlarging the plant to provide a peaking capability of about 7% (see Fig. 1-7).

A special situation for the application of TES exists when a plant is converted from oil to coal. This results in derating the boiler, thus leaving excess turbine capacity. For a typical 500 megawatt plant the extra 7% peaking capability would require a larger T-G costing about \$8.6 million. If this is available "free" in a conversion it considerably improves the TES economics. Moreover, installation of TES removes a disincentive to coal conversion, namely, the loss of capacity, which would require the utility to accelerate its new plant construction schedule.

	Cost
Earthwork and Grading	$ 8,200
Roads and Paving	1,300
Land and Land Rights	50,000
Foundations	93,000
Piping and Valving	1,166,800
Instrumentation and Control	50,000
Flash Tank	36,000
Recuperator	500,000
TES Units	7,800,000
TES Salt	1,219,000
Subtotal	$10,924,300
Contingency & Int During Constr at 15%	1,638,660
Engrg & Constr Mgmt at 12%	1,310,920
Increm T-G (37.36MW) & Elect Cost at $\$230/\mathrm{KW}_e$	8,592,000
Total	$22,465,860
System Breakeven = (37.36 MW) ($650/KW)	$24,284,000
Net Savings – New Plant or Plant w/o Excess T-G	$ 1,818,140
– Retrofit, Plant with Excess T-G	$10,410,140

2349-096D

Fig. 1-7 Total TES System Capital Cost-Ft. Martin, Feedwater Heating Case

Overall we feel that latent heat TES is a viable means of providing peaking capability on its own merits, compared to cycling a coal or nuclear plant. This does not necessarily mean that it is superior to other TES systems using sensible heat storage. Some of these systems use very inexpensive storage material (water, rock, etc.) and containers (underground caverns, etc.). Although our study has identified salts that are also relatively low in cost, heat exchanger costs are high due to the high temperature and pressure.

It is suggested, therefore, that a further evaluation of active heat exchanger designs that minimize heat exchanger area be performed to complete the assessment of the latent heat TES option.

Section 2

REFERENCE POWER PLANTS

2.1 SELECTION OF FIVE EXISTING ELECTRIC UTILITY POWER PLANTS

The initial task was to select existing power plants which typify the large central station units presently in service and are representative of future construction. These included:

- Cooper Nuclear Station Unit No. 1, located in Nebraska, which was used as a typical nuclear-fueled boiling water reactor power plant.
- Three Mile Island Unit No. 1, located in Pennsylvania, representative of a nuclear-fueled pressurized water reactor power plant.
- Fort Martin Unit No. 1, located in West Virginia, representative of a supercritical once-through boiler fossil-fueled central station power plant.
- Fort St. Vrain, located in Colorado, representative of a nuclear-fueled high temperature gas cooled reactor power plant.

In addition to these reactor and boiler types, a high pressure, drum type boiler, fossil fueled station using 2400 psig/1000° F steam was included, as these steam conditions are representative of the majority of large oil and coal fired central station power plants in the U.S. today. Roseton Unit No. 1, located in New York, was chosen as the representative 2400 psig unit, which is oil-fired. Figure 2-1 describes the reference power plants and lists unit sizes and steam conditions.

2.2 THERMODYNAMIC STATE POINTS AND PLANT PERFORMANCE

For each of these power plants the base load station heat balances were obtained and are included as Figures 2-2 through 2-6. Also included as Figure 2-7 are the associated heat rates and generating costs at the high side of the main transformer. Although the fossil fueled power plants are considerably more thermodynamically efficient (lower plant heat rate) than either the BWR or PWR nuclear plants, the nuclear plants have lower yearly operating costs per kw hours generated due to exceptionally low fuel cost. The Fort St. Vrain nuclear plant includes the advantages of both fossil and nuclear plants in that it has efficient 2400 psig/1000° F throttle conditions comparable to a fossil plant and lower fuel cost associated with nuclear plants.

Generic Type	Operating Station	Location	Net MW Output	Throttle Press, Psig	Throttle Temp., °F	Reheat, °F
1 Boiling Water Reactor	Copper Nuclear Station Unit #1	Nebraska	835	970	541	—
2. Pressurized Water Reactor	Three Mile Island Unit #1	Pennsylvania	870	910	565	—
3. Supercritical Fossil Fueled Boiler	Fort Martin Unit #1	W. Virginia	540	3500	1000	1000
4. High Temperature Gas-Cooled Reactor	Fort. St. Vrain Unit #1	Colorado	355	2400	1000	1000
5. High Pressure Fossil Fueled Boiler	Roseton Unit #1	New York	600	2400	1000	1000

2349-007D

Fig. 2-1 Reference Utility Power Plants

ORIGINAL PAGE IS
OF POOR QUALITY

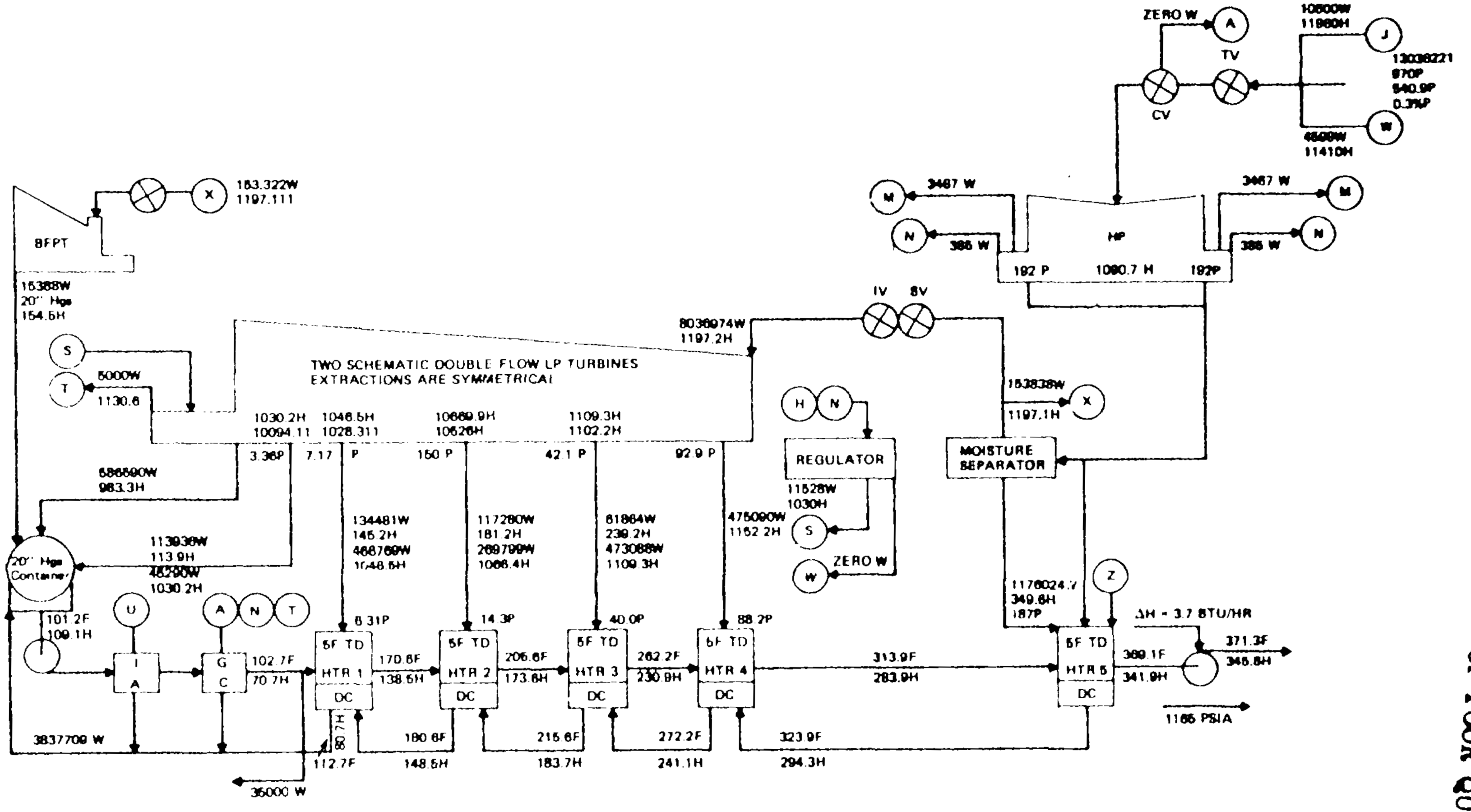

Fig. 2-2 Cooper Nuclear Station Unit #1 "Max Calculated"

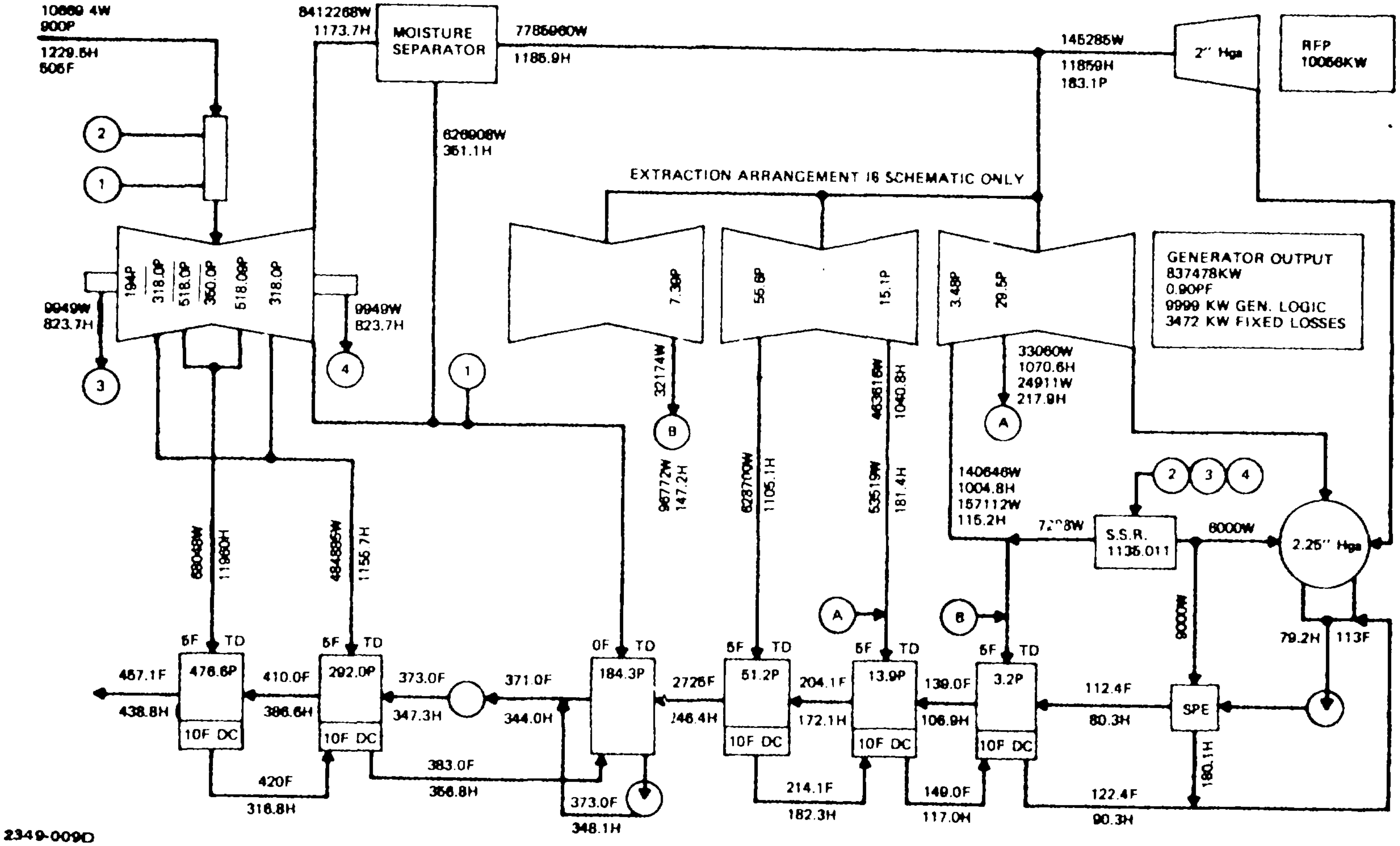

Fig. 2-3 Three Mile Island Unit #1 "Max. Calculated"

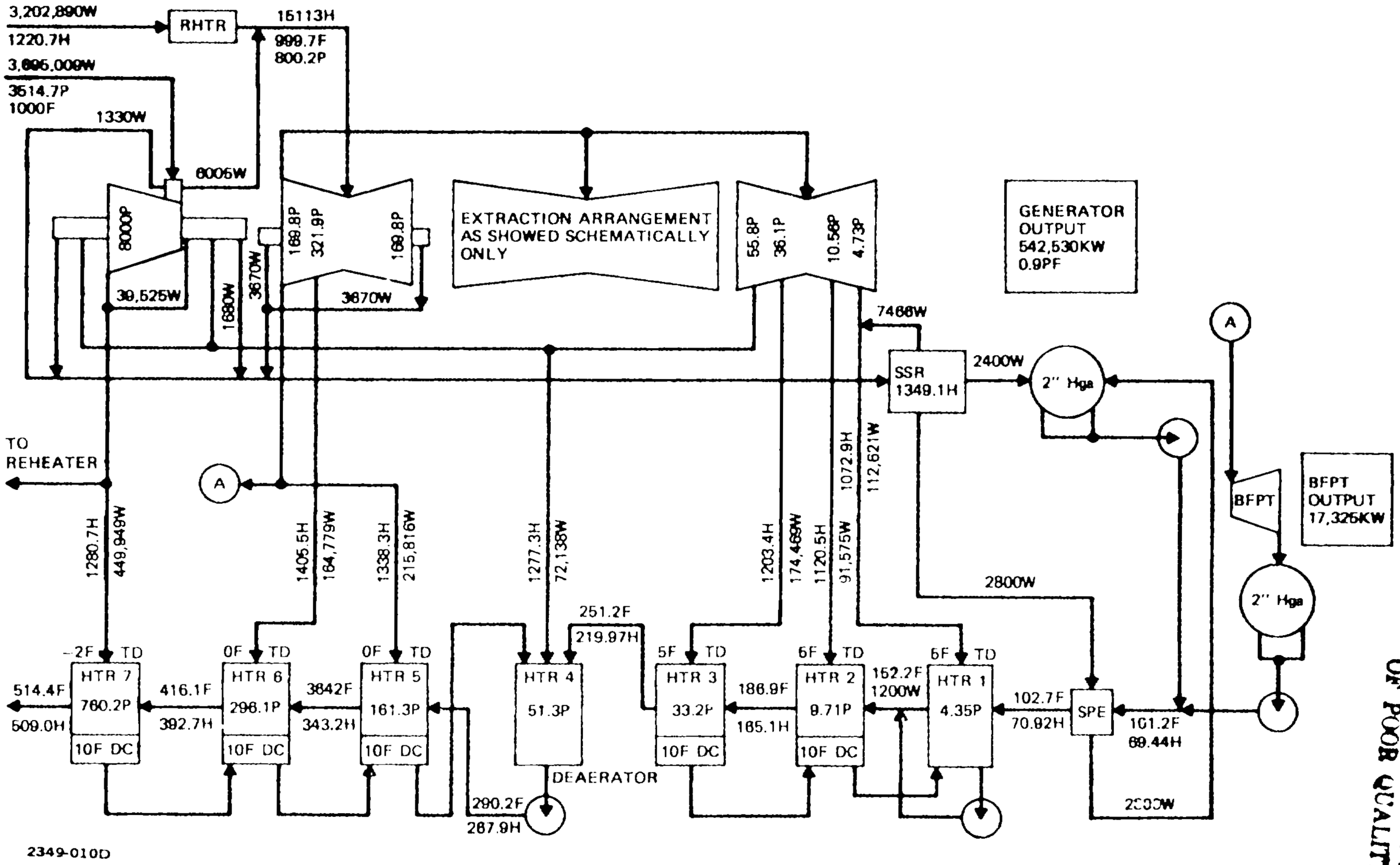

Fig. 2-4 Ft. St. Martin Unit #1 "Max. Calculated"

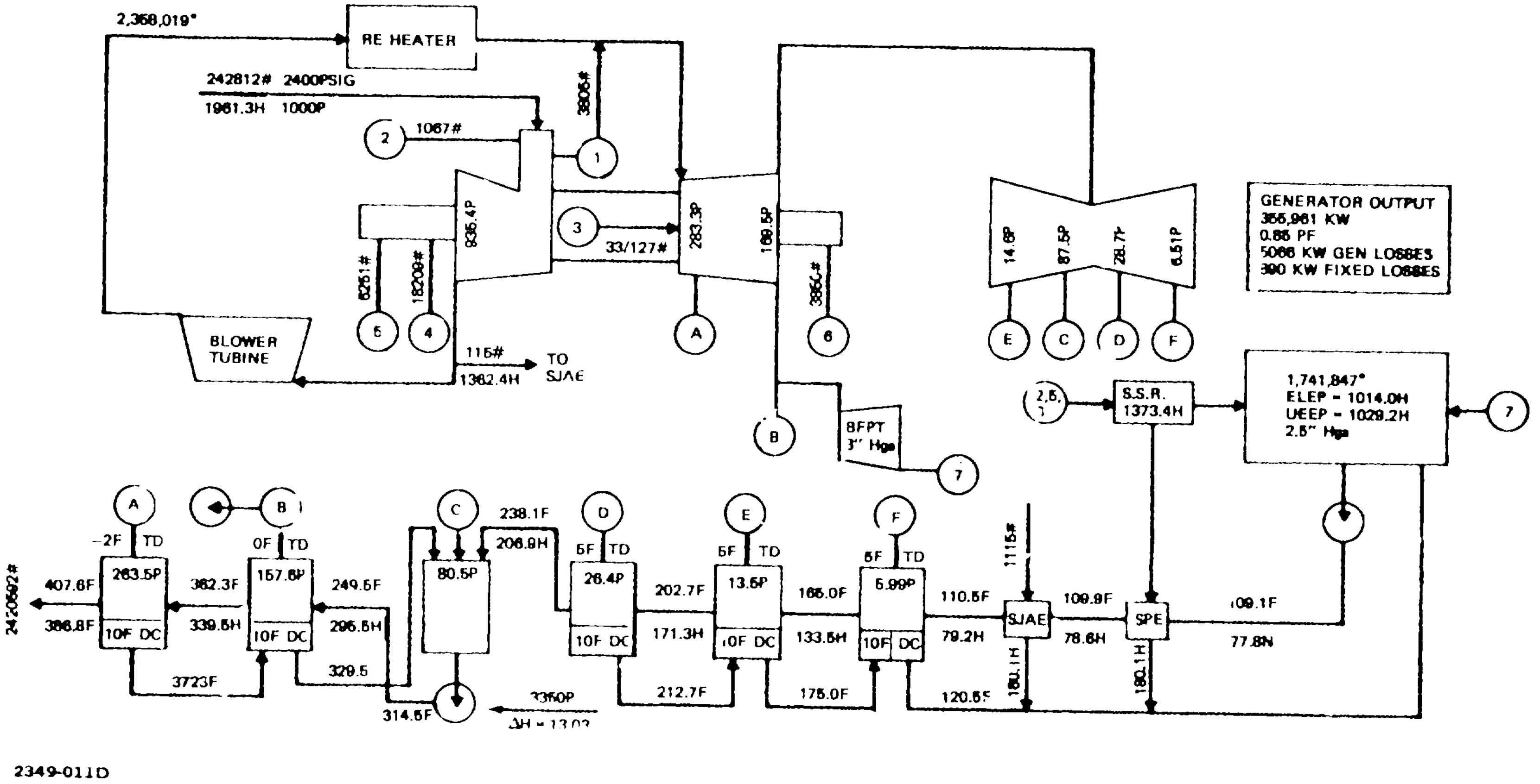

Fig. 2-5 Ft. St. Vrain Unit #1 "Max Calculated"

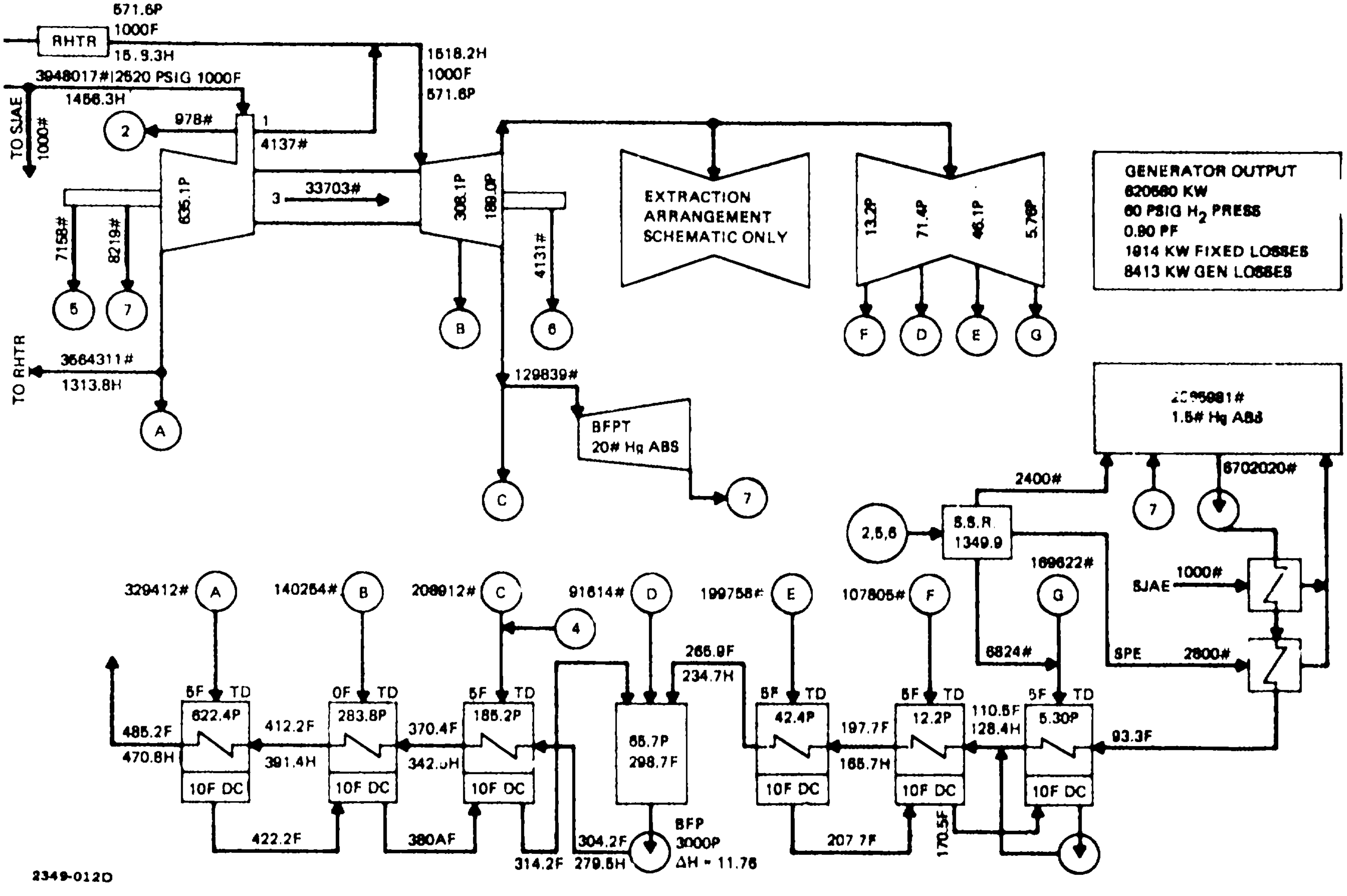

Fig. 2-6 Roseton Unit #1 "Max Calculated"

ORIGINAL PAGE IS
OF POOR QUALITY

The installed cost for the various power plants in the study varied from ~$132/KW$_e$ to $460/KW$_e$ with the two fossil plants at the low end of the scale, the HTGR next, and the BWR and PWR as the most costly, respectively. Note that although the nuclear plants were all initially placed in operation in 1974, construction costs varied from about $287 to $367/KW. In the case of fossil plants, Roseton's capital cost of $268/KW lies within this range, but Ft. Martin's figure of $132/KW must be adjusted to allow for its earlier construction period (initial operation, 1967).

Since a new TES installation should be compared to an incremental capacity increase of a new plant, we should base cost analysis on current plant costs which are shown in Figure 2-8. Here it can be seen that there is no significant difference between the costs for nuclear and fossil plants, therefore either can be considered for incorporation of a TES system. Since the near-term national goal is to reduce dependence on oil, presumably TES would be utilized in coal or nuclear plants. Roseton, although an oil-fired plant which was selected because of the availability of operating data, has steam conditions representative of many coal fired plants. It should also be mentioned that if an oil plant is converted to coal the boiler is derated, resulting in excess turbine capacity. This is an ideal situation since TES could then be added without requiring additional turbine/generator capacity.

GENERATING STATION	COOPER	THREE MILE ISLAND NO. 1	FORT MARTIN NO. 1	FORT ST. VRAIN	ROSETON NO. 1
GENERIC TYPE	BWR	PWR	SUPERCRITICAL FOSSIL (COAL)	HTGR	HIGH PRESSURE FOSSIL (OIL)
DATE OF INITIAL OPERATION	1974	1974	1967	1974	1974
INSTALLED CAPACITY (MW)	835	870	540	355	600
COST OF PLANT ($1000)	306,648	400, 929	71,410	102,000	160,885
COST/KW OF INSTALLED CAP.	$367.24	$460.84	$132.41	$287.33	$268.14
PRODUCTION EXPENSES					
a) FUEL, $1000 (MILLS/KWHR)	2,986(1.54)	19,933(2.45)	27,041(4.44)	N/A	41,624(9.56)
b) O&M, $1000 (MILLS/KWHR)	4,490(0.77)	11,235(1.84)	2,077(0.34)		1,239(0.28)
c) MISC., $1000 (MILLS/KWHR)	459(0.08)	2,991(0.49)	359(0.06)		1,241(0.29)
d) TOTAL, $1000	13,935	29,159	29,477		44,104
e) MILLS/NET KW-HR	2.38	4.78	7.30		10.13
FIXED CHARGES					
BASED ON FCR = 15%, $1000	45,997	60,139	10,712	15,300	24,133
HEAT RATES (BTU/KWHR)					
NET TURBINE	10,151	9,976	7,612	8,508	7,763
NET PLANT	10,685	10,501	8,836	8,956	8,936

2349-013D

Fig. 2-7 Plant Heat Rates and Generating Costs

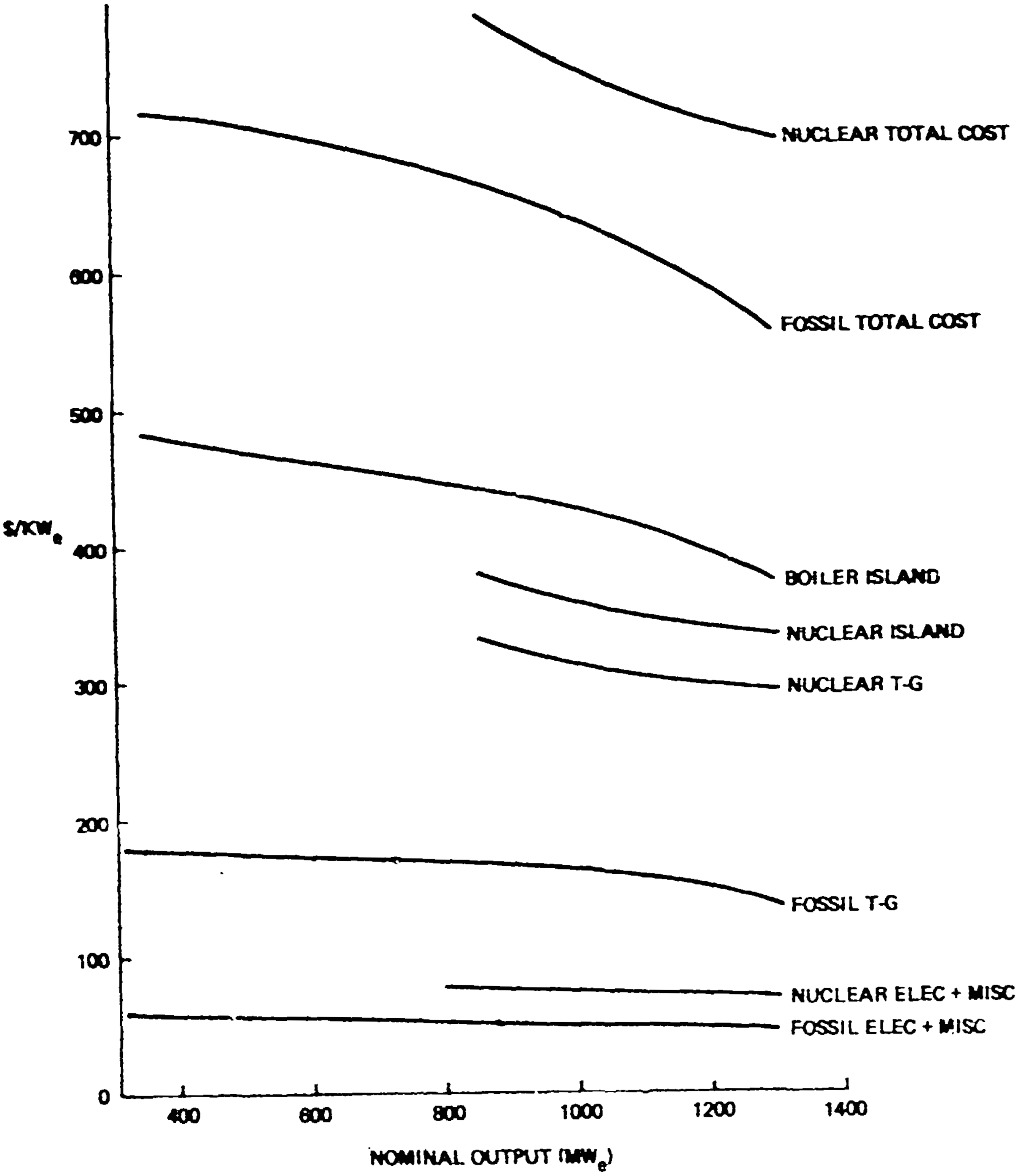

2349-014D

Fig. 2-8 1977 Utility Plant Construction Costs

Section 3

THERMAL ENERGY STORAGE LOCATIONS IN THE UTILITY PLANT CYCLE

3.1 CANDIDATE LOCATIONS

Thermal energy storage locations can be divided into several categories by characteristics. Locations are described as single loop and double loop. Single loop types are characteristic of fossil-fueled boilers and boiling water reactors where the steam produced directly enters the power conversion cycle. Double loop types represent PWR and HTGR plants where pressurized water and helium, respectively, are circulated in a primary loop. Heat is transferred in a boiling heat exchanger where feedwater is heated and evaporated to provide secondary steam to a power conversion cycle loop.

Latent heat stored in the fused salts contained in a thermal energy storage heat exchanger can also be classified by usage. This energy may be used to augment throttle flow, augment reheat flow, provide reheat energy, provide feedwater heating or provide energy to a separate power conversion cycle using steam or other working fluid.

The ten candidate TES heat exchanger locations selected for consideration in Task 2 were:

1. Double Loop Regenerative Heating Augmentation
2. Single Loop Regenerative Heating Augmentation
3. Double Loop Reheat Augmentation
4. Single Loop Reheat Augmentation
5. Double Loop Main Steam Augmentation
6. Single Loop Crossover Steam Augmentation
7. Double Loop Separate Power Conversion Loop
8. Single Loop Separate Power Conversion Loop
9. Double Loop Intermediate Heat Exchanger/Thermal Storage
10. Single Loop Intermediate Heat Exchanger/Thermal Storage

A schematic representation of each candidate location is included as Figure 3-1. Figure 3-2 contains a short description of each candidate location.

3.2 RECOMMENDED LOCATIONS

The ten TES locations combined with the five operating power plant types gives 50 combinations of power plant types and TES locations with feedwater temperature in the various cycles ranging from 100° F to 515° F and the main throttle steam temperature from 540° F to 1000° F. Considering the 10 candidate locations and the steam generator requirements of the five plants, 15 of the original 50 combinations were deleted as not applicable since these involved single loop power systems with double loop heat exchanger schemes (see Figure 3-3). Single loop heat exchanger schemes are, at this level of screening, all applicable to double loop power systems. A screening evaluation was then made of the remaining 35 applicable combinations considering effects on overall cycle performance, physical complexity of locating the TES units in a given cycle, operating limitations with TES units in the cycle, and licensing difficulties associated with implementation. Details of the Power Plant/TES Location matrix screening are presented in Appendix A.

For nuclear cycles, the main reason for elimination of cases was that the TES would often have to be located inside of the primary containment which would necessitate major containment redesign. The use of primary reactor fluid in the TES would necessitate shielding of the TES unit. This would require additional cost penalties and would subject the TES to NRC licensing requirements. Nuclear licensing requirements would have to be resolved before plant construction could proceed. Backfitting (retrofitting) these systems would be out of the question.

Some fossil plant cases were eliminated for a number of reasons. For example, one case (C-9) would have caused the boiler reheat section to be under-utilized when operating at rated conditions. Other reasons included heat exchanger temperature design problems (i.e., insufficient temperature difference between working fluids) and turbine cycle changes (e.g., excessive exit temperatures) that would have been necessary to implement the TES system which would have degraded performance instead of enhancing it. Handling large steam flows in the TES and matching stream pressures for readmission to low pressure turbine sections were avoided due to system and control complexities.

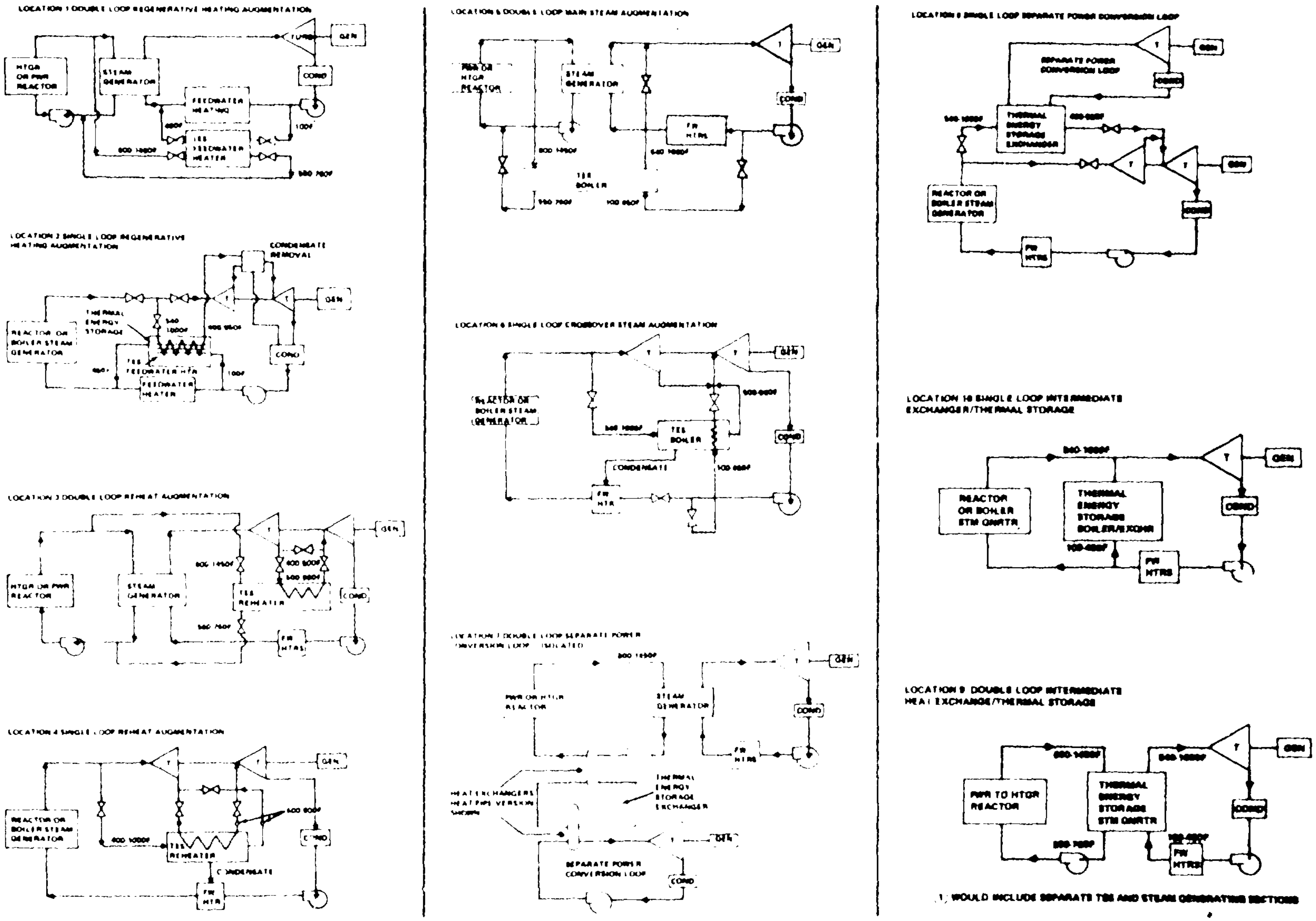

Fig. 3-1 TES Locations in Power Plant Cycles

Location No.	System Type	Thermal Energy Source	TES Extraction Point	TES Addition Point	Remarks
1	Double Loop Regererative Heating Augmentation	Pwr, Htgr	Hot Primary Loop	Feedwater	Parallel or Series Operation with Variable Number of Existing Heaters
2	Single Loop Regenerative Heating Augmentation	Boiler, Reactor	Main Steam	Feedwater	Parallel or Series Operation with Variable Number Existing Heaters. Alternate would Flash Condensate from Crossover Mixer to Feedwater Heaters instead of Dump to Condenser
3	Double Loop Reheat Augmentation	Pwr, Htgr	Hot Primary Loop	Crossover	TES is Crossover Steam Reheater
4	Single Loop Reheat Augmentation	Boiler, Reactor	Main Steam	Crossover	TES is Crossover Steam Reheater, TES Supply Steam to Crossover and Condensate Flashed for Feedwater Heating
5	Double Loop Main Steam Augmentation	Pwr, Htgr	Hot Primary Loop	Throttle	TES is Condensate Boiler, Auxiliary Steam Feed to Throttle Condensate Extraction Point Variable
6	Single Loop Crossover Steam Augmentation	Boiler, Reactor	Main Steam	Crossover	TES is Condensate Boiler, Auxiliary Steam feed to Crossover, TES Supply Steam to Crossover Flashed for Feedwater Heating, Condensate Extraction Point Variable
7	Double Loop Separate Power Conversion Loop	Pwr, Htgr	Cold Primary Loop	Separate Cycle	Isolated (Reflux Heat Pipe) Intertie, Variations include Isolated and Direct TES Exchange, with TES Heat from Cold and Hot Legs of Primary Loop
8	Single Loop Separate Power Conversion Loop	Boiler, Reactor	Main Steam	Separate Cycle	Variations include Isolated TES Exchange to Separate Power Cycle using Reflux Heat Pipes
9	Double Loop Intermediate Heat Exchanger/ Thermal Storage	Pwr, Htgr	Hot Primary Loop	Throttle	TES Isolates Thermal Energy Source from Power Cycle
10	Single Loop Intermediate Heat Exchanger/ Thermal Storage	Boiler, Reactor	Main Steam	Throttle	Brantley-NASA/Marshall Patent, TES is Parallel with Power Conversion Cycle and Thermal Energy Source Simultaneously

2349-016D

Fig. 3-2 Description of TES Locations

Power Plants

A. Cooper Nuclear Station (BWR)
B. Three Mile Island No. 1 (PWR), TMI
C. Fort Martin (Supercritical Fossil)
D. Fort St. Vrain (HTGR)
E. Roseton (High-Pressure Fossil)

TES Location Matrix

1. Double Loop Regenerative Heating Augmentation
2. Single Loop Regenerative Heating Augmentation
3. Double Loop Reheat Augmentation
4. Single Loop Reheat Augmentation
5. Double Loop Main Steam Augmentation
6. Single Loop Crossover Steam Augmentation
7. Double Loop Separate Power Conversion Loop – Insulated
8. Single Loop Separate Power Conversion Loop
9. Double Loop Intermediate Heat Exchanger
10. Single Loop Intermediate Heat Exchanger

TES LOCATION/ PWR PLT	COOPER A	TMI B	FT. MARTIN C	FT. ST. VRAIN D	ROSETON E
1	~~A1~~	B1	~~C1~~	D1	~~E1~~
2	A2	B2	C2	D2	E2
3	~~A3~~	B3	~~C3~~	D3	~~E3~~
4	A4	B4	C4	D4	E4
5	~~A5~~	B5	~~C5~~	D5	~~E5~~
6	A6	B6	C6	D6	E6
7	~~A7~~	B7	~~C7~~	D7	~~E7~~
8	A8	B8	C8	D8	E8
9	~~A9~~	B9	~~C9~~	D9	~~E9~~
10	A10	B10	C10	D10	E10

X CONCEPT NOT APPLICABLE FOR THIS PLANT

2349-017D

Fig. 3-3 Power Plant/TES Location Matrix

Based on this screening evaluation a total of ten combinations of TES cycle locations and power plants were recommended as worthy of further consideration as follows:

Power Plant Cycle Description	Power Plant Name	Plant Generic Type
Regenerative Heating Augmentation	Three Mile Island	Nuclear PWR
Regenerative Heating Augmentation	Fort Martin	Supercritical Fossil
Regenerative Heating Augmentation	Ft. St. Vrain	Nuclear HTGR
Regenerative Heating Augmentation	Roseton	High Pressure Fossil
Reheat Augmentation	Cooper	Nuclear BWR
Reheat Augmentation	Three Mile Island	Nuclear PWR
Crossover Steam Augmentation	Three Mile Island	Nuclear PWR
Separate Power Conversion Loop	Fort Martin	Supercritical Fossil
Separate Power Conversion Loop	Ft. St. Vrain	Nuclear PWR
Separate Power Conversion Loop	Roseton	High Pressure Fossil

These cases were selected for further evaluation because they all appeared to be technically achievable in that: (a) thermodynamically they presented no apparent problems, (b) physical complexity of the TES integration did not appear to present insoluble engineering problems, (c) nuclear cases did not violate the primary containment and lessened any chance of NRC licensing problems and (d) they did not appear to present unusual operating difficulties.

Preliminary state points for the recommended locations are given in Figure 3-4 through 3-7.

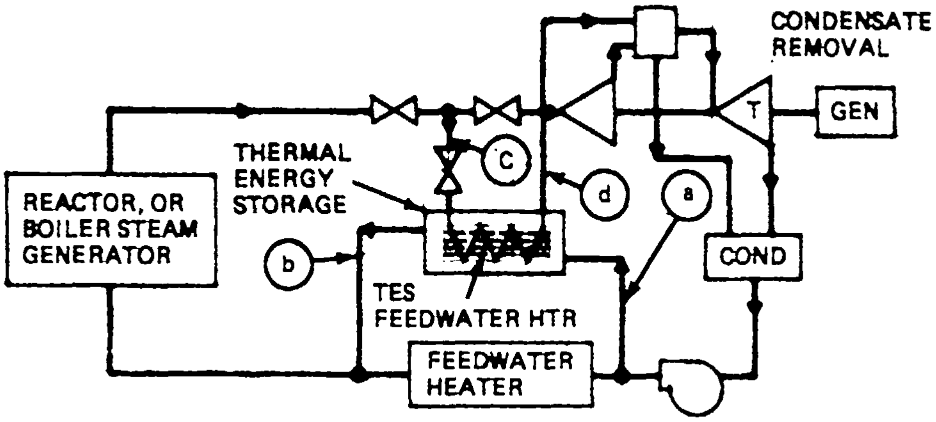

Generating Station	TES State Point Location Data					
Plt. Name	Matrix ID	Point	P (Psia)	T (°F)	$H\left(\frac{Btu}{Lb}\right)$	$W_{Max}\left(\frac{Lb}{Hr}\right)$
TMI	B2	a.		112.4	80.3	7,808,248
				139.0	106.9	7,808,248
				204.1	172.1	7,808,248
				277.5	246.4	7,808,248
				373.0	347.3	10,559,985
				410.0	386.6	10,559,985
		b.	TES Dependent			
		c.	900.0	565.0	1229.5	(Steam)
		d.	TES Dependent			
Fort Martin	C2	a.		102.3	70.3	2,313,230
				150.4	118.3	2,674,701
				184.9	152.8	2,674,701
				248.7	217.2	2,674,701
				227.3	264.8	3,519,057
				360.7	339.3	3,519,057
				412.0	392.6	3,517,067
		b.	TES Dependent			
		c.	3515 687.3	1000 1000	1424.0 1514.3	(Steam to HP) (Reheat to HP)

2349-018D

Fig. 3-4 Location 2 Single Loop Regenerative Heating Augmentation

Generating Station		TES State Point Location Data				
Plt. Name	Matrix ID	Point	P (Psia)	T (°F)	$H\left(\frac{Btu}{Lb}\right)$	$W_{Max}\left(\frac{Lb}{Hr}\right)$
Fort Martin	C2	d.	TES Dependent			
Fort St. Vrain	D2	a.		110.6	79.3	1,975,622
				163.2	131.7	1,975,622
				200.5	169.1	1,975,622
				235.6	204.4	1,975,622
				316.4	282.4	2,306,326
				358.7	335.8	2,306,326
		b.	TES Dependent			
		c.	2415	1000	1460.4	(Steam to HP)
			567.5	1000	1517.8	(Reheat to IP)
		d.	TES Dependent			
Roseton	E2	a.		93.5	61.5	2,573,847
				156.8	124.7	3,027,424
				193.4	161.4	3,027,424
				260.5	229.2	3,027,424
				298.0	273.0	3,761,016
				363.0	339.6	3,761,016
				403.8	382.3	3,761,016
		b.	TES Dependent			
		c.	2415	1000	1460.4	(Steam to HP)
			519.4	1000	1519.8	(Reheat to IP)
		d.	TES Dependent			

2349-019D

Fig. 3-4 Location 2 Single Loop Regenerative Heating Augmentation (Continued)

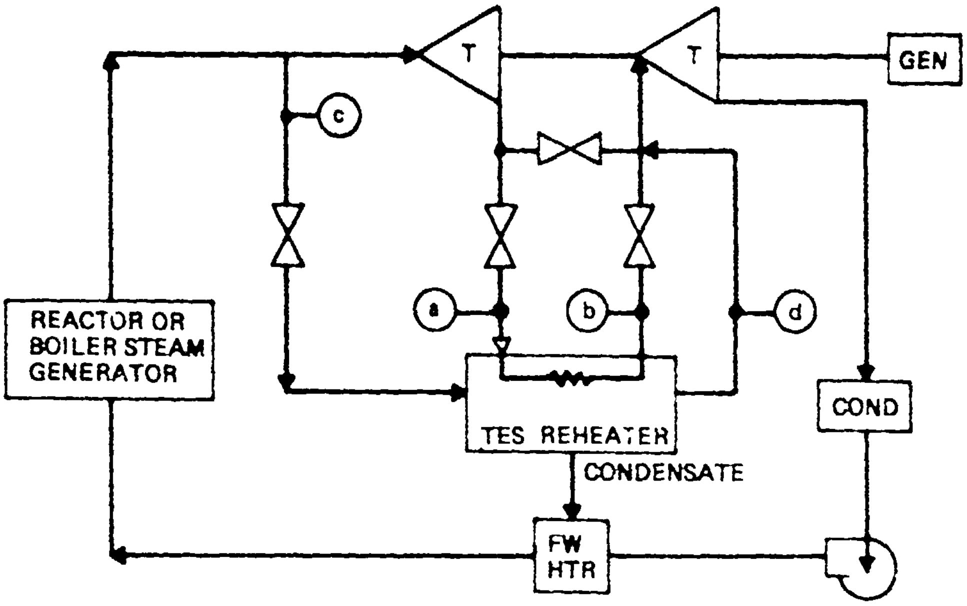

Generating Station	TES State Point Location Data					
Plt. Name	Matrix ID	Point	P (Psia)	T (°F)	$H\left(\frac{Btu}{Lb}\right)$	$W_{Max}\left(\frac{Lb}{Hr}\right)$
Cooper	A4	a.	170.0	370.0	1196.3	7,847,278
		b.	TES Dependent			
		c.	970.0	540.9	1191.0	(Steam)
		d.	TES Dependent			
TMI	B4	a.	183.1		1186.9	7,640,675
		b.	TES Dependent			
		c.	900.0	565.0	1229.5	(Steam)
		d.	TES Dependent			

2349-020D

Fig. 3-5 Location 4 Single Loop Reheat Augmentation

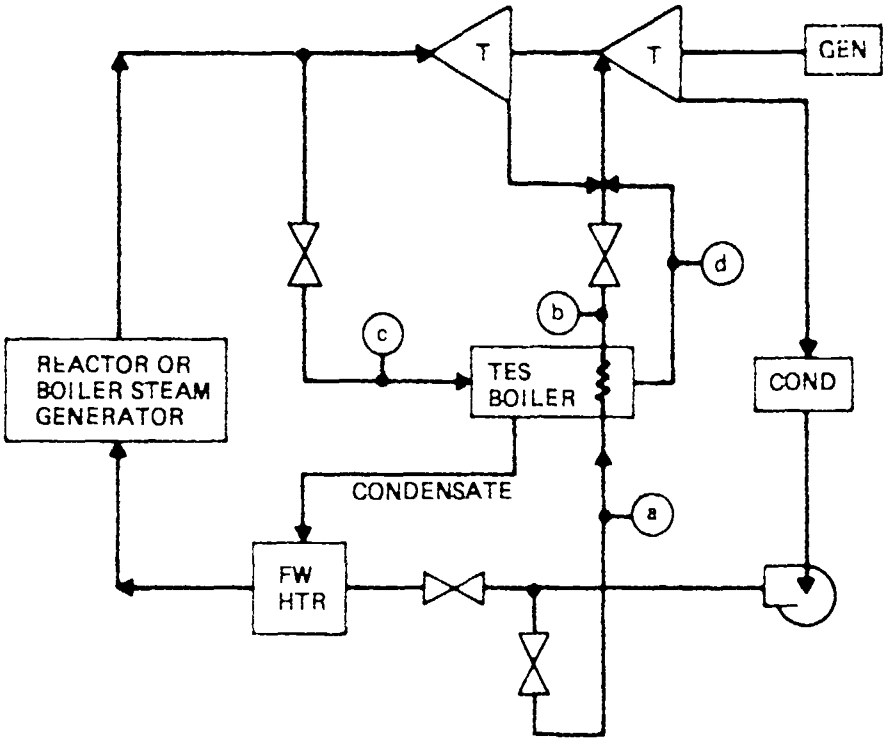

Generating Station		TES State Point Location Data				
Plt. Name	Matrix ID	Point	P (Psia)	T (°F)	H $\frac{Btu}{Lb}$	W_{Max} $\frac{Lb}{Hr}$
TMI	B6	a.		112.4	80.3	7,808,248
				139.0	106.9	7,808,248
				204.1	172.1	7,808,248
				277.5	246.4	7,808,248
				373.0	347.3	10,559,985
				410.0	386.6	10,559,985
		b.	TES Dependent			
		c.	900.0	565.0	1295.5	(Steam)
		d.	TES Dependent			

Fig. 3-6 Location 6 Single Loop Crossover Steam Augmentation

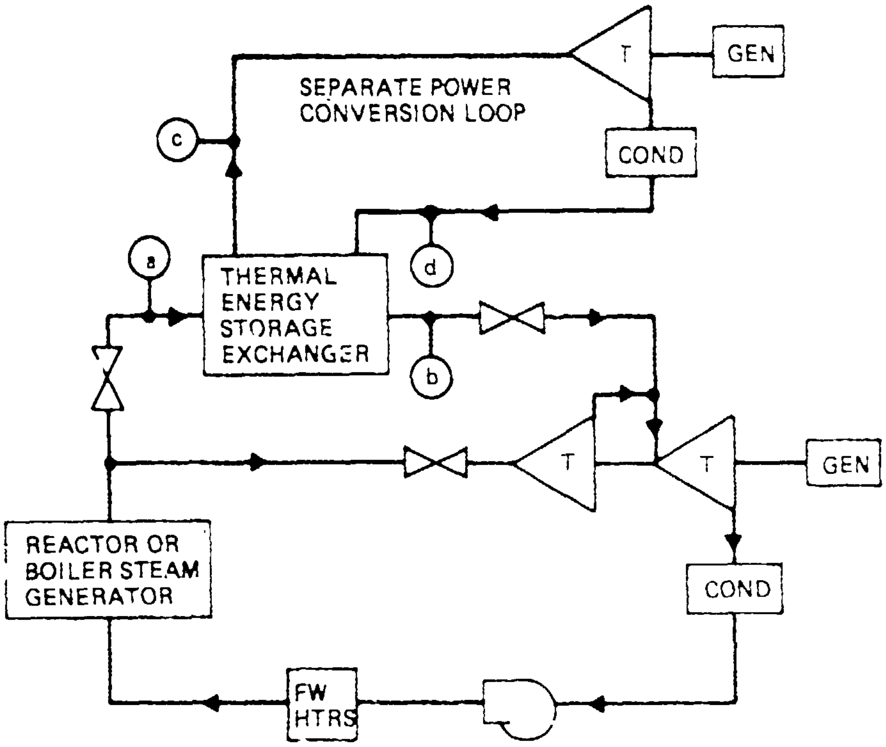

Generating Station		TES State Point Location Data				
Plt. Name	Matrix ID	Point	P (Psia)	T (°F)	$H\left(\frac{Btu}{Lb}\right)$	$W_{Max}\left(\frac{Lb}{Hr}\right)$
Fort Martin	C8	a.	3515.0	1000.0	1424.0	(Steam to HP)
		b.	TES Dependent			
		c.	TES/Loop Dependent			
		d.	TES/Loop Dependent			
Fort St. Vrain	D8	a.	2415.0	1000.0	1460.4	(Steam to HP)
		b.	TES Dependent			
		c.	TES/Loop Dependent			
		d.	TES/Loop Dependent			
Roseton	E8	a.	2415.0	1000.0	1460.4	(Steam to HP)
		b.	TES Dependent			
		c.	TES/Loop Dependent			
		d.	TES/Loop Dependent			

2349-021D

Fig. 3-7 Location 8-Single Loop Separate Power Conversion Cycle

Section 4

THERMAL ENERGY UNIT SIZING

This phase of the program (Task 3) consisted of two subtasks: PCM Selection and Heat Exchanger Concept Selection/Sizing. After selecting five representative (reference) power plants (Task 1) and recommending ten candidate locations for the TES in these cycles (Task 2), the next effort was to select and match the PCM to the concept (depending on specific plant state point conditions) and to develop suitable heat exchanger designs for each concept.

This effort began with a review of daily and seasonal load curves for each of the five reference utility systems. Since economical peaking capability is related to TES cost, we performed a simple capital cost evaluation based on the trade-off between boiler and TES system cost to establish system target cost, storage duration, and total heat stored. This enabled us to screen candidate salts (PCMs) and heat exchanger container materials.

Based on this information, a number of candidate heat exchanger concepts were reviewed including: tube/shell, heat pipe, macroencapsulated pumped loop, fluidized microencapsulated and moving PCM.

One or more salt eutectics were then matched with the heat exchanger concepts in order to select an integrated design for the ten plant cycle locations.

4.1 PLANT LOAD CURVES

As shown in Figure 4-1, each of the five reference power plants make up a portion of one or more utility systems. As part of its data collection role, the Federal Power Commission (FPC) annually compiles and distributes daily power consumption and peak plant capacity information. Using the FPC's latest published information, as a service the General Electric Company provided hourly load factors for each system for "average" weekday and weekend conditions recorded over the four seasons of the year. With this data, computer plots of the system's power consumption on an hourly basis for weekday and weekend periods were prepared (see Appendix B).

Since peak load conditions occur in different seasons depending on location, the seasonal period was selected during which peaking occurs for each plant (utility system). For example, in southern regions peak loads will usually be recorded during summer months when air-conditioning is in great demand; whereas in northern industrialized regions, winter heating and production requirements usually produce greater demand than other seasons. Regardless of season, peak energy is required during daytime hours (8 AM to 8 PM) and energy demand is greater during weekdays than over weekends.

Based on the highest average daily peak load demand for each system, a "normalized" peak demand curve was generated for each system. As shown in Figure 4-2, although they reflect different seasons and different capacities, the shape of the daily peak load curve for each system is remarkably similar. This daily peak could be provided by TES by storing heat overnight. The question arises whether it is also desirable to consider weekend heat storage for use during the week or even off-season storage for use during the peak usage season. Without detailed calculations it is clear that this is not as cost effective as daily energy storage. The purpose of TES is to reduce the required steam generation capacity at a saving of about $\$450/KW_e$. For a given KW_e reduction of the daily peak, weekend storage would require storing five times as much heat as daily storage and hence the TES system would be five times larger, even neglecting the fact that week long storage would result in additional heat losses from the system. Seasonal storage is, of course, even less cost competitive. Our study was therefore totally focused on a system utilizing over-night energy storage.

4.2 TES COST GOAL

Economics will play the critical role in the decision to adopt TES systems. We are not describing a system that will significantly change the plant's heat rate, and therefore will not vary the fuel consumed to generate electrical energy. The trade-off is based on potential capital equipment savings and on the operational advantages of baseloaded equipment. Although we will later show that a TES system may actually improve the plant's heat rate slightly, the economic trade-off primarily involves the question of increased boiler capacity versus the use of TES. That is, with a TES system we can "undersize" the boiler for a certain peak plant capacity requirement, with TES providing the peak energy demand.

GENERIC TYPE	OPERATING STATION CONSIDERED	LOC	SYSTEM
BOILING WATER REACTOR	COOPER NUCLEAR STA UNIT 1	NEBR	(NEPP) NEBRASKA PUBLIC POWER DISTRICT
PRESSURIZED WATER REACTOR	THREE-MI ISLAND UNIT 1	P.A.	(GPU) GENERAL PUBLIC UTILITIES
SUPERCRITICAL COAL FIRED BOILER*	FORT MARTIN UNIT 1	W. VA.	(ALGPS) ALLEGHENY POWER SYSTEM
HIGH TEMP GAS–COOLED REACTOR	FORT ST. VRAIN UNIT 1	COLO	(PSCO) PUBLIC SERVICE CO. OF COLORADO
HIGH PRESS. OIL FIRED BOILER*	ROSETON UNIT 1	N.Y.	(CEHG) CENTRAL HYDSON ELECTRIC & GAS

*TYPICAL CYCLES. COULD APPLY TO EITHER OIL OR COAL FIRED PLANTS.

2349-022D

Fig. 4-1 Reference Utility Power Plants

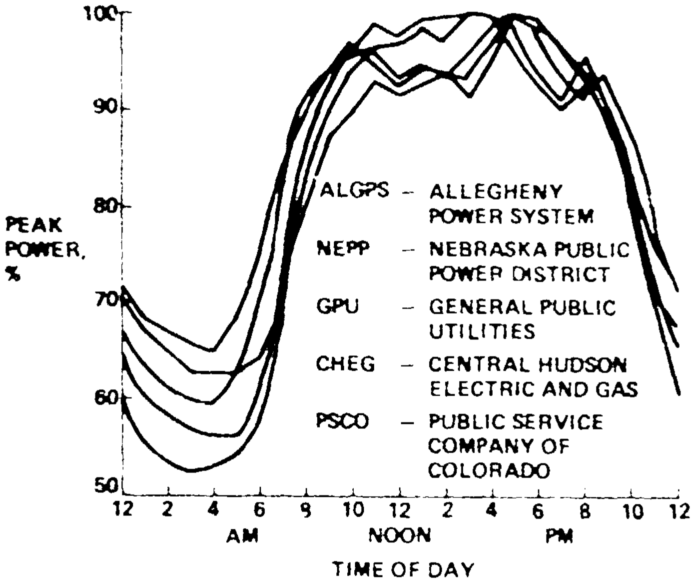

TYPICAL LOAD ABOVE	HOURS
95%	6
90%	12
85%	14

2349-023D

Fig. 4-2 Normalized System Average Weekday Load Curve (Peak Season)

To gain a first-cut insight into the relative economic advantage of TES and evaluate a target-cost for the PCM heat exchanger, we neglected operational considerations and performed a simple capital cost comparison. Here, the cost of boiler island capacity to TES system (salt, heat exchanger, fabrication, installation, etc.) costs must be traded off. Current (1977) costs for boiler (fossil) and nuclear islands range from \$350 to \$450 per electric KW (Figure 2-8). The cost of a TES system, however, is dependent not only on peak power level (KW) but on shape of the load curve, since the amount of phase change material required is a function of stored energy. Consider a typical daily load curve such as in Figure 4-3. The cost of thermal energy storage will be related to the area under this curve for any peak power reduction specified, i.e.:

$$\text{TES Cost} = K \frac{C_s}{\Delta H} \int_{P_{\text{shaved}}}^{P_{\text{peak}}} t\,dP$$

where C_s = salt cost per unit weight

ΔH = heat absorbed by salt (latent plus sensible)

K = cost multiplier for total system (heat exchanger, piping, land, etc.)

t = time

P = power (KW)

Comparing the option of TES storage to increased boiler capacity, it "pays" to store thermal energy as long as the incremental cost of the TES is less than, or at most equal to, the incremental cost of adding additional steam generating equipment. For each increment of power ΔP, the incremental TES cost is:

$$\Delta\text{TES Cost} = \frac{K C_s\, t\, \Delta P}{\Delta H}$$

Rearranging this expression:

$$\frac{\text{System Cost } (K\,C_s)}{\text{Unit Weight of Salt}} = \left(\frac{\Delta\text{ TES Cost}}{\Delta P}\right) \times \frac{\Delta H}{t} \qquad (4\text{-}1)$$

Setting the incremental TES cost per unit power generated (ΔTES Cost/ΔP) equal to the cost of additional boiler or nuclear island capacity allows us to determine the optimum TES cost per unit weight of salt for a specified usage duration. Before this point, savings will increase as usage increases, while beyond this, total savings will decrease as usage increases and system eventually becomes unprofitable (negative savings).

Using the foregoing expression, Figure 4-4 shows the relationship between salt heat storage (which for a first approximation can be considered to be latent heat), TES cost and operating time. Obviously, the higher the salt's latent heat of fusion, the more energy we can store at a given unit cost. For example, with a total TES cost of $1 per pound of salt, the figure shows that the optimum duration for which the TES system can supply peaking power is about 5-7 hours for salts with latent heats of about 70 cal/gm, which will be shown later to be typical of salts that are suitable for this application.

A subsequent review of the system load curves for the five utility plants (see Figure 4-2) showed that a 5-7 hour storage capability would result in a 5% peak reduction. Based on this goal we concluded that the TES system could cost no more than $1 per pound of salt. To allow for the expected high cost of the heat exchanger and associated piping, site preparation and land cost, engineering fees, etc., it is apparent that a suitable salt must be identified that costs much less than $1 per pound.

From the above analysis, we can determine the optimum operating time (hours) for the TES system based on a TES unit cost. Although this is independent of the plant load curve, the total dollar savings realized with the TES will depend on the load curve. For example, using a TES system with the steeper load curve illustrated in Figure 4-5 will result in greater total dollar savings than for the flatter curve. The total TES cost will be a function of the area under the load curve, but savings in steam generating capability is only proportional to the reduction in height of the peak. Therefore, net savings of the steeper load curve over the flatter one will be related to the indicated area.

This analysis also gave an indication of the potential containment materials that could be considered. Based on a "target cost" of $1 per pound of salt, we could not consider exotic metals such as Hastelloys or Inconel alloys for large surface area heat exchangers. In fact, this indicated that we were limited to low carbon or at most stainless steels. This latter decision obviously affected salt selection. Not only were we now

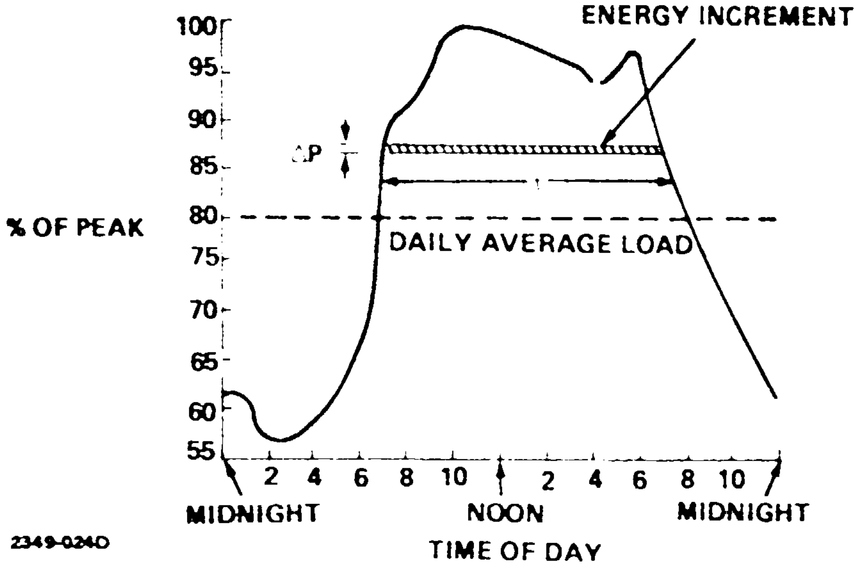

Fig. 4-3 Typical System Daily Load Variation Curve

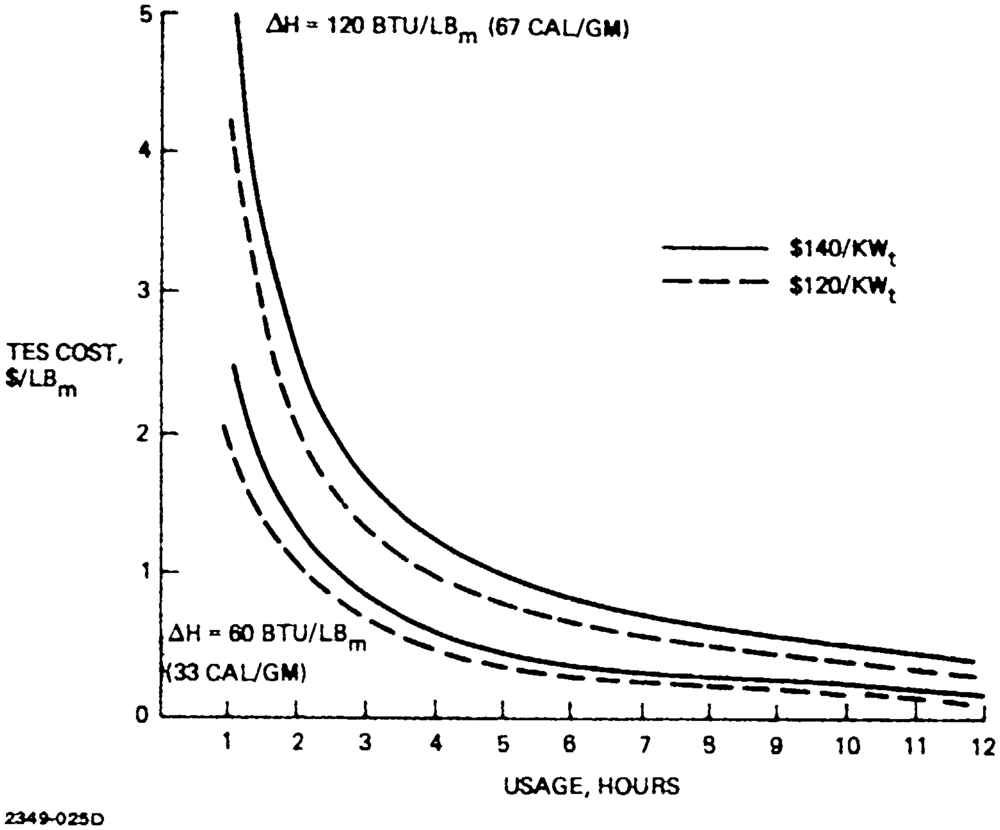

Fig. 4-4 Optimum Reduction in Peak Width vs TES Cost

looking to identify a salt costing less than, say, $.25/lb, but the salt or salt eutectics must also be sufficiently compatible with carbon or stainless steel to guarantee a system design life goal of 30 years.

As will be shown in the following paragraphs, much of our subsequent effort verified the conclusions reached from this relatively simple, preliminary economic study. We iterated many designs and potential salt decisions using this evaluation criteria.

4.3 SELECTION OF PEAKING CAPABILITY TO BE PROVIDED BY TES

As previously discussed (Section 4.1), a review of "normalized" system load curves indicated that these curves would be similar for each of the five reference systems under consideration (see Figure 4-2). Reviewing the system load data and comparing the inclusion of TES to the alternate cost of meeting peaking demands (cycling a large steam generator), it was concluded that the system could be most profitably used on a daily (rather than weekly or seasonal) basis to provide peaking capability of approximately 5% of capacity.

Therefore, as a first cut, using the normalized curves presented in Figure 4-2 we estimated the peak power saving (MW), the period (hours) for which the demand exceeded 5% and, therefore, the amount of energy that needed to be stored. Figure 4-6 summarizes the results of this analysis for each system under consideration. Notice that the period during which demand exceeds 95% of the "normalized" peak plant capacity ranges from 4.34 to 7.68 hours. On the average, then, for a "typical" system we may say that in order to increase system capacity by 5% we must store energy over about 18 hours which will subsequently be used to meet peaking requirements over the remaining 6-hour daily period.

After we design the TES system and determine its cost, an iterative evaluation is required to determine the correct optimum peak reduction for a specific plant and load curve.

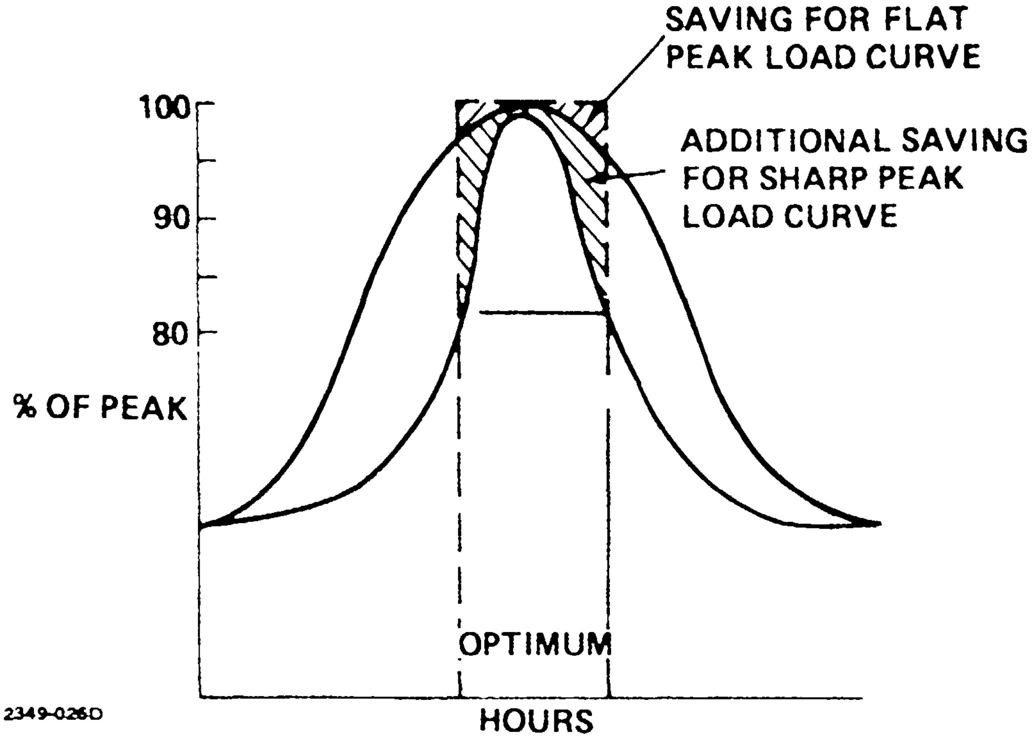

Fig. 4-5 Effect of Load Variation Curve on Peak Load Reduction

SYSTEM*	SEASON	PEAK POWER (MW)	5% SAVING (MW)	TIME POWER < 95%	ENERGY STORED	
					MWH_E	MWH_T
ALGPS	WINTER	3635	181.7	5.51 HOURS	426	1278
NEPP	SUMMER	1504	75.2	4.34 HOURS	166	498
GPU	WINTER	5244	262.2	5.98 HOURS	733	2199
CEHG	SUMMER	597	29.8	7.68 HOURS	156	468
PSCO	SUMMER	2080	104	7.29 HOURS	493	1479

*See Fig. 4-2

2349-027D

Fig. 4-6 Total Energy Storage Requirements for 5% Peaking Capability

4.4 CANDIDATE PHASE CHANGE MATERIALS/CONTAINER MATERIALS

4.4.1 Screening Criteria

As discussed in the previous section, our preliminary economic tradeoff indicated that the total TES system capital cost (including salt, heat exchanger fabrication, installation, etc.) would have to be less than about $1 per pound of salt.

Therefore, we initially set out to identify salts that could be purchased at relatively low cost and were sufficiently compatible with stainless steels to satisfy our 30-year life design goal. It was also important to establish the cost of additional purification beyond commercial grade levels that would be required for this application. This is a very real problem for which a definite answer is unavailable due to a scarcity of corrosion data. In reviewing data we also sought to evaluate other parameters of interest, such as safety, toxicity and environmental impact.

Although selection of salts for use in thermal energy storage systems has been given a great deal of attention by various researches in recent years, most of this work has consisted of analysis or experiments on specific salts so that less data has been developed than is desired, especially when attempting to evaluate a broad range of salts. Only partial data is available, therefore, regarding thermophysical properties, let alone containment, corrosion or purity information. Much of the existing data applies to salts when exposed to air (metal heat treating) which would tend to overstate corrosion problems, or to salts that have not been uniformly purified, so that data of different investigators do not agree. For certain single salts and for a very few specific eutectics, relatively complete data does exist which can be used to predict how similar salts may behave.

For our application, the following initial screening criteria were established for salt selection:

- Melting point between 200-500°C (400-900°F)
- Inexpensive (< $.25 per lb. as a guideline, based on large quantity costs published in the Chemical Marketing Reporter (CMR)).
- Few safety hazards beyond those ordinarily associated with hot liquids.
- Low corrosion rate with low carbon or stainless steel, so that 30-year design life is possible.

A number of salt families are candidates for latent heat thermal energy storage. These are fluorides, chlorides, hydroxides, nitrate/nitrites, carbonates, sulfates, bromides and some oxides. Various researchers have recommended salts from these families for specific thermal storage applications. Individual consideration of each of these types will be given below, together with our reasons for positive or negative recommendation for the electric utility application.

Initially, single salts were screened on the basis of price. Since it was not clear that a sufficient number would be identified on this basis, and as costs will vary depending on the quantity ordered, we began with salts costing up to almost $3/lb. Appendix C lists 175 candidate single salts initially selected from the CMR (Ref 2). From the literature and discussions with Drs. Janz and Borucka, our consultants, eutectics using these salts which melt in our desired range were determined. The cheapest were selected for further evaluation (Figure 4-7), making sure that our entire temperature range was covered. A discussion of salts by types is presented in the following paragraphs.

4.4.2 Fluorides

In general, fluorides possess the "best" thermal properties and therefore have received a great deal of attention. Many researchers have developed TES systems using fluoride salts (Reference 1, 3 and 4). For our application, however, fluorides were rejected, since costs are relatively high although thermal properties are excellent. According to Reference 2, the cost of commonly considered fluorides are:

KF	$ .62/lb
NaF	$ .32/lb
LiF	$ 2.62/lb

These costs are not the last word on the subject since Reference 4 lists possible revised prices based on a large increase in production rates and improved production techniques. Under these circumstances the prices might become:

KF	$ .19-.36/lb
NaF	$ .05-.26/lb
LiF	$1.16-1.51/lb

According to Reference 3, the only fluoride mixtures which melt below 500°C (1000°F) contain large amounts of LiF, BeF_2 or MBF_4 (where M = alkali metal). Of these, BeF_2 is expensive and highly toxic and therefore was rejected. MBF_4 has a significant vapor pressure

Melting °C	Point °F	Salt (A·B·C)	Percent Composition By Weight (A-B-C)
83	181.4	$AlCl_3 \cdot NaCl \cdot KCl$	64-20-16
142	287	$KNO_3 \cdot NaNO_3 \cdot NaNO_2$	53- 7-40
179	364	$KNO_3 \cdot NaNO_3 \cdot NaNO_2$	Unknown
190	374	$AlCl_3$	100
204	399	$Ca\ (NO_3)_2\ NaNO_2$	48.3-51.7
220	428	$NaNO_3 \cdot KNO_3$	45.7-54.3
228	442.4	$KCl \cdot 2NCl_2$	31.8-68.2
474	476	$Na\ NO_3 \cdot NaOH$	84.5-15.5
252	485	$Li\ NO_3$	100
262	503.6	$KCl \cdot Zn\ Cl_2$	18.3-81.7
262	503.6	$NaCl \cdot ZnCl_2$	22.6-77.4
262	503.6	$LiOH \cdot LiCl_2$	63 – 37
282	541.4	$ZnCl_2$	100
287	549	$KNO_3\ BA\ (NO_3)_2$	73.2-26.8
297	567	$NaCl\ NaNO_3$	4.6-95.4
307	585	$NaNO_3$	100
318	604.4	$NaOH$	100
338	608	$KCl \cdot KNO_3$	4.5-95.5
360	680	KOH	100
385	725	$KCl\ NaCl\ Mg\ Cl_2$	14.5-22.3-63.2
397	747	$K_2(CO_3)\ Li_2CO_3Na_2CO_3$	34.5-32.1-33.4
418	784.4	$NaCl\ Ba\ Cl_2\ MgCl_2$	28.4-31.8-34.8
426	799	$LiF \cdot LiOH$	65 – 35
432	809.6	$KCl\ ZnCl_2$	54.3-45.7
435	815	$KCl \cdot Mg\ Cl_2$	61.4-38.6
450	842	$NaCl\ Mg\ Cl_2$	60.1-39.9
454	849	$NaF\ KF\ LiF$	11.7-59.1-29.2
462	864	$LiOH$	100
465	869	$CaCl_2\ KCl \cdot NaCl$	64.5-6.5-29
470	878	$KCl\ Mg\ Cl_2$	36.2-63.8
487	908.6	$KCl\ Ca\ Cl_2Mg\ Cl_2$	25-26.7-48.3
496	925	$Li_2CO_3 \cdot Na_2CO_3$	44 – 56
492	917	$LiF\ KF$	
500	928	$NaCl \cdot CaCl_2$	33 – 67
504	939	$KCl\ NaCl\ CaCl_2$	5-29-66

2349-028D

Fig. 4-7 Preliminary Candidate Salt/Salt Eutectics from BF_3 and can be extremely corrosive even to high nickel content alloys and was rejected. LiF is relatively expensive and poses the problem of availability. Even modest TES systems for utility plants will require approximately 10 million lbs. of salt per plant. Foote Mineral, the largest manufacturer of LiF (and of Li salts in general), informed us that their potential production capacity of LiF was only 4 million lbs. per year; that any program to significantly increase this would require 18 to 24 months lead time before production would commence, and would involve considerable capital investment (Reference 5). For this reason, the use of LiF in the immediate future in large systems was considered impractical. Fluorides were therefore eliminated from further consideration since eutectics having acceptable melting points were not available in large quantities at reasonable prices. Other objections to fluorides include the fact that they give off toxic fumes when heated, especially LiF and MgF_2 (Reference 6). However, this objection may not be a problem in a well designed system. KF (Reference 1) is hygroscopic. In second generation systems using a TES unit which stores heat directly from the boiler at high temperatures, fluorides should be considered. Reference 1 contains results of complete experimental investigations of all important containment and safety questions related to a fluoride eutectics.

4.4.3 Chlorides

Chlorides do not exhibit thermal properties as desirable as fluorides, nor is there as much data available. However, several chloride eutectics exist which melt in our desired temperature range and meet our target cost criteria, so that chlorides are among our recommended salts. Initially, we considered eutectics made of the following single chloride salts:

	Cost of Industrial Grades (Reference 2)
NaCl	\$ .02/lb
KCl	\$ .02/lb
$MgCl_2$	\$ .127/lb
$ZnCl_2$	\$1.39/lb
$BaCl_2$	\$ .153/lb
$CaCl_2$	\$ .03/lb

$ZnCl_2$ was subsequently eliminated not only because of its relatively high cost, but since it has a tendency to supercool (form a glass, Reference (6)), is very corrosive (at least in the presence of moisture) and gives off toxic fumes when heated strongly. The decision to eliminate $ZnCl_2$ was reluctant, since it has a low melting point (541°F) and would have permitted the use of chloride salts down to 442°F in a eutectic mix. Some eutectics of $AlCl_3$ exist which melt at low temperatures, but these were ruled out since $AlCl_3$ reacts vigorously with water yielding HCl. Fumes of HCl are produced when $AlCl_3$ comes into contact with moist air and $AlCl_3$ is corrosive to skin (Reference 7). Furthermore, under atmospheric pressure, $AlCl_3$ does not melt but sublimes. It is felt that this would result in excessive safety and handling problems. The five (5) remaining chloride salts form eutectics which melt above 725°F so that chlorides are recommended for the high end of energy storage only (800-1000°F).

Thermal property data on chloride salts are scarce, and that for eutectics is almost non-existant. Reference 8 lists properties (ρ, ΔH_{fs}, c_p, k) for these salts with some exceptions; e.g., no values are presented for liquid thermal conductivity for any of the listed salts and values of solid thermal conductivity are included only for NaCl and KCl. It is worth noting that authorities argue that much of the data that does exist is unreliable or even contradictory (References 3 and 8). It is important that the properties of the eutectic salts under discussion here cannot, in general, be estimated from values of the constituent salts. Experimental determination of properties is a prerequisite to any hardware program.

Authorities agreed that even if present in minute amounts, water would cause excessive corrosion with chloride salts. Littlewood (References 9 and 10) Koger (Reference 11), Susskind (Reference 12) and DeVan (Reference 13) support the hypothesis that molten chlorides can be contained in mild steel if they are dry and pure. Susskind tested a eutectic of $NaCl \cdot KCl \cdot MgCl_2$ in 1020 mild steel for 1000 hours at 500°C and noted no intergranular or mass transfer corrosion. The penetration depth was .7 mils/yr. It must be pointed out that extreme care was taken with material preparation. All apparatus in which salts were prepared were thoroughly cleaned and leak tested using a He mass spectrometer detector. Inert atmospheres of helium or argon were used and these were purified by passage ofer titanium chips at 850°C. The eutectic was prepared by vacuum-melting and outgassing at 500°C to a pressure of less than 20 μ. Reagent grade salts and anhydrous $MgCl_2$ were used. Reference 14 reports successful containment of chlorides after removal of water with a gettering metal (aluminum or magnesium). Obviously, if such strict purification standards must be met for the quantities of salt involved in a utility installation, it will materially increase the PCM cost. This will be discussed in a later section on salt corrosion/purification.

$MgCl_2$ and $CaCl_2$, when heated give off toxic fumes which could be a problem if a TES unit ruptures. Also, chlorides have a very large volume change on fusion. For example, for NaCl the volume change from solid to liquid is 25%, so that significant salt movement will occur during cycling. $CaCl_2$ is a dessicant, so that an exothermic reaction will occur if it contacts water. Chlorides should be operated under a dry N_2 atmosphere. $Mg(OH)_2$ contamination of $MgCl_2$ results in the formation of oxichloride cement (MgOCl), which could be a problem.

4.4.4 Hydroxides

The hydroxides considered were:

LiOH	$1.97/lb, Reference 15
NaOH	$ .13/lb, Reference 15
KOH	$ .075/lb, Reference 2

Of these, LiOH was eliminated because of cost and availability, although it had the best thermal and corrosive properties.

Data on the properties of hydroxides are more available than for chlorides. Reference 8 gives a complete set of data for NaOH except for solid phase thermal conductivity. It should be noted that NaOH in addition to a solid-liquid transformation at 610°F, which has a $\Delta H_{fs} = 38$ cal/gm, also exhibits a solid-solid phase transformation at 565°F, with an additional $\Delta H = 38$ cal/gm.

A non-eutectic mix of NaOH (91%), $NaNO_3$ (8%) and 1% unspecified corrosion control additives is marketed under the name "Thermkeep"$^{(R)}$ by Comstock and Wescott, Inc. (Reference 16), at a cost of about $.20 per lb.

Two contaminants which pose a corrosion problem in NaOH are H_20 and $C0_2$, which can be absorbed from the atmosphere. Use of a blanket atmosphere is essential and References 3 and 17 agree it should be H_2. Reference 3 notes that this introduces possible long-term problems with hydrogen embrittlement of the alloys and weldments of the containment unit. The danger of explosion inherent in a pressurized H_2 atmosphere (Reference 17) suggests that satisfactory results might be obtained using a mixture of 10% H_2 and 90% N_2 which would reduce the risk. Reference 15 questions the seriousness of $C0_2$ contamination and points out some contradictions in existing data regarding water contamination. Most authorities (Reference 8 and 15) suggest using stainless steel, however, Comstock and Wescott use mild steel in their "Thermkeep" system apparently made possible by their use of a corrosion inhibitor. Corrosion problems may be expected to be worse for KOH than NaOH (Reference 15).

Hydroxides are extremely hygroscopic and any contact with water would cause a highly exothermic reaction, possibly explosive in nature. In addition, hydroxides are caustic and could be a danger to personnel in the vicinity of a ruptured container. According to Reference 6, NaOH may give off toxic fumes when strongly heated.

4.4.5 Nitrates/Nitrites

While the thermal properties of nitrates/nitrite eutectics are not as good as those of chlorides and hydroxides, the low costs, good corrosion properties and low melting points make them good candidates for our TES application. The specific salts considered are:

KNO	\$ .095/lb, Reference 2
$NaNO_3$	\$ .076/lb, Reference 2
$NaNO_2$	\$ .3095/lb, Croton Chemical

Eutectic mixtures of these three salts have been available under various trade names as heat transfer fluids since the late 1930's (U-TEC-TIC, HITEC, HTS, Partherm). Reference 18 describes a 290°F melting point eutectic called "HTS", which is identical to HITEC, Partherm 290, and U-TEC-TIC, References 19 and 20. Fairly complete data is available for these salts because of their long use.

The properties of several eutectics of these salts are available, particularly of the 290°F melting point eutectic. No problems are envisioned in obtaining data for these salts.

Nitrates/nitrites are superior to most salts in that they form a passivating layer on steels by the formation of surface oxide layers. Moreover, the presence of small amounts of water does not appear to increase the corrosion rate significantly (Reference 3). Kirst, et al, give a corrosion rate on mild steel of .0003 in/month at 850°F (Reference 18). Most corrosion problems will result from solid impurities in the melt, particularly with Na_2SO_4 and Al oxides. A blanketing atmosphere of N_2 is recommended by several sources (Reference 3, 17 and 18).

Nitrites do not pose some of the hazards associated with other salts; they evolve no toxic gases nor are they caustic. They should, however, be kept out of contact with cyanide, aluminum, and organic matter (fire hazard). At temperatures above 454°C, nitrites continuously degrade by $5\ NaNO_2 \longrightarrow 3NaNO_3 + Na_2O + N_2$. This represents the upper limit to which the salts are useful and care should be taken to prevent nitrite containing TES units from overheating. Baker Chemical lists the decomposition point of $NaNO_3$ as 380°C. Compared to chlorides, nitrates present much less of a problem from volume change on fusion, the increase for $NaNO_3$ being 10.7%, that for KNO_3 only 3.3% and that for $NaNO_2$ less than 20% (Reference 8).

4.4.6 Carbonates

Reference 15 recommends carbonates over chlorides and hydroxides as heat storage salts. However, all of the recommended eutectics which melt below 1000°F contain Li_2CO_3. Hence, the same cost problem ($ .76/lb) and availability problems which apply to LiF also apply to Li_2CO_3, although to a slightly lesser degree. In any case, significant production capacity would have to be built before large scale use of carbonates can be considered. This is unfortunate since carbonates have very good thermal properties. Moreover, the presence of the Li_2CO_3 appears to have a passivating effect on steel surfaces. Research carried out at IGT (Reference 15) has shown that the 300 series Stainless Steels are compatable with alkali carbonates for periods over five years. Reference 3 lists a eutectic mix of 57% K_2CO_3 and 43% $MgCO_3$ which melts at 860°F and as such would be suitable for our system. It was eliminated from our list of recommended eutectics since it is more expensive (K_2CO_3, $.0975 lb, $MgCO_3$, $.30/lb.) than the selected chloride eutectic which melts at 864°F and which has a higher heat of fusion. This carbonate eutectic would probably be more aggressively corrosive than eutectics containing Li_2CO_3 since work by Janz has shown that it is the formation of a $LiFeO_2$ passivating layer which is responsible for slowing the corrosion of these systems.

4.4.7 Sulfates

Sulfates were rejected because of their extremely corrosive nature. When heated, sulfates tend to form sulfides which result in rapid steel corrosion (Reference 3). An oxygen atmosphere has been suggested to retard sulfide formation, but the presence of 0_2 results in a different set of corrosion problems as the steel is prone to oxidize.

4.4.8 Oxides

Reference 3 discusses the possible use of B_2O_3 as a PCM, but rejects its use since it is corrosive and difficult to purify. Reference 15 disagrees on the corrosion point in the case of stainless steel but the tests were only conducted for a few hours. The thermal properties of B_2O_3 are similar to those for hydroxides and it melts at 450°C. Since there is no lack of chloride salt mixtures with better thermal properties, B_2O_3 is not recommended.

4.4.9 Thermal Mass Transfer Corrosion

In addition to the corrosion problems mentioned above we should mention that of thermal mass transfer corrosion. According to Reference 8, when a temperature gradient exists in a flowing salt system, thermal potentials exist which remove metal at hot points and deposit metal at cooler points. These reactions are electrolytic and are called Faradaic mass transfer. Susskind (Reference 12) conducted mass transfer tests on a chloride eutectic. Plugging occurred in a 1/2 inch stainless steel tube loop after 4000 hours of operation. This indicates that mass transfer corrosion may be a concern with a flowing salt system. Although this phenomenon could conceiveably occur in static salt systems with large temperature gradients, it is not expected to be a problem in our case since temperature gradients are small and heat exchangers are configured so that salt is heated from the top and cooled from the bottom which minimizes convection currents.

4.4.10 Salt Thermophysical Data

Along with the chemical composition of each selected salt compound, Figure 4-8 also lists the thermophysical data required in order to design the PCM heat exchanger; i.e., the latent heat of fusion (ΔH_{fs}), specific heat (c_p), solid and liquid thermal conductivity (k_s and k_l), and solid and liquid density (ρ_S and ρ_L). Unfortunately, thermophysical salt data are difficult to compile. Different experimenters report different properties and available analytical procedures are questionable for predicting what cannot be measured. In the following paragraphs, therefore, a brief discussion of the sources of data for each of the thermophysical properties is presented, along with qualitative evaluation of the accuracy of tabulated data. Footnotes in Figure 4-8 identify how each piece of data was obtained. The salts listed are the cheapest available in their temperature range on a \$/ ΔH_{fs} basis.

Densities (ρ_S ρ_L) - For most of the single salts considered, experimental values for the densities of the solid and liquid phases are available. This is not the case with most of the eutectics considered. We have, therefore, estimated the eutectic densities by ratioing densities of the constituent salts by the weight percentages of each salt present in the eutectic. Various sources (e.g. References 8 and 15) doubt the accuracy of this method but offer no preferrable method. Both References present eutectic densities, but disclaim their accuracy.

Heats of Fusion (ΔH_{fs}) - The state of data for heats of fusion is similar to that for density, and we have treated them the same way. Estimated values given by References 8 and 15 are similar, but both Borucka and IGT feel these numbers are not accurate.

Salt Element A – B – C	Melt Point[a] °C (°F)		Composition[a] Weight %			Heat of Fusion, ΔH_f Cal/gm (BTU/lb)	Specific Heat Cal/gm °C		Thermal Conductivity 10^3 x cal/sec °C cm (BTU/hr ft °F)		Density gm/cc (lb/ft^3)	
			A	B	C		Solid ($c_{p,s}$)	Liquid ($c_{p,l}$)	Solid (K_s)	Liquid (K_l)	Solid (ρs)	Liquid (ρl)
$KNO_3 \cdot NaNO_3 \cdot NaKO_2$	142	(287)	53	7	40	19.5[m] (35)	.29[n]	.32[m]	1.38[c] (.33)	1.38[m] (.33)	1.97[c] (123)	1.97[m] (123)
$KNO_3 \cdot NaNO_3 \cdot NaNO_2$	179	(354)	Partherm		350[b]	19.5 (35)[d]	.29[d, n]	.32[d]	1.38[c, d] (.33)	1.38[d] (.33)	1.97[c, d] (123)	1.97[d] (123)
$Ca(NO_3)_2 \cdot NaNO_2$	204	(399)	48.3	51.7	--	31.2[c] (56)	.33[n]	.38[e]	1.70[c, e] (.411)	1.70[e] (.411)	2.34[c] (146)	2.34[f] (146)
$NaNO_3 \cdot KNO_3$	220	(428)	45.7	54.3	--	32.8 (58.8)[f]	.38[f]	.36[f]	1.17[f] (.28)	1.368[f] (.33)	2.18[g] (136)	1.88[g] (117)
$NaNO_3 \cdot NaOH$	248	(475)	84.8	15.5	--	42.8[f] (76.5)	45[f]	.45[f]	1.56[c, f] (.377)	1.56[f] (.377)	2.24[f] (140)	1.933[f] (120.7)
$NaCl \cdot NaNO_3$	297	(567)	4.6	95.4	--	46.8[f] (84)	44[f]	.43[f]	1.48[f] (.36)	1.48[f, h] (.36)	2.26[f] (141)	1.88[f] (117)
$NaNO_3$	307	(585)	100	--	--	43.5[m] (78.1)	45[m]	.44[m]	1.35[m] (.33)	1.45[m] (.35)	2.26[m] (141)	1.90[m] (119)
$NaOH$	318	(605)	100	--	--	76[g] (138)[q]	48[m]	.50[m]	2.2[m, c]	2.2[m]	2.73 (170)	1.74 (109)
$KCl \cdot KNO_3$	320	(608)	4.5	95.5	--	28.21[f] (47)	28[f]	.29[f]	1.15[f] (.278)	1.15[f, h] (.278)	2.11[f] (132)	1.86[f] (116)
KOH	360	(680)	100	--	--	32.1[m] (57.8)	32[g]	.38[m]	2.20[c, d] (.53)	2.20[d] (.53)	2.04[m] (127)	1.73[m] (108)
$KCl \cdot NaCl \cdot MgCl_2$	385	(725)	14.5[g]	22.3[g]	63.2[g]	110[g] (197)	23[f]	.248[f]	3.6-3.8[j] (.87-.92)	1.9-2.4[j] (.47-.58)	2.25[g] (140)	1.63[g] (102)
$NaCl \cdot BaCl \cdot MgCl_2$	418	(784)	28.4[g]	31.8[g]	39.8[g]	81.6[g] (146)	19[f]	.21[f]	3.6-3.8[j] (.87-.92)	1.9-2.4[j] (.47-.58)	2.76[g] (172)	2.12[g] (132)
$NaCl \cdot MgCl_2$	450	(842)	60	40	--	111[g] (199)	.22[k]	.24[k]	3.6-3.8[j] (.87-.92)	2.27[k] (.55)	2.23[k] (139.1)	1.61[g] (100)
$CaCl_2 \cdot KCl \cdot NaCl$	485	(905)	64.5	6.5	29	77.8[f] (139)	21[f]	.23[f]	3.6-3.8[j] (.87-.92)	1.9-2.4[j] (.47-.58)	2.15[f] (134)	1.86[f] (116)
$NaCl \cdot CaCl_2$	500	(928)	33	67	--	67[k, l] (121)	20[k]	.24[k]	3.6-3.8[j] (.87-.92)	2.44[k] (.59)	2.16[k] (134)	1.89[g] (118)
$KCl \cdot NaCl \cdot CaCl_2$	504	(939)	5[g]	29[g]	66[g]	67[k, l] (120)	.28[k]	.24[k]	3.6-3.8[j] (.87-.92)	2.39[k] (.58)	2.16[k] (134)	1.90[g] (119)

Footnotes – Table 1.

(a) Values for melting point and composition are experimental data provided by Drs. Janz and Borucka.

(b) Partherm salts are proprietary products of the Park Chemical Co and the composition is unavailable.

(c) Due to a lack of information, value listed for solid is that of liquid phase of same salt.

(d) Value given is that of a different eutectic having the same or similar constituents (similar anions).

(e) Value given is for one of the eutectics constituent salts as values for the other(s) have not been found.

(f) Value determined by ratioing values for constituent salts by weight.

(g) Source (Ref. 8) states: "Not Accurate. Calculation based on assumed ideality, not true in most cases."

(h) Due to a lack of information, value given for liquid is the same as for solid phase.

(i) Values given are for KCl and NaCl.

(j) Values given bracket range for Cl salts listed in Ref. 15 which are referred to as estimates.

(k) Values given in Ref. 15 are referred to as estimates.

(l) ΔH_f data sources disagree for this salt. Ref. 13 lists value as 77.8 cal/gm, but since Ref. 15 lists 67 cal/gm this figure was (conservatively) used.

(m) Experimental data.

(n) Value of $c_p(s)$ determined from $c_{pl}/c_{ps} = 1.10$, as per Ref. 13.

(o) Solid densities at 25°C.

(p) Liquid densities at melt point.

(q) Includes solid-solid transformation at 565°F (296°C).

Fig. 4-8 Thermophysical Property Data of Selected Salts

ORIGINAL PAGE IS OF POOR QUALITY

Specific Heats - Slightly less data appears to be available for specific heats, and often data is available only for one phase (solid or liquid). Borucka suggests using a factor of $c_{pl}/c_{ps} = 1.10$ to estimate the specific heat of a phase when a value for the other phase is available. We present numbers from Reference 8 and 15 when available, and ratio by weight (%) the values for single salts when they are not.

Thermal Conductivities - The least data are available for thermal conductivities. Bramlette et al, Reference 3, state that data for chlorides are so sparse and inaccurate that they can not even present it. Analytical procedures exist for the thermal conductivity of the liquid phase, but they are considered to be inaccurate. Complicating this is the fact that, according to Borucka, accurate measurements of thermal conductivity is difficult so that such experimental values as do exist must be substantiated to establish accuracy.

We have listed data and estimates presented in Reference 8, 15 and 3. Other values have been set by also using values of the liquid phase for that of the solid phase or by assigning approximate values found for some salts for all salts in that family (chlorides).

As gathered from the above discussion, much of the data presented in Figure 4-8 is unavoidably suspect. The question is whether this uncertainty is significant to our overall goal of determining the basic feasibility of a latent heat thermal energy storage system. We will answer this in a later section with a sensitivity study of a specific heat exchanger configuration. By taking reasonable variations on critical salt properties, we can determine the overall impact on the total system cost and hence feasibility.

4.4.11 Salt Purity

The required degree of salt purification can only be estimated. First, it was necessary to determine purity levels of commercially available salts. Suppliers of salt in large quantities were contacted including Foote Mineral, Croton Chemical Company, Morton Salt Company, Hooker Chemicals and Plastics Corporation, Dow Chemical, and IMC Chemical Group. The data received for $CaCl_2$, $MgCl_2$, NaCl, KOH, NaOH, $NaNO_2$, KNO_2 and $Ca(NO_3)_2$ is presented in Appendix D.

The purity of the salts range from 90 to 99.5% (not including water of crystallization) with a variety of impurities. In the case of $MgCl_2 \cdot 6H_2O$ and $CaCl_2 \cdot 2H_2O$, roughly 50% and 20% H_2O, respectively, are contained in the crystal lattice. To determine which of the various impurities might pose problems and have to be removed, these data were sent to Drs. Borucka and Janz for their comments. Although both consultants expressed reservations about estimating the added purification required without supporting test data, we felt that including this cost was important to a fair economic evaluation of the TES concept. Therefore, we asked that they give us their opinions on this subject. Dr. Borucka contacted the five suppliers and found that none appeared interested in further purifying the salts prior to delivery. For purification she was referred to J. T. Baker Chemical or Mallinckrodt, who produce small quantities of reagent grade materials. This may indicate that extra purification will have to be undertaken by the TES user. Both Drs. Janz and Borucka agreed that water and oxygen are critical contaminants and that water must be removed from salts to the maximum degree possible. Both further felt that traces of Na_2SO_4 could be troublesome, especially if it were to separate from the bulk mass and collect in one location. Dr. Borucka further commented that removal of Al oxides, K_2SO_4, $KClO_3$, Hg metal and $Mg(OH)_2$ traces might be required. Her comments are summarized in Figure 4-9.

Both investigators stressed the need for further research on the effect of these trace impurities on corrosion. Janz and Borucka described similar techniques for removal of traces of water and oxygen. Both agree that such purification should be undertaken after the salt has been placed in the TES heat exchanger, so that atmospheric contact will not occur after purification. It is noteworthy that the cost of fuel oil to heat the salt for this purpose would be only 1/2 ¢/lb at 40¢ per gallon of oil. Other costs are difficult to estimate. The need for a vacuum freeze/thaw purification cycle can increase thickness of the TES heat exchanger walls, thus increasing system costs. Alternately a larger vacuum shell could be constructed to hold the heat exchanger so that only one very heavy walled unit would be required which could purify many units. The capital cost per unit will be lower as more units are processed so that if TES use becomes wide spread the cost could become quite low. The cost of a pressure vessel to contain a TES heat exchanger would be about $300,000, or only about $.02/lb of salt for a TES system for a single 1000 megawatt utility plant. The procedure to remove solid impurities ($NaSO_4$ primarily) was described by Dr. Borucka as best conducted in aqueous solutions of the parent salt by selected chemical reactions. This would indicate that solid purification might best be undertaken by the salt manufacturer.

Bulk prices for our recommended salts are given in Figure 4-10. Column 1 gives the bulk cost for "as received" salt quoted in Reference 2. Column 2 gives prices per pound quoted by suppliers in truckload quantities (> 20,000 lbs, the largest lot quoted and therefore the lowest price). As previously mentioned, Reference 18 suggests that a significant increase in demand of fluoride salt could result in a cost reduction. The same may be true for our recommended salts, so that the advent of widespread TES usage could result in lower prices than those quoted. In the other direction, prices will increase due to added purification costs. In two extreme cases ($MgCl_2$ and $CaCl_2$), crystalline water accounts for

Salt	Supplier	Objectionable Impurities To Be Removed		Required Protective Gas Atmosphere
$NaNO_2$	Croton		All Traces of Water and Oxygen	N_2
$NaNO_3$		Na_2SO_4		
KNO_3		Al oxides		
KCl				
$Ca(NO_3)_2$				
$NaOH$	Hooker	Na_2SO_4		H_2
$NaCl$	Morton			N_2
KOH	IMC	K_2SO_4, $KClO_3$, Hg		H_2
$MgCl_2$ (a,b)	Dow	$Mg(OH)_2$		N_2
$CaCl_2$ (b)		?		
$BaCl_2$ (c)	?	?		

(a) $MgCl_2$ "flake" is in fact: $MgCl_2 \bullet 6H_2O$, i.e. about + 50% water content.

(b) Purity Specifications not detailed sufficiently.

(c) Supplier and purity not identified so far.

2349-0300

Fig. 4-9 Suggested Salt Purification Requirements roughly 50% and 20% of the salt weight respectively so that in order to get 1 lb of anhydrous $MgCl_2$, 2 lbm of $MgCl_2$ crystals must be purchased; this effectively doubles the cost of this salt even without including water removal cost. This adjusted purchase price as shown in Column 4 includes an allowance of \$.05/lb on all salts for the energy required for water removal, amortization of a vacuum vessel and pumping station for vacuum bakeout, and provisions for extra supplier charge for solid impurity removal. It will be shown later than even if this estimate is somewhat optimistic it will not significantly affect our cost/benefit analyses.

SALTS	BULK PRICES CHEMICAL MARKETING REPORTER (7 - 19 - 76)	BULK PRICES MANUFACTURER'S TRUCKLOAD > 20,000 LB	QUANTITY COST CORRECTED FOR WATER CONTENT	TOTAL COST[1] INCL \$.05/LB FOR WATER, O_2, AND SOLID IMPURITIES REMOVED
$MgCl_2 \cdot 6H_2O$	.1275	.0850	.2550/.170	.305
$CaCl_2 \cdot H_2O$	.0275	.0440	.035 /.055	.105
NaCl	.02	.0177	–	.07
KCl	.02	.0755	–	.13
$NaNO_2$	–	.3095	–	.3595
$NaNO_3$	.065	.1095	–	.1595
KNO_3	.095	.1825	–	.2350
NaOH	.25	.143	–	.193
KOH	.075	.22	–	.27
$BaCl_2$	.155	–	–	.205
$Ca(NO_3)_2$	–	.1175	–	.1675
U-TEC-TIC*		.30	–	.35

*U-TEC-TIC = HITEC/HTS/PARTHERM

(1) Based on highest bulk price indicated in column (2) or (3)

Fig. 4-10 Cost Estimates – Salts Recommended for TES Systems

2349-0310

4.5 CANDIDATE HEAT EXCHANGER CONCEPTS

As previously stated, a goal of the study was to consider a reasonable number of heat exchanger designs so that a selection of promising TES configurations could be made. The intention was not to optimize a single design, but rather to demonstrate design feasibility and determine overall cost effectiveness of latent heat thermal storage. In keeping with this philosophy we considered the following heat exchanger designs:

- Tube/Shell
- Heat pipe
- Macroencapsulated PCM
- Intermediate pumped metal loop
- Fluidized microencapsulated PCM,
- Moving PCM.

Although preliminary calculations were performed on each concept, more work was done on the tube/shell which we selected as our baseline design.

4.5.1 Tube/Shell

Tube/shell heat exchangers for feedwater heating are currently in widespread use in the utility industry. They are generally constructed with U-tubes and a single tube sheet as shown in Figure 4-11A but can also be double tube sheet construction as shown in Figure 4-11 B & C. A large plant can employ six or more feedwater heaters in series to raise the temperature of water leaving the condenser from 100–110° F to approximately 500–550°F prior to entering the boiler. Feedwater in the tubes is heated by steam on the shell side which is extracted from various points in the turbine(s). These heaters are usually installed horizontally and can be up to 50 ft. long. They are typically 8–10 ft. in diameter. Our proposed TES tube/shell heat exchanger is a variation on this design. In order to prevent rupture of the unit which could occur if melting salt is not free to expand, our tube/shell design must provide a free liquid surface with the melt line proceeding down from the top of the unit. The most direct way to accomplish this is to use a double tube sheet, single pass unit mounted vertically as conceptually shown in Figure 4-12. A single tube sheet, single pass unit mounted vertically with the tube sheet at the top might also work, but was considered a greater risk for initial designs because of the possibility of blocked liquid relief paths due to settling of the solid. During energy storage, steam from the boiler enters the top of the unit and flows downward through the tubes so

ORIGINAL PAGE IS
OF POOR QUALITY

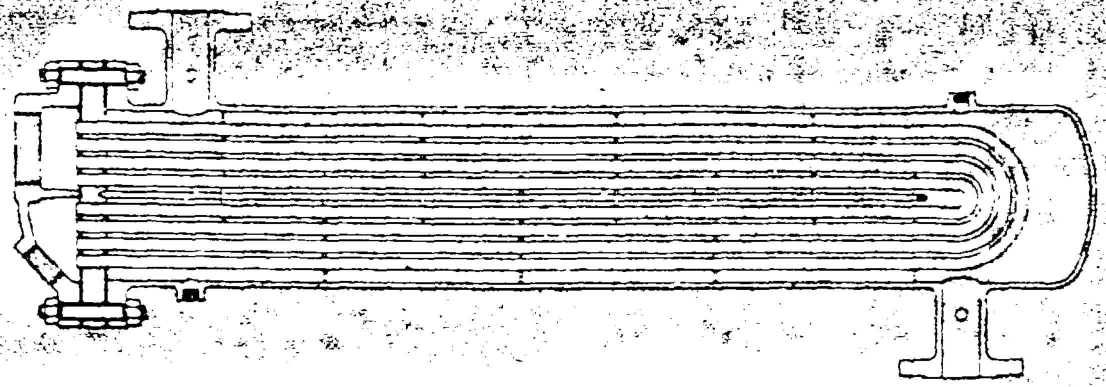

A) U-TUBE, BAFFLED SINGLE-PASS SHELL, SHELL-AND-TUBE HEAT EXCHANGER, (COURTESY PATTERSON-KELLEY CO.)

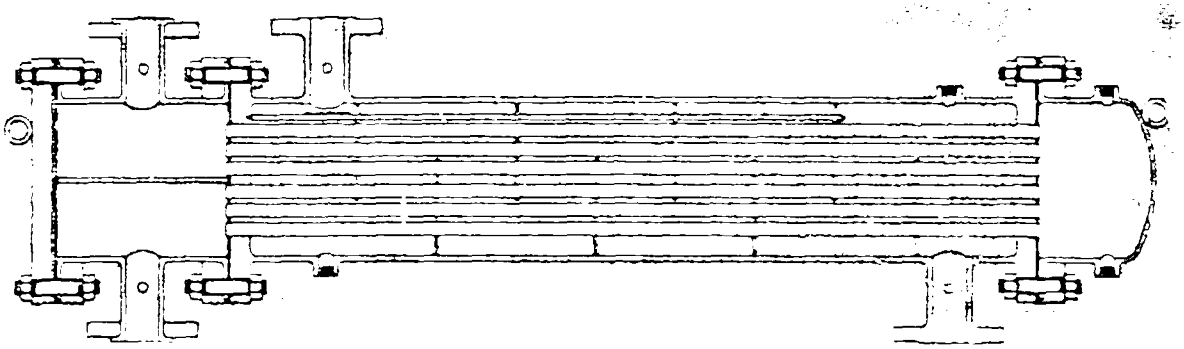

B) TWO-PASS TUBE, BAFFLED SINGLE-PASS SHELL, SHELL-AND-TUBE HEAT EXCHANGER DESIGNED FOR MECHANICAL CLEANING OF THE INSIDE OF THE TUBES. (COURTESY PATTERSON-KELLEY CO.)

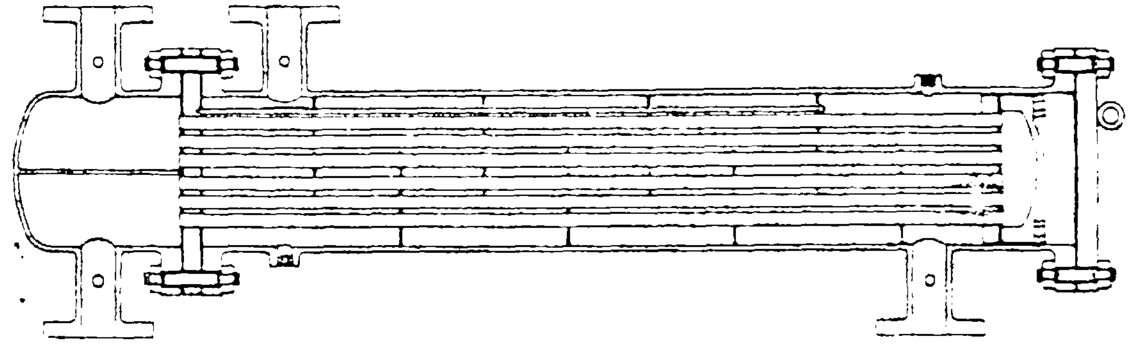

C) HEAT EXCHANGER SIMILAR TO B EXCEPT WITH A FLOATING HEAD TO ACCOMMODATE DIFFERENTIAL THERMAL EXPANSION BETWEEN TUBES AND SHELL. (COURTESY PATTERSON-KELLEY CO.)

2349-032D

Fig. 4-11 Tube & Shell Heat Exchanger Designs

ORIGINAL PAGE IS
OF POOR QUALITY

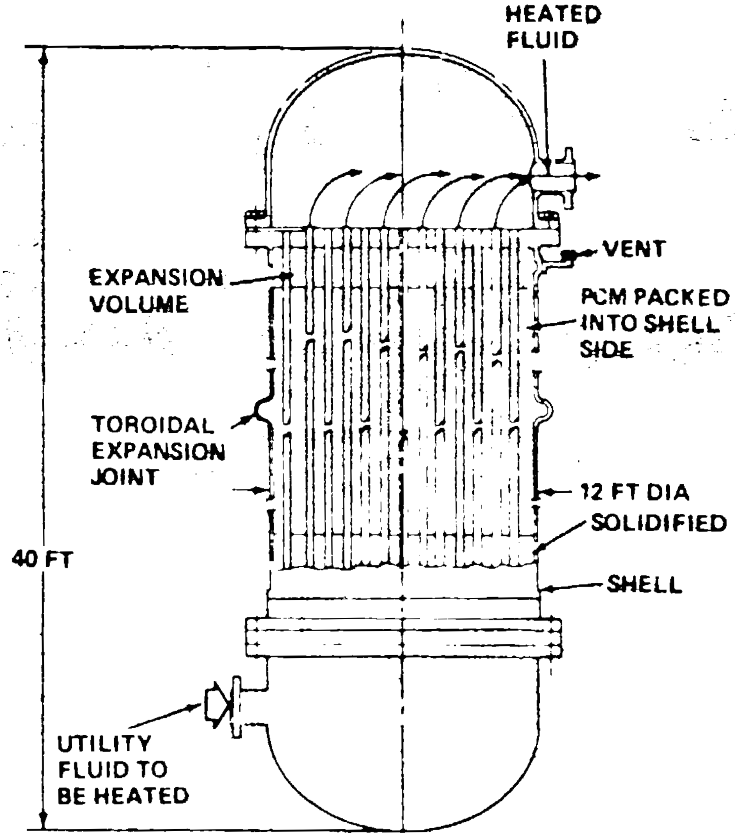

2349-033D

Fig. 4-12 TES Shell and Tube Heat Exchanger Concept that salt melting progresses from top to bottom of the unit. The shell contains the salt phase change material. During energy usage, feedwater enters the bottom of the unit and salt is solidified from the bottom up.

To minimize the number of heat exchanger modules, each unit should be as large as practical. Reasonable limits for railroad car shipping without special provisions are 40 ft. long by 15 ft. diameter. This size unit will weight (including salt) approximately 400,000 lbs. which is also acceptable for on-site hoisting by crane. Within overall size constraints the design problem is to determine tube size and spacing that meets performance requirements at minimum cost.

Although the bulk of our analytical efforts for other designs relied on closed-form solutions and hand calculations, a computer analysis was performed for the tube/shell design. This analysis verified the adequacy of the hand calculation methods and permitted more rigorous evaluation of our baseline design. The analysis was performed to size the TES heat exchangers required for feedwater heating at the Ft. Martin plant. Figures 4-13 and 4-14 present the preliminary state point conditions and net plant heat rates during energy storage and usage (peaking) modes.

A thermal network and computer program was set up to model the performance of our baseline tube/shell TES heat exchanger. The program represents one tube of a 30 foot long heat exchanger, and was initially set up with six salt and five extraction locations (see Figure 4-15).

The model includes a sub-routine to control extraction of steam from the unit on the storage side and water on the usage side as a function of exit temperature from each of the sections. During energy storage, the logic was written to permit fluid flow from one section into the next as long as the temperature was greater than or equal to a control temperature (Tc_2). Once temperature dropped below this control point, the program would divert the flow out of the unit so that further fluid cooling could not occur. During energy storage the steam enters at 1,000°F and should exit at 705°F (see Figure 4-13). Therefore, for the initial run (Case 1) we set the control temperature during storage at 705°F, which is the desired outlet temperature. Similarly, during energy usage the program permitted the fluid to flow through the salt sections until its temperature equals or exceeds another control point (Tc_1). Here (Case 1) we set this limit to the desired outlet temperature of 514°F for our initial runs.

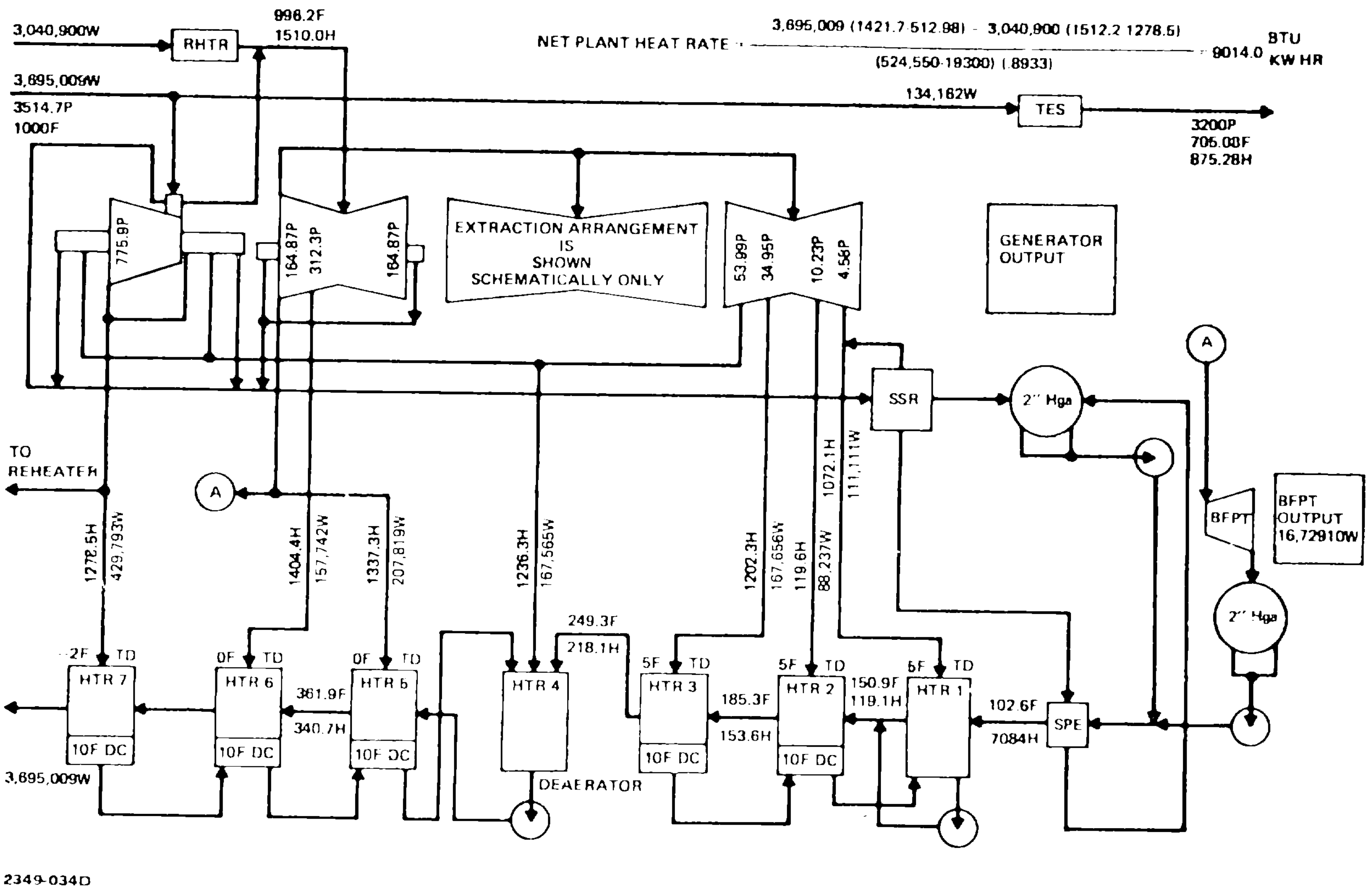

Figure 4-13. Ft. Martin Heat Balance, Feedwater Heating Storage Mode

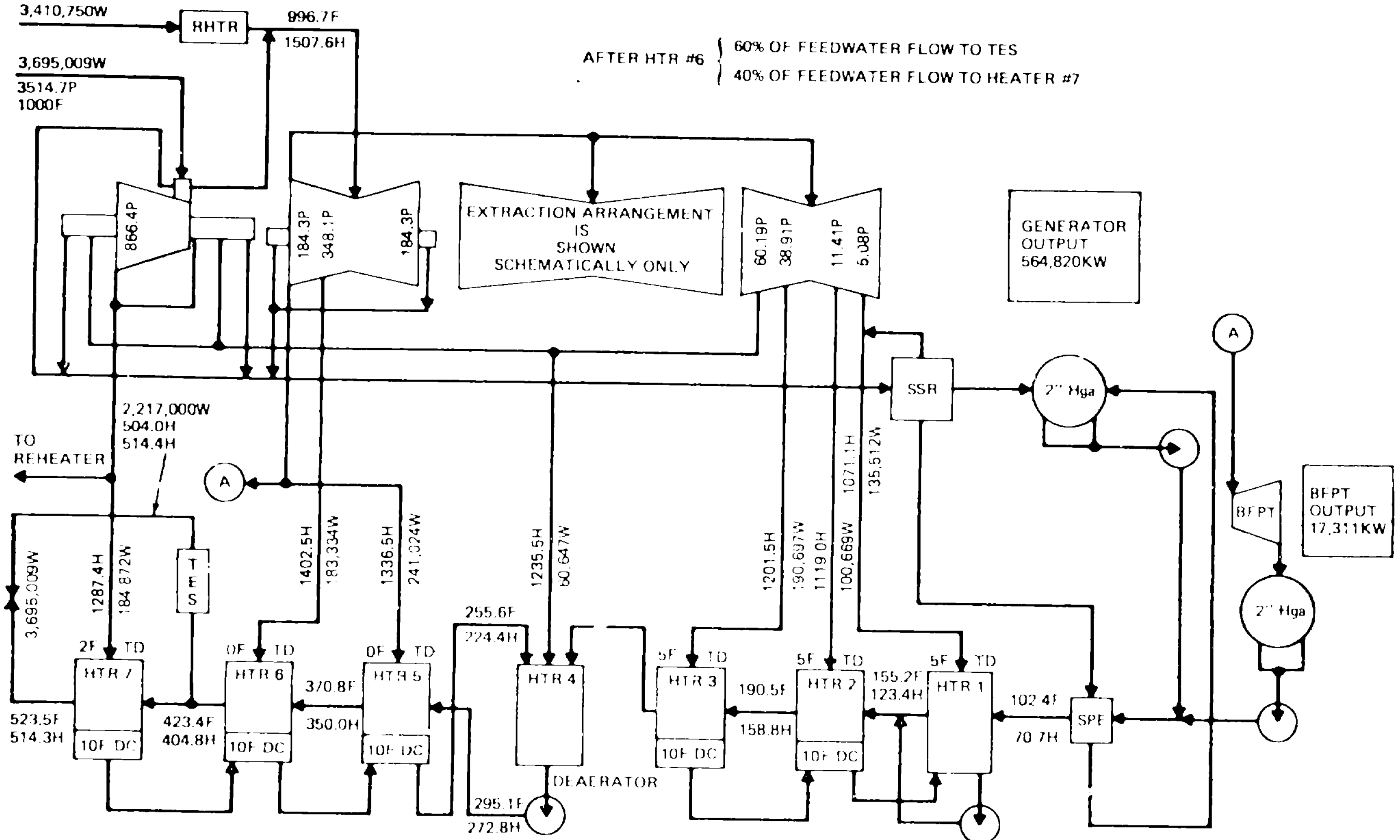

$$\text{NET PLANT HEAT RATE} = \frac{3{,}695{,}009\,(1421.7-508.13) + 3{,}410{,}750\,(1509.5-1287.4)}{(564{,}820-19{,}900)\,(.8925)} = 8498.4\ \frac{\text{BTU}}{\text{KW HR}}$$

2349-035D

Fig. 4-14 Ft. Martin Heat Balance, Feedwater Heating Usage (Peak) Mode

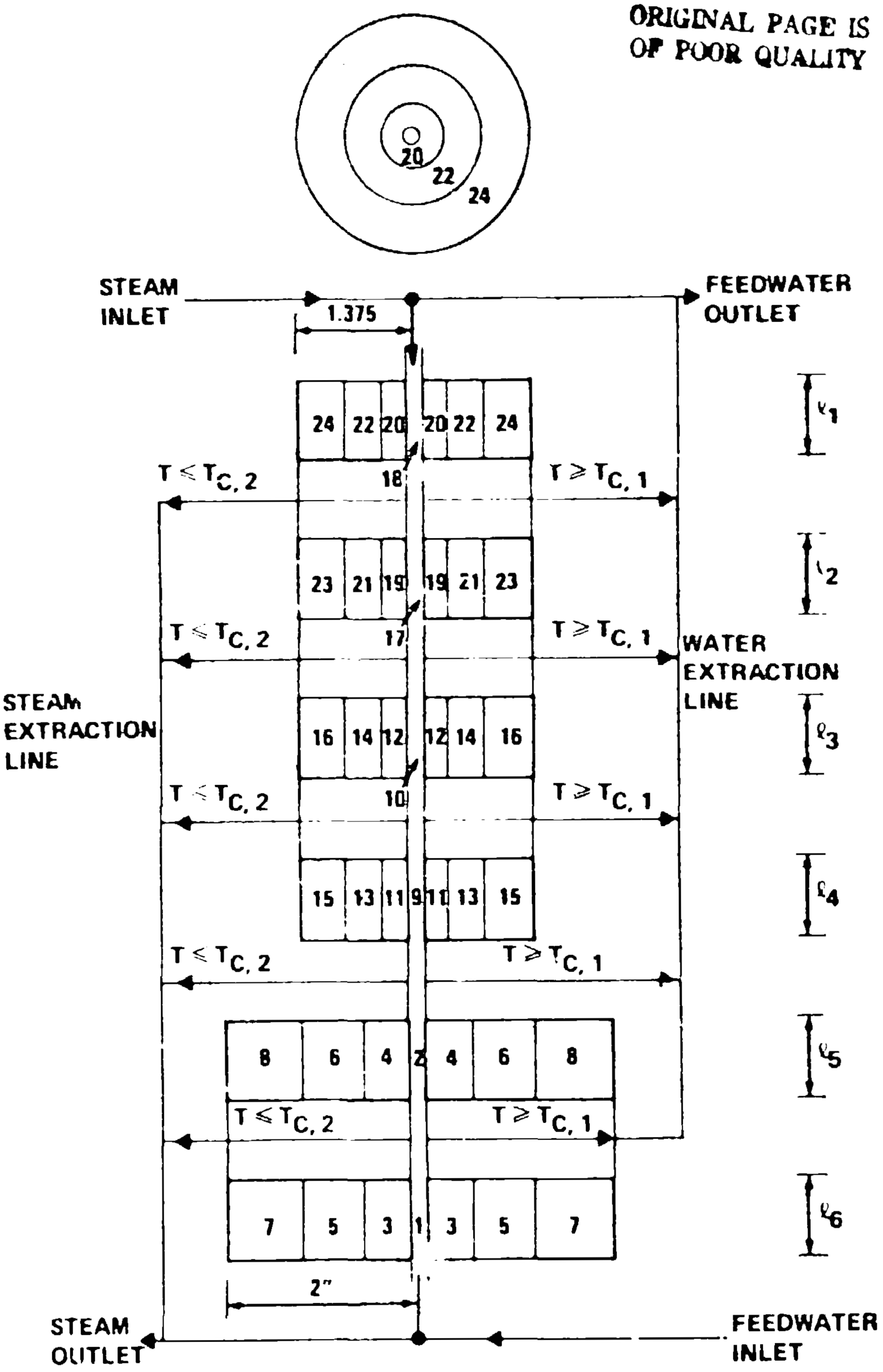

234J-036D

Fig. 4-15 TES Heat Exchanger Nodal Diagram

Figure 4-16 describes the overall logic that was used to size and evaluate the tube shell heat exchanger. As shown, the first step was to select an overall heat exchanger length for evaluation which we took as 40 ft. Following this, we determined the type and mass of salt required from an energy/temperature plot for each case (see Figure 4-17). Next, based on these energy requirements, we segmented the total heat exchanger length amongst the various salts selected. We then estimated the required pipe spacing for the various salts based on maintaining a minimum temperature difference of about 100°F between the fluid line and the salt melt point using a hand calculation. As will be discussed in more detail later, we calculated the melt line position based on a simplified one-dimensional heat transfer equation from Carslaw and Jaeger (Reference 21).

Using the total mass of salt required, the length of salt segments and pipe spacing determined above, we then calculated the total number of pipes required and the mass flow rate (and velocity) through each pipe. We then ran the program to determine performance of the TES unit.

Salts and dimensions shown in Figure 4-18 were determined using this procedure for the Ft. Martin/feedwater heating case. As shown, Cases 1 and 2 have different flow control temperatures (Tc_1 & Tc_2). Note that for these calculations, we used preliminary power plant information. For subsequent design refinement, detailed computer analyses were used to integrate the TES into the plant cycle and change these initial thermodynamic conditions (see Section 5.1).

Since we chose to analyze a single tube throughout the heat exchanger, the number of pipes was based on the minimum spacing dictated by the various salts. Thus, in a two-salt unit, if salt #1 required a minimum spacing of 4 inches and salt #2, 5 inches, the total number of pipes required was then calculated based on the 4 inch spacing. Alternately, we could have varied tube spacing in the various salts by varying the mass flow rate through the tube in the various salt sections. Obviously, we would then require a different number of tubes in the various sections of the unit. In our design refinement effort (Section 5.1,) a more realistic appraisal of tube spacing and flow arrangement was made.

Step (1): Select overall heat exchanger length based on practical constraints.

Step (2): Determine component salts and mass required based on energy/temperature profile.

Step (3): Based on energy requirements, aportion total heat exchanger length amongst component salts.

Step (4): Determine pipe spacing for component salts based on preliminary hand calculations.

Step (5): Based on results of Steps (2), (3), and (4), calculate total number of pipes required and mass flow rate and velocity through single pipe.

Step (6): Run program to evaluate performance — outlet temperature profile, transient salt temperature profile and energy stored.

2349-035D

Fig. 4-16 Heat Exchanger Design/Analysis Logic

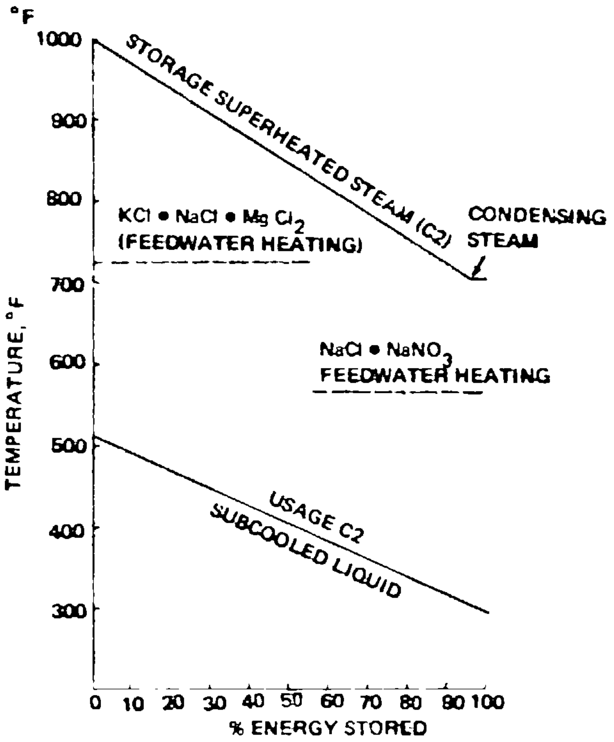

(a) FEEDWATER HEATING (C2)

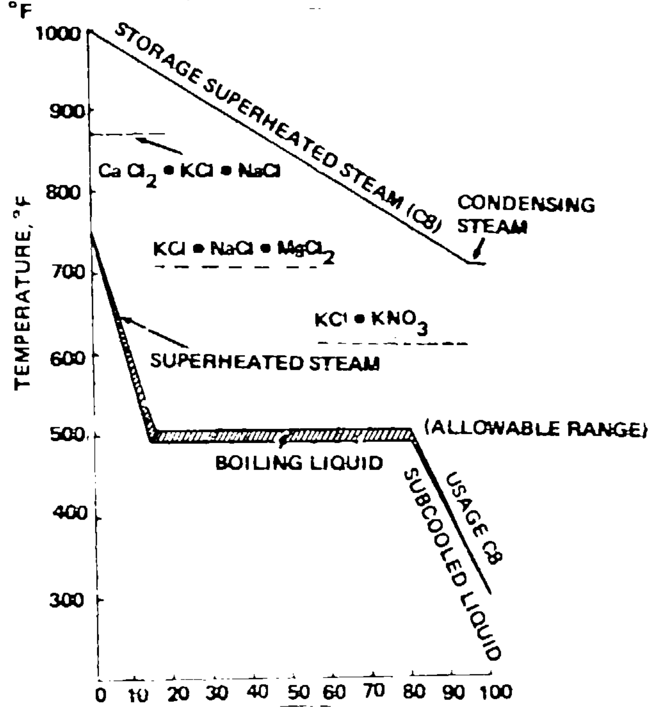

(b) AUXILIARY POWER SUPPLY (C8)

NOTE: SALT CHOSEN TO ALLOW ABOUT 100°F TEMPERATURE DIFFERENCE BETWEEN SALT MELT TEMPERATURE AND EXIT FLOW TEMPERATURE

2349-037D

Fig. 4-17 Location of Energy Stored in TES Cycle for Ft. Martin Feedwater Heating and Auxiliary Power Designs

ORIGINAL PAGE IS OF POOR QUALITY

Flow Rate per Pipe:	53 lbm/hr, water side (storage) 3.2 lbm/hr, steamside (usage)	
Total Flow Rate:	2,217,000 lbm/hr, water side 134,162 lbm/hr, steam side	
Number of 1" OD Pipes:	41,830	
Total H/X Length:	30 feet	
Total Pipe Length:	1,254,900 feet	
Pressure Drop: (ignoring entrance effects)	.2055 psf water side .0058 psf steam side	
Salt Sections:	Salt #1	Salt #2
Salt Type:	4.6 $NaC1 + 95.4 NaNO_3$	14.5 $KC1$ + 22.3 $NaC1$ + 63.2 $MgC1_2$
Salt Weight (total):	4,826,310 lbm	4,213,306 lbm
Salt Section Length:	10'	20'
Pipe Spacing (centers):	4"	2.75"
Section Diameter:	68'	46'
Bypasses:	2	4
Energy Stored/Used:*	Case 1	Case 2
BTU/Tube		
Total:	33,146/30,152	29,954/29,615
Latent:	20,780/23,591	28,438/25,986
BTU, Total H/X		
Total:	(1.386) 10^9/(1.26) 10^9	(1.25) 10^9/(1.20) 10^9
Latent:	(.869) 10^9/(.987) 10^9	(.76) 10^9/(1.09) 10^9
Control System Logic:	$T_{c,1}$ = 514°F $T_{c,2}$ = 705°F	464°F 755°F

*Results are based on initial salt temperature of 1000°F and correspond to two days after start. Energy stored not equal to energy used implies that quasi-steady state has not been reached.

2349-037D **Fig. 4-18 Salient Physical Characteristics – Analysis Cases 1 and 2**

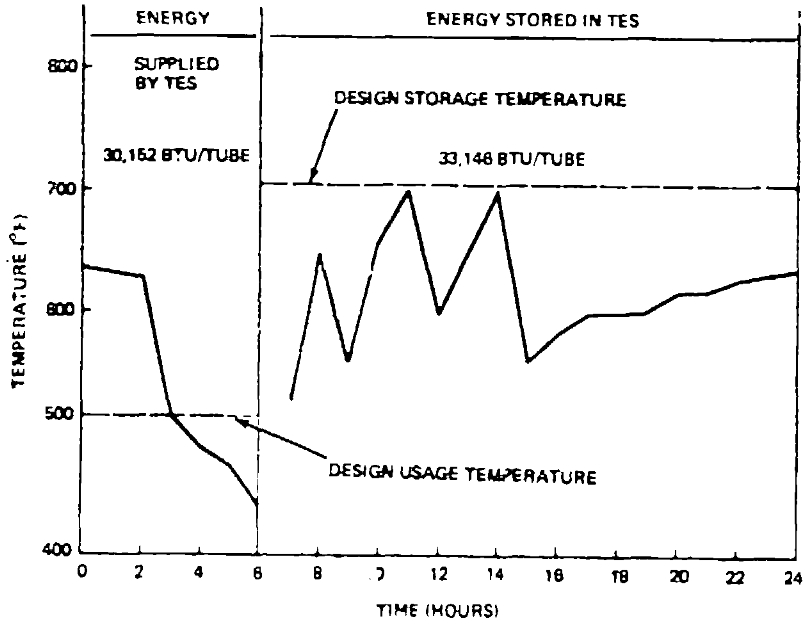

2349-038D

Fig. 4-19 TES Outlet Fluid Temperature, Ft. Martin Feedwater Heating – Case 1

Based on the initial temperature/energy profile of the Ft. Martin/feedwater heating case it was decided that a two-salt unit, using $NaCl \cdot NaNO_3$ and $KCl \cdot NaCl \cdot MgCl_2$ eutectics would be satisfactory (Figure 4-17). Neglecting the sensible heat storage of each salt, it was initially determined that each salt would store an equal amount of energy and, therefore, the total heat exchanger length was segmented into two equal sections of 20 feet each. Preliminary analysis, however, showed that the sensible heat contribution would be significant (~30% of total) and that ten feet of the $NaCl \quad NaNO_3$ unit would be inactive. The analysis was therefore run for a 30 foot long heat exchanger.

Pressure drop calculations and the total and latent energy stored and used (supplied) are also presented in Figure 4-18. As shown, pressure drop through the heat exchanger section neglecting entrance effects, elbows, etc., will be insignificant. The energy data presented has been extracted from our computer runs and corresponds to the third day of operation from an initial stable salt temperature of 1,000°F.. For this case we want to store 1.26×10^9 BTU. Storage of a larger amount of energy indicates that the mass of salt, and hence the heat exchanger size, can be decreased. Obviously, energy stored should equal energy used. The imbalance between these parameters indicates that a daily steady state condition was not fully achieved.

Figure 4-19 presents a plot of the exit water and steam temperature during the energy usage and storage periods for this analysis. As shown, over significant time periods the feedwater outlet temperature was significantly higher or lower than the desired outlet temperature of 514°F, and the steam temperature was about 100°F below the desired outlet temperature of 705°F over most of the energy storage phase. This figure represents conditions after 48 hours of operation, starting from an initial salt temperature of 1,000°F. Fig. 4-20 presents energy used and stored (BTU's) as a function of time for this case. As shown, $(1.26)\ 10^9$ BTU's were supplied during the energy usage phase, while $(1.39)\ 10^9$ BTU's were stored during the energy storage period. This implies that steady state has not been reached and that the program would have to execute more cycles to achieve final conditions.

Figure 4-21 presents a map of nodal temperatures at the end of the storage and usage periods. This plot enables us to evaluate the adequacy of our preliminary pipe spacing calculation and also how much (if any) of the salt will remain inactive. As shown, it appears that our hand calculations can adequately specify the required pipe spacing. Looking at the end of storage, we see that the salt temperature at the farthest locations and greatest depth

ORIGINAL PAGE IS
OF POOR QUALITY

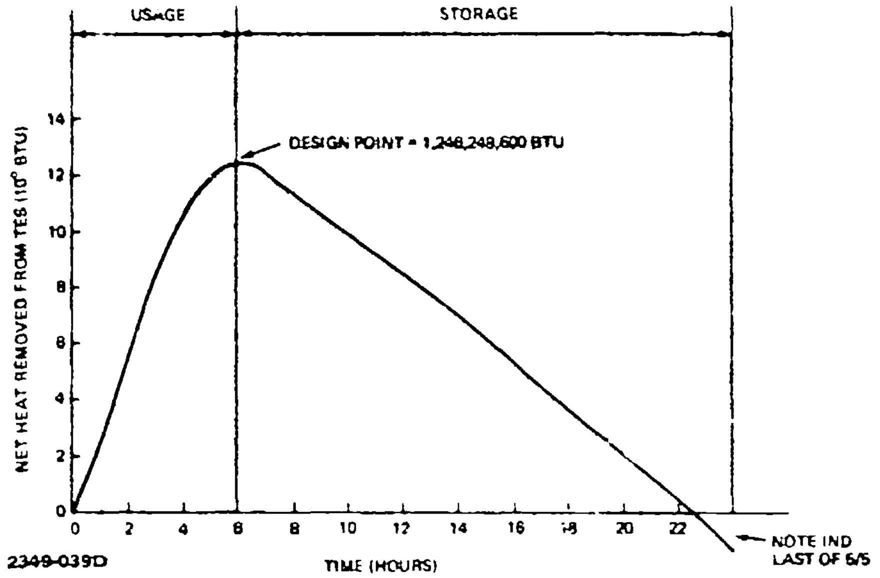

Fig. 4-20 Transient Energy Supplied/Stored by TES – Case 1

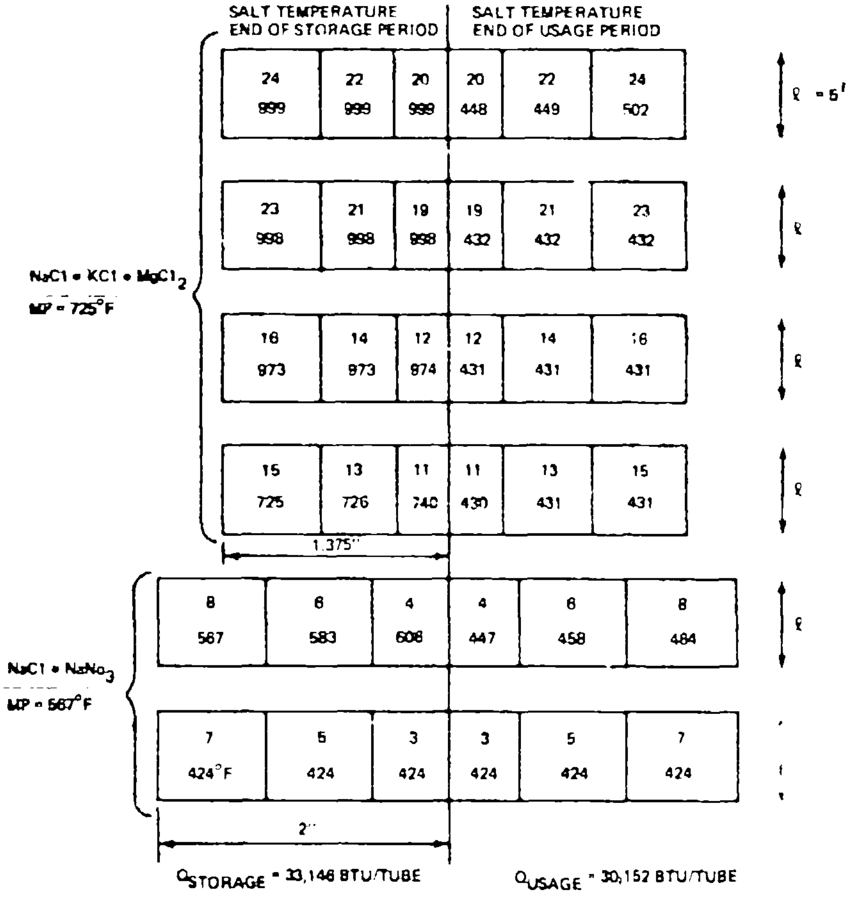

2349-040D

Fig. 4-21 Salt Temperature Map - Case 1

starting from the entrance are at the melting point for each of the salts (Node 15 = 725° F, Node 8 = 567° F). This implies that increasing the active salt radius would not increase the latent heat contribution of the salt. It is significant that the lower section of the heat exchanger (nodes 3, 5, and 7) remains at constant temperature (424° F) throughout the usage and storage periods. This suggests that we have oversized the heat exchanger and that we can eliminate another five (5) feet of total length, reducing the final unit to 25 feet long. This reduction may be attributed to our preliminary method of sizing the TES unit based on latent heat storage only. Note that if we wish to maintain the 40 ft. length we can increase the flow through the tube and thus require fewer total modules.

Our analysis extracts fluid from the unit in discrete steps based on two control temperatures. Another case (Case 2) was run to examine the influence of this parameter with the same conditions as above, except that steam control temperature ($T_{C,2}$) was set 50° F higher than before (755 rather than 705° F) and water control temperature ($T_{C,1}$) was set 50° F lower (464 rather than 514° F). This change did not significantly affect the final results in terms of fluid outlet temperature, although some parts of the PCM did run significantly hotter (see Figures 4-22 and 4-23).

Concluding this series, in order to evaluate the effect of pipe length the analysis was repeated for a sixty (60) foot long TES unit using the 705° and 514° F control temperatures of Case 1. In this case, the mass flow rate was doubled to compensate for the longer heat exchanger length. Here again, the results were not very much different from Case 1 (Figures 4-24, 4-25, and 4-26) and the bottom section (10 feet) was inactive.

Evaluations of these results indicated that more effective and less expensive control systems would improve TES performance. It was decided that using a conventional regenerative fluid/fluid heat exchanger would give better control of the TES outlet temperature and also simplify heat exchanger construction. The results of a preliminary run made for this system with a heat exchanger effectiveness of 30% is presented in Figure 4-27. As shown, the design does lower the variation in outlet temperature. This design can be improved further by including a bypass around the modulating heat exchanger (Figure 4-28).

Summary:

We concluded this preliminary evaluation of the tube/shell unit and proceeded to evaluate alternate concepts. The preliminary analysis provided us with several major analytic and design conclusions. It showed (for a realistic duty cycle) that a significant amount of energy (~30%) is available as sensible heat, decreasing our previous estimates of salt quantities required. It also verified several analytical techniques, particularly our method of calculating tube spacing, and helped to develop analytical techniques used in our design refinement efforts (see Section 5). It also revealed that the inclusion of a simple regenerative heat exchanger with bypasses would be an effective method of controlling TES fluid outlet conditions on tube/shell units. Some method of outlet temperature control is required in all static salt systems since the heat exchanger effectiveness decreases with time as the melt (or solidification) line progresses away from the tube surface. Since a major portion of the energy is stored as latent heat, the thermal resistance between the utility fluid (steam or water) and the melt line directly affects the heat transfer rate. The major advantage of the moving salt systems discussed later is that this thermal resistance can be minimized.

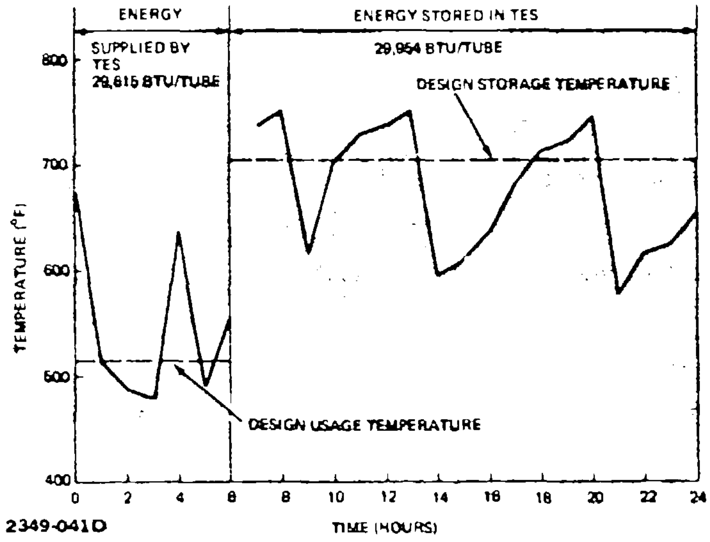

Fig. 4-22 TES Outlet Fluid Temperature, Ft. Martin Feedwater Heating – Case 2

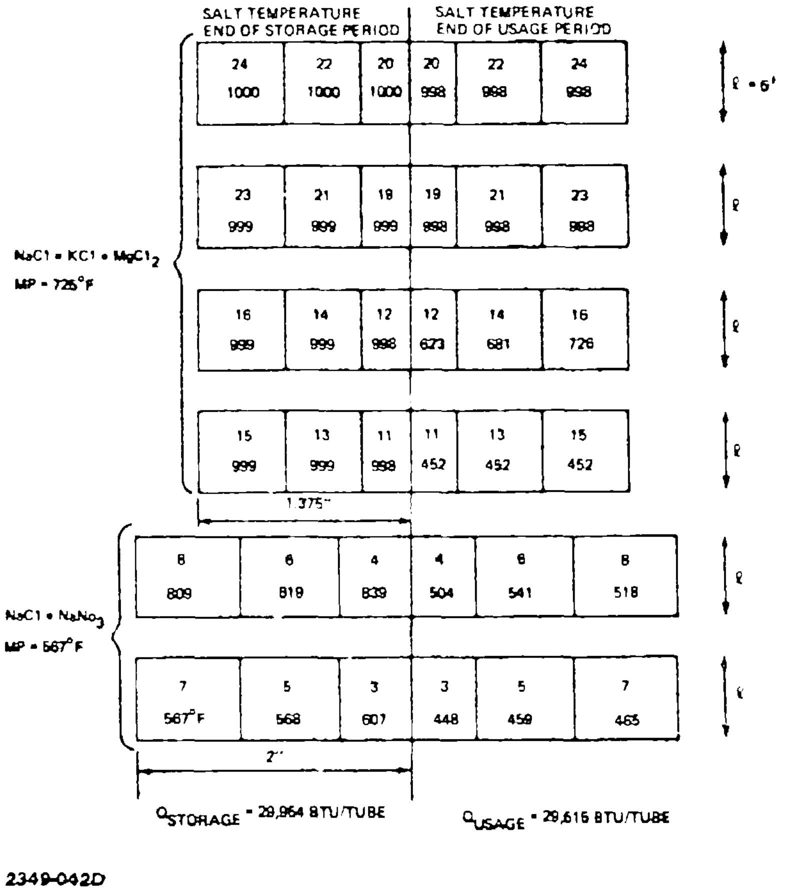

Fig. 4-23 Salt Temperature Map - Case 2

ORIGINAL PAGE IS
OF POOR QUALITY

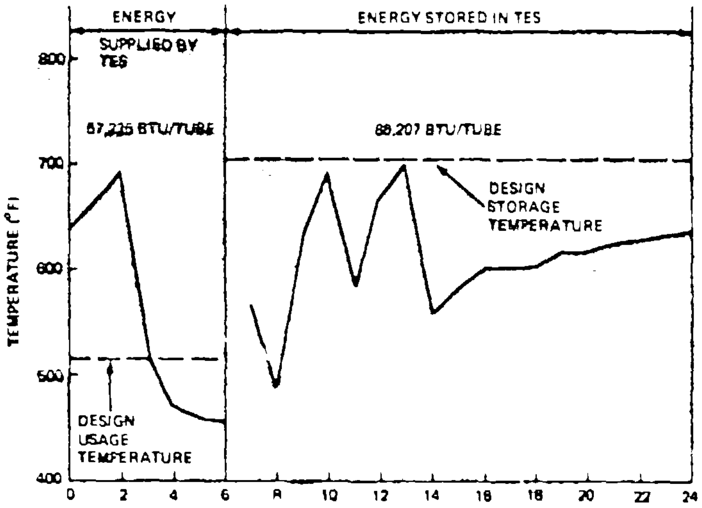

2349-043D

Fig. 4-24 TES Outlet Fluid Temperature, Ft. Martin Feedwater Heating — Case 3

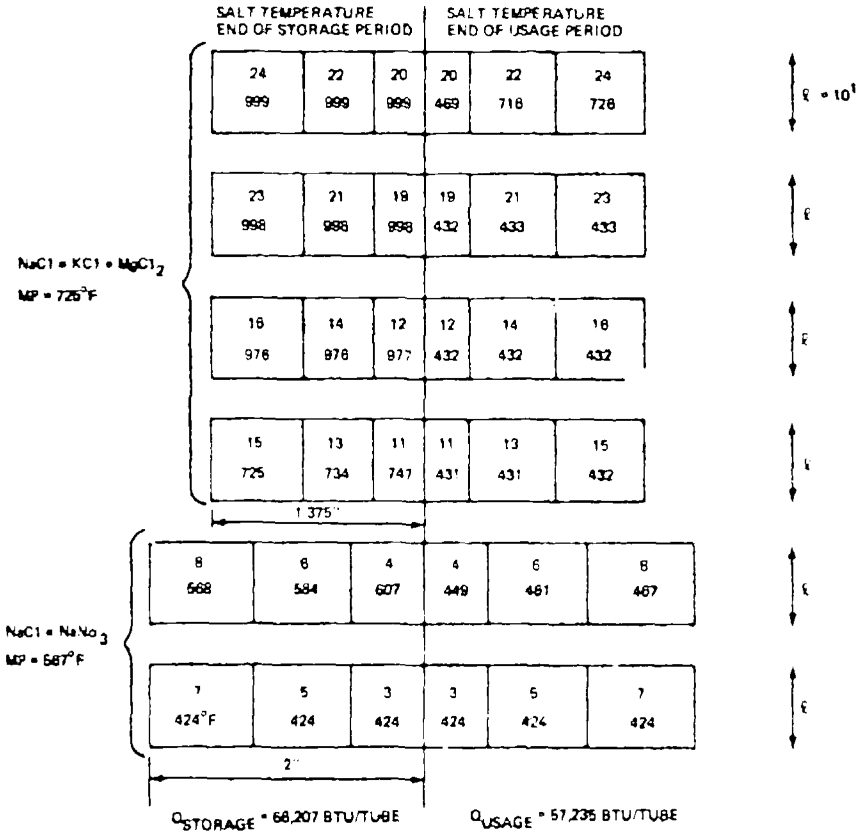

SALT TEMPERATURE END OF STORAGE PERIOD			SALT TEMPERATURE END OF USAGE PERIOD		
24 999	22 999	20 999	20 469	22 716	24 728
23 998	21 998	19 998	19 432	21 433	23 433
16 976	14 976	12 977	12 432	14 432	16 432
15 725	13 734	11 747	11 431	13 431	15 432
8 568	6 584	4 607	4 449	6 461	8 467
7 424°F	5 424	3 424	3 424	5 424	7 424

2349-044D

Fig. 4-25 Salt Temperature Map - Case 3

Flow Rate per Pipe:	106 lbm/hr, water side (storage) 6.4 lbm/hr, steam side (usage)	
Total Flow Rate:	2,217,000 lbm/hr, water side 134,162 lbm/hr, steam side	
Number of 1" OD Pipes:	20,916	
H/X Length:	60 feet	
Total Length of Pipe:	1,254,900 Feet	
Pressure Drop: (ignoring entrance effects)	.8223 psf water side .023 psf steam side	
Salt Sections:	Salt #1	Salt #2
Salt Type:	4.6 NaCl • 95.4 $NaNO_3$	14.5 KCl • 22.3 NaCl 63.2$MgCl_2$
Salt Weight (Total):	4,825,310 lbm	4,213,306 lbm
Salt Section Length:	20'	40'
Pipe Spacing (centers);	4"	2.75"
Section Diameter:	46'	31'
Bypasses:	2	4
Energy Stored/Used*		
BTU/Tube		
Total:	66,207/57,235	
Latent:	41,789/43,481	
BTU, Total H/X		
Total:	$(1.39)\ 10^9/(1.20)\ 10^9$	
Latent:	$(.87)\ 10^9/(.91)\ 10^9$	
	Control System Logic:	
	$T_{c,1} = 514°F$	
	$T_{c,2} = 705°F$	

*Results are based on initial salt temperature of 1000°F and correspond to two days after start. Energy stored not equal to energy used implies that quasi-steady state has not been reached.

2349-045D

Fig. 4-26 Salient Physical Characteristics, Analysis Case 3

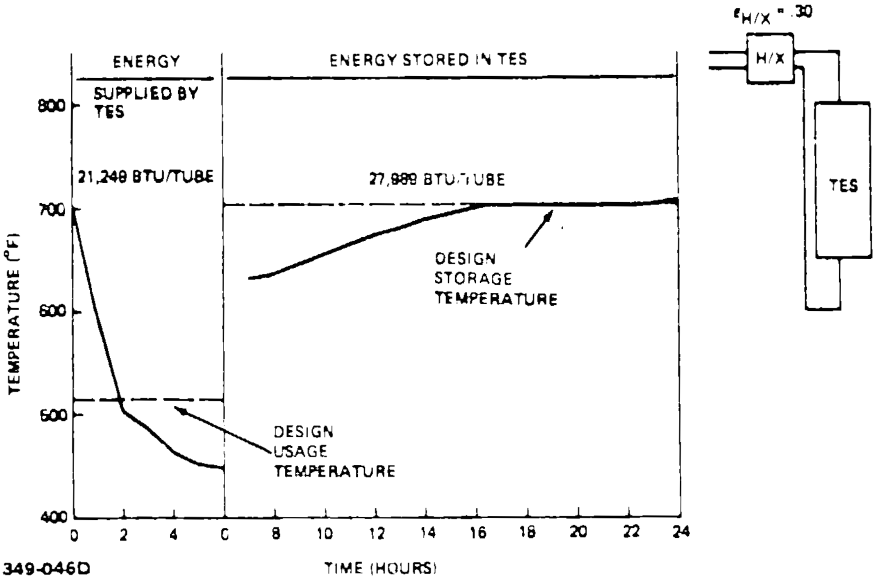

Fig. 4-27 TES Outlet Fluid Temperature, Ft. Martin Feedwater Heating – Case 4

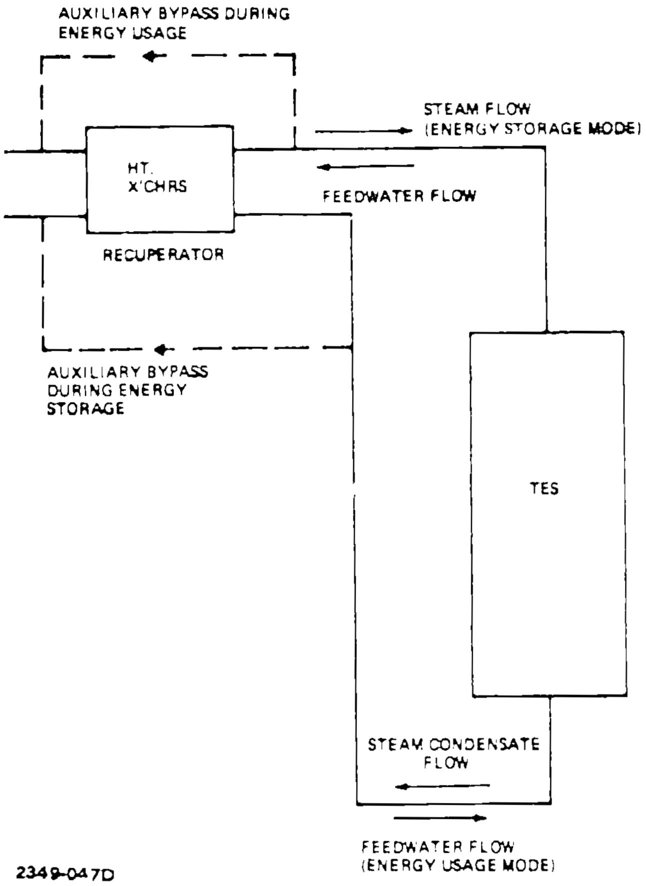

Fig. 4-28 TES Control System

4.5.2 Heat Pipe Heat Exchanger Concept

The heat pipe heat exchanger is superficially similar to the tube/shell heat exchanger except that the tubes extend into the manifold regions (which become tube/sink heat exchangers) and are individually sealed heat pipes. Heat pipes are relatively high conductance devices, but they still introduce some additional thermal resistance compared with the tube/shell. They have a number of advantages, however, which may offset this:

- Vapor pressure of the working fluid in the heat pipes is generally lower than that of the steam or feedwater, permitting thinner tubing to be used.
- The amount of working fluid in an individual heat pipe is small (less than 1/2 lbm), minimizing the potential hazards of reactions with the PCM if a leak develops.
- Burst diaphragms can be provided in end caps at both ends of each heat pipe, so that if a leak develops with either source or sink fluid, the heat pipe will simply become an open conduit between these lines, minimizing any chance of bursting a pipe and reacting with the PCM.
- Failed individual pipes must be recapped to close the leakage path, but cause very little loss in total storage capacity.

One of the problems in designing a heat pipe/TES system is lack of suitable heat pipe working fluids for the 600-800° F temperature range. Nuclear plants operate below this temperature range, and are, therefore, better suited to this TES concept than a fossil fueled plant. For example, the Three Mile Island plant was considered with TES used to eliminate most of the steam extraction for the final feedwater heater during peak power periods. A schematic of the system is shown in Figure 4-29.

The TES unit is sized to permit approximately 5% additional power generation for a six-hour usage period. The storage part of the cycle takes 18 hours. For the temperatures involved, the use of a single PCM, a sodium nitrate, sodium hydroxide eutectic (84.5% $NaNO_3$, 15.5% NaOH) with a melt temperature of 475° F was selected. The heat pipes must be capable of operating over the full temperature range of 410° F to 565° F to cover extremes of the storage and usage cycles. For these temperatures, Dowtherm A, a 26.5% diphenyl, 73.5% diphenyl oxide eutectic working fluid (also marketed under a variety of other tradenames) was selected for the heat pipes, based on compatibility with steels, relatively low vapor pressure (495° F boiling point), and an anticipated low level of reactivity with the phase change material. From a heat pipe performance point of view, the principle disadvantage of Dowtherm A is its relatively low liquid thermal conductivity 065 BTU/hr° F), which will

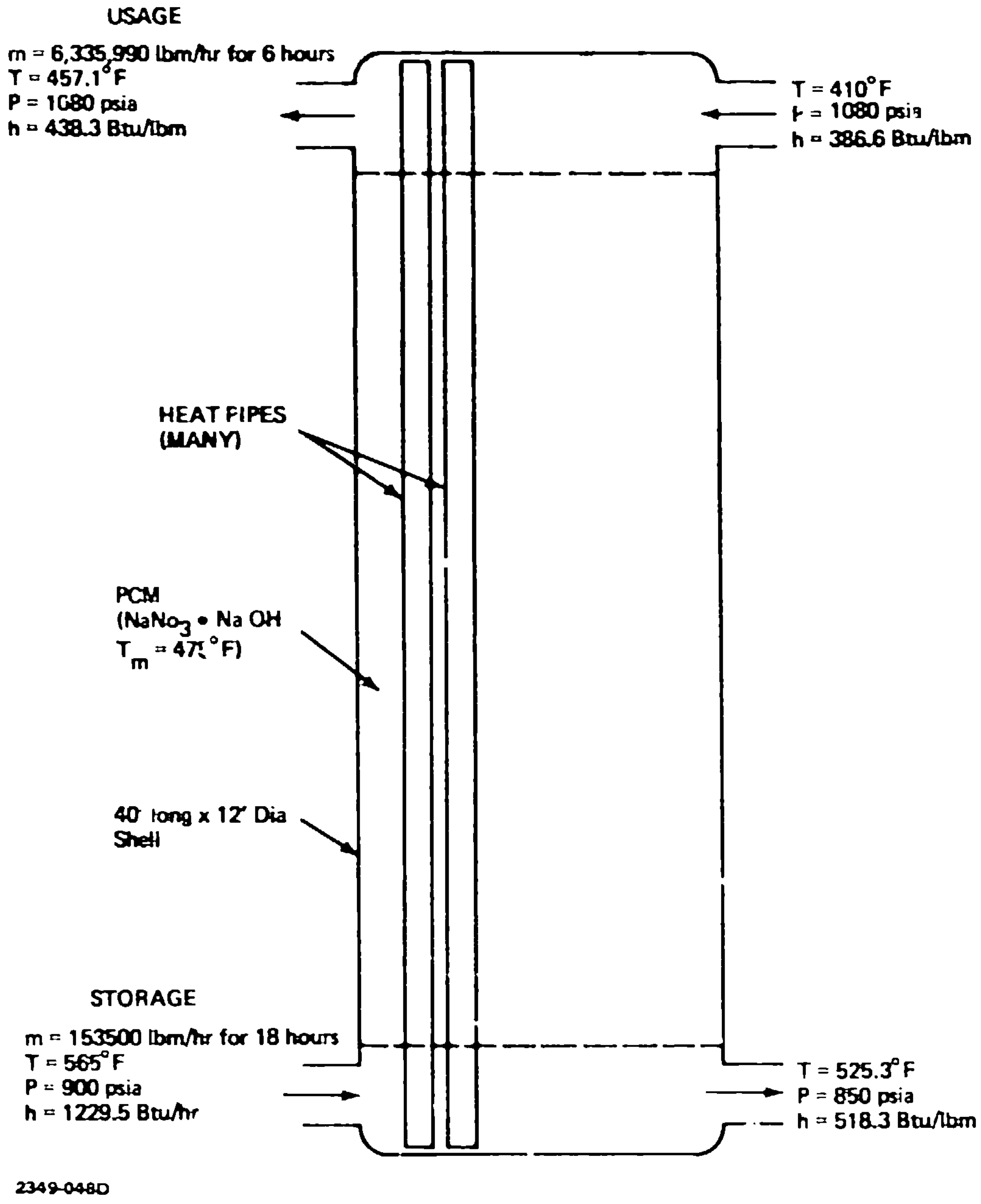

Fig. 4-29 Heat Pipe Heat Exchanger/TES Cannister Schematic

require a good internal wick design to avoid excessive temperature drops. Water, with approximately 4 times the liquid thermal conductivity, might also be used as a working fluid, but might require use of monel tubing rather than steel, has high vapor pressure at these temperatures, and would react with the PCM should a pipe burst.

With the heat pipe/TES canister arrangement shown in Figure 4-29, heat pipes are oriented vertically, and heated at the bottom end (the evaporator) during heat storage. The length of pipe located in the PCM canister acts as a condenser during heat storage, and condensate returns to the evaporator assisted by gravity. For usage, the feedwater heat exchanger is located at the top of the canister. This portion of the heat pipes now acts as a condenser, the PCM region acts as evaporator, and gravity again assists condensate return from condenser to evaporator. Volumetric expansion of the PCM (liquid density = 120.7 lbm/ft^3, solid density = 140 lbm/ft^3) on melting is accommodated by arranging the heat exchangers so that they correspond in effect to a counterflow arrangement, though separated by the PCM. In this way, the hottest heat pipe during storage is also the hottest during usage, and will be the first pipe to initiate melting during usage. Since the heat pipe is virtually isothermal along its length, the melt layer should form continuously along its length, providing a flow path for liquid to reach the void volume at the top of the canister. In addition, a melt layer should form adjacent to the metal plate separating the storage heat exchanger and the PCM. This should permit liquid PCM to flow from any partially melted pipe region (possibly as a result of mild longitudinal temperature gradients) to fully melted regions, minimizing pressure gradients in the PCM

With this arrangement, tube spacing is based on propagation rates of the liquid solid interface in a manner similar to that used for the tube-shell heat exchanger, allowing for additional thermal resistance of the heat exchanger and heat pipe. An approximate equation for the melt radius, R, at any time, t for constant fluid temperature, T_f, is then:

$$\beta\,[\ell n \beta + K_1] = K_1 + K_2 t \qquad (4\text{-}2)$$

where,

$$\beta = (R/a)^2$$

$$K_1 = \frac{2k_s}{aU}\;\frac{\ell_{PCM}}{\ell_{H/X}} + \frac{4k_s}{h_{HP} d_i} - 1$$

$$K_2 = \frac{4\,|Tm - Ts|\,k_s}{\Delta H_{fs}\,\rho_s\,a^2}$$

In the expression for K_1, ℓ_{PCM} and $\ell_{H/X}$ refer respectively to the lengths of heat pipe in the PCM and the active heat exchanger; U, is the overall coefficient of heat transfer in the active heat exchanger (including the heat pipe film coefficient in the heat exchanger region), and h_{HP} is the heat pipe film coefficient for the length of pipe in the PCM region. Tube spacing is calculated for the usage mode in this example since the PCM melt temperature (T_m = 475° F) is closer to fluid temperature during usage than during storage, and since usage heat flux is 3 times that of storage. For this case, the water side film coefficient is estimated to be 300 BTU/hr $ft^{2\circ}$ F). The heat pipe functions as a condenser in the heat exchanger, with condensing film coefficient, for Dowtherm A working fluid, estimated to be 2000 BTU/hr $ft^{2\circ}$F. This is based on a gravity-assisted wick design developed at Grumman, using data obtained with Freon-12 working fluid, adjusted for the difference in liquid conductivity. The overall coefficient of heat transfer is then

$$U = \frac{1}{\dfrac{1}{h_{H_2O}} + \dfrac{1}{h_{cond}}} = 261 \text{ BTU/hr ft}^{2\circ}\text{F} \tag{4-3}$$

The PCM region of the heat pipes acts as an evaporator, with h_{EVAP} estimated at 600 BTU/hr $ft^{2\circ}$F, extrapolated from Freon-12 data for a gravity assisted wick.

Wall thickness, t_w, based on buckling considerations is approximately given by:

$$\frac{t_w}{d} = \left[\frac{(S.F.)(\Delta P)}{2.2E}\right]^{1/3} \tag{4-4}$$

For a safety factor, SF = 3, a maximum pressure of 1080 psi (neglecting internal pipe pressure), and a modulus of elasticity, $E = 29 \times 10^6$ for steel:

$$\frac{t_w}{d} = \left[\frac{3 \times 1080}{2.2 \times 29 \times 10^6}\right]^{1/3} = 0.037$$

or t_w = .037" for a 1" diameter tube.

With this value of t_w, d_i = 0.926" for a 1" tube and,

$$K_1 = \frac{2K_s}{aU}\,\frac{\ell_{PCM}}{\ell_{H/X}} + \frac{4k_s}{h_{HP}\,d_i} - 1$$

$$K_1 = \frac{2 \times 0.377}{\frac{1}{24}(261)}(10) + \frac{4(.377)}{600\left(\frac{.926}{12}\right)} - 1 = -.274$$

The fluid temperature, T_f, during usage varies from 410° F to 457.1° F, giving a mean temperature difference (with $T_m = 475°$ F) of:

$$T_m - \overline{T}_f = \frac{(T_m - T_{fmin}) - (T_m - T_{fmax})}{\ln\left(\frac{T_m - T_{fmin}}{T_m - T_{fmax}}\right)} = 36.5° \text{ F}$$

from which, for a six-hour usage period,

$$K_2 t = \left(\frac{4 \left| T_m - \overline{T}_s \right| k_s}{\Delta H_{fs} \ \rho_s \ a^2}\right) t = \frac{4 \times 36.5 \times .377}{76.5 \times 140 \left(\frac{1}{24}\right)^2} \times 6 = 17.76$$

Then,

$$\beta\left[\ln\beta - 0.274\right] = 17.49$$

from which $\beta = 9.06$, $R/a = 3.01$, since $a = 1/2''$, $R = 1.50''$, and the pipe centers should be put on 3" spacing. Energy storage associated with the phase change process is ΔH_{fs} = 76.5 BTU/lbm.

In addition, there is some sensible heat storage,

$$\Delta E_{SEN} = c_{ps}(T_m - \overline{T}_s) = c_{pl}(\overline{T}_l - T_m) \tag{4-5}$$

where $\overline{T}_s$ = average temperature of the solid PCM at the end of usage

$\overline{T}_l$ = average temperature of the liquid PCM at the end of storage.

With the approximation:

$$\overline{T}_s \cong \frac{T_m + \overline{T}_{fusage}}{2} = \frac{475 + 438.5}{2} = 456.8° \text{ F}$$

$$\bar{T}_1 \cong \frac{T_m + T_{f\,storage}}{2} = \frac{475 + 533.9}{2} = 504.5°\,F$$

$$\Delta E_{SEN} = 0.45\,(475 - 456.8) + .45(504.5 - 475) = 21.5\ \frac{BTU}{lbm}$$

Then, $$\Delta E_{total} = 76.5 + 21.5 = 98\ BTU/lbm$$

Energy stored per foot of pipe is then,

$$E' = \Delta E_{total}\,\rho_s\,\pi a^2\,(\beta - 1) = 602.8\ \text{BTU/ft of pipe}$$

and for $l_{PCM} = 36'$:

$$E = 21,700\ \text{BTU/pipe}$$

The pipes are assumed to be arranged in a hexagonal array as shown in Figure 4-30. We require an amount of active PCM per foot of pipe given by:

$$M' = \rho_s\,\pi a^2\,(\beta - 1) = 140\,\pi\,(\tfrac{1}{24})^2\,(9.06 - 1)$$

or, $$M' = 6.151\ \text{lbm PCM/ft of pipe}$$

Each hexagon must contain sufficient mass for 3 heat pipes, with sufficient area to accommodate the liquid phase, $\rho_\ell = 120.7\ \text{lbm/ft}^3$, hence:

$$3M' = \rho_\ell\,(\tfrac{3}{2}\sqrt{3}\,S^2 - 3\pi\,a^2)$$

or $$S = \left[\frac{2}{\sqrt{3}}\left(\frac{M'}{\rho_\ell} + \pi a^2\right)\right]^{1/2} = 3.06\ \text{inches}$$

The cross-sectional area associated with each pipe is then,

$$A_x = \frac{\sqrt{3}}{2}\,S^2 = 8.124\ \text{square inches}$$

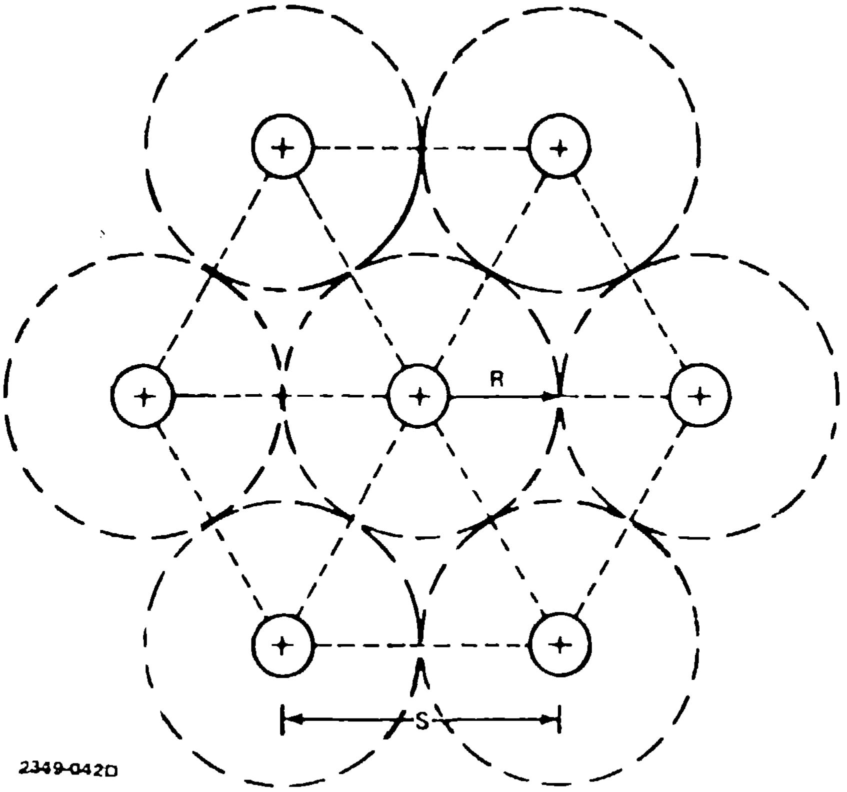

Fig. 4-30 Hexagonal Arrangement of Heat Pipes in Cannister

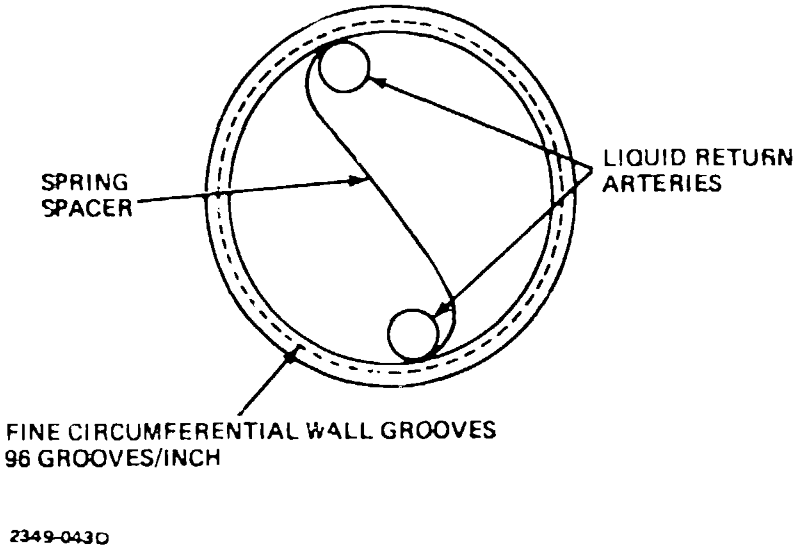

4-31 Gravity Assisted Wick Cross-Section-Schematic

If we use canisters with diameter d_c = 12', the number of pipes per canister is:

$$N_p = \frac{\frac{\pi}{4} d_c^2}{A_x} = \frac{\frac{\pi}{4} (12)^2}{(8.124/144)} = 2004$$

and the heat storage per canister is:

$$Q_c = N_p E = 43.5 \times 10^6 \text{ BTU/canister}$$

For a total storage requirement of:

$$Q_T = 1.965 \times 10^9 \text{ BTU}$$

the number of canisters required is:

$$n_c = Q_T/Q_c = 45.2 \longrightarrow 46 \text{ canisters}$$

The mass of PCM required is:

$$M_{pcm} = N_c \left[\frac{\pi}{4} dc^2 - N_p \pi a^2\right] \ell_{PCM} \rho_\ell \qquad (4\text{-}6)$$

$$= 20.42 \times 10^6 \text{ lbm}$$

The heat pipes, as stated earlier, use Dowtherm A working fluid and a gravity assisted wick design. The wick design used in these calculations (Reference 22) is shown schematically in Figure 4-31. The maximum heat flux, $\dot{Q}_{max}$, each pipe must carry occurs during the usage cycle, with

$$\dot{Q}_{max} = \frac{E}{t_{usage}} = \frac{21700}{6} = 3617 \text{ BTU/hr} \qquad (4\text{-}7)$$

For this heat flux, two arteries are required, each about .051" in diameter. The wall wick consists of fine circumferential grooves, 96/inch of length, approximately 8 mils deep and 4 mils wide. The arteries are forced against the wall by a spring type spacer. It should be noted that these arteries are somewhat different from those used in heat pipes designed for space applications. The arteries are open at the ends and do not require capillary integrity. For this reason, they should be relatively inexpensive to fabricate. Machining the fine circumferential grooves will be a major item in fabrication cost of the heat pipes. It may be possible, however, to reduce the number of grooves required, particularly in the PCM region which has the greatest length and lowest heat flux. This is left for a more detailed design phase.

The use of heat exchangers at both top and bottom ends at the heat pipes presents an additional problem in heat pipe design, since the bottom heat exchanger will tend to trap inactive working fluid when the top heat exchanger is working. Fortunately for this case, the bottom heat exchanger can be made with a very short vertical height. The steam side will have a condensing film coefficient:

$$\bar{h} = 0.943 \sqrt[4]{\frac{g\rho_\ell(\rho_\ell - \rho_v)\, k^3_\ell\, \Delta H_{fs}}{\ell_{H/X}\Delta T}} = \frac{Q_{max\ storage}}{2\pi a\, \ell_{H/X}\Delta T} \qquad (4\text{-}8)$$

for which:

$$\ell_{H/X}\Delta T = \left(\frac{Q_{max\ storage}}{0.943 \times 2\pi a}\right)^{4/3} \left[\frac{\mu}{g\rho_\ell(\rho_\ell - \rho_v)\quad \Delta H_{fs}}\right]^{1/3} \qquad (4\text{-}9)$$

where,

$$Q_{max\ storage} = \frac{21700}{18} = 1206 \text{ BTU/hr}$$

then,

$$\ell_{H/X}\Delta T = \left[\frac{1206}{0.943(2\pi/24)}\right]^{4/3} \left[\frac{0.250}{418 \times 10^6 \times 47.6(47.6 - 1.9)\,(.336)^3(639.1)}\right]^{1/3} = 1.824 \text{ ft}^\circ\text{F}$$

$$\text{For } \ell_{H/X} = 1/2 \text{ ft}, \Delta T = 3.65^\circ \text{F}$$

The inside of the pipe at the bottom will be functioning as an evaporator, with $h_{EV} \simeq 6600$ BTU/hr ft$^{2\circ}$F. Then,

$$T_{EV} = \frac{Q}{\pi d_i\, \ell_{H/X} h_{EV}} = \frac{1206}{\pi\left(\frac{.926}{12}\right)(.5)\,600} = 8.3^\circ \text{F}$$

The total $\Delta T_{H/X}$ at the bottom during storage will then be:

$$\Delta T_{H/X} = 3.6 + 8.3 = 11.9^\circ F$$

This is acceptable considering the overall temperature difference between the condensing steam and the phase change temperature:

$$T_{cond} - T_{PCM} = 525 - 475 = 50^\circ F$$

Despite the short length required for the bottom heat exchanger, the heat pipe must be designed to minimize the extent of flooding of the evaporator surfaces during the storage period, since this will act to increase the evaporator ΔT. This problem can be minimized by using a plug to reduce vapor space volume at the bottom of the pipe, thereby reducing the excess liquid available for flooding. Also, since flooding will result in pool boiling in the evaporator, with associated liquid expulsion, it should be possible to design a liquid trap which would collect any liquid entrapped in the vapor. The liquid trap would be designed to return liquid at a very slow rate to the evaporator. In this way the trap would run partially full during the heat storage period, and empty during the heat usage period.

4.5.3 Macroencapsulated PCM Concept

In this concept, relatively large quantities of PCM are encapsulated with thin layers of containment material (steel) which would deform to accommodate volumetric changes associated with change of phase. Relatively small quantities of containment material would be required, since the thickness would have to be small to minimize bending stress. One such configuration, consisting of long "plank" shaped blocks of PCM, is shown in Figure 4-32 (A). The plank cross-section would be essentially rectangular when the PCM is at maximum density in the solid state. The edges would be relatively stiff, and top and bottom surfaces would bulge outward as indicated to accommodate volumetric expansion associated with melting. The planks would be stacked in a pressure vessel, as shown in Figure 4-32 (B), with gap regions provided for fluid flow. The gap height would be adjusted by design of the plank edge shape to be as small as possible consistent with allowable flow pressure drops and required film coefficient for heat transfer. High overall packing density is desirable to minimize pressure vessel size and cost.

For the configuration shown, the liquid pressure, P_ℓ, on melting is:

$$P_\ell = 30\,E\,\frac{at^3}{b^4}\left(\frac{\rho_s}{\rho_\ell} - 1\right) \qquad (4\text{-}10)$$

where E = modulus of elasticity of the containment material. The maximum bending moment occurs at the edge, where (per unit length of plank):

$$M = -\frac{P_\ell\ b^2}{12}$$

with associated bending stress,

$$\sigma = \frac{P_\ell\ b^2}{2\,t^2}$$

Substituting for P_ℓ

$$\sigma = 15E\left(\frac{at}{b^2}\right)\left(\frac{\rho_s}{\rho_\ell} - 1\right)$$

from which it is apparent that stress varies directly with thickness of the containment material.

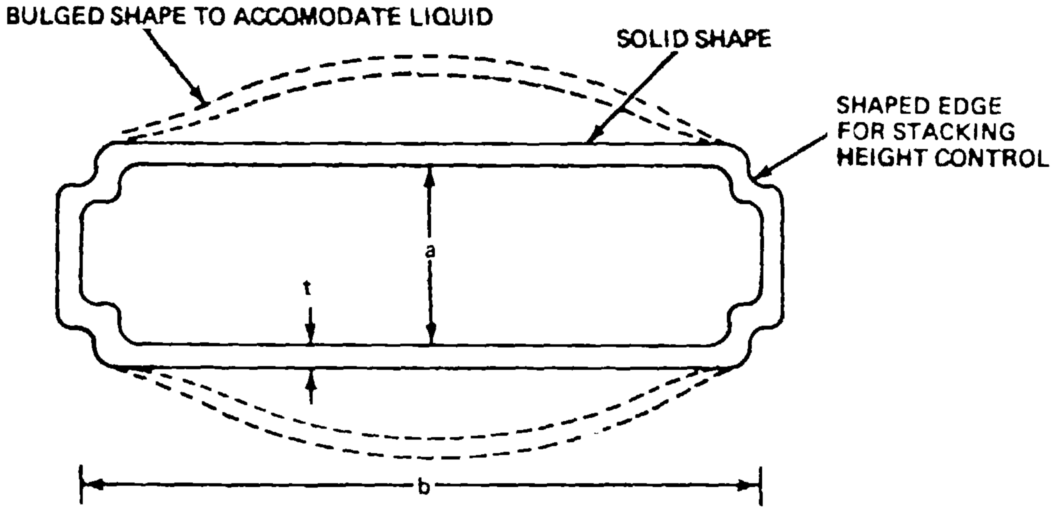

(A)

Macroencapsulated PCM - Cross-Section

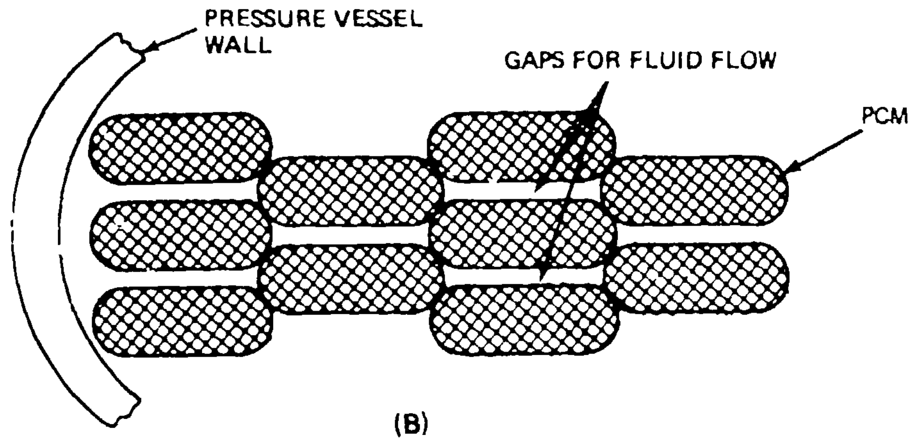

(B)

Fig. 4-32 Stacking Arrangement – Macroencapsulated PCM

As an example, consider a PCM with high volumetric density change, such as the $KCl \cdot NaCl \cdot MgCl_2$ eutectic used for the high temperature salt in the Fort Martin feedwater heating application. Using stainless steel for the encapsulating material, with b = 24", a = 3", and t = .012"

$$\sigma = 15 \times 30 \times 10^6 \, \frac{(3)\,(.012)}{(24)^2} \left(\frac{140}{102} - 1 \right) = 10{,}500 \text{ psi}$$

which is below allowable design stress levels for many stainless steels. Note that the thickness of .012" is arbitrary. The planks of PCM need be handled at ambient temperature only during initial installation, with the PCM in a solid state.

The mass of stainless steel required for encapsulation per pound of PCM, for the dimensions used above, is:

$$\frac{m_{ss}}{m_{pcm}} = \frac{\rho_{ss}}{\rho_{s,\,pcm}} \times \frac{2\,(a + b)\,t}{ab} = 0.031$$

This is small enough to indicate that costs of macroencapsulation should be modest.

The time, τ, required to freeze the PCM, based on a one-dimensional heat transfer calculation using only the flat top and bottom surfaces of the PCM blanks for heat transfer, is given by:

$$\tau = \frac{\rho_s\,(\Delta H_{fs})}{|T_m - \overline{T}_f|} \left(\frac{a^2}{8\,k_s} + \frac{a}{h} \right)$$

Where $\overline{T}_f$ is the mean fluid temperature and h is the film coefficient for heat transfer to the external PCM surface. For a given τ, this equation may be rearranged to solve for the film coefficient required:

$$h = \frac{a}{2 \left[\frac{(T_m - \overline{T}_f)\,\tau}{\rho_s\,\Delta H_{fs}} - \frac{a^2}{8\,k_s} \right]} \qquad (4\text{-}11)$$

For the Fort Martin feedwater heating case, using the high temperature PCM with a a = 3", and considering the usage mode:

$$h = \frac{3/12}{2 \left[\frac{(725 - 491.2)(6)}{140 \times 197} - \frac{(3/12)^2}{8\,(.90)} \right]} = 2.97 \text{ BTU/hr ft}^2\,{}^\circ\text{F}$$

Flow rates and gap height between planks of the PCM would have to be sized to provide at least this value of film coefficient, but this should be easily accomplished.

The principal disadvantage of this concept is cost of the required pressure vessels. An intermediate low pressure circulating gas loop might be considered to eliminate the pressure vessels, but cost of the heat exchangers for such a loop would probably be comparable to the cost of the equivalent boiler capacity being replaced. A better approach, primarily suited to very large TES applications, might be to locate the macroencapsulated PCM in deep underground cavities, taking advantage of lithostatic pressure to substantially reduce pressure vessel costs.

4.5.4 Intermediate Pumped Loop

The use of a low pressure intermediate liquid metal circulating loop is an attractive variation of the baseline tube/shell PCM concept. The low pressure would permit significant reductions in wall thickness for the tubes and shell domes. This would be off-set to some extent by the cost of heat exchangers, pumps, and piping for the liquid metal loop. Heat exchanger bypass lines could be provided in the loop with bypass flow varied to compensate for the variable thermal resistance within the PCM associated with movement of the liquid solid interface. This bypass control should result in more uniform steam and water outlet temperatures.

Film coefficients for circulating liquid metal are very high (of the order of 10^4 BTU/hr $ft^{2}{}^\circ F$) compared to steam and water flow (50 to 10^3 BTU/hr $ft^{2}{}^\circ F$) and these, in turn, are high compared to the equivalent thermal conductance, $k/(a \cdot \ln\ (r/a))$, for the PCM (3-20 BTU/hr $ft^{2}{}^\circ F$). The heat transfer areas required for the heat exchangers can therefore be correspondingly smaller than that of the tube surface area provided in the PCM, providing only that temperature drops on the steam and/or water sides are acceptable.

4.5.5 Fluidized Encapsulated PCM

Microencapsulating the PCM, using particle sizes comparable to that of pulverized coal (e.g., 50-100 μ) is attractive because it eliminates the need for heat exchangers, though this may be off-set by encapsulation cost. The concept is illustrated in Figure 4-33, using a one-bin empty system. For heat storage, cold encapsulated PCM is drawn from a filled bin, entrained by carrier steam, and deposited hot in the next (empty) bin. One bin is depleted as the other fills. When full, valves are adjusted to repeat the process of taking PCM from another cold bin and putting it into the previously emptied bin. Bins

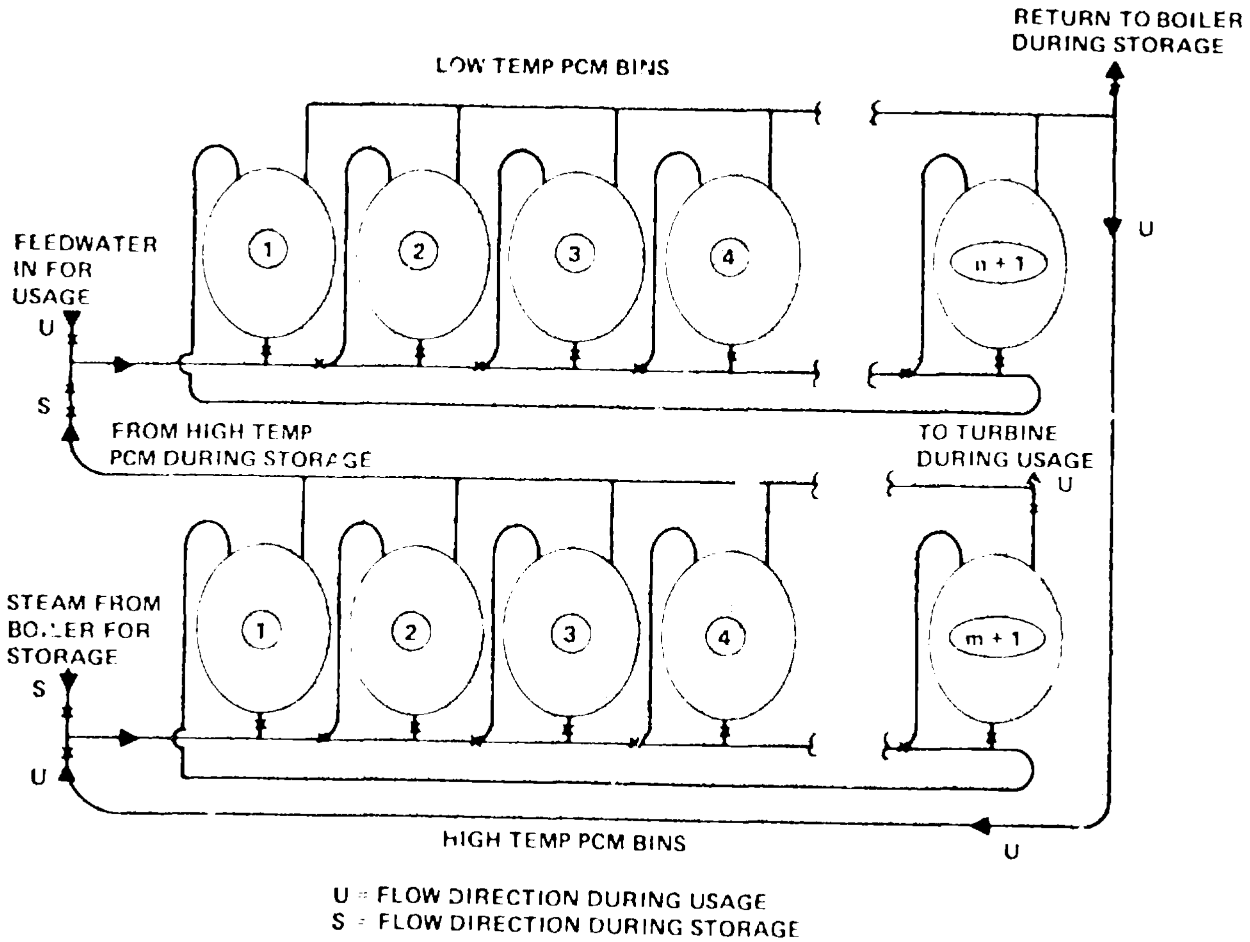

2349-051D

Fig. 4.32 Fluidized Microencapsulated PCM Concept would be large enough to permit particle settling, with the carrier fluid drawn off at the top. For heat removal, the carrier fluid would be liquid water in the feedwater heating case, or liquid evolving to steam in the auxiliary power cycle case. As with the other PCM concepts, several PCM's with different melt temperatures might be used, using separate sets of bins for each PCM, each based on a one-bin-empty concept. The microencapsulated PCM system would differ from a pulverized coal system in having to take full cycle pressure. Provision for bin-to-bin venting would be required to minimize pressure variations during PCM transfer. Also, it would be desirable to have

$$\frac{\dot{m}_{H_2O}}{\dot{m}_{PCM}} = \frac{\Delta H_{fs} + \Delta H_{sensible}}{(\Delta h)_{H_2O}} \tag{4-12}$$

so that all the heat transfer for each PCM could be accomplished with a single entrainment. The sensible energy storage would be greater for microencapsulated PCM than for other concepts, since the PCM would quickly approach the carrier fluid temperature, with negligible exit temperature differences. This permits use of smaller quantities of PCM.

Taking the Ft. Martin feedwater heating case as an example (See Fig. 4-17), using the same carrier fluid temperatures and PCM's for both storage and usage as for the tube/shell case, the high temperature salt (KCl, NaCl, $MgCl_2$) (see Fig. 4-8) would store heat at 800°F, and cool to 514.4°F after giving up its heat. The heat stored would then be:

$$\Delta H_T = c_{p_\ell} (T_{hot} - T_m) + \Delta H_{fs} + c_{p_s} (T_m - T_{cold}) \tag{4-13}$$

$$= 0.248\ (800-725) + 197 + .23\ (725-514.4)$$

or, $\Delta H_T = 264$ BTU/lbm

This compares to 230 BTU/lbm for the same PCM used in the shell and tube heat exchanger. The additional 34 BTU/lbm would reduce the amount of PCM required by 12.9%. For the low temperature PCM (NaCl · $NaNO_3$, see Fig 4-8).

$\Delta H_T = 0.43\ (705-567) + 84 + .44\ (567-487) = 178.5$ BTU/lbm compared with 135.3 BTU/lbm estimated for the shell tube case. The additional 43.2 BTU/lbm would permit a reduction of 24% in the amount of PCM required. No allowance has been taken in these numbers for the sensible heat stored in the encapsulating material. While all systems will have containment material with associated sensible heat storage, the mass of such material may be somewhat larger for microencapsulation than it would be for other concepts.

The ratios of carrier fluid mass flow rate to PCM mass flow rate for this example during storage would be 1.46 and 0.49 for the high and low temperature PCM's, respectively. The low mass ratio for the low temperature PCM could present a design problem (e.g., high pressure drops or two entrainments). During usage, the corresponding carrier fluid flow rate ratios would be 24 and 8.1, which should be adequate. It should be noted that these mass flow ratios would be constant during the storage and usage processes. This may be a significant advantage for the microencapsulation technique when compared to heat-exchanger concepts which require bypass lines and outlet temperature controls.

For the encapsulation process, the PCM may be considered as enclosed in a spherical shell, with internal diameter large enough to accommodate the PCM at its lowest density state (i.e., highest temperature liquid state). Some void volume would exist at all other states. The shell would then have to be thick enough to resist buckling in the high pressure carrier fluid environment, with thickness given by:

$$\frac{t}{r} \approx \sqrt{\frac{5\,(S.F.)\,P}{E}} \tag{4-14}$$

where P is carrier fluid pressure, S.F. is Safety Factor, E is shell material modules of elasticity, and r is shell radius (shell assumed thin). For the Ft. Martin conditions assuming encapsulation with nickel, and using a safety factor of 3,

$$\frac{t}{r} = \left(\frac{5 \times 3 \times 4323}{29 \times 10^6}\right)^{1/2} = .0473$$

For $r = 50\,\mu$, $t = 2.36\,\mu$. If such capsules could be made, the mass, M_e of the encapsulating material required would be given by:

$$\frac{M_e}{M_{PCM}} = \frac{\rho_e}{\rho_{1,\ PCM}} \times \frac{3t}{r} \tag{4-15}$$

For nickel (sp. g. = 8.9) and NaCl · $NaNO_3$ (sg. gr. = 1.88),

$$\frac{M_e}{M_{PCM}} = \frac{8.9}{1.88} \times 3 \times .0473 = 0.671$$

The mass of nickel in this case would be 67% of that of the PCM, and bulk encapsulating material costs would be significantly greater than the PCM costs. Low cost encapsulating materials (perhaps non-metallics) as well as low cost encapsulating process would appear necessary for this concept to be viable.

Fluidizing and entraining the particles is not anticipated as a problem. For turbulent duct flow, with a friction factor of 0.005, carrier fluid velocities for the lowest and highest density fluids (1000°F, 3500 psia steam at 4.86 lbm/ft^3, and 423°F, 4323 psia liquid at 52.6 lbm/ft^3) of 20 and 5 ft/sec, respectively, would appear adequate to entrain 100 μ sized particles in a vertical duct. The corresponding terminal sink velocity of such particles would be approximately 1 and 0.25 ft/sec for low and high density carrier fluids, and adequate residue time would have to be provided in the bins to permit the particles to settle.

The time required for heat transfer should be at least as small as the particle transport time. Most of this time will be associated with the phase change process. An approximate solution for the freezing process, allowing for the temperature rise of the carrier fluid as freezing proceeds, is:

$$t = \frac{1}{3} \left(\frac{\dot{m}_f}{\dot{m}_{PCM}} \right) a \rho_s c_{p_f} \left\{ \left(\frac{a}{k_s} \right) f(\varphi) + \left(\frac{1}{h} + \frac{a}{k_s} \right) \ln \left(1 + \frac{1}{\varphi 3}\right) \right\} \tag{4-16}$$

where,

$$\varphi = \left[\left(\frac{\dot{m}_F}{\dot{m}_{PCM}} \right) c_{p_f} \left(\frac{T_m - T_{fi}}{\Delta H_{fs}} \right) - 1 \right]^{1/3}$$

and,

$$f(\varphi) = \frac{1}{\varphi} \left\{ \frac{1}{2} \ln \frac{(\varphi^2 - \varphi + 1)}{(\varphi + 1)^2} + \sqrt{3} \left[\frac{\pi}{6} - \tan^{-1} \frac{(\varphi - 2)}{(\varphi \sqrt{3})} \right] \right\} \tag{4-17}$$

For the Fort Martin case the freezing times for the high and low temperature PCM's would be 0.35 and 0.27 seconds, respectively. With a carrier fluid velocity of 5 ft/sec, heat transfer would occur over distances less than two feet, which is well under the flow lengths required for bin-to-bin mass transfer. Hence, no additional residence time would be required for the heat transfer process.

From a safety point of view, microencapsulation presents two problems, failure of encapsulating shells and failure of the pressurized bins. Encapsulating shell failure would release small quantities of PCM which could react with carrier fluid, with some particle agglomeration probable. Use of relatively course mesh screens or periodic bin cleaning might be required. Bin structural failure, as with any pressure vessel, is a serious problem, but only the void volume in the bin would contain high pressure fluid capable of contributing work of expansion. Also, the encapsulated particles should present somewhat less hazard than the bulk PCM.

Major drawbacks of the microencapsulated system are unknowns associated with materials and processes for encapsulation. If encapsulated PCM could be provided at moderate cost (~ $1/lbm), the system would be more attractive but would still result in added cost for pressure vessel and high pressure valves. Development of hardware and flow relations associated with handling microencapsulated PCM are not trivial problems, but appear soluable with straight forward engineering effort. This would only be warranted, however, if the encapsulation problems were solved.

4.5.6 Moving PCM Concept

The moving PCM concept attempts to minimize required heat transfer surface area by eliminating most of the thermal resistance within the PCM. The liquid-solid interface is always kept close to the heat transfer surface. This concept is illustrated schematically in Figure 4-34. During usage, liquid PCM flow through slit nozzles on to rotating drums. The heat sink fluid flows through the drums, cooling the surfaces and freezing the PCM. The solid PCM is scraped off after making a partial rotation, falling into a storage bin. For heat storage, the source fluid is fed through heat exchangers located at the bottom of the bin which has a pitched floor arranged so that the PCM drains off as it melts. The liquid PCM is pumped into an insulated storage tank until needed for the usage part of the cycle.

Many heat exchanger manufacturers were contacted during this study to obtain information on rotating drum heat exchangers and available hardware. This effort was largely unsuccessful. Most manufacturers felt that special equipment whould have to be developed for this application. Accordingly, what follows is a discussion of heat exchanger characteristics essentially developed from basic principles.

For the drum freezing process the PCM thickness, δ , which can be frozen during rotation through an angle θ (less than 2π), at a rotational speed, Ω , neglecting sensible energy contributions and assuming one-dimensional heat transfer, may be approximated by the relation:

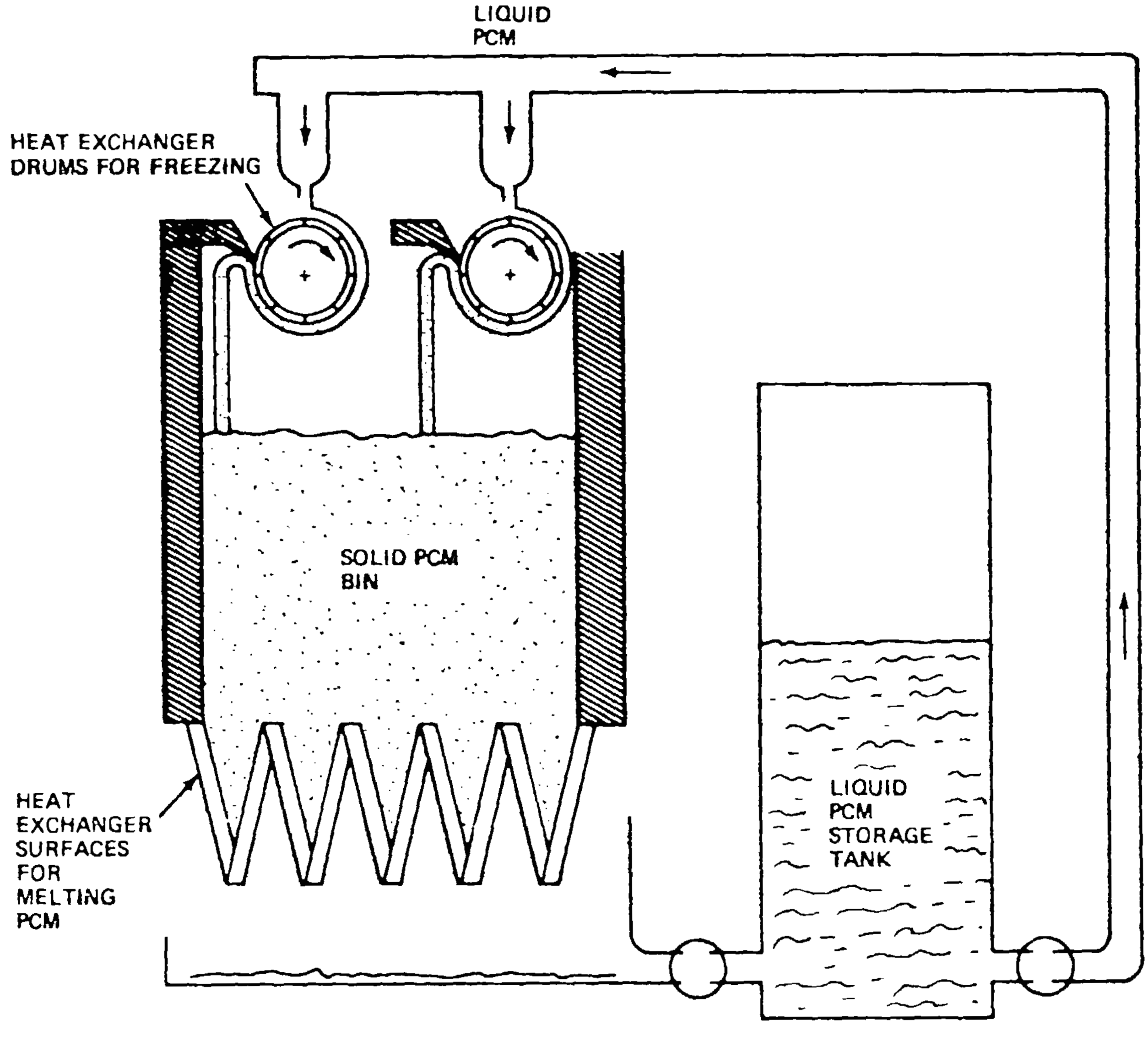

Fig. 4-34 Moving PCM Concept - Schematic

$$\delta = \frac{k_s}{U}\left[\sqrt{1 + \frac{B}{\Omega}} - 1\right] \tag{4-18}$$

where, $B = \frac{2U^2}{k_s} \; \frac{(T_m - \overline{T}_f)\,\theta}{\rho_s \;\; \Delta H_{fs}}$

and, $\frac{1}{U} = \frac{1}{h} + \frac{t_w}{k_w}$

with,

h = sink fluid film coefficient

t_w = drum wall thickness

k_w = drum wall thermal conductivity

T_f = mean sink fluid temperature

The rate at which PCM can be frozen by an individual drum of length, L, and radius, R, is then:

$$\dot{m} = \rho_s \, LR\Omega\delta$$

or, $\dot{m} = \rho_s LR \, \frac{k_s}{U}\,\Omega \left[\sqrt{1 + \frac{B}{\Omega}} \;\; -1\right]$

from which it can be seen that the mass freezing rate, $\dot{m}$, increases monotonically with Ω, asymptotically approaching an upper limit:

$$\dot{m}_{\Omega \to \infty} = \rho_s \, LR \, \frac{B}{2} \, \frac{k_s}{U} = \frac{L\,R\,U\,(T_m - \overline{T}_f)\theta}{\Delta H_{fs}} \tag{4-19}$$

High values of U and θ are clearly desireable. Some drum manufacturers have expressed doubts that the solidified PCM will adhere to a stainless steel surface. In the calculations which follow, θ has been taken as $3\,\pi/2$, assuming liquid to be supplied to the drum somewhat before top center, and removed somewhat after bottom center. Special techniques to assure adhesion may be required to accomplish this.

To obtain high values of U, we need high values of h and a relatively thin wall, t_w. This can be accomplished by putting the sink fluid through multiple passages adjacent to the drum surface, using many stiffening ribs, as shown in Figure 4-35. The drum surface will tend to bulge outward between the ribs due to high sink fluid pressure. The deflection, δ_w, for given rib spacing, wall thickness and sink fluid pressure is

$$\delta_w = \frac{p \ell^4}{32 E t_w^3} \qquad (4\text{-}20)$$

For specified values of δ_w and t_w, this expression can be rearranged to compute the rib spacing, ℓ.

To provide some information on the size and performance of the rollers and bin bottom heat exchangers for this concept, limited calculations were performed applying this concept to the high temperature salt used in the Ft. Martin feedwater heating case. Some representative numbers, taken from the tube-shell study, are given below for the salt and the source and sink fluids:

(1) Salt: $KCl \cdot NaCl \cdot MgCl_2$ eutectic

$T_m = 725°F$

$\Delta H_{fs} = 197$ BTU/lbm

$\rho_s = 140$ lbm/ft^3

$k_s = 0.90$ BTU/hr ft °F

$M_T = 1.68 \times 10^6$ lbm

(2) Heat Sink Fluid: Feedwater,

$T_{in} = 487°F$

$T_{out} = 514.4°F$

$p = 4323$ psia

$\dot{m}_f = 2.217 \times 10^6$ lbm/hr

Six-hour usage period

(3) Heat Source Fluid: Steam

T_{in} = 1000°F

T_{out} = 800°F

p = 4200 psia

$\dot{m}_f$ = 134,162 lbm/hr

Eighteen hour storage period

For this case, a roller design was developed, not optimized, as follows (see Figure 4-35.

No. of rollers = 20

Roller Radius, R = 6"

Roller Length, L = 12'

Wall thickness, t_w = 0.120"

Rib thickness, t_f = 0.235"

No. of ribs = 36

Rib Span, = 0.812"

Passage height, S = 0.24"

With feedwater flowing through the rollers in parallel, the flow velocity would be nearly 13 ft/sec, providing a film coefficient, h = 5460 BTU/hr ft^{2}°F, with a pressure drop of about 5 psia. The overall coefficient of heat transfer is about 570 BTU/hr ft^{2}°F. If the rollers rotate at 30 RPM, and the PCM adheres over 3/4 of the circumference ($\theta = \frac{3\pi}{2}$), it should be possible to freeze a layer of PCM with thickness δ = 0.021". The amount of PCM solidified is then approximately 1200 lbm/hr/ft of roller length, and the rollers would have to be 11.6 ft. long to solidify all the PCM in the 6 hour period. Bulging of the roller surface, δ_w, should be only a little more than .001" due to the high pressure of the feedwater, and should not present a problem in stripping off the solidified PCM.

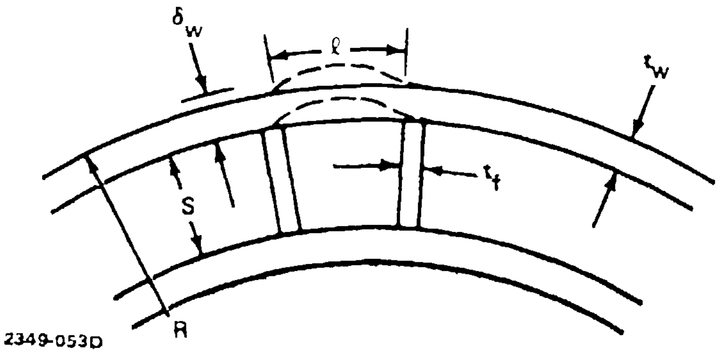

Fig. 4-35 Drum Heat Exchanger Schematic

For the bottom heat exchanger used to melt the PCM, a passage geometry similar to that used on the roller was assumed. Since the steam is under high pressure similar to that of the feedwater, at a steam velocity of 20 ft/sec, the steam side film coefficient would be approximately 465 BTU/hr ft$^{2\circ}$F. At this team velocity, approximately 265 channels, corresponding to a width exceeding 23 ft would be required to handle the total steam flow. The log mean temperature difference for storing the heat is about 154°F, and the heat transfer rate needed is about 7.33×10^7 BTU/hr, hence the heat transfer surface area required is about 1640 ft^2. Given the width of 23 ft, the length would have to be about 71 ft. The steam pressure drop associated with this length would be about 10 psi, which should be acceptable.

Bin dimensions must be established to fit this heat exchanger into the bin. The mass of PCM requires a volume of 12,000 ft^3. Allowing some void volume, this could be provided by a 24 ft. cube. The bottom heat exchanger could then be made up of 48 panels, each 1.5 ft. wide by 24 ft. long, arranged in accordion fashion as indicated in Figure 4-34. Panels would be divided into 3 sets of 16 each. Steam would flow in parallel through the 16 panels of each set, and in series through the 3 sets. The panels would have a slight longitudinal pitch so that liquid would be drawn off by gravity as it formed. The solid would be forced against the panel surfaces by gravity.

This rotating drum concept has several advantages over the other concepts discussed, as it minimizes the high pressure heat exchanger surface area, while permitting a low pressure PCM storage vessel. The principal disadvantage is mechanical design of the rotating drum, which requires rotating seals for the high pressure sink fluid. The seals could be pressurized with the same inert gas used to provide blanket pressure over the PCM, but some of this gas would then enter the sink fluid and have to be removed by the condenser air removal system. Alternatively, a seal scavenging system might be used to remove any water or steam leakage before it could contaminate the PCM. In addition, there are several other moving heat exchanger concepts which eliminate the seal problem but introduce other mechanical design problems. If rotating heat exchangers were available, the moving PCM concepts would be very attractive, and might well be the lowest cost approach for utilizing latent heat TES.

4.6 FINAL PCM SELECTION FOR PLANT/CYCLE LOCATIONS

Initially, the quantity of salt required was calculated based on the latent heat stored. However, it was shown that the sensible heat contribution would be significant (~30%). Hence, a more refined procedure was required in order to select the final quantity of salt required. To select a salt for a given application, it is necessary to know the temperatures at which energy is available or must be delivered. Salts must be chosen which allow sufficient temperature difference (ΔT) between the fluid flow temperature and the salt melt temperature for both the storage and usage parts of the cycle. As an illustration of our final salt selection process, consider the Ft. Martin feedwater heating and auxiliary power generation cases:

Figure 4-36 shows the flow stream temperature as a function of percent of total energy for these cases. Also shown are selected salts. These salts were chosen from the list of recommended salts in Fig. 4-8 on the basis of melting points, allowing sufficient temperature differences between the melt point and the flow temperature to affect heat transfer. Where more than one salt could have been chosen, the cheaper salt, on an energy stored/cost basis, was chosen. From the salt melt temperature the total percentage of energy which can be stored in each salt can be found directly. As shown, 33% of the total energy will be stored in the high temperature salt and 67% in the low temperature salt for the feedwater heating case.

For the shell and tube designs energy will be stored as both sensible and latent heat. In order to estimate the total mass of salt needed, the contributions of each type must be taken into account. In order to do this an estimate of the salt temperature profile at the end of the usage period and at the end of the storage period was made. The general procedure used was as follows:

- From inlet and outlet temperatures and enthalpies, salts were selected and a percentage of the total energy stored was assigned to each salt (as shown in Figure 4-36).
- The "average" salt temperature was determined assuming that the salt average temperature profile follows the fluid stream temperature profile and that the difference between them is equal to the difference between the salt melt point and the fluid temperature closest to the salt melt point.
- The total available latent and sensible storage capacities for each salt was then calculated.
- The weights of each salt were determined.

ORIGINAL PAGE IS OF POOR QUALITY

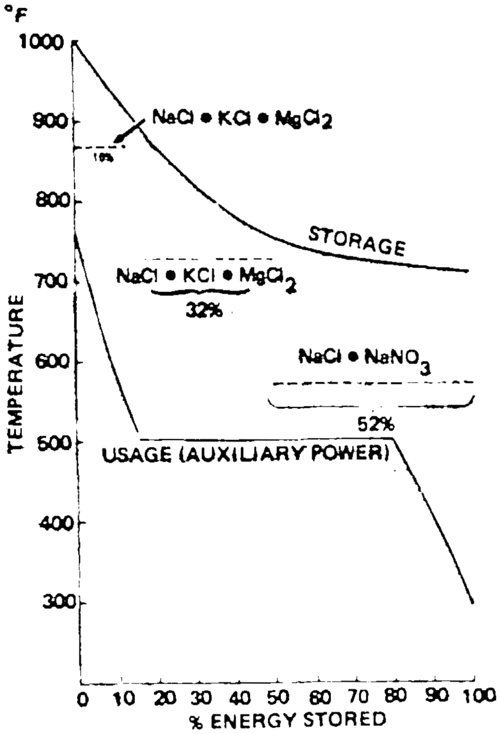

(a) AUXILIARY POWER SUPPLY (C8)

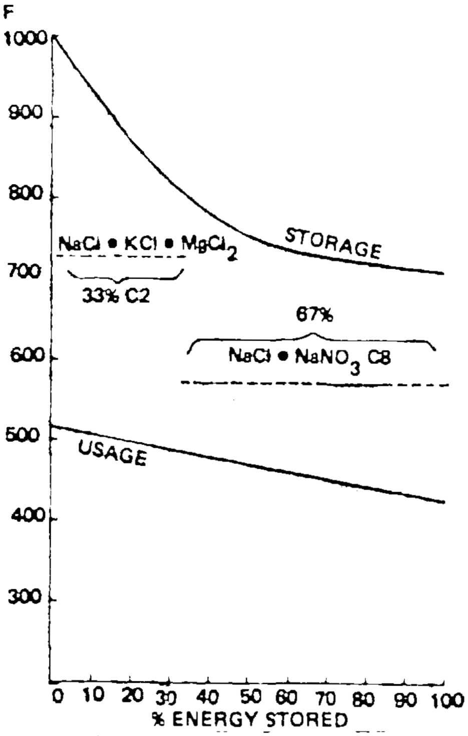

(b) FEEDWATER HEATING (C2)

Fig. 4-36 Energy Storage and Usage vs. Temperature Ft. Martin Plant

2349-054D

As stated, it was assumed that average salt temperature would follow fluid temperature. Therefore, the difference between salt temperature at the maximum radius (tube spacing/2) and the fluid stream was a constant, being equal to the minimum fluid temperature in the module minus the salt melt temperature. From the average salt temperature the total available energy per unit mass of salt was calculated as follows:

$$Q_{available} = \Delta H_{fs} + c_{p,s}(T_m - T_s) + c_{p,\ell}(T_\ell - T_m) \qquad (4\text{-}21)$$

where

T_m = salt melt temperature

T_s = average solid salt temperature

T_ℓ = average liquid salt temperature

$c_{p,s}$, $c_{p,\ell}$ = solid and liquid salt specific heats

ΔH_{fs} = Salt Latent Heat of Fusion

For example, during the storage period of the Ft. Martin feedwater heating case, the salt will extract heat from superheated steam, cooling it from 1000°F to 705°F. The high temperature salt will extract 33% of this energy bringing the steam down to a temperature of 800°F. At the exit of this module, therefore, assuming that the salt at the mid-point between the tubes is at the melting temperature (725°F), a maximum temperature difference of 75°F is developed. Hence, based on our earlier assumption, a constant temperature difference of 75°F is assumed between the fluid steam and salt at this radial position throughout the module. Therefore, the salt temperature at the module inlet will be 925°F (1000 - 75°F).

The "average" salt temperature was then set equal to the average steam temperature (900°F) minus 1/2 of the difference between the steam and salt outer radius temperatures (75°F); i.e., average salt temperature is

$$T_{salt} = 900° - 75/2 = 862.5°F$$

Hence, for a specific heat of .24 BTU/lbm°F, a sensible contribution of 33 BTU/lbm was calculated. Appendix E presents a complete description of these design calculations for the Ft. Martin and Roseton cases. Fig. 4-37 summarizes the total salts required for each of these plants as determined by this procedure.

As shown in the following section, the other plants under consideration were eliminated for other reasons. Therefore, we did not perform similar detailed calculations for them. However, as part of our screening process we did select salts and perform an economic evaluation for each of the remaining plant/concepts.

System	Total Energy Stored x 10^9 BTU	Salt		Energy (%)
		Type	Amount 10^6 LB	
Fort Martin	1.319	$KCl \bullet NaCl \bullet MgCl_2$ (14.5/22.3/63.2)	1.68	33
(Feedwater Htg)		$NaCl \bullet NaNO_3$ (4.6/95.4)	5.32	67
Fort Martin	1.791	$CaCl_2 \bullet KCl \bullet NaCl$ (64.5/6.5/29)	1.53	16
(Aux Pwr System)		$KCl \bullet NaCl \bullet MgCl_2$ (14.5/22.3/63.2)	2.35	32
		$NaCl \bullet NaNO_3$ (4.6/95.4)	5.04	52
Roseton (Feedwater Htg)	1.462	$NaCl \bullet NaNO_3$ (4.6/95.4)	6.82	100
Roseton	1.869	$NaCl \bullet BaCl_2 \bullet MgCl_2$		
		(28.4/31.8/39.8)	1.53	16
(Aux Pwr Sys)		$NaNO_3$	8.00	84

2349-055D

Fig. 4-37 Salt Amounts for Tube and Shell TES Units

4.7 PERFORMANCE/COST SCREENING OF CONCEPTS

4.7.1 Recommended Plant and Cycle Locations

Initially we considered using only the sensible heat of the steam for charging the TES units, but flow rates to the TES units could be reduced considerably if latent as well as sensible heat was utilized. The method of condensing charging steam changed the appearance of the various concepts in that fluid leaving the TES after charging was liquid, not vapor, and this made it necessary to find a method to dispose of this high pressure liquid source. It was then decided to utilize a pressure control valve to reduce the flow stream pressure. The fluid became two-phase after the valve and a flash tank was utilized to separate vapor and liquid. From there this vapor and liquid were directed to a high pressure feedwater heater. A schematic representation of this process appears in Figure 4-38.

Next, the ten candidate cases were re-examined in more detail in order to determine if there were any remaining technical or economic problems to be overcome. Heat exchanger temperature/energy profiles were drawn (Figures 4-39) for the ten cases and various problems appeared. For example Case A4 (Case designations are derived from Power Plant/TES Location Matrix in Figure 3-3) had only a 50°F temperature difference on one side of the heat exchanger. Also, information from turbine vendors revealed that the application of super-heat to low pressure turbines could not be tolerated for extended periods of time because of choking of the lowest pressure stages. This also applied to Case B4. The heat exchanger curve for Case C2 revealed that the pressure chosen for condensing hot reheat steam was too low. Condensing at this pressure resulted in a low condensing temperature. This caused a temperature crossover in the heat exchanger curve where the fluid to be heated during peaking would actually lose heat. The same problem existed in several other cases. To eliminate this problem it was decided that the highest pressure steam available should be used to charge the TES units. Condensing of this fluid, which occurs in the TES unit, was to take place at the highest possible pressure with its corresponding high saturation temperature. Since Cases A4, B2, B4 and B6 had no higher pressure steam supplies and due to the various problems inherently associated with nuclear plants, such as shielding of the TES units, licensing difficulties, and choking of the last stage turbine group, these cases were omitted from further consideration. Also Cases D2 and D8 were eliminated from further consideration when it was discovered that Ft. St. Vrain, a unique installation, was not operating at the time because of reactor plant modifications. This left four cases to be analyzed in further detail, namely Ft. Martin and Roseton Single Loop Regenerative Heating Augmentation and Single Loop Separate Power Conversion Loop cases.

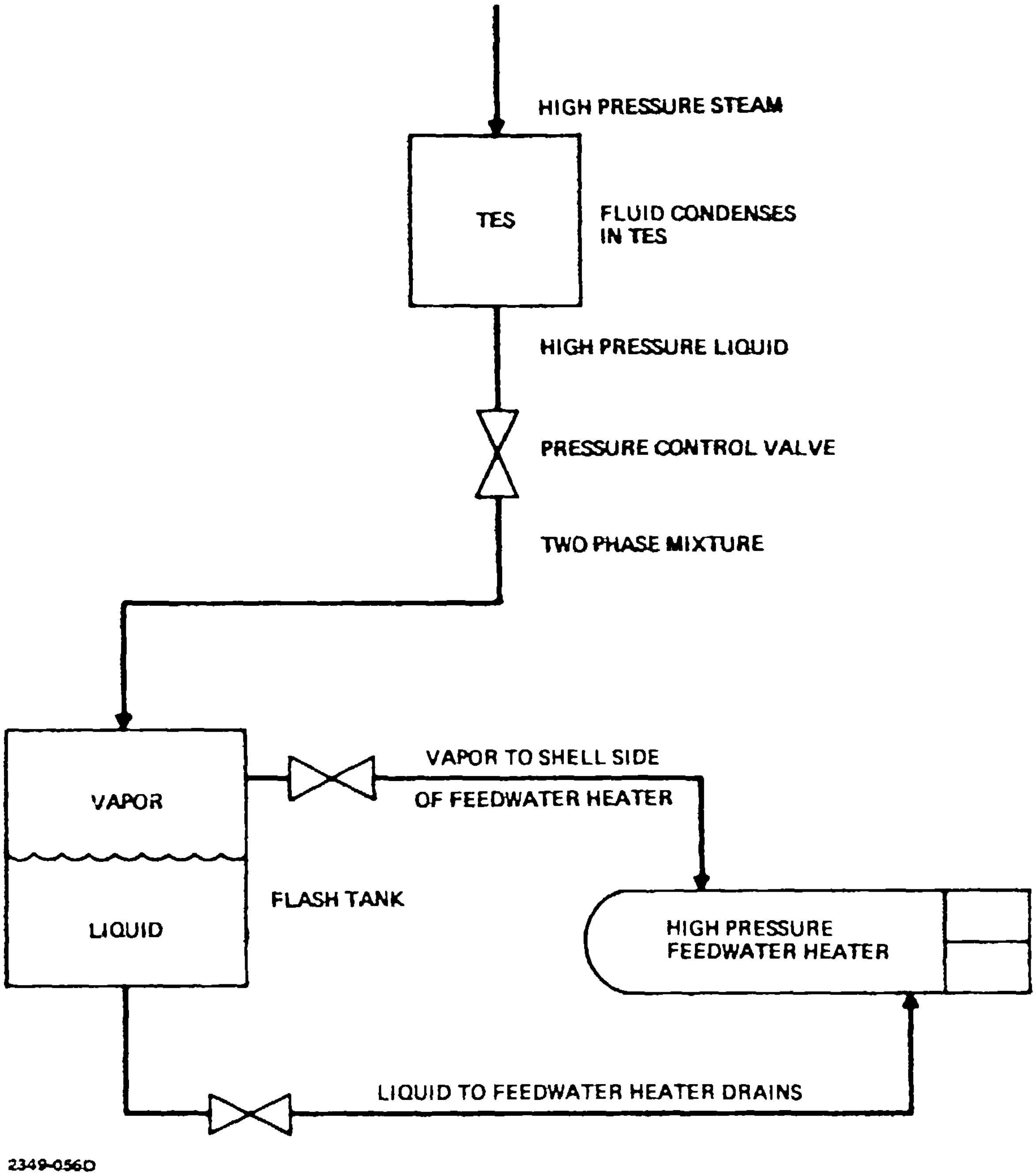

Fig. 4-36 Schematic of TES Sysem Utilizing Steam Latent Heat

CASE A4

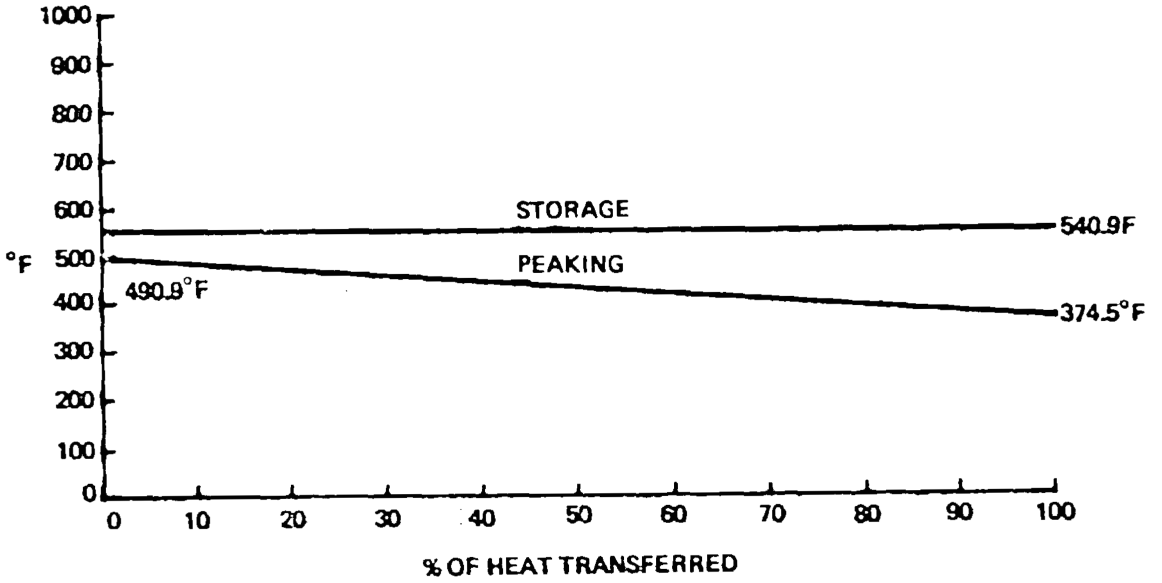

CASE B2

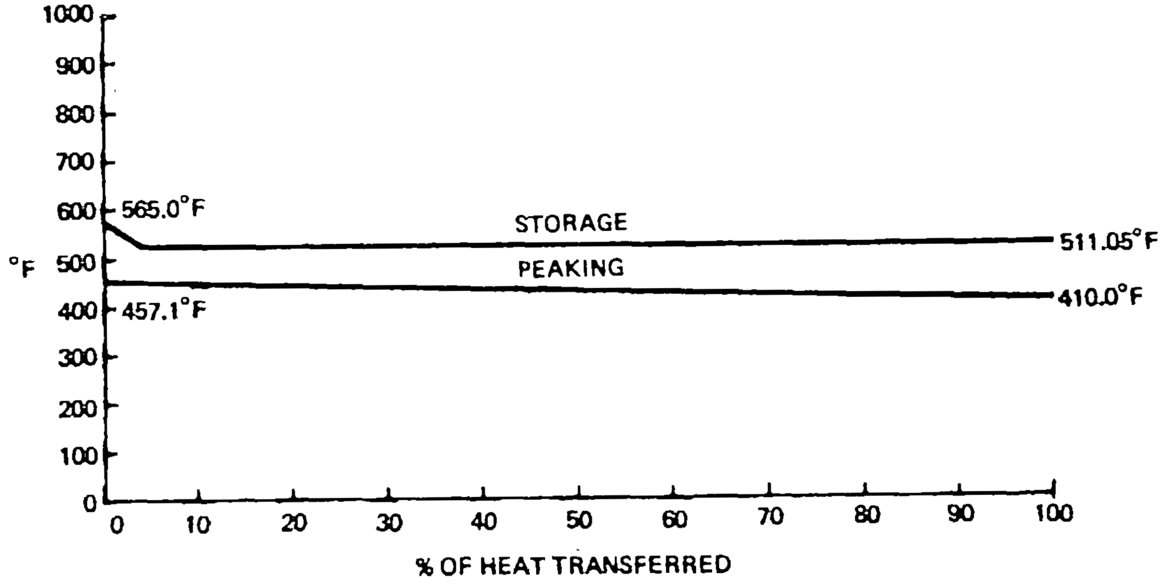

2349-057D

Fig. 4-39 Heat Exchanger Temperature/Energy Profile

CASE B4

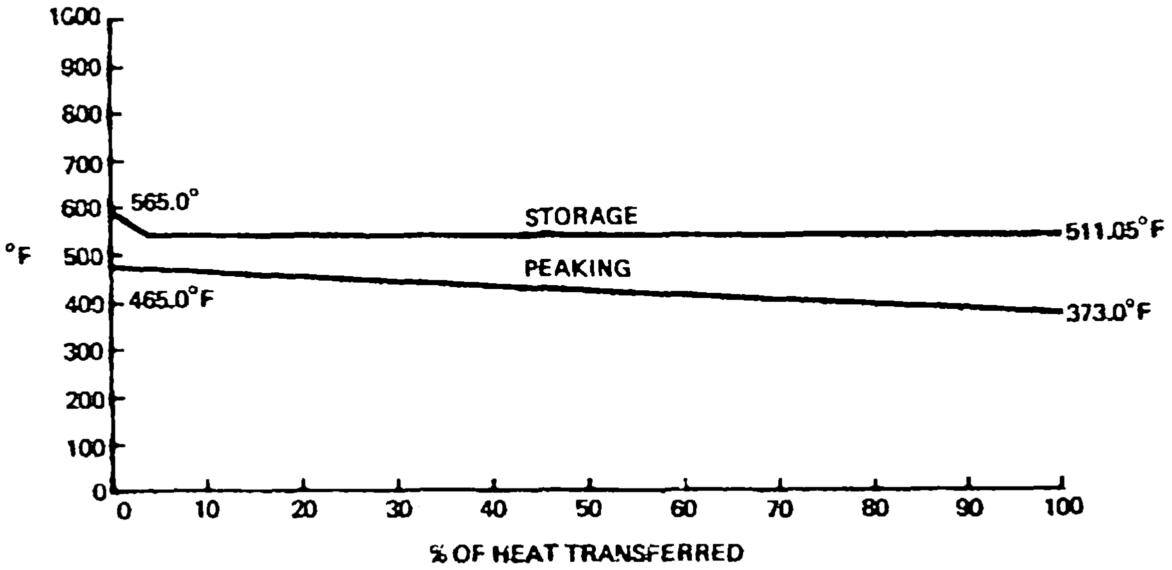

CASE B6

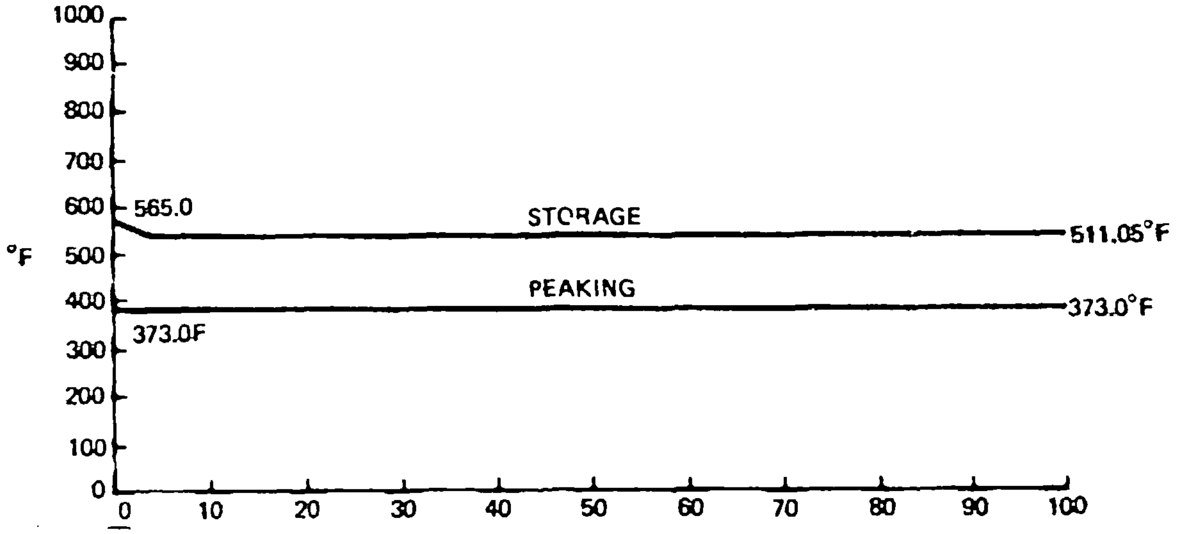

2349-058D

Fig. 4-39 Heat Exchanger Temperature/Energy Profile (Cont'd)

CASE C2

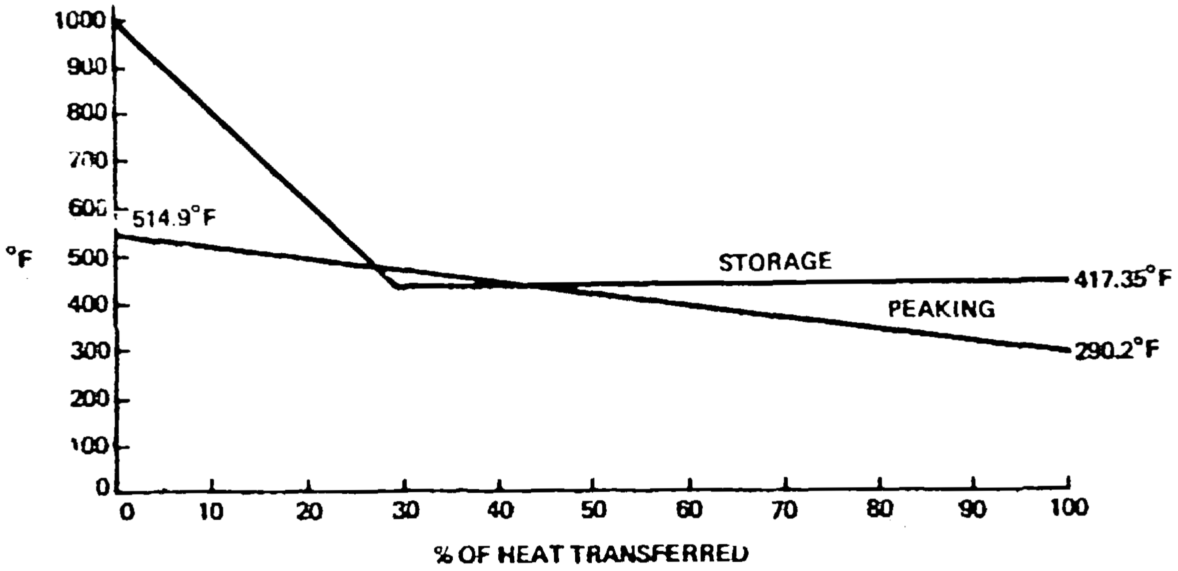

CASE C8

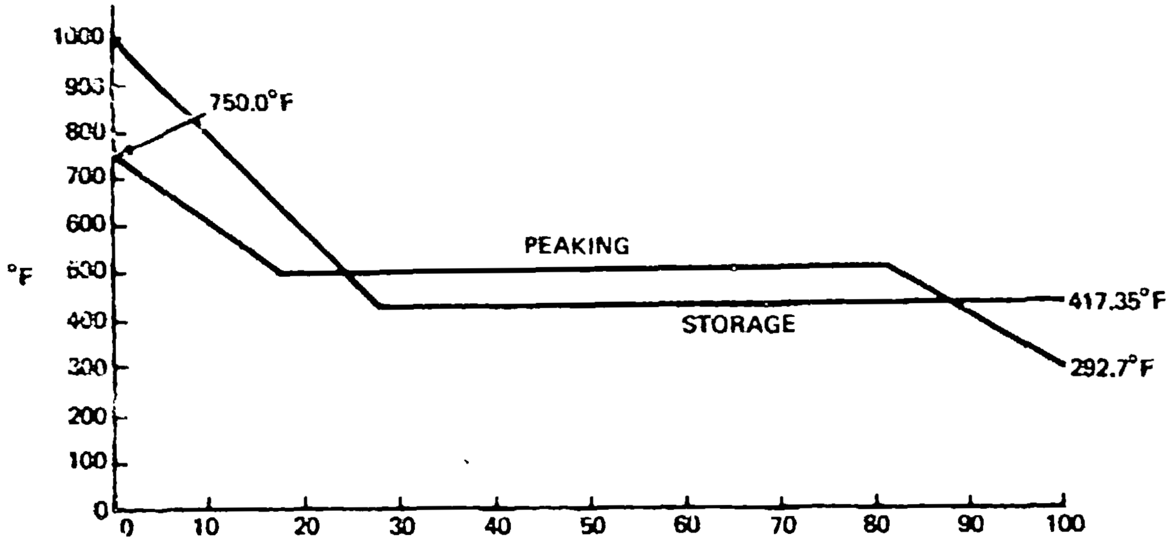

2349-0590 **Fig. 4-39 Heat Exchanger Temperature/Energy Profile (Cont'd)**

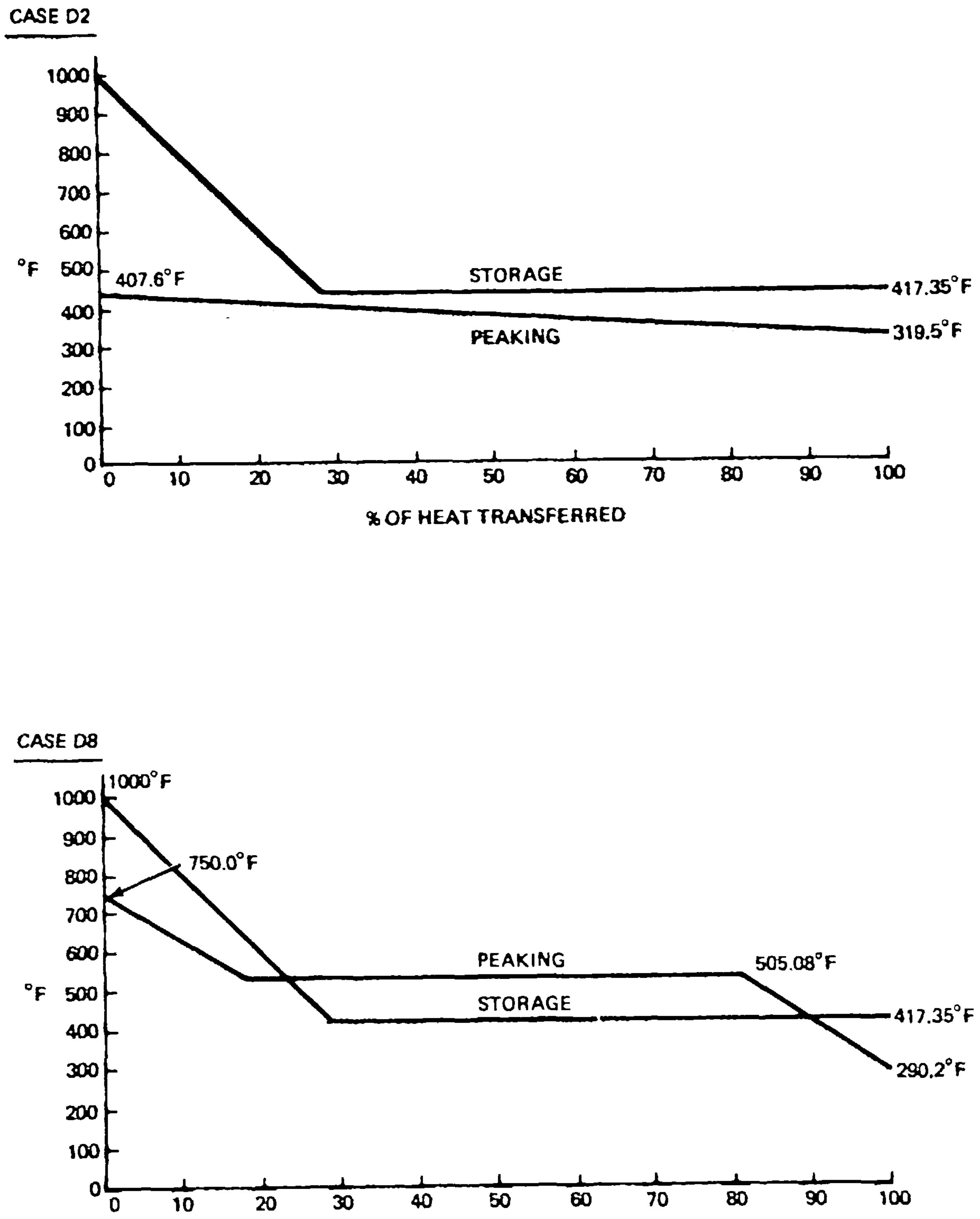

2349-060D

Fig. 4-39 Heat Exchanger Temperature/Energy Profile (Cont'd)

CASE E2

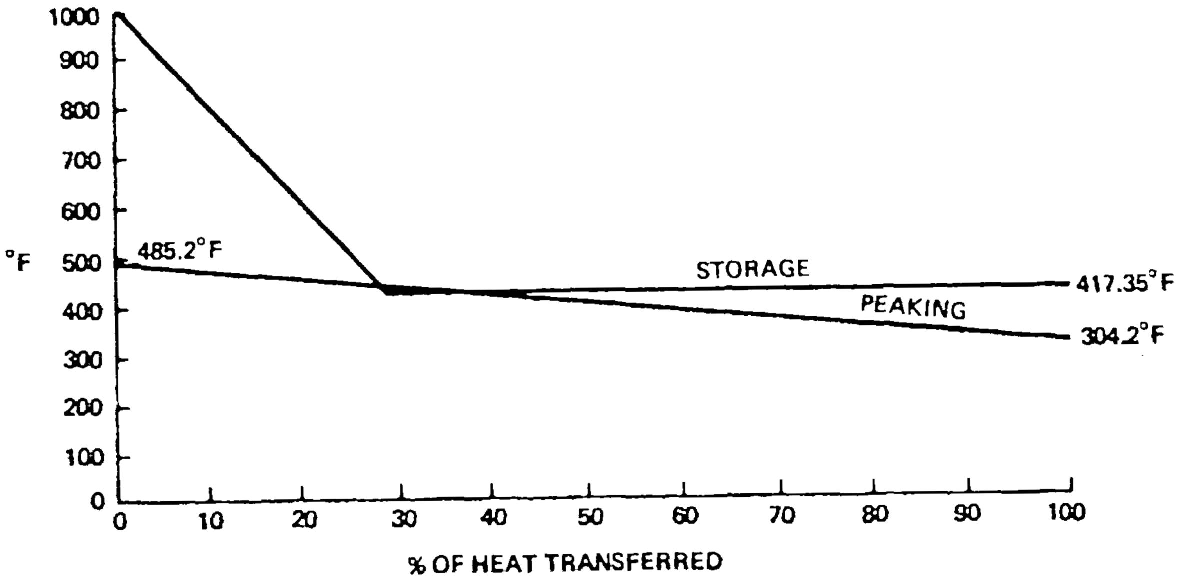

CASE E8

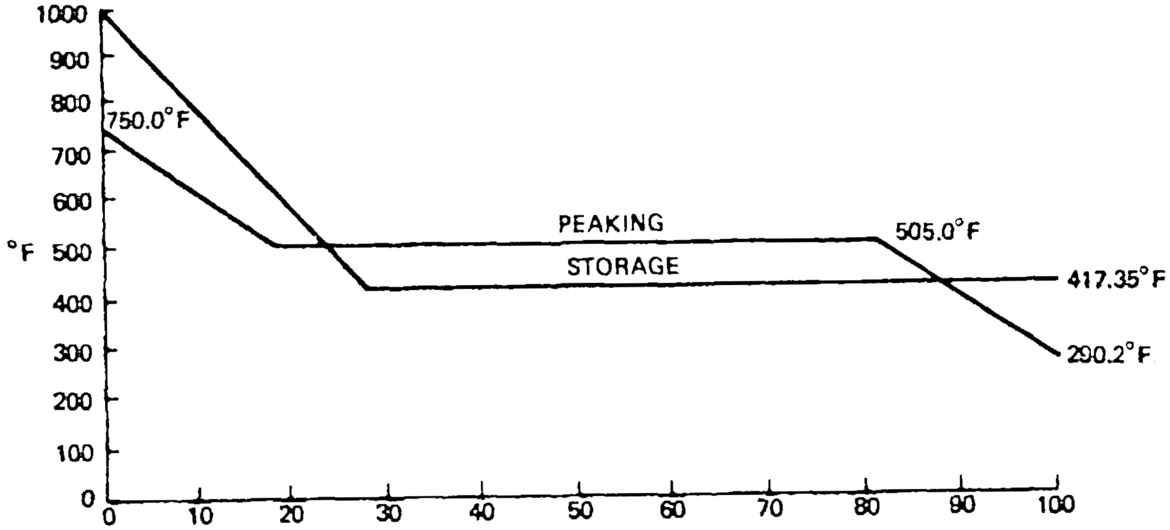

2349-061D Fig. 4-39 Heat Exchanger Temperature/Energy Profile (Cont'd)

The use of throttle steam to provide energy to the TES units made it possible to raise the condensing temperature. This in turn increased minimum temperature differences in the TES units. New flow rates were then calculated (Figure 4-40) and new heat exchanger diagrams were drawn (Figure 4-41) corresponding to the new steam and liquid conditions. This increased the minimum temperature difference (in any of the four remaining cases) to 144°F, which was acceptable.

At this time a heat balance computer analysis was made for both Cases C2 and C8.* That is, all heat and mass components were balanced under the prescribed operation conditions. This was done to determine the off-design performance of the power plant with and without the inclusion of TES.

It became apparent in Case C2 (the Single Loop Regenerative Heating Case) that with three feedwater heaters removed from service more than the 5% additional peaking was produced. Also, the low pressure turbine stage group was experiencing choked flow. Subsequent computer analyses revealed that to produce only the additional 5% peaking, only 60% of the flow to the highest temperature heater needed to be bypassed to TES during peaking. Using this criterion, heat balances were done in both peaking and storage modes. The Single Loop Separate Power Conversion Loop for Ft. Martin (Case C8) was within acceptable limits in the original computer runs and flow rates to the TES units during peaking and storage were not altered. The new flow rates for Case C2 are included in Figure 4-42. The heat balances for the Ft. Martin base plant and for both feedwater heating and separate cycle TES modes are included in Figures 4-43 through 4-47. A summary of the net plant heat rates (NPHR) for Ft. Martin is presented in Figure 4-48.

As shown in Figure 4-48, it is obvious that there would be a penalty for operating a base plant with TES as a peaking unit in comparison with steady 100% operation of the base plant. The increase in daily average heat rates for cases C2 and C8 can be translated into additional fuel consumption. Based on a heating value of 12,075 BTU/lb for West Virginia coal, Case C2 would consume an additional 9,107 tons of coal per year and Case C8 would consume an additional 16,134 tons of coal. Using a cost of $1.25 per 10^6 BTUs for this coal the additional fuel consumption translated into an additional expense of $275,140 and $487,450 respectively. If the plant without TES were to be operated as a peaking plant the daily average heat rate would have been calculated for the plant operating at 77.4% output for 18 hours and at 100% output for 6 hours. This would produce the same daily generation as Cases C2 and C8. The corresponding net plant heat rates are 8950 BTU/KWHR and 8838 BTU/KWHR,

*Ft. Martin, feedwater Heating (C2) & Auxiliary Power (C8) - See fig. 3-3

CASE: C2 (3 HEATERS REMOVED FROM SERVICE, WITH CONDENSING OCCURING @ 3200 PSIA

PEAKING

T_{pi}	=	290.	°F
P_{pi}	=	4323.0	Psia
h_{pi}	=	267.8	BTU/lbm
T_{po}	=	514.4	°F
P_{po}	=	4323.0	Psia
h_{po}	=	504.0	BTU/lbm
F_p	=	3694.940	lbm/hr
t_p	=	6	hr

STORAGE

T_{si}	=	1000.0	°F
P_{si}	=	3500.0	Psia
h_{si}	=	1421.7	BTU/lbm
T_{so}	=	705.08	°F
P_{so}	=	3200.0	Psia
h_{so}	=	875.5	BTU/lbm
t_s	=	18	hr

$$Q = F_p\,(h_{po} - h_{pi})\,t_p = 3{,}694{,}940\,\frac{\text{lbm}}{\text{hr}}\;504.0\left(\frac{\text{BTU}}{\text{lbm}} - 267.8\,\frac{\text{BTU}}{\text{lbm}}\right)6\ \text{hr}$$

$$\boxed{Q = 5.2365 \times 10^9\ \text{BTUs}}$$

$$F_s = \frac{Q}{(h_{si} - h_{so})\,t_s} = \frac{5.2365 \times 10^9\ \text{BTU}_s}{\left(1421.7\,\frac{\text{BTU}}{\text{lbm}} - 876.5\,\frac{\text{BTU}}{\text{lbm}}\right)18\ \text{hr}}$$

$$\boxed{F_S = 532{,}616\ \text{LBM/HR}}$$

CASE: C8 (5% PEAK SHAVING, WITH CONDENSING AT 3200 PSIA)

PEAKING

T_{pi}	=	294.02	°F
P_{pi}	=	715.0	Psia
h_{pi}	=	264.8	BTU/lbm
T_{po}	=	750.0	°F
P_{po}	=	615.0	Psia
h_{po}	=	1380.05	BTU/lbm
F_p	=	267,834	lbm/hr
t_p	=	6	hr

STORAGE

T_{si}	=	1000.0	°F
P_{si}	=	3500.0	Psia
h_{si}	=	1421.7	BTU/lbm
T_{so}	=	705.08	°F
P_{so}	=	3200.0	Psia
h_{so}	=	875.5	BTU/lbm
t_s	=	18	hr

$$Q = F_p\,(h_{po} - h_{pi})\,t_p = 257{,}834\,\frac{\text{lbm}}{\text{hr}}\left(1380.05\,\frac{\text{BTU}}{\text{lbm}} - 164.8\,\frac{\text{BTU}}{\text{lbm}}\right)6\ \text{hr}$$

$$\boxed{Q = 1{,}7922 \times 10^9\ \text{BTUs}}$$

$$F_s = \frac{Q}{(h_{si} - h_{so})\,t_s} = \frac{1.7922 \times 10^9\ \text{BTUs}}{\left(1421.7\,\frac{\text{BTU}}{\text{lbm}} - 876.5\,\frac{\text{BTU}}{\text{lbm}}\right)18\ \text{hr}}$$

$$\boxed{F_S = 182{,}290\ \text{LBM/HR}}$$

2349-062D

Fig. 4-40 Revised Flow Rates for Recommended Four Plant Cycle Locations

CASE: E2

PEAKING

T_{pi}	= 304.2	°F
P_{pi}	= 3000.0	Psia
h_{pi}	= 278.6	BTU/lbm
T_{po}	= 485.2	°F
P_{po}	= 3000.0	Psia
h_{po}	= 470.8	BTU/lbm
F_p	= 3,948,017	lbm/hr
t_p	= 6	hr

STORAGE

T_{si}	= 1000.0	°F
P_{si}	= 2400.0	Psia
h_{si}	= 1461.3	BTU/lbm
T_{so}	= 649.45	°F
P_{so}	= 2200.0	Psia
h_{so}	= 695.5	BTU/lbm
t_s	= 18	hr

$$Q = F_p\,(h_{po} - h_{pi})\,t_p = 3{,}948{,}017\ \frac{\text{lbm}}{\text{hr}}\left(470.8\ \frac{\text{BTU}}{\text{lbm}} - 279.5\ \frac{\text{BTU}}{\text{lbm}}\right)6\ \text{hr}$$

$$\boxed{Q = 4.5315 \times 10^9\ \text{BTUs}}$$

$$F_s = \frac{Q}{(h_{si} - h_{so})\,t_s} = \frac{4.5315 \times 10^9\ \text{BTUs}}{\left(1461.3\ \frac{\text{BTU}}{\text{lbm}} - 695.5\ \frac{\text{BTU}}{\text{lbm}}\right)18\ \text{hr}}$$

$$\boxed{F_S = 328{,}744\ \text{LBM/HR}}$$

CASE: E8

PEAKING

T_{pi}	= 294.02	°F
P_{pi}	= 715.0	Psia
h_{pi}	= 264.8	BTU/lbm
T_{po}	= 750.0	°F
P_{po}	= 615.0	Psia
h_{po}	= 1380.05	BTU/lbm
F_p	= 300,000	lbm/hr
t_p	= 6	hr

STORAGE

T_{si}	= 1000.0	°F
P_{si}	= 2400.0	Psia
h_{si}	= 1461.3	BTU/lbm
T_{so}	= 649.45	°F
P_{so}	= 2200.0	Psia
h_{so}	= 695.5	BTU/lbm
t_s	= 18	hr

$$Q = F_p\,(h_{po} - h_{pi})\,t_p = 300{,}000\ \frac{\text{lbm}}{\text{hr}}\left(1380.04\ \frac{\text{BTU}}{\text{lbm}} - 264.8\ \frac{\text{BTU}}{\text{lbm}}\right)6\ \text{hr}$$

$$\boxed{Q = 2.0075 \times 10^9\ \text{BTUs}}$$

$$F_s = \frac{Q}{(h_{si} - h_{so})\,t_s} = \frac{2.0075 \times 10^9\ \text{BTUs}}{\left(1461.3\ \frac{\text{BTU}}{\text{lbm}} - 695.5\ \frac{\text{BTU}}{\text{lbm}}\right)18\ \text{hr}}$$

$$\boxed{F_S = 145{,}632\ \text{LBM/HR}}$$

2349-063D

Fig. 4-40 Revised Flow Rates for Recommended Four Plant Cycle Locations (Cont'd)

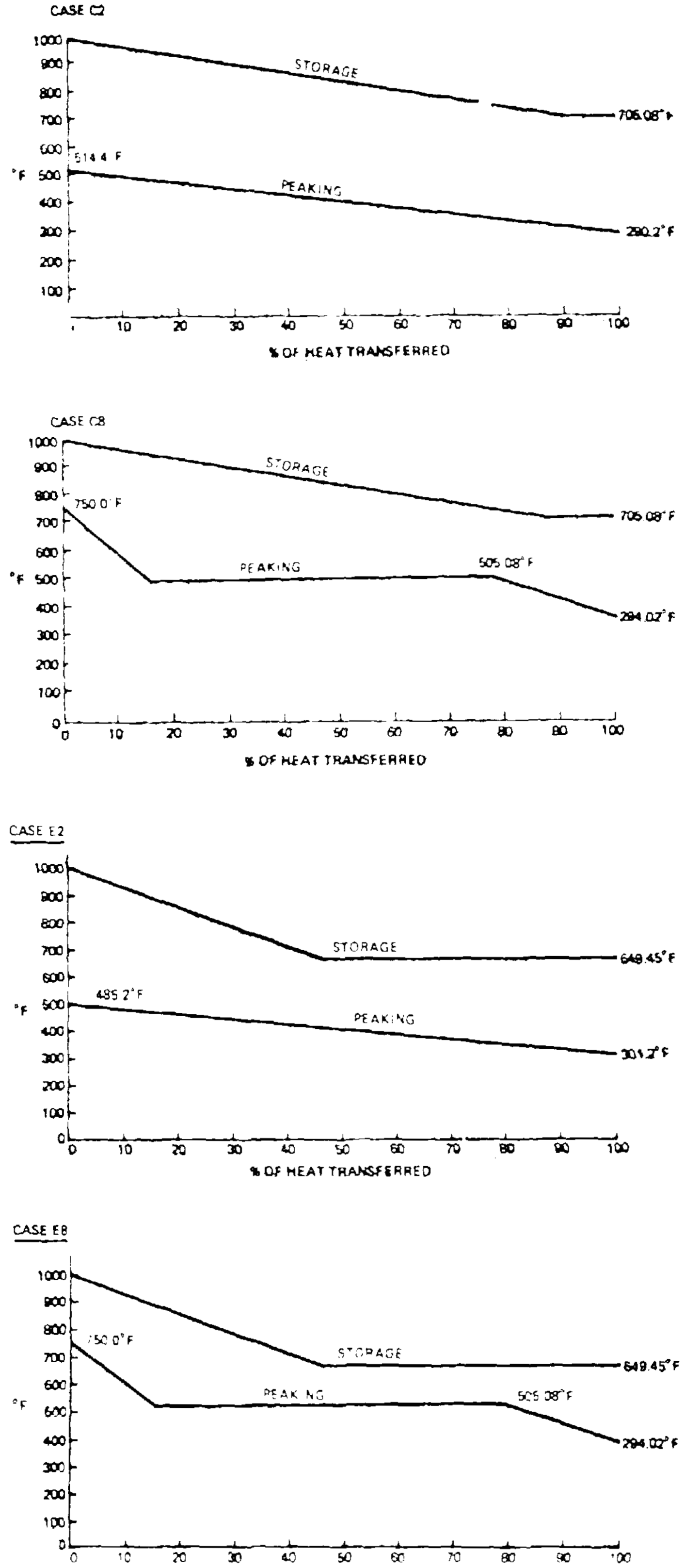

2349-064D

Fig. 4-41 Heat Exchanger Temperature for Recommended Four Cycle Locations

CASE: C2   60/40 SPLIT OF FEEDWATER FLOW TO TES DURING PEAKING

PEAKING

T_{pi}	= 423.4	°F
P_{pi}	= 4323.0	Psia
h_{pi}	= 404.82	BTU/lbm
T_{po}	= 514.4	°F
P_{po}	= 4323.0	Psia
h_{po}	= 504.0	BTU/lbm
F_p	= 2,217,000	lbm/hr
t_p	= 6	hr

STORAGE

T_{si}	= 1000.0	°F
P_{si}	= 3500.0	Psia
h_{si}	= 1421.7	BTU/lbm
T_{so}	= 705.08	°F
P_{so}	= 3200.0	Psia
h_{so}	= 875.5	BTU/lbm
t_s	= 18	hr

$$Q = F_p (h_{po} - h_{pi})\, t_p = 2{,}217{,}000 \, \frac{\text{lbm}}{\text{hr}} \left(504.0 \, \frac{\text{BTU}}{\text{lbm}} - 404.82 \, \frac{\text{BTU}}{\text{lbm}} \right) 6 \text{ hr}$$

$$\boxed{Q = 1.3193 \times 10^{9} \text{ BTUs}}$$

$$F_s = \frac{Q}{(h_{si} - h_{so})\, t_s} = \frac{1.3193 \times 10^{9} \text{ BTUs}}{\left(1421.7 \, \frac{\text{BTU}}{\text{lbm}} - 875.5 \, \frac{\text{BTU}}{\text{lbm}} \right) 18 \text{ hr}}$$

$$\boxed{F_S = 134{,}162 \text{ LBM/HR}}$$

2349-065D

Fig. 4-42 Revised Flow Rates for Ft. Martin Feedwater Heating Case

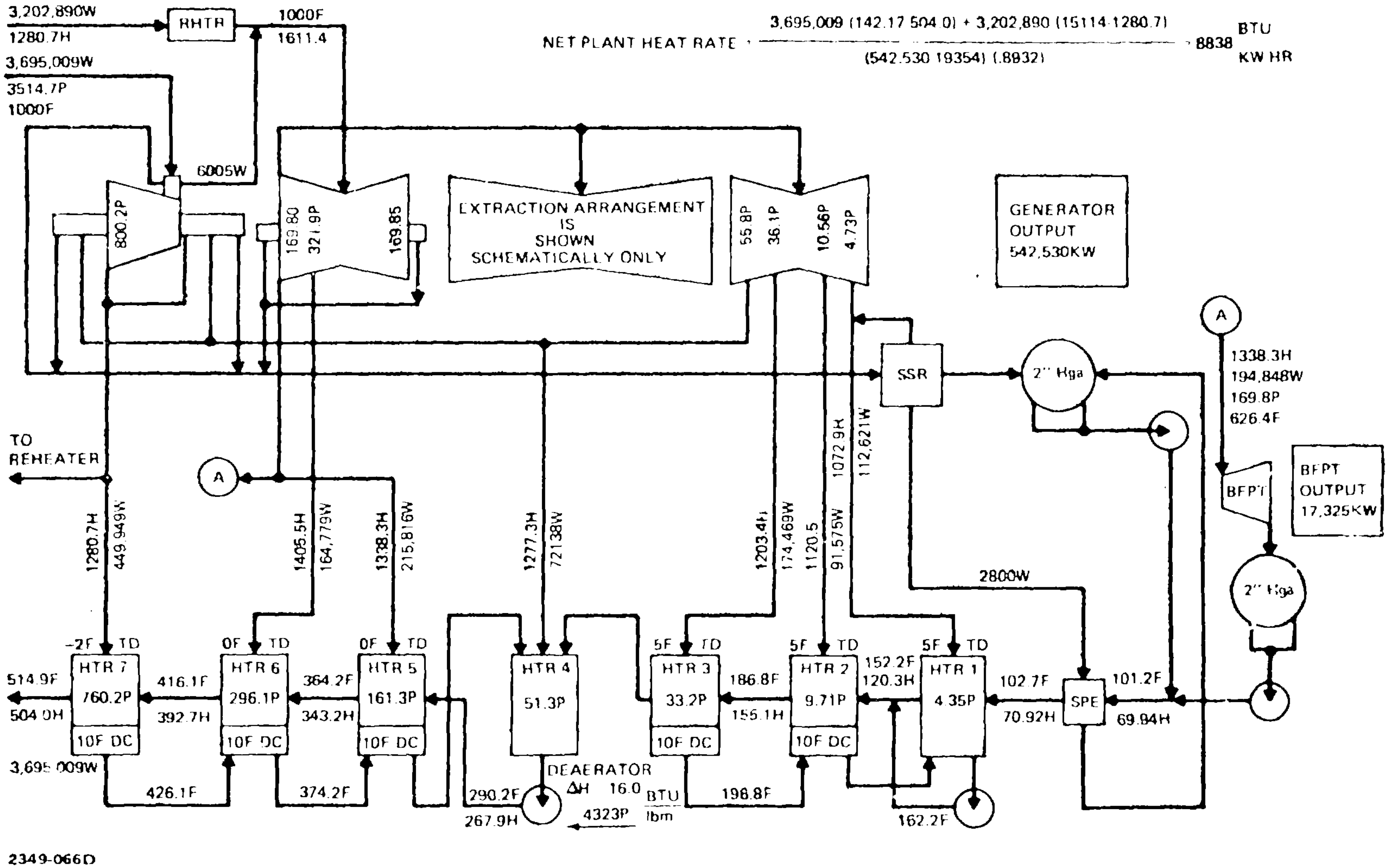

Fig. 4-43 Heat Balance Ft. Martin - Base Case

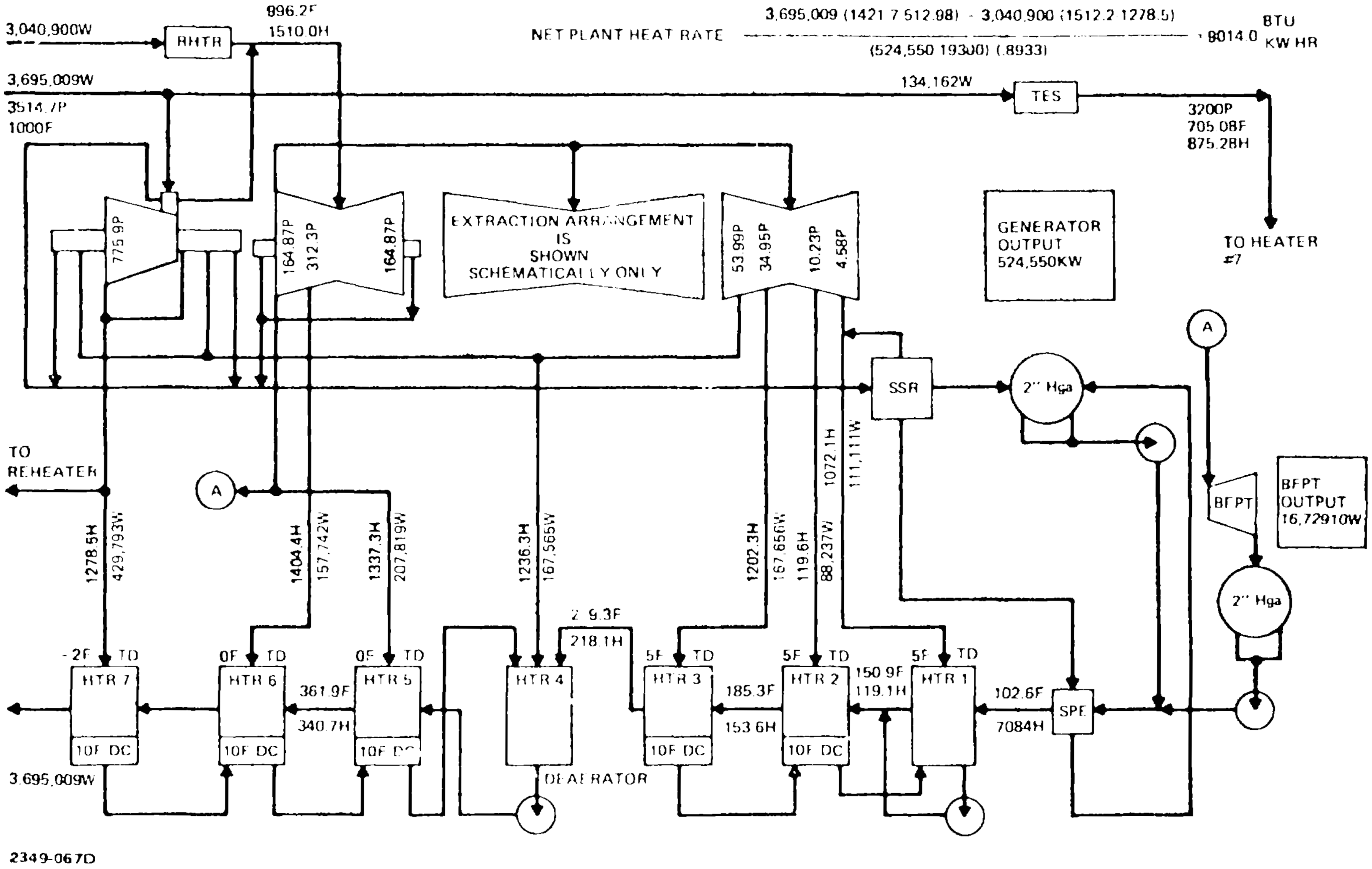

Fig. 4-44 Heat Balance, Ft. Martin, Feedwater Heating - Storage Mode

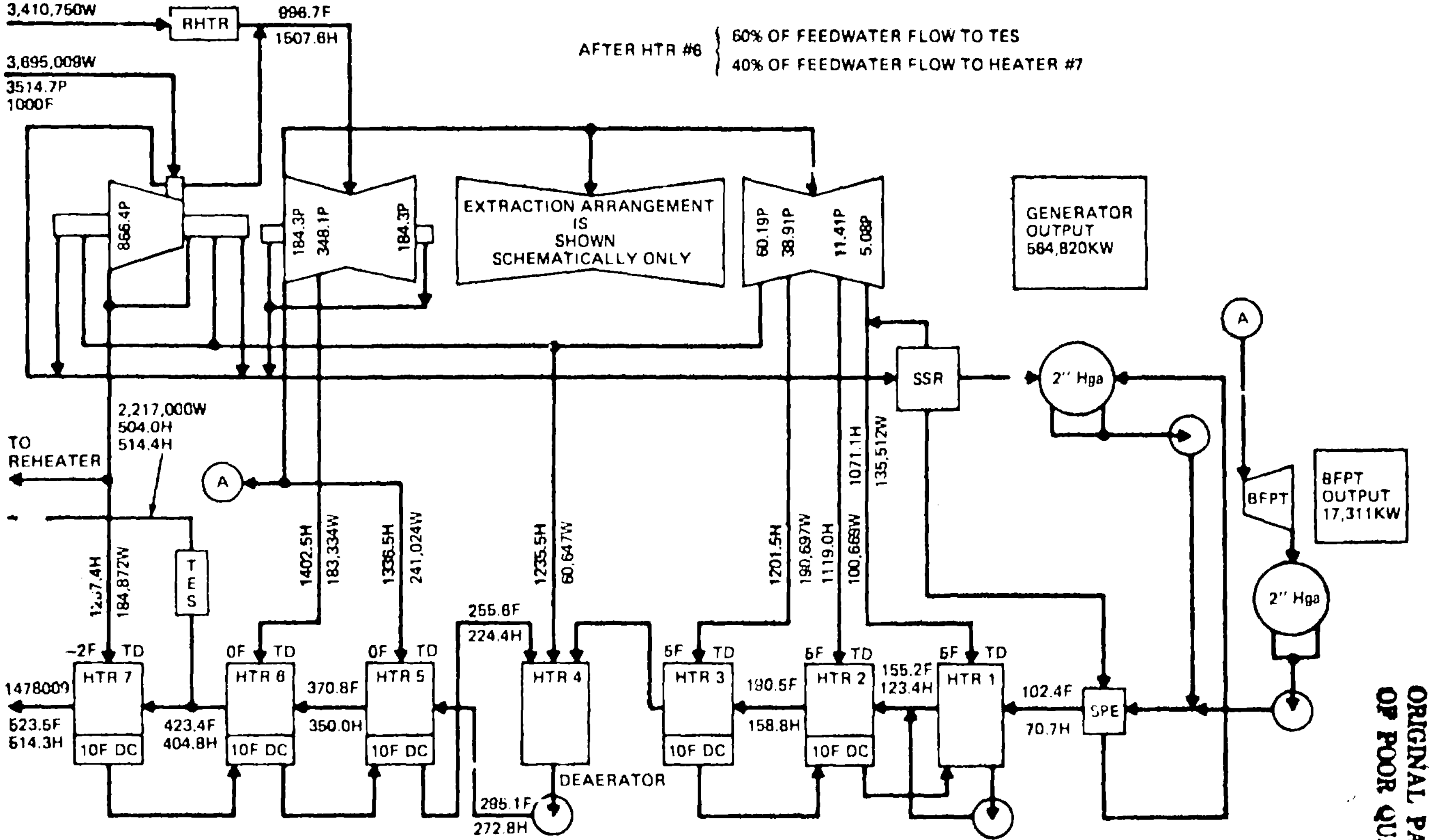

$$\text{NET PLANT HEAT RATE} = \frac{3{,}695{,}009\ (142.17-508.13) + 3{,}410{,}750\ (1509.6-1287.4)}{(584{,}820-19{,}900)\ (.8925)} = 8498.4\ \frac{\text{BTU}}{\text{KW HR}}$$

2349-068D

Fig. 4-45 Heat Balance, Ft. Martin, Feedwater Heating - Peaking Mode

ORIGINAL PAGE IS OF POOR QUALITY

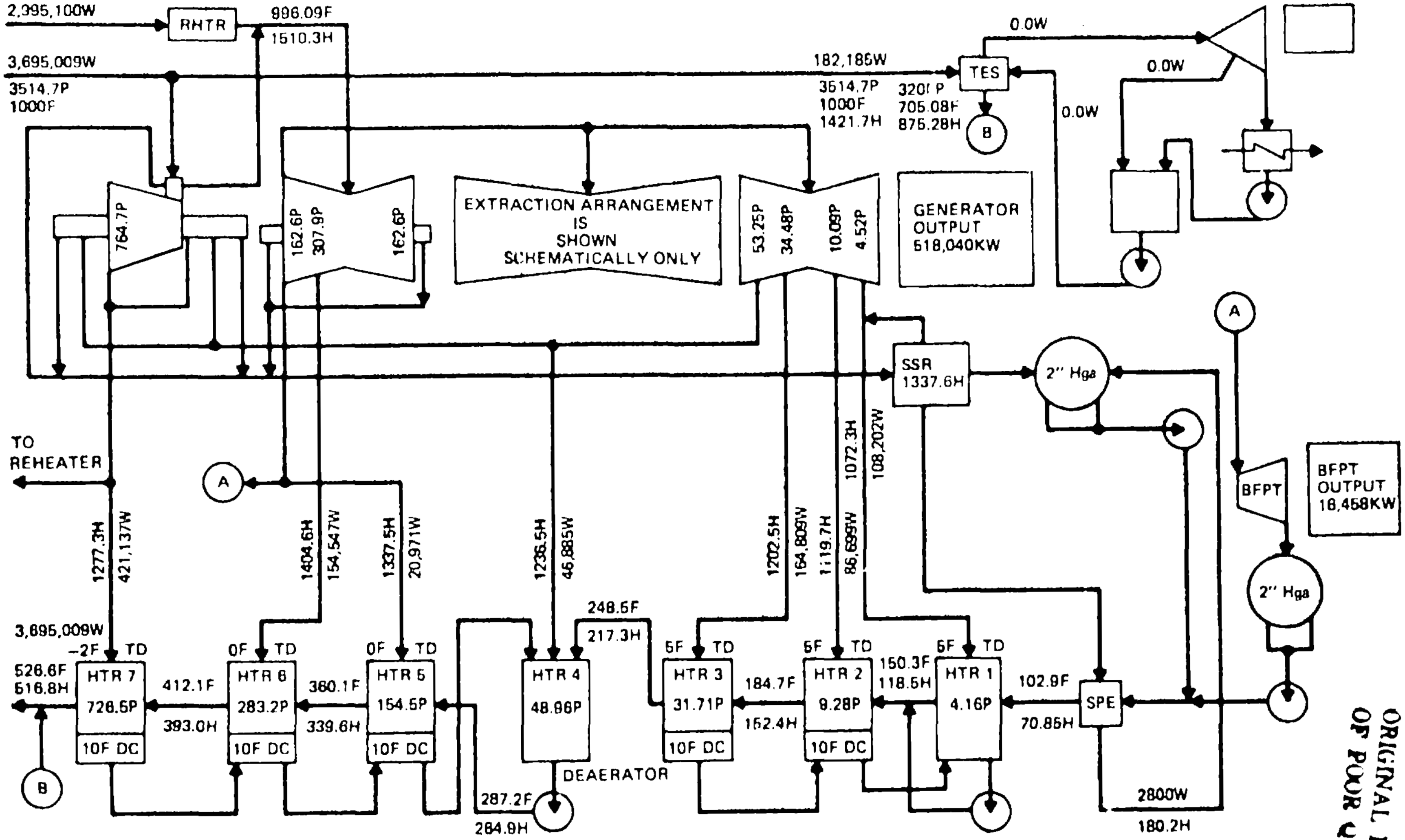

$$\text{NET PLANT HEAT RATE} = \frac{3{,}695{,}009\,(1421.7-516.8) + 2{,}986{,}100\,(1612.5-1277.3)}{(518{,}040-19270)\,(.8932)} = 9086.5\ \frac{\text{BTU}}{\text{KW HR}}$$

2349-069D

Fig. 4-46 Heat Balance, Ft. Martin, Auxiliary Cycle – Storage Mode

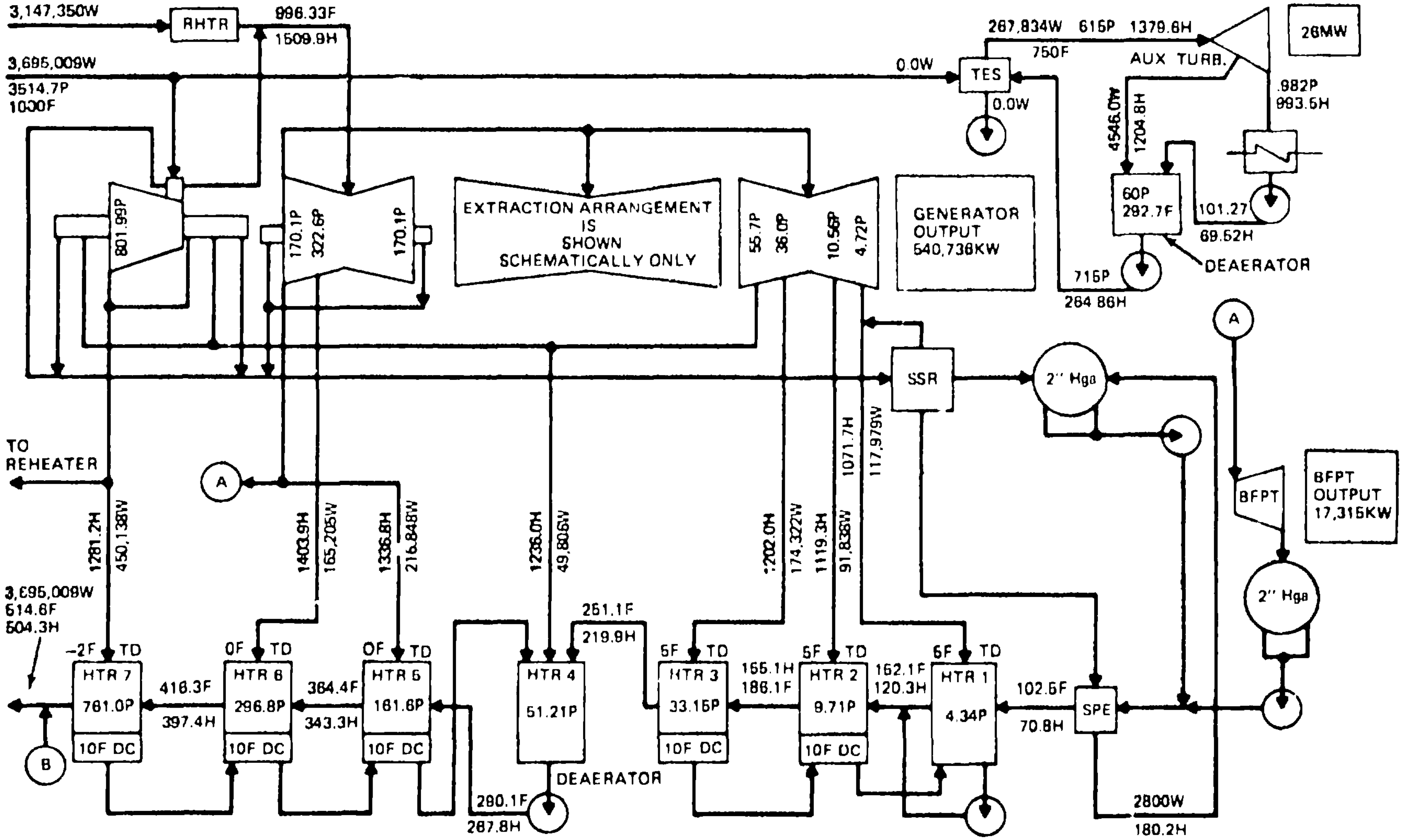

$$\text{NET PLANT HEAT RATE} = \frac{3{,}695{,}009\ (1421.7-504.28) + 3{,}197{,}350\ (1511.4-1281.2)}{(568{,}740-19{,}900)\ (.8926)} = 8430.2\ \frac{\text{BTU}}{\text{KW HR}}$$

2349-070D

Fig. 4-47 Heat Balance, Ft. Martin, Auxiliary Cycle – Peaking Mode

Case	Mode	NPHR (Btu/Kwhr)	Hours of Operation	Change from Base
Base	Normal (100%)	8838.0	24	–
Feedwater	Storage	9014.0	18	–
Heating	Peaking	8498.5	6	–
(C2)	Daily Average	8885.0	24	47
Auxiliary	Storage	9086.5	18	–
Power Supply	Peaking	8430.2	6	–
(C8)	Daily Average	8922.0	24	84
Cycled	Partial Load (77.4%)	8950	18	–
Base	Peaking (100°)	8838	6	–
Plant	Daily Average	8922	24	84

Fig. 4-48 Summary of Net Plant Heat Rates – Ft. Martin

2349-0710

which yield a daily average heat rate of 8922 BTU/KWHR. Comparing this to the daily average heat rates of Cases C2 and C8 showed an increase in the heat rate of 37 BTU/KWHR and 0 BTU/KWHR.

Therefore, it was concluded that Case C2 was more efficient than cycling the base plant and Case C8 showed no efficiency difference in comparison to the cycled base plant. Since Cases E2 and E8 are identical in principle to Case C2 and C8, little would be gained from including both of these plants in the final evaluation. Roseton, therefore, was eliminated, and all subsequent design refinement was based on incorporating thermal energy storage into the Ft. Martin plant for either feedwater heating or to supply energy to a separate power conversion loop.

4.7.2 Recommended Heat Exchanger Concepts

As discussed in 4.5, many heat exchanger concepts can fulfill the TES requirements. Moving PCM systems are theoretically superior since the required heat exchanger area can be greatly reduced. A unit with heat transfer to and from the salt provided by heat pipes offers important salt/water isolation advantages but currently only appears feasible for the lower temperature conditions of nuclear plants. Since our overall goal is to determine with a reasonable degree of confidence whether a latent heat thermal energy storage system is cost effective, we felt that it was necessary to perform the design refinement and economic analysis on those heat exchanger concepts for which performance and cost estimates will be most realistic. These are clearly the basic tube/shell and the liquid metal intermediate loop tube/shell. Tube/shell units are in widespread use in the utility industry and the required liquid metal technology has been applied in nuclear power plants.

4.8 CONCEPTS RECOMMENDED FOR DESIGN REFINEMENT

In review then, Power plant applications retained for further design refinement were the Regenerative Feedwater Heating Augmentation and the Single Loop Separate Power Conversion Loop case, both integrated into the Ft. Martin supercritical fossil (coal) plant.

During storage for subsequent feedwater heating, 134,162 lbm/hr of main steam flow at 3500 psia and 1000°F will be directed to the TES units. This fluid leaves the TES unit at 3200 psia and 705.08°F and the TES stores 1.319×10^9 BTUs. During peaking, 60% of the feedwater flow between the sixth and seventh heaters is diverted to the TES units. Thus, 2,217,000 lbm/hr enters the TES units at 423.4°F and leaves at the final feedwater temperature of 514.4°F. Average daily heat rate is 8885 BTU/KWHR and daily generation (deducting auxiliary power) is 1.2364×10^7 KWHRs representing an average net output of 515,168 KW.

For the separate loop case, 182,185 lbm/hr of main steam flo[illegible] bypassed to the TES units during storage. During peaking, 267,834 lbm/hr of flo[illegible]e auxiliary cycle is heated from 294°F and 715 psia to 750°F and 615 psia. This requires the TES units to store 1.791×10^9 BTUs. The daily average heat rate is 8922/BTU/KWHR and daily generation is 1.2259×10^7 KWHRs, representing an average net daily output of 510,788 KW. Fig. 4-49 contains detailed information relating to these two cases. These temperature and flow conditions were used for design refinement analyses of tube/shell and intermediate loop tube/shell heat exchanger modules integrated into the Ft. Martin Plant presented in the following section.

	Fort Martin Plant	
	Feedwater Heating	Separate Cycle
Storage (18 hours)		
Inlet Temperature, °F	1,000	1,000
Outlet Temperature, °F	705	705
Inlet Pressure, psi	3,500	3,500
Outlet Pressure, psi	3,200	3,200
Inlet Enthalpy, BTU/lb	1,421.7	1,421.7
Outlet Enthalpy, BTU/lb	875.5	875.5
Flow Rate, lbm/hr	134,162	182,188
Heat Rate, BTU/KWHR	9,014.0	9,086.5
Gross Output, KW	542,550	518,040
Net Output, KW	505,250	498,770
Usage (6 hours)		
Inlet Temperature, °F	423.4	294
Outlet Temperature, °F	514.4	750
Inlet Pressure, psi	4,323	715
Outlet Pressure, psi	4,323	615
Inlet Enthalpy, BTU/lb	404.8	264.8
Outlet Enthalpy, BTU/lb	504.0	1,379.4
Flow Rate, lbm/hr	2,217,000	267,834
Heat Rate, BTU/KWHR	8,498.5	8,430.2
Gross Output, KW	564,820	566,740
Net Output, KW	544,920	546,840
Total Energy Stored, BTU:	1,319,000,000	1,791,000,000
$KW_e h$	133,800	156,000

2349-072D

Fig. 4-49 Fort Martin Revised Fluid Conditions and Heat Balance Information

Section 5

DESIGN REFINEMENT

5.1 HEAT EXCHANGER DESIGNS

To make our final cost/benefit analysis as realistic as possible, the tube/shell and intermediate loop tube shell concepts were selected for design refinement. This does not imply that the other concepts are less desirable, only that we felt more design effort was required to refine these approaches for accurate costing than was possible in this initial study. Before beginning the design refinement, certain parameters were established from other considerations. The salt eutectics were selected from our recommended list (Figure 4-8) for the appropriate heat exchanger temperature levels discussed in 4.6. Maximum overall dimensions of a heat exchanger module were taken as 40 ft. long and 15 ft. diameter based on railroad car shipping and on-site handling constraints. In this regard, it should be pointed out that as several heat exchanger manufacturers recommended as maximum diameter of 12 ft. some of our calculations are based on this constraint. As discussed in 5.1.2, we feel that this limit is design-dependent and at least one of our two structural arrangements can be fabricated in the 15 ft. diameter size. Tube inside diameter was also fixed for the majority of our analysis. This is a tradeoff between material cost and labor (welding) cost. As tube diameter is increased there is more surface area to transfer heat to the salt, so tube spacing can be increased; however, the tube wall thickness increases to contain the pressure with a larger diameter. Fewer tubes, however, reduces the number of tube/tube sheets welds although each weld is longer. In addition to spacing, structural and labor considerations, the selection of inside diameter also effects fluid flow velocities through the tube and hence the inside heat transfer coefficient. Our basic thermal and structural design analysis was based on a pipe inside diameter of one inch. The question of optimum tube diameter was examined separately so that final designs could be iterated if necessary.

5.1.1 Thermal Analysis

Tube and Shell:

The equations which describe the heat flow into or out of a pipe surrounded by a salt are given by several standard heat transfer equations. Considering single one-dimensional heat transfer, the energy flux per unit length of pipe may be written:

$$\frac{\dot{Q}}{L} = \left[\frac{4\pi k_s}{\ell n \, (R/a)^2} \right] (T_w - T_m)$$

where k_s = salt thermal conductivity in solid state

T_w = pipe outside wall temperature

T_m ≡ salt melting point

a = pipe outer radius

R = salt melt radius

It may also be expressed in terms of film coefficient and pipe wall thermal resistance as

$$\frac{\dot{Q}}{L} = 2\pi r_i \left\{ \frac{1}{\frac{1}{h} + \frac{r_i \ell n \left(r_o / r_i \right)}{k_w}} \right\} \left(T_f - T_w \right)$$

where h is the fluid film coefficient

r_i is the pipe inner radius

r_o = a = pipe outer radius

k_w = pipe wall thermal conductivity

T_f = fluid bulk temperature

T_w = pipe outer wall temperature

Ignoring energy stored as sensible heat, energy stored in the salt is:

$$\int \frac{\dot{Q}}{L}\, dt = \Delta H_{fs}\, \rho_s\, \pi \left(R^2 - a^2 \right)$$

Setting these equations equal to each other, integrating and rearranging gives:

1) $$\left(\frac{R}{a}\right)^2 \ln\left(\frac{R}{a}\right)^2 + \left[\left(\frac{R}{a}\right)^2 - 1\right] \left\{ \frac{2k_s}{r_i} \left[\frac{1}{h} + \frac{r_i}{k_w} \ln\left(\frac{a}{r_i}\right) \right] - 1 \right\} = \frac{\left(T_f - T_m\right) 4 t k_s}{\Delta H_{fs}\, \rho_s\, a^2}$$

which describes the relationship between active time, t, pipe spacing, temperature difference and film coefficient.

The internal film coefficient, h, may be expressed as follows (Reference 23, pg. 219):

2) $$h = \frac{k_f}{D} (.023) \left(\frac{\rho V D}{\mu}\right)^{0.8} Pr^{0.4} = X_1 V^{0.8}$$

where:

3) $$V = \frac{\dot{M}}{N\rho \frac{\pi D^2}{4}}$$

where $\dot{M}$ = mass flow rate

N = number of pipes

and X_1 = constant

4) $$N = \frac{M_s}{\rho_\ell \, \pi \, (R^2 - a^2)}$$

where, M_s = mass of salt

This set of four equations may be used to size the system once the pipe wall thickness $(a - r_i)$ has been determined from pressure containment and corrosion considerations. Pipes will be spaced on hexagonal centers. The total TES unit diameter, therefore, can be estimated from the total cross sectional area per pipe, since $A = \pi R^2$ or $R = \sqrt{A/\pi}$. In our case:

$$A = N \sin(60^\circ)(2R)^2$$

$$\text{so that diameter} = 2\sqrt{\frac{N\,(2R)^2\,(.866)}{\pi}}$$

For example, consider the Ft. Martin feedwater heating case. Modules for each salt eutectic used are separately sized. Consider, first, the high temperature salt modules. From Section 4.6, salt for high temperature storage will be KCl· NaCl· $MgCl_2$ and 1,679,500 lbm of this salt will be required. Since in our design concept the same pipes will be used during both storage and usage phase, that phase requiring the most total pipes will size the system.

As discussed in 5.1.2 a tube wall thickness of .18 inches is required, including a small allowance for corrosion.

Considering first the storage side, since steam flow will cool from 1000°F to 800°F, properties are evaluated at 900°F. Then,

ρv = 5.2 lbm/ft^3

μ = .109 lbm/hr ft

k = .04 BTU/hr ft°F

Pr = 2.7

Total Flow Rate = 134,162 lbm/hr

Equation 2 thus becomes $h = .0495\,(V^{.8})$ and

equation 3 becomes $V = 4,730,414/N$

On combining 2 and 3 we obtain $h = 10,827/N^{.8}$

The following properties were used for the high temperature salt:

$\Delta H_{fs} = 197$ BTU/lbm

$\rho\, s = 140$ lbm/ft^3

$\rho\, 1 = 102$ lbm/ft^3

$k_s = .9$ BTU/hr ft°F

After eliminating "h" using Equation 5 then equation 1 becomes:

$$7) \qquad (R/a)^2 \ln(R/a)^2 + ((R/a)^2 - 1)\,(N^{.8}/425.6 - .97) = 66.33$$

Equation 4 for this case is $L = 3818.5/N\,(R^2 - .0032)$

The above Equation 7 uses the log mean average ΔT across the heat exchanger for $(T_f - T_m)$.

In similar manner the equivalent of Equation 7 for the usage case can be calculated using water properties at 400°F:

$\rho = 49$ lbm/ft^3

$\mu = .26$ lbm/hr ft

$k = .349$ BTU/hr ft°F

$Pr = .87$

Flow Rate = 2,217,000 lbm/hr

Equations 2 and 3 then become: $h = .827\,(V^{.8})$

$V = 8,295,000/N$

or $h = 283,517/N^{.8}$

Using this and the same salt properties as before we get:

$$8) \qquad (R/a)^2 \ln\,(R/a)^2 + ((R/a)^2 - 1)\,(N^{.8}/6563 - .97) = 54.63$$

The expression for the number of pipes, (N, Equation 4) is the same for both cases.

Comparing Equation 7 and 8 it can be seen that since the term on the right of Equation 8 is smaller than the same term in Equation 7 and since the denominator under the N^8 term is larger, this equation will give the smaller spacing. Therefore, the usage case dominates.

Examining Equation 8 it is apparent that since the factor of 6563 under N^8 is so large, N may vary over a large range without significantly affecting the value of R. Taking advantage of this we estimate the value of R taking N = 0. For this case $(R/a)^2 + 24.2$ and R = 3.345 inches.

From Equation 8 for a 12 foot diameter this would require 423 tubes (N) which is small compared to 6563 ($N^8 = 126$). The total length of tubing required, L, becomes L = 166 feet, which would make 5 modules having 32.2 feet active salt length leaving 6.8' for headers and vapor space. Module size for the low temperature salt was done in exactly the same manner.

At this point we may consider different flow patterns through the TES modules. The choice is between parallel series, or combination flow patterns. In a parallel arrangement, the flow would be evenly divided among a number of modules. Each module or group of modules (which can contain more than one salt) acts independently on a portion of the flow. While this has isolation advantages, a disadvantage of a parallel flow approach is that it results in low vapor velocity in the energy storage mode. Since the total flow rate and heat storage (and hence mass of salt) are determined from power plant considerations, the flow velocity per pipe is determined by the number of pipes used. In the parallel flow case, this is the number of pipes per module times the number of modules.

Preliminary calculations indicated that for the Ft. Martin cases this design would result in such a low vapor velocity that the vapor to pipe wall heat transfer resistance would be large, preventing the system from meeting design requirements. The velocity can be increased by placing some or all of the modules in series, where the outlet of one module becomes an inlet of the next. Alternately, inserts within the pipes can be used to increase the internal heat transfer coefficient. For this study, however, it was felt that this approach would be more expensive than choosing the "proper" flow pattern.

Based on this type of analysis, it was decided that the five high temperature salt modules required for the Ft. Martin feedwater heating case should be in series. Similar calculations performed for the low temperature salt indicated that adequate thermal performance would be achieved with a combination of five groups of three modules in series.

	Hot Salt (KCl NaCl $MgCl_2$)	Cold Salt (NaCl $NaNO_3$)
Number of Modules	5	15
Flow Pattern	Series	5 groups of 3 in series
Salt Mass (lbm)	1,679,500	5,319,300
Pipes Per Module (1" ID, .18" wall)	423	737
Pipe length (feet)	33.2	32
Pipe Spacing (inches)	6.69	5.05
Module Diameter (feet)	12	12
Total Energy Stored (%)	33	67

2349-073D

Fig. 5-1 Tube and Shell Design, Fort Martin Feedwater Heating

	Hot Salt ($CaCl_2$ KCl NaCl)	Middle Salt (KCl NaCl $MgCl_2$)	Cold Salt (NaCl $NaNO_3$)
Number of Modules	4	7	14
Flow Pattern	Series	Series	7 groups of 2 in series
Salt Mass (lbm)	1,476,000	2,348,000	5,061,000
Pipes per Module (1" ID, .18" wall)	605	675	600
Pipe Length (feet)	33.3	35	32
Pipe Spacing (inches)	5.57	5.23	5.6
Module Diameter (feet)	12	12	12
Total Energy Stored (%)	16	32	52

2349-074D

Fig. 5-2 Tube and Shell Design, Fort Martin Auxiliary Power

Considering the question of parallel versus series flow, if the denominator of N^8/X term in Equation 8 is large enough the value of N determined may be doubled or tripled without affecting the value of R. The preliminary designs for the Ft. Martin C2 (feedwater heating) and C8 (auxiliary power cycle) are summarized in Figures 5-1 and 5-2.

Liquid Metal Run-Around Loop

A design which separates the water and salt is the pumped liquid-metal-run-around loop system. Similar to nuclear reactor cooling technology, the pumped-loop system can consist of a sodium-water/steam heat exchanger, a sodium salt TES unit, and a pumped sodium run-around loop (Figure 5-3). If a pipe in the salt fails, the liquid metal leakage will not exothermically react with the salt. A water leak into the liquid metal loop would be relieved by a blowout plug located external to both salt and water heat exchangers so that no significant damage would result to the liquid metal-water heat exchanger.

For this initial study it was assumed that the sodium-water/steam heat exchanger will consist of water tubes surrounded by sodium annuli (see Figure 5-4). This will simplify containment of high pressure water (3500–4300 psi). It is envisioned that each salt (by generic type) will be connected to an independent sodium loop, in order that different required heat flux rates at different temperatures may be accommodated.

From Rohsenow & Choi (Reference 24), the overall heat transfer coefficient (h) from a liquid metal stream to a tube wall is:

9) $$h = \left[\left(\frac{k}{D}\right)(6.7 + .0041\,(\mathrm{Re}\,\mathrm{Pr})^{.793}\,e^{(41.8)(\mathrm{Pr})}\right]$$

Size of the heat transfer coefficient predicted by this equation, using the annulus equivalent hydraulic diameter, was so large as to be negligible in the system design.

Since the liquid metal heat transfer resistance is very small compared to other resistances in the system, the flow loop analysis follows directly from the tube and shell case. (See Figure 5-5). However, temperatures seen by the salt and water are the same in the run-around loop case as in the tube and shell case. If the liquid metal temperature drop is small, size and configuration of the salt module must be similar. Likewise, length of the water flow path in the liquid metal/water heat exchanger must be the same as the water flow length in the shell and tube case. Based on this, the design for the Ft. Martin case is summarized in Figures 5-6 and 5-7.

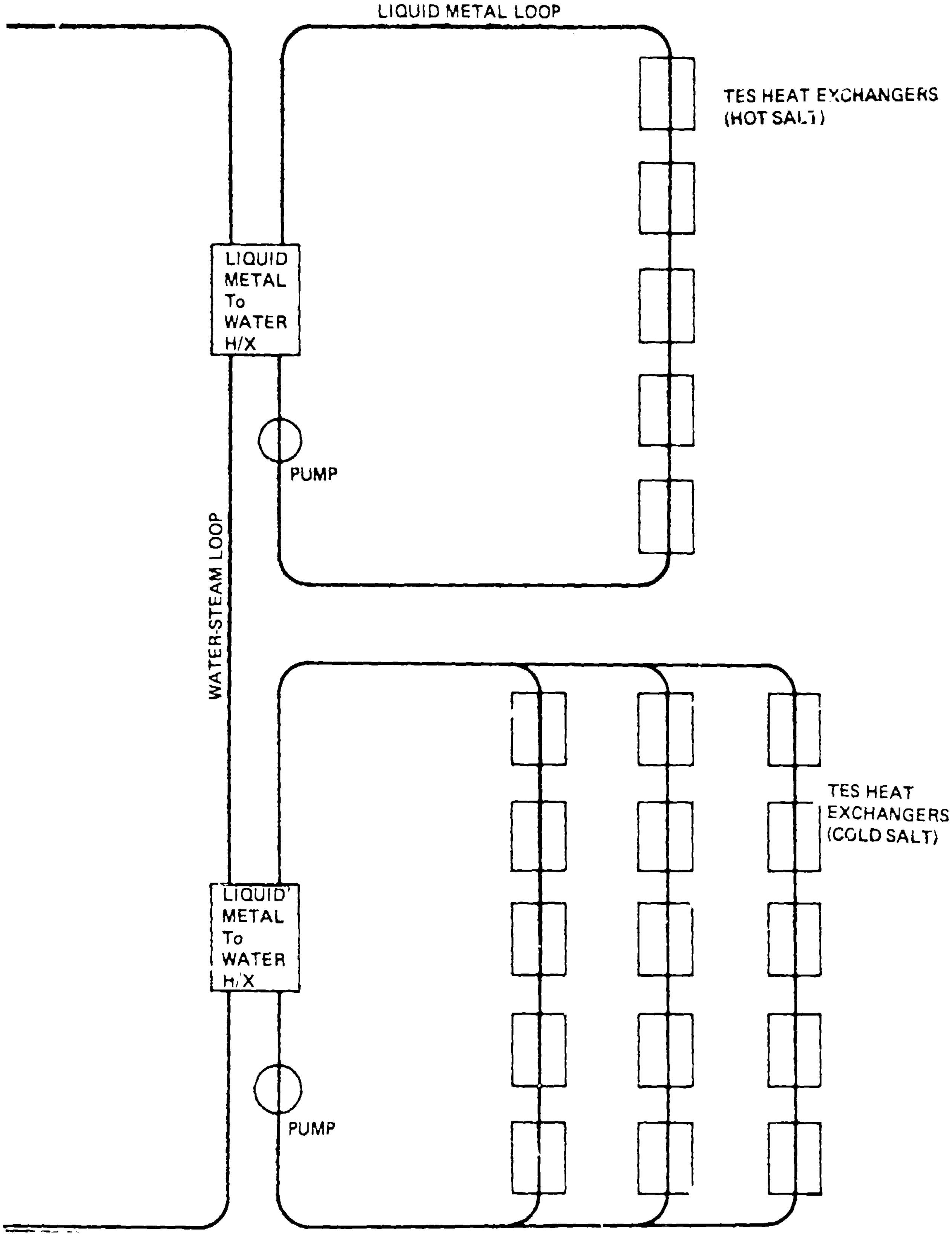

2349-075D

Fig 5-3 Liquid Metal Intermediate System Fort Martin Feedwater Heating

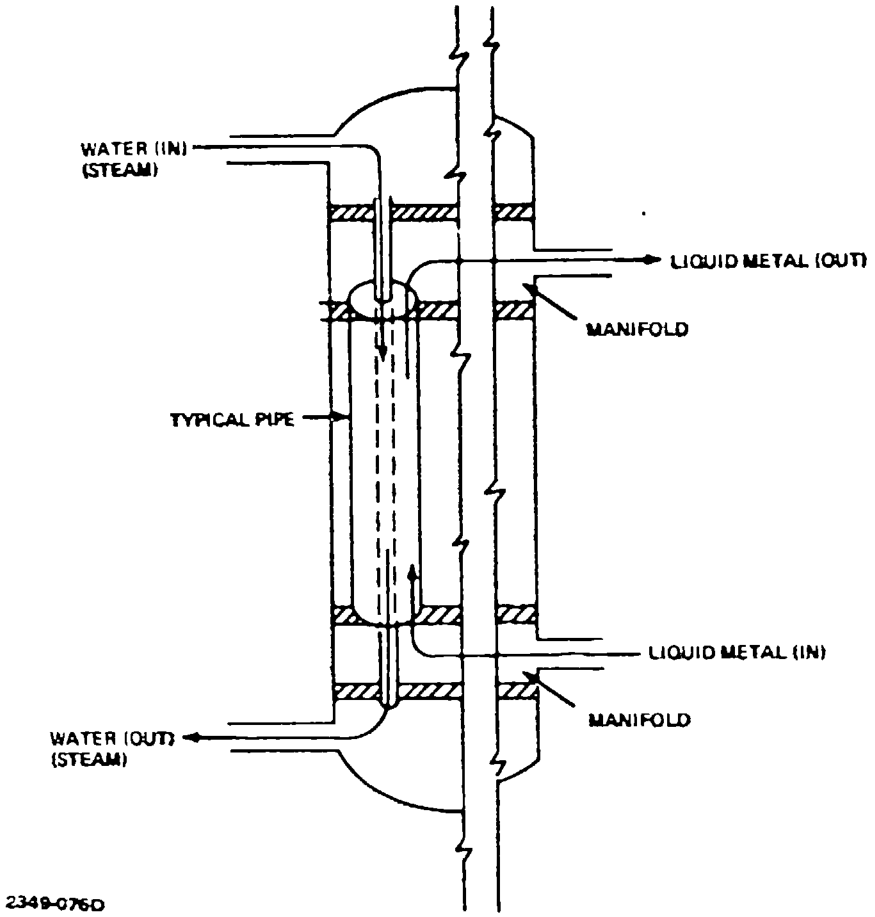

Fig. 5-4 Liquid Metal/Water Heat Exchanger

RESISTANCES FOR SHELL AND TUBE CASE:

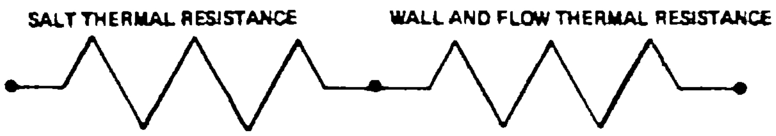

RESISTANCES FOR LIQUID METAL INTERMEDIATE CASE

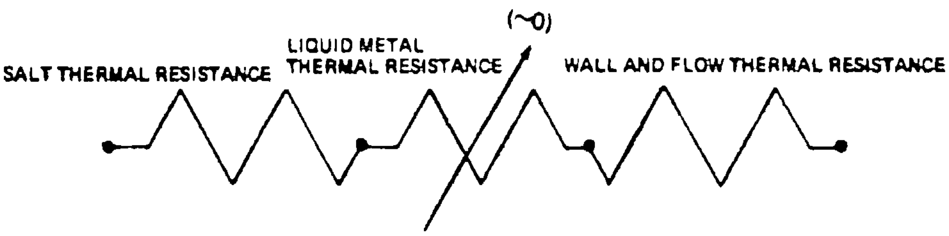

Fig. 5-5 Comparison of Thermal Resistances – Tube/Shell & Liquid Metal Designs

2349-077D

As previously stated, the water/liquid metal heat exchanger consists of annular tubes with water flowing in the inner tube and liquid metal flowing in the annulus.

In order to check the assumption of low liquid metal heat transfer resistance a sample calculation was performed using a sodium flow velocity of 1 ft/sec, and an annular thickness of .25" and sodium properties evaluated at 700° F.

Equation 9 then produces:

$$h = (41.8/.0416)\,(6.7 + .0041)\left(\left(\frac{53.7\ (3600)\ .0416}{.7}\right)(.005)\right)^{.793} e^{41.8(.005)}$$

$$= 6860 \text{ BTU/hr ft}^{\circ}\text{F}$$

which is large compared to the heat transfer coefficient of 60 to 1500 BTU/hr ft° F for steam/water.

The amount of required sodium may be estimated from the volume of sodium pipes. Each foot of pipe in the module contains .00545 ft^3 of sodium volume so the total volume in the TES canisters is:

C2: $(.00545)(5(423)(33.2) + 15\,(737)(32)) = 2290\ \text{ft}^3$ of Na or about 122,000 lbm

C8: $(.00545)(4(33.3)(605) + 7\,(675)(35) + 14\,(32)(600)) = 2805\ \text{ft}^3$ or about 149,000 lbm of Na

Additional amounts will be required for the heat exchangers and connecting pipe volumes, perhaps 20-30% more in each case.

The salt quantities required for our heat exchanger designs neglected thermal losses to the surroundings, since this effect will be negligible. As an illustration, consider the feedwater heating design for New York City weather conditions. The heat transfer coefficient to the air is (Reference 25)

$$h = (1 + .3V) \text{ BTU/hr ft}^{2\circ}\text{F}$$

where V is wind speed in miles per hour. For January the average wind speed is 11 mph in New York City, so,

$$h = (1 + .3(11)) = 4.3 \text{ BTU/hr ft}^{2\circ}\text{F}.$$

A typical high temperature insulation in wide use by the utility industry is calcium silicate, which exhibits a thermal conductivity of about .065 BTU/hr ft°F.

For a 1 foot thick layer of insulation, then, the total coupling from the TES unit to air is:

$$U = \frac{1}{1/4.3 + 1/.065} = .064 \text{ BTU/hr ft°F}$$

Conservatively assuming that during the 18-hour storage the air temperature will be 0°F (average fan air temperature = 34°F, Reference 26), and the TES unit will be at 1000°F throughout this period, losses for this case (20 modules) would be:

$$Q = 18\ (20)\ \pi\ (12)\ 33(.064)\ (1000 - 0) = 2.8 \times 10^7 \text{ BTU}$$

This quantity represents only 2% of the total energy stored. Hence, even with this conservative analysis, which neglects that the average module temperature will be less than 1000°F during the 18-hour period and uses a low value for air temperature, the insulation loss represents only about 2% of the total energy stored. Within the preliminary nature of this total analysis, this amount can be neglected at this point.

5.1.2 Structural Analysis

Our two recommended designs are both tube and shell units, the difference being that in the liquid metal intermediate loop case, the salt heat exchanger need not be designed for high pressure. In the basic tube shell case the utility fluid (steam or feedwater) passes through the tubes so the tubes and domes must be designed for high pressure. The maximum pressure is somewhat at the discretion of system design. The main steam (energy source) at Ft. Martin is 3500 psia, but a pressure drop can exist prior to the salt heat exchanger. Likewise, feedwater entering the boiler is at 4323 psia and in the present plant layout the last pump is before the number 5 feedwater heater so the last three feedwater heaters are designed on the tube side for 4323 psi and a maximum temperature of 514°F (see Figure 4-42). Since the last heater steam extraction is at 800 psi it should also be possible to use a lower pressure pump before the number 5 heater and add a final pump after the number 7 heater. This would reduce design pressure to the TES heat exchanger. If we assume that we maintain the present Ft. Martin layout, then the TES unit will see 4323 psi feedwater at the end of a storage cycle when the upper dome is at 1000°F and maximum salt temperature is about 900°F. Even with an extra pump the unit would still see high pressure steam at 1000°F during energy storage.

Since our TES heat exchanger requirements are similar to those for the last stage feedwater heaters at Ft. Martin, vendor quotes should be obtainable. However, since our design temperature is nearly 500°F higher and the cost of the heat exchanger is so important to the overall cost effectiveness of our proposed system, we decided to do some limited structural analysis to define problem areas and perhaps suggest an approach to reduce costs.

For our calculations we took the design case as 1000°F and 3500 psi for the tubes and domes and 1000°F and 100 psi for the shell. The first configuration to be considered (Figure 5-8) has forged spherical domes and tube sheets in tension and compression, respectively. The material selected was 321 stainless steel with a 14 ksi strength (ASME Boiler Code, Section VIII). The spheres share a common chord at the plane of the centroid of an end ring with a cross-section of 36" x 24", with a 72" radius to the centroid from the longitudinal axis.

For the 80" radius sphere in tension,

$$\text{Thickness} = pR/2\sigma = 3500 \times 80 / \left[2\ (14{,}000)\right] = 10''$$

For the 93" radius sphere in compression,

$$\text{Thickness} = pR/2\sigma = 3500 \times 93 / \left[2\ (14{,}000)\right] = 11.6''$$

Stress in the ring due to outward force exerted by the compressed sphere (ignoring the slight help from the tensile sphere) is:

$$\sigma = \left[\frac{3500 \text{ psi} \times 93''}{2}\right] \times .707 \times \left[\frac{1}{36'' \times 24''}\right] = 13{,}300 \text{ psi}$$

which is within the allowable.

Buckling pressure for the 93" radius sphere assuming $E = 25 \times 10^6$ psi is,

$$p_{cr} = .2\,E\left(\frac{t}{R}\right)^2 = .2 \times .25 \times 10^6 \left(\frac{11.6}{93}\right)^2 = 78{,}000 \text{ psi}$$

Thus, buckling does not govern the thickness.

The shell design for 100 psi and 100°F is,

$$\text{Thickness} = pR/\sigma = 100 \text{ psi} \times 90 \text{ in}/14{,}000 \text{ psi} = .64''$$

Salt TES units — — same as in Shell and Tube Design

Water/Sodium Heat Exchangers

Annular Tubes:

annulus (water) 1" ID .18" thick
1.36" OD
annulus: .25"
outer pipe: 1.85" ID
2.15" OD

Hot Salt:

5 H/X 423 pipes
33.2 feet long

Cold Salt:

15 H/X 737 pipes
32 feet long

2349-078D

Fig. 5-6 Liquid Metal Loop Design, Ft. Martin Feedwater Heating

Salt TES units ———— same as in Shell and Tube Design

Water/Sodium Heat Exchangers:

Annular Tubes:

water tube (inside) 1" ID – 1.36" OD
sodium tube (outside) 1.85" ID – 2.15" OD

Hot Salt:

4 H/X, 606 annular pipes, 33.3 ft. long

Middle Salt:

7 H/X, 675 annular pipes, 35 ft. long

Cold Salt:

14 H/X, 600 annular pipes, 32 ft. long

2349-079D

Fig. 5-7 Liquid Metal Loop Design, Ft. Martin Auxiliary Power Cycle

DESIGN FOR 3500 PSI, 1000 F
MATERIAL: 321 SS

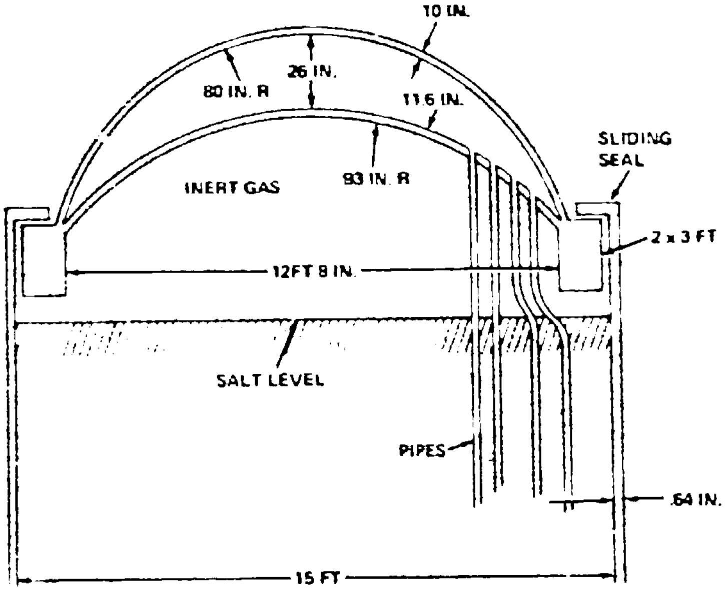

2349-080D

Fig. 5-8 Tube and Shell Heat Exchanger - Standard Configuration

In this design we assume that relative thermal expansion between the thin wall tubes and the heavier (and slower responding) shell will be accommodated by a sliding seal between the shell and upper ring. The end load must then be carried by the total number of straight tubes. Additional bent tubes could be used (as shown in Figure 5-8) in order to fully utilize the shell volume for energy storage.

Tubes designed for 3500 psi and 1000°F require a wall of,

$$\text{Thickness} = Pr/\sigma = 3500 \times .5''/14{,}000 = .125''$$

The tube area in cross section is $\pi \times 1'' \times .125 = .38\ \text{in}^2$. At a tube spacing of 6.7" the end load per tube is 100 psi x 6.7" x 6.7" = 4500 lbs.

However, the straight tubes only extend to a radius of 68" while the 100 psi shell pressure acts over a 90" radius for an area ratio of $(90/68)^2 = 1.75$. The end load per straight tube is then 1.75 x 4500 lbs = 7,870 lbs.

Tube area required to carry the end load is thus

$$A = \text{load}/\sigma = 7870/14{,}000 = .56\ \text{in}^2$$

or tube,

$$t = A/\pi\ D = .56\ \text{in}^2/\pi = .18\ \text{in.}$$

The end load and not internal pressure, thus designs the tubes.

The foregoing summarizes what might be termed a conventional tube/shell design. It can be seen that at these high pressures and temperatures the domes and end ring become massive. In addition to material and forging cost, large labor costs can be anticipated to make the deep welds joining the domes to the rings.

As an alternate, therefore, we considered a stayed construction as shown in Figure 5-9. In this design each heat exchanger tube is welded to a heavy well hollow strut which in turn is welded to the external dome and the domed tube sheet. Since this is a more efficient structure we used a higher design pressure, 4500 psi, to cover the case where the final feedwater pump is before the TES.

ORIGINAL PAGE IS
OF POOR QUALITY

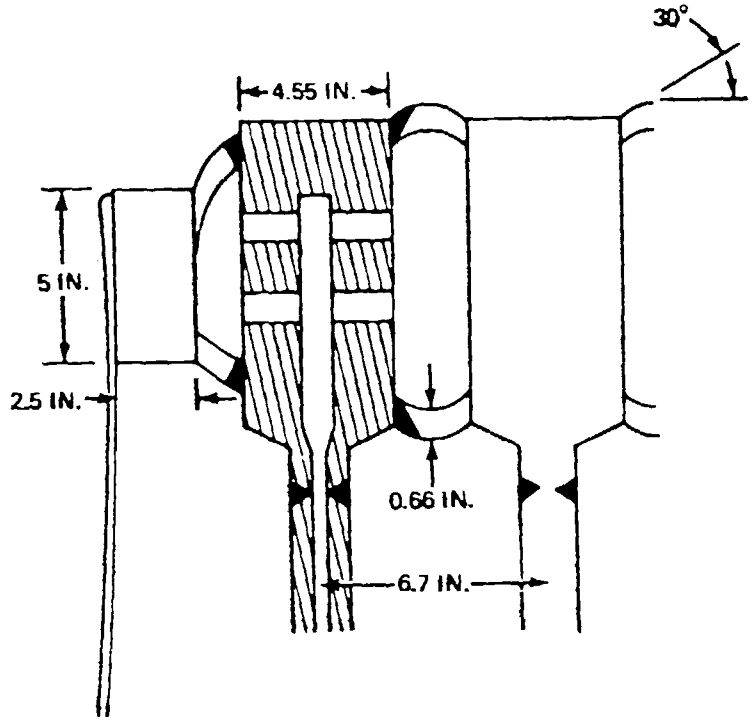

2349-0050

Fig. 5-9 Stayed Configuration Tube and Shell Heat Exchanger

At a tube spacing of 6.7 inches the load on each stay is 4500 psi x 6.7" x 6.7" = 202,000 lbs. The net stay area must be

$$A = 202{,}000/14{,}000 = 14.5 \text{ in}^2$$

Allowing a 1.5" diameter hole (area = 1.8 in^2) for flow in and out of the tubes the total gross stay area must be 16.3 in^2

$$\text{Stay Diameter} = \sqrt{16.3/.785} = 4.55''$$

For the top and bottom sheets (domes) assume the skin next to the stay is formed into a 30° cone as shown in Figure 5-9, then,

$$P/2\pi R = 202{,}000/(6.28 \times 2.28) = 14{,}200 \text{ lbs/in.}$$

The membrane load/inch = 14,200/.5 = 28,400 lbs/in

The thickness required is:

$$t = 28{,}400/14{,}000 = 2.04''$$

For a bulge height of 0.29" at the shortest span between stays and 0.66" on a 45° line between stays,

$$\text{Span} = 6.7 \times \sqrt{2} - 4.55 = 4.93''$$

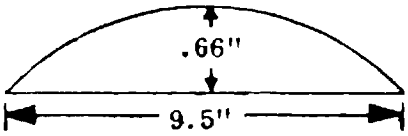

R = 4.93"

As a sphere, the thickness required,

$$t = [4500 \times 6.05] \;/\; [2 \times 14{,}000] = .97'', \quad 2'' \text{ provided}$$

where the radius of curvature has been increased to 6.05" to allow for double curvature effects. The end ring is pulled inward by the membrane load $N\phi$,

$$N\phi = PR/2 = 4500 \times 6.05/2 = 13{,}600 \text{ lbs/in.}$$

with a horizontal component = .833 x 13,600 :: 11,300 lbs/in.

To make the end rings small, height should be selected so that pressure load balances the N loads from each of the two plates:

$$4500\ h = 2 \times 11,300$$
$$h = 5''$$

Designing the ring as a beam simply supported between the plates,

$$M = 1/6\ t^2 \times 14,00 = 1/8 \times 4500 \times 5^2$$
$$t = 2.5''$$

In summary, the stayed configuration reduces dome thicknesses from 10-12 inches to 2 inches and the ring from 24" x 36" to a 2-1/2" x 5" cross-section, while also extending the pressure capability from 3500 psi to 4500 psi (both at 1000°F). Benefits of this approach are summarized in Figures 5-10 and 5-11, where the material and welding requirements for each configuration are computed. It can be seen that the stayed configuration requires 450,000 lbs less steel resulting in significant cost reduction possibilities as will be discussed in Section 7.

Standard Configuration

	Volume (ft^3)	Weight (lbm)
80" Domes 10" thick	424	206900
93" Domes 11.6" thick	342	166896
Rings 15'OD 1" ID 3' thick	490	239120
Tubes 650 1" ID 1.36" O.D.	105	51240
Shell .66" thick 35' long 15' dia	91	44408
Total		708564

Stayed Configuration

	Volume (ft^3)	Weight (lbm)
Stays 2 x 650 → 4.5"	55	26840
Rings 15' OD 14.58' ID 3" thick	8	3904
Domes, 2" thick	285	139080
Tubes as above	105	51240
Shell as above	91	44408
Total		265470

2349-082D

Fig. 5-10 Heat Exchanger Weight Breakdown

STANDARD CONFIGURATION

Circumferential Length: 68" x 2 x π x 4 = 1720 in.
Vol of welds/in = 1/2 (10" x 10") = 50 in^3/in
Volume of Weld· 86,000 in^3
Pipe Length: 1300 x 1" x π = 4084"
Volume of Weld/in = 1/2 x .18" x 1" = .09 in^3/in
Volume = .09 (4084) = 367 in^3
Total = 86,367 in^3 of weld

STAYED CONFIGURATION

Circumferential Length: 180" • π • 4 = 1008 inches
Volume of Weld/in = 2 cu. in/in
Total = 2016 in^3
Stays
Number of Stays = 1300
Circumference = π 5" = 15.7 inches
Total: 2 x (1400) (15.7) = 40,820 in. circumference
Volume of Weld/in = 2 in^3/in
Total Volume for Stays = 81,640 in^3
Total = 83,656 in^3

2349-083D

Fig. 5-11 Total Volume of Welds

5.1.3 Design Sensitivity

Since much of the available salt thermophysical property data is questionable, and since in many cases eutectic values must be estimated, it is important to examine the sensitivity of our designs to possible changes in the design values used. The salt properties of importance are density (ρ , solid and liquid), specific heat (c_p, solid and liquid), thermal conductivity (k, solid and liquid) and latent heat of fusion (ΔH_{fs}).

First consider the magnitude of expected variations. According to Dr. Borucka (Reference 8), molten salt property experimental data obtained by different workers in many cases show considerable differences. She suggests that available data for ΔH_{fs}, c_p and k be assumed at best to be only ±10% accurate. Reference 3 considers available data for the thermal conductivity of chlorides to be so inaccurate as not even worth presenting, and even Dr. Borucka presents k data for KCl, NaCl and then only in the solid phase. Value for densities are considered fairly accurate, at least for solid densities.

An added complication is that very little real data exists for eutectic mixtures. Values presented for eutectics usually are estimates from values for the single salt. It is possible that this results in gross inaccuracies. IGT presents a comparison of real data with data from accepted estimation techniques for k, (see Figure 5-12). As can be seen, values from the estimation technique are satisfactory for certain single salts, but quite wrong for the three eutectics listed. It is generally difficult to establish a range of inaccuracy which would apply. For preliminary purposes, however, we assumed that data for ΔH_{fs}, c_p and k may vary by ±25%.

To judge how such variation would affect our design, we repeated the design calculations for the Ft. Martin feedwater heating case. Consider the high temperature salt, $KCl \cdot NaCl \cdot MgCl_2$, values from Figure 4-8:

k_l = .47 - .59, used .53 BTU/hr ft ^oF

k_s = .87 - .92, used .9 BTU/hr ft ^oF

c_{pl} = .248 BTU/# ^oF

c_{ps} = .23 BTU/# ^oF

ΔH_{fs} = 197 BTU/#

Salt	$k_{experimental}$[14]	$k_{estimated}$ Gambill[9]	$k_{estimated}$ Vargaftik[46]
	Btu/hr °F ft		
LiBr	0.23	0.79	--
NaOH	0.53	0.53	1.14
LiCl	0.28	1.97	0.63
KNO_3	0.26	0.41	0.64
NaCl	0.58	--	0.51
KCl	0.39	--	0.38
Li_2CO_3	1.14	--	1.27
Na_2CO_3	1.06	0.81	1.04
$ZnCl_2$	0.20	0.45	0.63
$NaNO_3$	0.33-0.35		1.06
$74NaNO_3$ $26KNO_3$*	0.27	0.51	0.95
24NaCl $76ZnCl_2$*	0.21	0.48	0.63
12NaF 59KF-29LiF*	2.6	2.24	1.08

*Composition on a weight basis

2349-084D

Fig. 5-12 Comparison of Estimated and Experimental Thermal Conductivity Values for Several Molten Salts and Salt Mixtures

If ΔH_{fs} and c_p are reduced 25% to,

$$c_{pl} = .186 \text{ BTU/\# }^{o}\text{F}$$

$$c_{ps} = .1725 \text{ BTU/\# }^{o}\text{F}$$

$$\Delta H_{fs} = 148 \text{ BTU/\#}$$

then the required salt mass will increase from 1,679,500 lbm to 2,276,300 lbm. Likewise for a similar 25% change the mass of the cold temperature salt, NaCl $NaNO_3$ increases from 5,319,300/lbm to 7,079,600 lbm. This would mean an increase of 25% in the number of modules required in this case from 20 to about 25. If we now look at the equation which regulates pipe spacing, Equation 1 (page 5-3), and noting that the term $(4K/hd_i)$ is not significant for the cases considered, then the thermal salt properties appear only on the right hand side of the equation in the form $C\ k/\rho_s\ \Delta H_{fs}$. The larger this term, the larger the pipe spacing and the fewer pipes that will be required. Therefore, if ΔH_{fs} is lower than we estimate (which requires more salt and therefore more modules), the effect is to increase spacing, which is beneficial. Thus, changes in "ΔH_{fs}" will hurt on one hand and help on the other. Since the sensitivity of spacing to this term is small there is an overall penalty if ΔH_{fs} is smaller than the value used.

The sensitivity of tube spacing (R) to changes in the right hand term are shown in Figure 5-13. As is shown, large changes in the term result in much smaller percentage changes in "R" and "R^2". For the Ft. Martin feedwater heating case (high temperature salt module) a decrease in k of 25% would result in a change of R from 3.345" to 3.0" or 10%. This would mean an increase in the number of pipes of about 20% but no increase in the number of modules. If both k and ΔH_{fs} varied by -25%, then the tube spacing is unchanged but the number of modules required increases by 25% due to the decrease in ΔH_{fs}. The sensitivity of a heat exchanger design to salt thermophysical properties is summarized in Figure 5-14.

$(R/a)^2$	R ($a = .68''$)	$\frac{Ck}{\rho_s \Delta H_{f_s}}$
30	3.72	73
25	3.4	56.47
20	3.04	40.91
15	2.63	26.62
10	2.15	14.02

2349-085D

Fig. 5-13 Tube Spacing Sensitivity to Salt Properties

	Effect of Property Change of 10%*		
Salt Property:	Tube Spacing	No. of Tubes	Salt Quantity (Volume No. of Modules)
ΔH_{fs}	−.03%	−5%	−5%
c_{p_l}	——	−2.5	−2.5
c_{p_s}	——	−2.5	−2.5
k_l	——	——	——
k_s	+.03%	−.01	——
ρ_s	−.03	−10	−10

2349-086D

*BASED ON 50% LATENT AND 50% SENSIBLE HEAT STORAGE.

Fig. 5-14 Summary of Typical Heat Exchanger Design Sensitivity to Salt Properties

5.2 SYSTEM LAYOUTS

To determine the system layout it was first necessary to establish all equipment in the system. A schematic diagram was drawn to illustrate all components of the system. The feedwater heating system schematic is shown in Figure 5-15. From this schematic, it was seen that the following equipment and incidentals were necessary in order to provide a complete system:

- Earthwork and grading
- Roads and paving
- Land and land rights
- Foundations
- Piping and valving
- Instrumentation and control
- Flash tank
- TES units

The number and dimensions of the heat exchangers for this case are given in Section 5.1.1. It lists five high temperature salt modules in series and fifteen low temperature modules in series by threes. All heat exchangers are 40 feet long and 12 feet in diameter. A schematic layout of the heat exchanger field is shown in Figure 5-16. Since all the heat exchangers were to stand on end to facilitate growth of the salt melt line, a minimum exclusion distance about each unit was chosen. It was decided that the array should be kept as small as possible to keep land costs down and localize safety considerations as much as possible. The heat exchangers were laid out with 40 feet centers as optimum for safety, land costs and accessibility.

Next, a plan view was drawn of buildings and equipment at the Fort Martin plant (Figure 5-17). From this and the layout of the TES array, a combined layout was drawn. As seen in Figure 5-18, there is no building around the TES units. This was done in order to eliminate an additional cost penalty, and reduce construction time. Also, the units themselves need no more protection for the elements than any other type of outdoor heat exchanger. No provision was necessary for cranes because the TES units will be rigged into place by contract during installation and removed in the same manner if module failure occurs.

Equipment sizing was done next. The flash tank was sized for a ten minute liquid holding capacity. This led to a cylindrical tank 6 feet in diameter and 20 feet tall with a volume

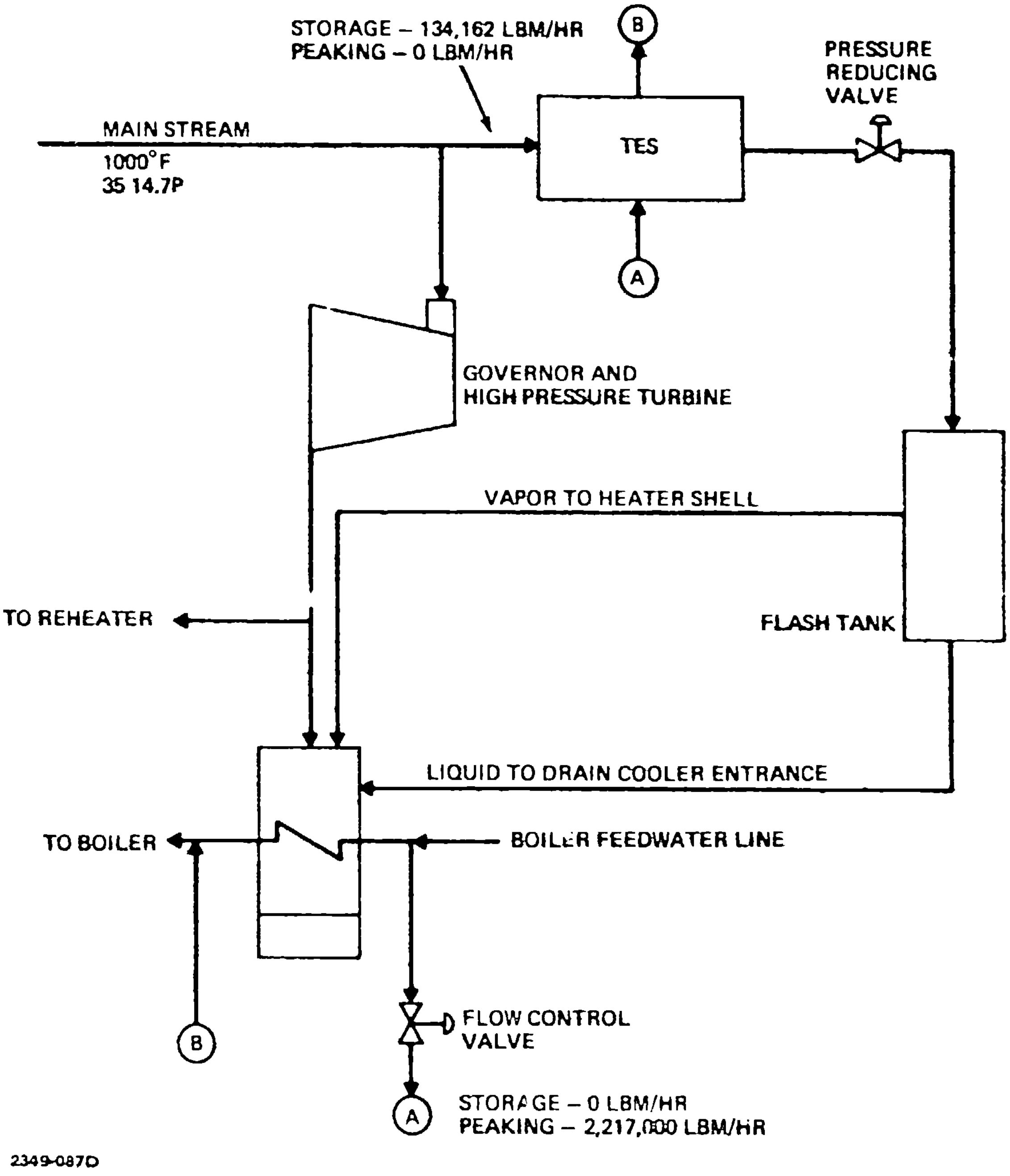

Fig. 5-15 Feedwater Heating System Schematic

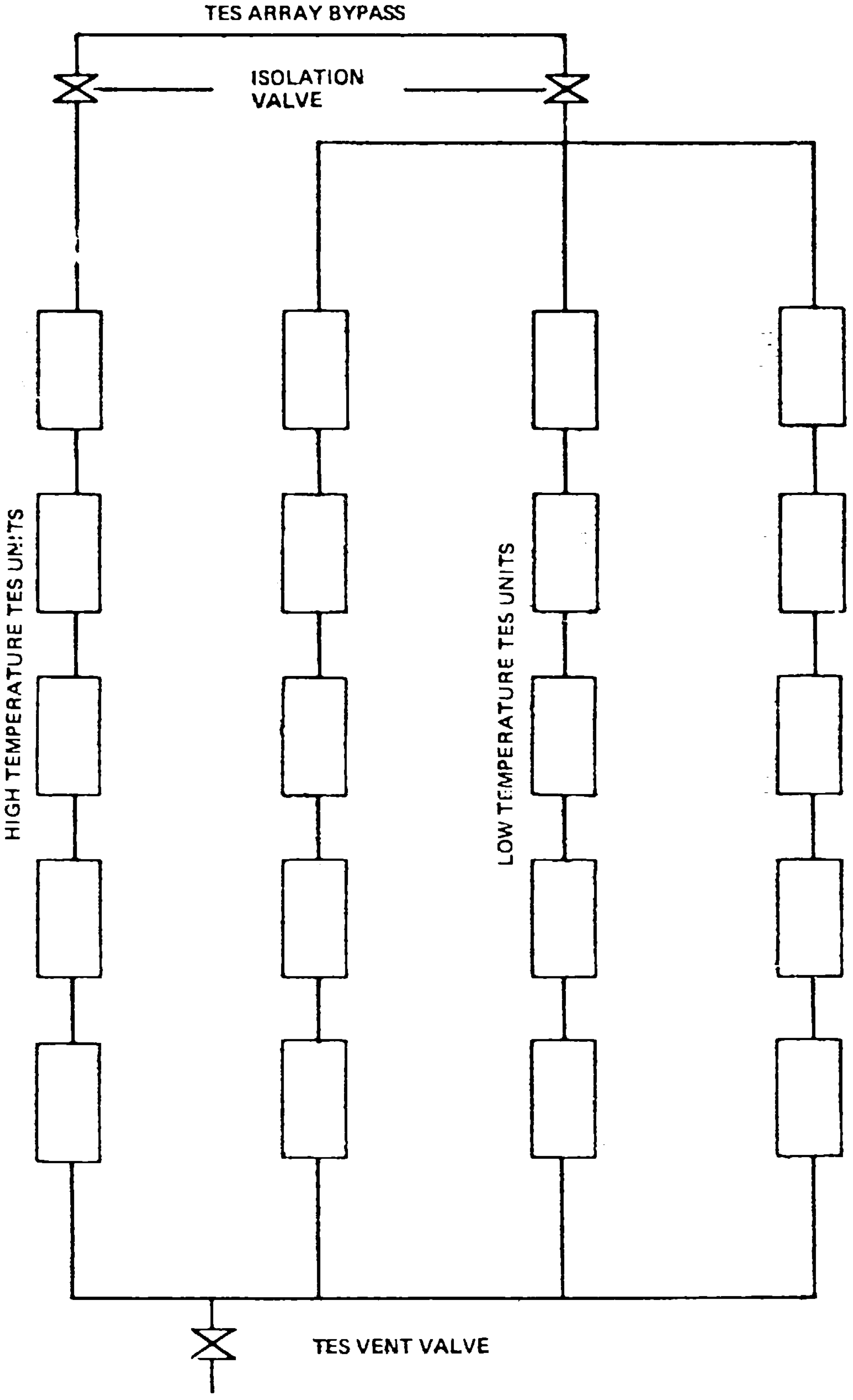

2349-088D

Fig. 5-16 Schematic Layout of TES Array

of 565.5 cubic feet. Tank thickness was determined from a design pressure of 1000 psia and resulted in a thichness of 1.53 inches. This vessel is to be constructed of carbon steel and has an approximate weight of 6 tons.

The next task was to determine all piping necessary for addition of the TES system. This included:

		Description	Flow Rate (lbm/hr)	Specific Volume (ft^3/lbm)
	1)	Main Steam Supply to TES units	134,162	.2066
STORAGE	2)	Main Condensed Liquid Line to Flash Tank	134,162	.04472
	3)	Vapor Lines to Heaters 7A and 7B Shell	71,146	.56896
	4)	Liquid Lines to Heaters 7A and 7B Drain Coder Entrance	63,016	.02087
USAGE	5)	Feedwater Line to Low Temperature TES Units	2,217,000	.01899
	6)	Feedwater Line Branches to Low Temperature TES Units	739,000	.01950
	7)	Feedwater Line to High Temperature TES Units and to Regain Boiler Feedwater Line	2,217,000	.02077

To determine inside diameter of the piping, an allowable velocity of 1,000 fpm/in of inside diameter up to 10,000 fpm was chosen to govern steam flow and 15 fps to govern liquid flow. For steam:

From continuity:

$$\dot{m} = \rho AV = AV/u$$

where V = (1000 ft/min)(60 min/hr) d_i

$$\dot{m} = d_i^2 \frac{(60,000\, d_i)}{4v(144)}$$

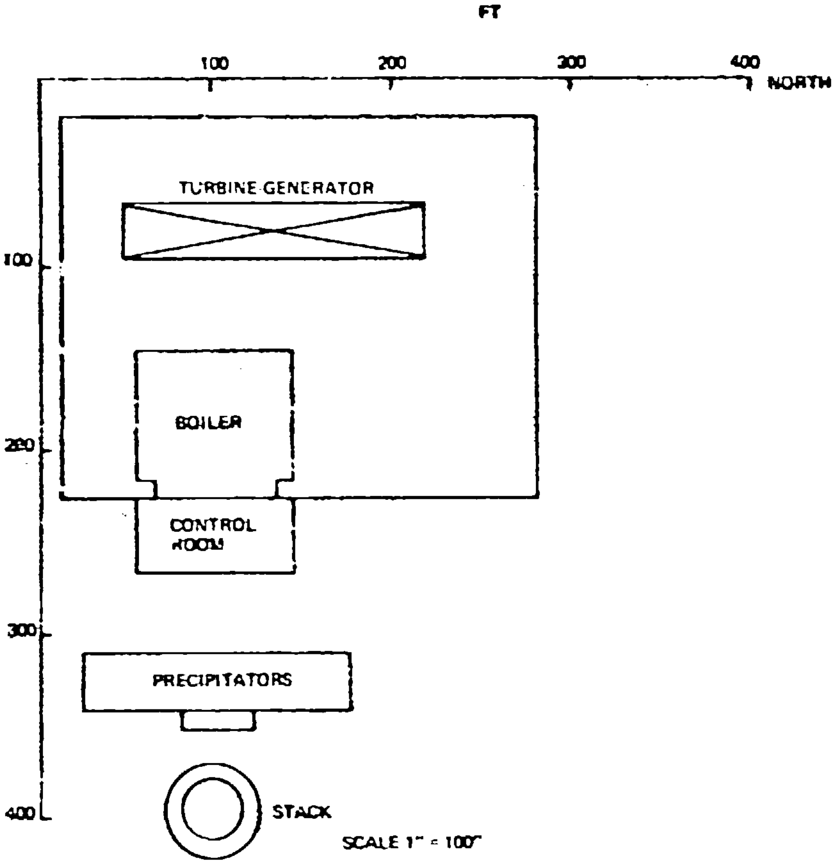

Fig. 5-17 Fort Martin Plan View

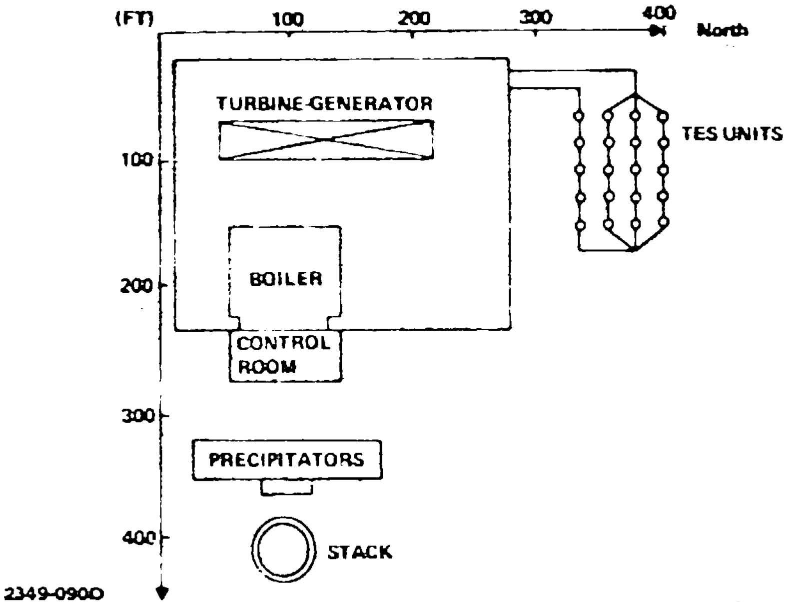

Fig. 5-18 Plan View — Ft. Martin, Feedwater Heating

therefore,

$$d_i = \sqrt[3]{\frac{m\ v}{104.167}}$$

$\dot{m}$ = flow, lbm/hr
ρ = density, lbm/ft^3
v = specific volume, ft^3/lbm
A = Area, ft^2
d_i = inside diameter, in.
V = velocity, ft/hr

and for liquids,

$$\dot{m} = \rho AV = AV/v$$

where V = 15 ft/sec = 54,000 ft/hr

so:

$$\dot{m} = \frac{d_i^{\,2}\ (54,000)}{4V(144)}$$

therefore,

$$d_i = \sqrt{\frac{\dot{m}v}{93.75}}$$

Pipe thickness was calculated by referring to the American National Standards Institute Code No. B31.1 where

$$t_m = \frac{pD + 2Sc + 2y\ pc}{2(S + (y - 1)p)}$$

$$t_n = \frac{tm}{.875}$$

p = Pressure, psig
D = Inside diameter, in.
S = Allowable Stress, psi
y = Temperature coefficient
c = Corrosion allowance, in.
t_m = Minimum wall thickness, in.
t_n = Nominal wall thickness, in.

A summary of piping dimensions is listed in Figure 5-19.

Pipe lengths for each type of line were scaled from the various figures and listed in Figure 5-20.

The amount of additional land necessary for the TES field was calculated by multiplying length by width of the array and adding 10% for a border around the field. This yielded approximately one-half acre. A foundation would be necessary for the units and it was determined that a two foot thick concrete slab should be used. The total amount of concrete necessary was 350 cubic yards. Additionally, a road for service vehicles would be constructed requiring 250 square yards of paving.

Pipe No.	Minimum Inside Diameter, In.	Nominal Thickness, In.	Pipe Weight lb/ft
1	4.39	.979	44.94
2	4.51	.744	41.75
3	4.98	2.53	14.14
4	2.11	.163	3.96
5	11.96	2.557	396.45
6	6.99	1.493	135.27
7	12.50	2.667	432.02

2349-091D

Figure 5-19 Pipe Dimensions

Pipe No.	Material	Pipe Lengths (ft)	Total Weight Weight
1	Stainless Steel	600	26,964
2	Stainless Steel	50	2,088
3	Carbon Steel	400	5,656
4	Carbon Steel	400	1,584
5	Carbon Steel	350	138,758
6	Carbon Steel	600	81,162
7	Carbon Steel	450	194,409

2349-092D

Figure 5-20 Pipe Lengths and Weight

Pipe No.	Material	Usage	Pipe Lengths (Ft)	Total Pipe Weight (lbs)
1	Stainless Steel	Main Steam	600	26,964
2	Stainless Steel	TES to Flash Tank	50	2,088
3	Carbon Steel	Flash Tank Return (Vapor)	400	5,656
4	Carbon Steel	Flash Tank Return (Liquid)	400	1,584

2349-093D

Fig. 5-21 Piping Characteristics — Auxiliary Power Design

For the Auxiliary Power Conversion Loop Case, additional land will be required to accommodate the additional five heat exchangers necessary. This would entail a field of .65 acres. Also, proportional increases could be expected in foundations, roads, and paving. Foundations would increase to 450 cubic yards and roads and paving to 225 square yards.

Piping for this case would basically include a main steam line to the TES units for charging, and the flash tank lines. Auxiliary loop piping is included in the auxiliary cycle cost analysis which follows. A list of the appropriate piping is included in Figure 5-21.

Auxiliary power conversion loop pricing must include an engineered steam turbine plant. This steam turbine plant is equivalent to a 26 MW_e net output plant minus the steam generator but would include the following:

Steam Turbine Generator
Condenser
Condensate Pumps
Heat Sinks
Auxiliary Turbine - Generator Building Equipment
Foundations
Earthwork and Grading
Roads and Paving
Piping and Valves
Circulating Water Piping and Valves
Turbine Generator Building
Overhead Crane
Control Room
Electrical Cabling and Switch gear
Land and Land Rights
Circulating Water Pump and Drivers
Switchyard
Deaerator
Feedpump and Driver

5.3 CONTROLS

Controls for integration of the TES into a power plant were divided into two categories. First, controls necessary for normal operation of the system and second, those necessary for safety considerations.

For TES use during normal plant operation the major categories of control can be divided into two basic categories, flow control and unit monitoring. Flow control can be accomplished by various pressure, flow and liquid level control valves. These control valves must have built-in logic so that they operate automatically. Also, control must be incorporated so that plant operators are able to override any of these valves if necessary.

Positive shut-off valves were also provided for isolation of individual TES units or strings so TES units could be removed from service. These would operate on signal if the heat exchangers became over-pressurized as in the event of a tube failure. They also must have override control to isolate TES units.

Unit monitoring can be accomplished by integrating all valve signals into a microprocessor and then tying this unit into the main plant control system. It would incorporate signals to show normal operating and faulted conditions. Redundancy could be provided if the hazards posed by TES malfunction are considered great enough to warrant it.

Additional controls are necessary for monitoring the auxiliary power cycle. This essentially be a scaled-down version of the control system incorporated into the base plant.

5.4 INTERFACE WITH PLANT

Integration of TES into a power plant is divided into two categories, mechanical and electrical. For this the plant must be shut down to accomplish incorporation. All other work such as heat exchanger installation, roadwork, paving, earthwork, grading and inter-TES piping installation can be done while the plant is under normal operation.

For the feedwater heating system the mechanical work will include tapping to the main steam line so that flow may be directed to the TES units during storage. The feedwater lines must also be tapped into so that auxiliary regenerative feedwater heating can be accomplished during peaking. The separate cycle does not affect plant operation during peaking, but does require connection into the main steam line for the energy source.

Electrical interface would include the integration of the TES control center into the main plant control center, and in the separate cycle case also tying the switchyard of the auxiliary power cycle into the power grid of the base plant.

5.5 SAFETY CONSIDERATIONS

A tube leak in the heat exchanger will result in two different sets of problems depending on whether the TES system is in the peaking or the storage mode. If a tube leak occurs near the end of the peaking stage at a time when the salt is all or partially solidified the tube pressure may be transferred through the salt directly to the shell. The heat exchanger will be provided with blow-out panels to prevent catastrophic failure.

The heat exchangers will also be provided with strain gauge sensors on the shell to predict overpressurization. If this signal is received, the next step is to isolate the system and relieve shell pressure. This will be done automatically by closing the isolation valves at the inlet and exit of the TES array and bypassing TES flow back to the plant. The TES vent valve will next open to relieve pressure in the inter-TES piping and consequently in the heat exchangers.

Release of the high temperature molten salt will be taken care of passively by constructing a small earthen dike about the TES array to prevent spread.

With some salts there may be a release of toxic gases from the molten salt. The TES system will be located cutside and personnel access restricted to prevent hazard. Salts that would pose a hazard to nearby communities will not be selected.

If a tube leak occurs during the storage mode or when the salt is almost completely molten, shell side pressure protection will actuate a safety relief valve on the shell located in the void volume area. A signal will then be sent to the control room. The system is also automatically isolated and depressurized by the forgoing system. In this case there may be some release of molten salt but this would be relatively small since the inert gas blanketing above the salt would mainly be ejected from the TES and the system would begin depressurization on actuation of the pressure relief valve.

Section 6

MANUFACTURING CONSIDERATIONS

6.1 HEAT EXCHANGER FABRICATION

As discussed in the previous section, the high design pressure and temperature of the tube/shell unit results in a thick spherical dome which is difficult to forge and weld but appears to be producible with existing technology. The stayed configuration greatly reduces weight and required depth of welds. The bulged domes can be fabricated using technology developed at Grumman. Recuperators required to control the TES heat exchanger outlet temperature are standard steam/steam or water/water units that can be procured from several suppliers.

The intermediate fluid loop design eliminates the need for the recuperator since a bypass or variable speed pump in the liquid metal loop can be used to control the system utility stream outlet temperature. The TES heat exchanger can be designed for low pressure so that standard tube/shell technology is applicable. The liquid metal heat exchanger does not present special fabrication problems.

6.2 SALT PROCESSING

An advantage of our modular heat exchanger approach is that each module can be fabricated, loaded with salt and the salt purified in the unit at the heat exchanger manufacturer. A sealed unit is shipped to the utility site. As discussed in 4.4.10, removal of solid impruities may be possible at the salt supplier and O_2 and H_2O will be eliminated by temperature-cycling the loaded TES unit while maintaining a vacuum.

6.3 SHIPPING AND ON-SITE INSTALLATION

The TES units are sized for standard railroad car shipping and on-site rigging by crane. The only connections required are welding of steam and feedwater lines. The entire TES can be assembled and all lines checked prior to plumbing into the existing plant. Plant downtime for the connection is expected to be short and the TES will include isolation valves so the plant can operate independently of the TES.

Section 7

COST EVALUATION

7.1 ITEMIZED CAPITAL COST BREAKDOWN

The major factor in determining if TES is cost effective is comparison of TES capital cost for a given peaking capability to the capital cost increment required to "enlarge" a plant by the same increment. For this tradeoff we decided to cost our baseline tube shell unit since this represents the technology most similar to current practice. As discussed in earlier sections, other concepts may in fact be superior but require additional design refinement to obtain realistic cost estimates. Even the tube and shell approach requires a somewhat innovative design approach (as discussed in 5.1.2) to avoid expensive heavy walled units.

To cost the tube and shell TES unit we took several approaches to check the estimates and also understand design features that contribute the major cost burdens. First, we contacted several suppliers of feedwater heaters and supplied them with a design definition (number of tubes, length and diameter, pressure and temperature). This resulted in estimates of about $900,000 for a 40 ft. high by 12 ft. diameter stainless steel unit. We then evaluated data on currently supplied feedwater heaters (Figure 7-1) and determined material cost. Subtracting this from the selling price resulted in an estimate of added value (supplier labor, overhead and profit). This indicated an added value of approximately $150,000 to $300,000 for units somewhat longer but only about one-half the diameter of our baseline TES unit. These feedwater heaters however contained up to five times the number of tubes as our unit, so welding labor could be expected to be higher even allowing for our thicker wall construction.

In parallel we performed an in-house design study of a "standard" 15 ft. diameter tube shell configuration and estimated the total weight (see 5.1.2) as 709,000 lbs. At a cost for 321 stainless steel of $2.10 per lb for tubing and $1.10 per lb for sheet the total material cost would be $830,700 for the basic heat exchanger, neglecting the support structure, weld metal, scrap, etc. Reducing this to a 12 ft diameter but adding some allowance for these items results in a material estimate of about $550,000. Assuming the value added of $150,000 from our feedwater heater data (for a unit with the same number of tubes) we would estimate the cost of a standard tube shell configuration at $700,000 or $200,000 less than the suppliers quick-look estimate. This is fairly consistent since we expected the supplier's quotes to be

		1 X 3	2 X 3	3 X	4 X 3	5 X 2	6 X 2	Steam Evaporator CKU
Conditions (Shell/Tube)								
Design Pressure,	psi	50/775	50/775	50/775	75/775	200/775	400/1950	250/425
Test Pressure,	psi	75/1163	75/1163	75/1163	113/1165	113/1163	600/2925	375/638
Design Temperature,	°F	380/300	380/300	380/300	430/330	390/390	450/450	410/450
Corrosion Allowance,	in			1/16				
Tubes								SB-163
Material			SA-249 TP 304 -- Material					Incology 800
Number		2000	1,277	1,226	782	3,129	3,225	228
CD/Thickness, in x BWG		3/4 x 20	7/8 x 20	1 x 20	1 x 20	3/4 x 20	5/8 x 18	3/4 x 18
Pitch	in	1-3/16	1-11/16	1-1/4	1-3/8	15/16	13/16	1-1/8
Average Length	ft	89.4	85.4	85.6	81.7	62.6	62.8	27.5 eff.
Shell								
Material			SA-515-70 -- Material					
OD/Thickness, in x in		90 x 1/2	82 x 1/2	81 x 1/2	72 x 1/2	95.5x3/4	98.5 x 1-1/4	65.37 x 11/16
Overall Length,	ft	49.50	47.00	47.25	44.75	40.00	42.00	32.25
Heat Exchanger								
Effective Surface,	ft^2	34,226	24,367	26,841	16,340	37,109	31,707	2,509
Gross Surface,	ft^2	35,052	24,936	27,423	16,678	38,416	33,087	2,535
Tube Bundle Weight,	lb	123,000	91,000	90,000	60,000	123,000	118,000	10,400
Dry Weight,	lb	151,000	11[illegible]	111,000	78,000	152,000	162,000	29,500
Thermal Duty,	M Btu	276,237	189,082	257,600	141,879	497,500	453,500	43,460
Original Price								
Per Shell	$/Shell	338,194	149,421	154,115	107,925	224,890	244,158	51,833
Per Eff. Surface	$/ft^2	5.99	6.13	5.74	6.60	6.06	7.70	20.68
Per Gross Surface	$/ft^2	5.85	5.99	5.62	6.47	5.85	7.38	20.47
Per Bundle Weight	$/lb	1.67	1.64	1.71	1.80	1.83	2.07	4.99
Per Dry Weight	$/lb	1.36	1.32	1.39	1.38	1.48	1.51	1.76
Per Million Btu $/mm	Btu	742	790	598	762	452	538	1,194
Year for above		1971.5	1971.5	1971.5	1971.5	1971.5	1971.5	1972.5
1976.5 Extrapolation								
Handy Whitman Index								
Per Eff. Surface	$/ft^2	9.03	9.24	8.66	9.95	9.14	11.61	
Per Gross Surface	$/ft^2	8.82	9.03	8.47	9.76	8.82	11.13	
Per Bundle Weight	$/lb^2	2.52	2.47	2.58	2.71	2.76	3.12	
Per Dry Weight	$/lb	2.20	1.99	2.08	2.08	2.23	2.28	
Thermal Duty	$/10^6 Btu	1119.00	1191.00	902.00	1149.00	682.00	811.00	

B&R Information Source:

Feedwater Heaters – WPPSS Spec. No. 2808-10

Steam Evaporator – WPPSS Spec. No. 2808-26

Fig. 7-1 Low Temperature Shell – Tube Heat Exchanger Prices conservative because we provided very limited information and not the detailed specification necessary for an accurate quote. Also our thicker wall will increase welding and forging costs.

It was obvious from the breakdown that the unit cost was too high, mostly because of the large amount of steel required. This motivated our evaluation of the stayed configuration. Only one of many stayed approaches was considered (see 5.1.2) but this resulted in a unit weight of 265,500 lbs and material cost of $343,000. For a 12 ft diameter we estimate a material cost (including 10% for support structure, etc.) of $240,000. Domes for this configuration are relatively thin (2 in.), which simplifies welding. Also the domes are not forged but bulged in a low-cost proprietary Grumman process so that a value-added estimate of $150,000 should be realistic for stayed construction. This results in a total heat exchanger cost of $390,000, which is the figure used in our detailed cost breakdown. The recuperator cost has been estimated by suppliers as $500,000. Since this is standard shell and tube technology, this cost is considered to be reasonably accurate.

Expenses were broken down into various unit cost categories. Figure 7-2 contains a list of unit costs for the various items.

For the regenerative feedwater heating case, Fig. 7-3 gives the total cost breakdown for the individual items. For the single loop separate power conversion loop an investment cost summary for the auxiliary steam plant is included as Fig. 7-4. Fig. 7-5 includes the same items as the regenerative feedwater heating case with the addition of the steam turbine cycle and excluding an incremental turbine-generator and electrical cost.

As shown, the use of TES for both feedwater heating or auxiliary power generation is less costly than increasing boiler capacity. It should be pointed out that neither design achieved the optimum (or target) cost figure, suggesting either that less peaking energy should have been stored and/or that further design refinement is required. A review of the actual power profile for Ft. Martin indicated that the power plant capacity could be reduced by about 7% for the energy storage values indicated in Fig. 4-49. This is because the actual power savings is reflected by a variable, rather than the step-wise 5% reduction used in our earlier cases. Hence, for the feedwater heating and auxiliary power supply cases the power plant capacity would be increased by 37.36 and 41.56 MW, respectively.

Earthwork and Grading	$16,375/acre
Roads and Paving	$5.38/square yard
Land and Land Rights	$100,000/acre
Foundations	$2.66/cubic yard
Piping and Valving	

Regenerative Feedwater Heating System Pipe No.	Cost $/foot	Auxiliary Power Loop Pipe No.	Cost $/foot
1	337	1	337
2	313	2	313
3	35	3	35
4	10	4	10
5	991		
6	338		
7	1080		

Instrumentation and Control	$50,000
Flash Tank (6 ft. diameter)	$3/lb

Fig. 7-2 Typical Unit Costs

		Cost
Earthwork and Grading		$ 8,200
Roads and Paving		1,300
Land and Land Rights		60,000
Foundations		93,000
Piping and Valving		1,166,800
Instrumentation and Control		50,000
Flash Tank		36,000
Recuperator		500,000
TES Units		7,800,000
TES Salt		1,219,000
	Subtotal	$10,924,300
Contingency & Int During Constr at 15%		1,638,650
Engrg & Constr Mgmt at 12%		1,310,920
Increm T-G (37.36MW) & Elect Cost at $230/KW$_e$		8,592,000
	Total	$22,465,860
System Breakeven = (37.36 MW) ($650/KW)		$24,284,000
Net Savings — New Plant or Plant w/o Excess T-G		$ 1,818,140
— Retrofit, Plant with Excess T-G		$10,410,140

2349-096D

Fig. 7-3 Total TES System Capital Cost – Ft. Martin, Feedwater Heating Case

	Captial Costs:	$1,000
a)	Steam Turbine Generator	4,152
b)	Condenser	837
c)	Condensate Pumps	36
d)	Heat Sinks	327
e)	Aux T-G Building Equipment	56
f)	Foundations	132
g)	Earthwork & Grading	23
h)	Roads & Paving	33
i)	Piping and Valves	33
j)	Circ. Water Piping & Valves	54
k)	T-G Building (Shell)	318
l)	Overhead Crane	103
m)	Control Room	40
n)	Elect. Cabling & Switchgear	140
o)	Land & Land Rights	127
p)	Circ. Water Pumps & Drivers	353
q)	Switchyard	344
r)	Deaerator	48
s)	Feed Pump + Driver	53
	Total Direct Cost	$7,183

2349-095D

Fig. 7-4 Investment Cost Summary – Auxiliary Power Steam Turbine Plant

	Cost
Earthwork and Grading	$ 10,300
Roads and Paving	1,600
Land and Land Rights	63,000
Foundations	120,000
Piping and Valving	235,900
Instrumentation and Control	50,000
Flash Tank	48,900
Recuperator	500,000
TES Units	9,750,000
TES Salt	1,530,700
Auxiliary Steam	7,183,000
Subtotal:	19,493,400
Contingency and Interest During Construction at 15%	2,924,010
Engrg and Constr Management at 12%	2,339,200
Total System Cost	24,756,618
System Breakeven = (41.36 MW) ($650/KW) =	$26,884,000
Net Savings	$ 2,127,382

2349-094D

Fig. 7-5 Capital Costs of Separate Power Conversion Loop, Ft. Martin

7.2 PLANT PERFORMANCE - OPERATING AND MAINTENANCE EXPENSES

7.2.1 Operating Expenses

As discussed in Section 4.7.1, (Figure 4-48), inclusion of the TES system to meet peaking requirements will decrease the net plant heat rate and, therefore, require less fuel consumption for the feedwater heating case compared to a cycled plant. As shown, a difference of 37 BTU/KWH was predicted for this case. Using this, with a fuel cost of $\$1.25/10^6$ BTU during a yearly operating period of 7000 hours (full year minus planned maintenance), a fuel savings of $182,893 can be expected. Neglecting fuel cost escalation and using an interest factor of 15% this corresponds to a capital savings of about $1,555,000. Hence, accounting for this savings lowers our capital cost estimate from about $22.5 million to $21.5 million, and therefore, the system economics appear even more favorable in this case. As previously mentioned in the use of the auxiliary power cycle, no change in the plant heat rate is projected and the capital cost of about $25 million therefore remains the same.

7.2.2 Maintenance Expenses

The expense of implementing TES in a power plant system should be in the same range as heat exchangers of similar type. With the fixed head shell and tube design these units are comparable to feedwater heaters except that when a unit is taken out of service it cannot be repaired on site but must be shipped to the factory for service. All other attendant mechanical and electrical equipment should incur the same operating and maintenance expenses because the items are identical to those presently in use. The TES system is basically a passive unit except for twice a day valve actuation. Considering the small number and use of the TES active components, unusually high operating and maintenance costs are not expected.

7.3 COST/BENEFIT ANALYSIS

We have shown in this section that a latent heat thermal energy storage system can be incorporated into a new supercritical fossil plant to provide approximately 7% peaking capability at less cost than enlarging the plant capacity by 7%. This conclusion requires innovative variation on the standard tube shell concept and some further design refinement on module length, site spacing, etc. It is also possible that some of the other concepts identified in this report may prove even more effective upon further detailed evaluation.

For a retrofit situation there is a special case where TES is very cost effective. This is when an oil plant is converted to coal resulting in excess turbine capacity. Referring to Figure 7-3 it can be seen that if the T-G is already available the TES can provide a peaking capability at a significantly lower cost than the cost of building this capability into a new plant. Providing that land is available, the TES system design and cost estimate should be valid for retrofit installations.

The TES thus can be used to counteract the disincentive which exists in converting from oil or coal, namely that capacity is lost thus accelerating the requirement for new plant construction. An added benefit of the TES approach that cannot be fully assessed is the reliability of operating plants at base load. This should extend the life and reduce the maintenance of the plant.

7.4 INSTALLATION IN NEW VERSUS EXISTING PLANTS

The implementation of TES in existing plants is bound by the physical layout of the plant and its operating conditions. That is, land for the TES array must be available close to the plant to minimize expensive piping costs. This is not always the case. In urban areas land is usually at a premium and energy peak loads are usually met with older fossil units. Ideally, this would be a good technical location for the use of TES but it may not be economically feasible if nearby land cannot be acquired. Another point concerns operation of the plant and its cycle. An existing fossil plant will operate at the point that will yield the best heat rate and output for a given time period. The introduction of TES tends to upset the balance and would incur operational changes. This is because the plant has been designed for specific thermodynamic conditions, flow rates, etc. and is now forced to operate essentially off-design.

New plant use of TES would allow the designer to modify the power plant cycle to achieve optimum peak shaving before equipment is purchased. Investigation of relationships between heat rate, output, amount of peak shaving and cost could be made to determine the most economical alternative. Then equipment sizing and system layouts could also be optimized to complete the economic feasibility picture.

President Carter has urged conversion of oil and natural gas plants to coal to reduce consumption of foreign oil. The conversion of an oil or natural gas boiler to coal creates a problem to most utilities in that the boiler, when coal-fired, is then undersized, resulting in excess capacity in the existing turbine generator unit. Boiler output could be augmented by TES to produce the previously oil-fired boiler output with a coal-fired boiler, since excess turbine-generator capacity would more easily allow cycling of the turbine-generator set. This would appear to be the case that would be most applicable to the future of the utility industry, but each utility must determine the economics of TES for an individual site and then determine if its use is justified.

Section 8

ACTION REQUIRED FOR SYSTEM IMPLEMENTATION

This report represents a reasonably detailed first look at the feasibility of energy storage in the latent heat of salt eutectics. The concept appears cost effective but certain key issues must be more fully explored before a public utility would implement the system for electrical power generation. The critical TES element is the heat exchanger that we have designed with only a small allowance for corrosion based on our consultants' review of available data. Corrosion tests of selected salts purified to various levels and contained in stainless steel are required to verify this assumption. The tests can be small scale.

Various heat exchanger concepts have been discussed and a tube and shell with a stayed structural arrangement recommended for minimum development within a cost target. More detailed design and costing of this unit is required to verify this selection. The advantages of our alternate concepts should be more fully explored for specific applications (such as the heat pipe unit for nuclear plants) and for longer term applications allowing time for further development of active heat exchanger concepts. Finally, a pilot demonstration should be undertaken at a participating utility to evaluate the system under actual operating temperature and duty cycles.

APPENDIX A

EVALUATION OF PROPOSED TES LOCATIONS

LOCATION 1 DOUBLE LOOP REGENERATIVE HEATING AUGMENTATION

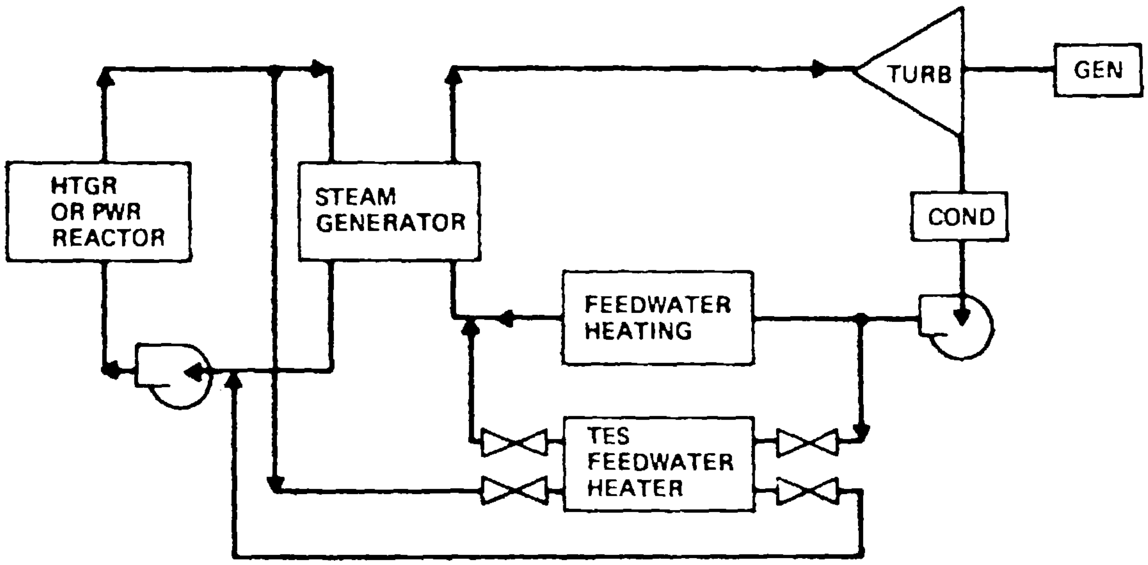

Generating Station		Evaluation of TES Location
Plt. Name	Matrix ID	
Cooper	A1	TES Location not applicable for direct cycle bwr.
TMI	B1	Use of primary cycle fluid as heat source for TES feedwater heater not recommended. a) TES F.W. htr. would be required to be located inside of primary containment. Due to radioactivity of primary cycle fluid. b) Extensive containment redesign required to accommodate TES, e.g., pentrations, isolation valves, piping, equipment arrangement. c) Additional NRC licensing required regarding pipe break & pipe whip analyses, location and safe shutdowns.
Fort Martin	C1	TES location not applicable for supercritical fossil plt.
Fort St. Vrain	D1	Use of primary cycle fluid (helium) as heat source for TES f[illegible] heater not recommended. a) Primary coolant system is entirely encapsulated [illegible] prestressed concrete reactor vessel (PCRV), hence [illegible]ing connections to this loop would be extremely difficult.
Fort St. Vrain	D1	b) Because TES would be subjected to radioactive primary fluid, it must be placed within the primary containment (PCRV). This would require an extensive redesign.
Roseton	E1	TES location not applicable for high pressure fossil plt.

2349-097D

Fig. A-1 Evaluation of Proposed TES Location No. 1

LOCATION 2 SINGLE LOOP REGENERATIVE HEATING AUGMENTATION

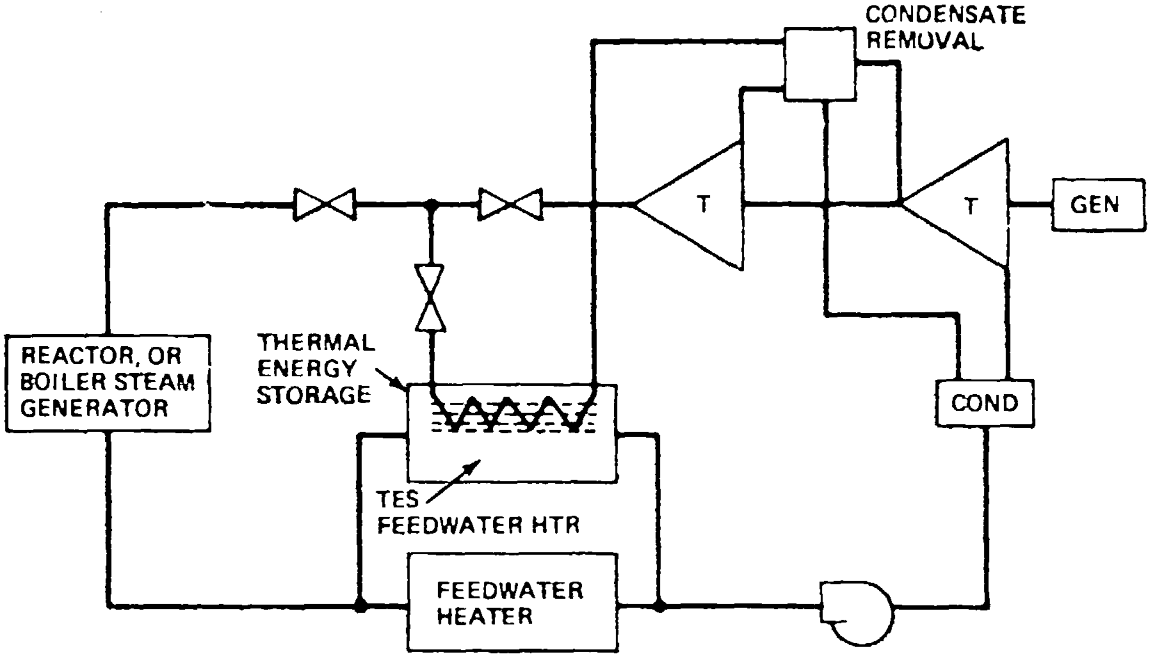

Generating Station		
Plt. Name	Matrix ID	Evaluation of TES Location
Cooper	A2	TES location not recommended a) Bwr condensate & main steam contain radioactive hazards, thus TES FW. HTR. must be shielded.
TMI	B2	TES location is candidate for further evaluation.
Fort Martin	C2	TES location is candidate for further evaluation.
Fort St. Vrain	D2	TES location is candidate for further evaluation.
Roseton	E2	TES location is candidate for further evaluation.

LOCATION 3 DOUBLE LOOP REHEAT AUGMENTATION

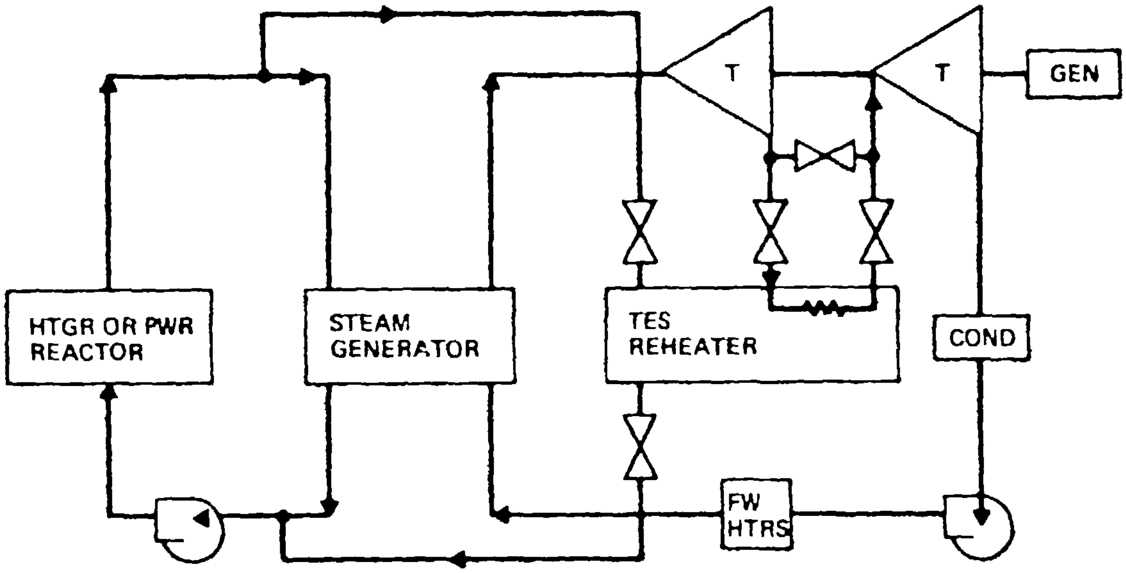

Generating Station		Evaluation of TES Location
Plt. Name	**Matrix ID**	
Cooper	A3	TES location not applicable for direct cycle BWR.
TMI	B3	TES location not recommended, see comments for B1.
Fort Martin	C3	TES location not applicable for supercritical fossil plt.
Fort St. Vrain	D3	TES location not recommended, see comments for D1.
Roseton	E3	TES Location not applicable for high pressure fossil plt.

LOCATION 4 SINGLE LOOP REHEAT AUGMENTATION

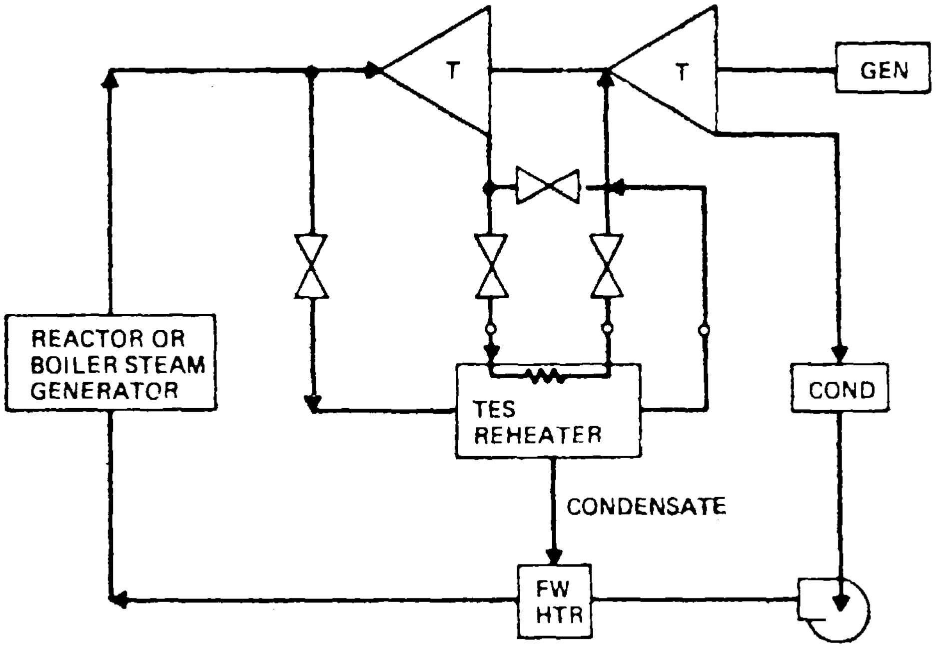

Generating Station		Evaluation of TES Location
Plt. Name	Matrix ID	
Cooper	(A4)	TES location is candidate for further evaluation.
TMI	(B4)	TES location is candidate for further evaluation.
Fort Martin	C4	TES location in supercritical fossil plt. not recommended. a) Boiler reheat section underutilized when operating in rated condition. b) Reheating HP turbine exhaust steam to 1000°F using a heat source at 1000°F would require a TES system having a 0° approach, such a system would be extremely large.
Fort St. Vrain	D4	TES location not recommended, see comments for C4.
Roseton	E4	TES location not recommended, see comments for C4

LOCATION 5 DOUBLE LOOP MAIN STEAM AUGMENTATION

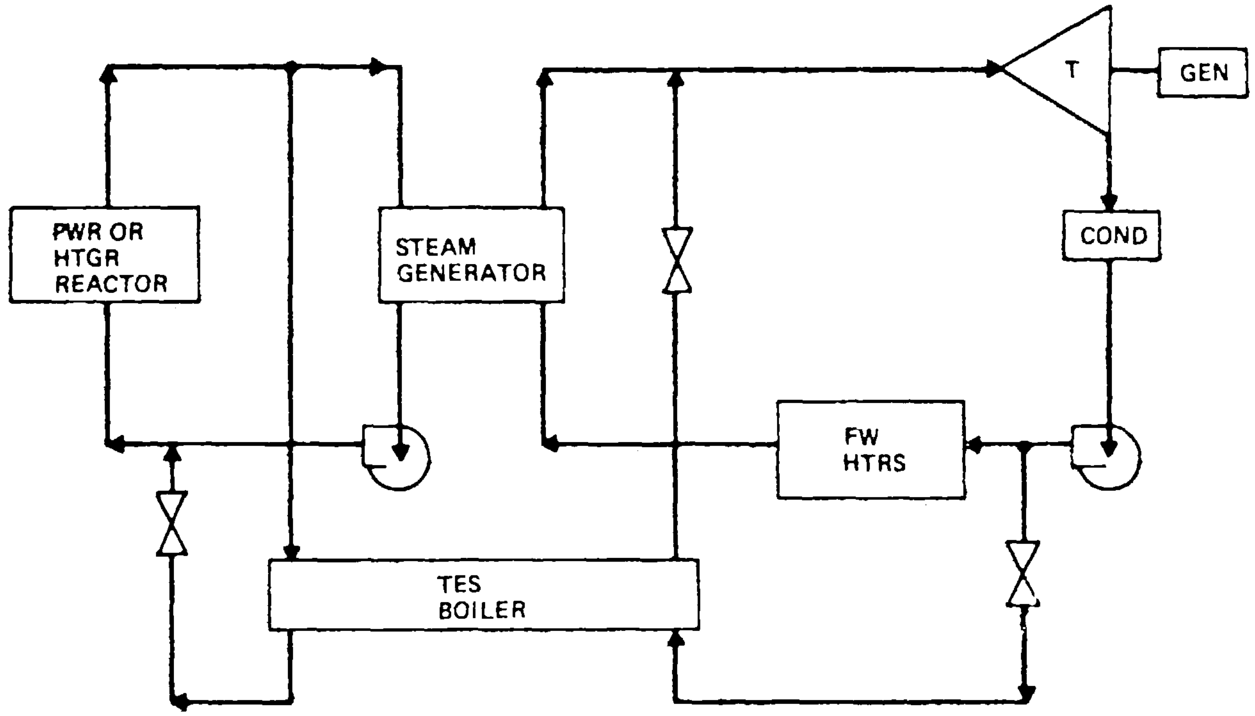

Generating Station		Evaluation of TES Location
Plt. Name	Matrix ID	
Cooper	A5	TES location not applicable for direct cycle BWR.
TMI	B5	TES location not recommended, see comments for B1.
Fort Martin	C5	TES location not applicable for supercritical fossil plt.
Fort St. Vrain	D5	TES location not recommended, see comments for D1.
Roseton	E5	TES location not applicable for high pressure fossil plt.

2349-099D

LOCATION 6 SINGLE LOOP CROSSOVER STEAM AUGMENTATION

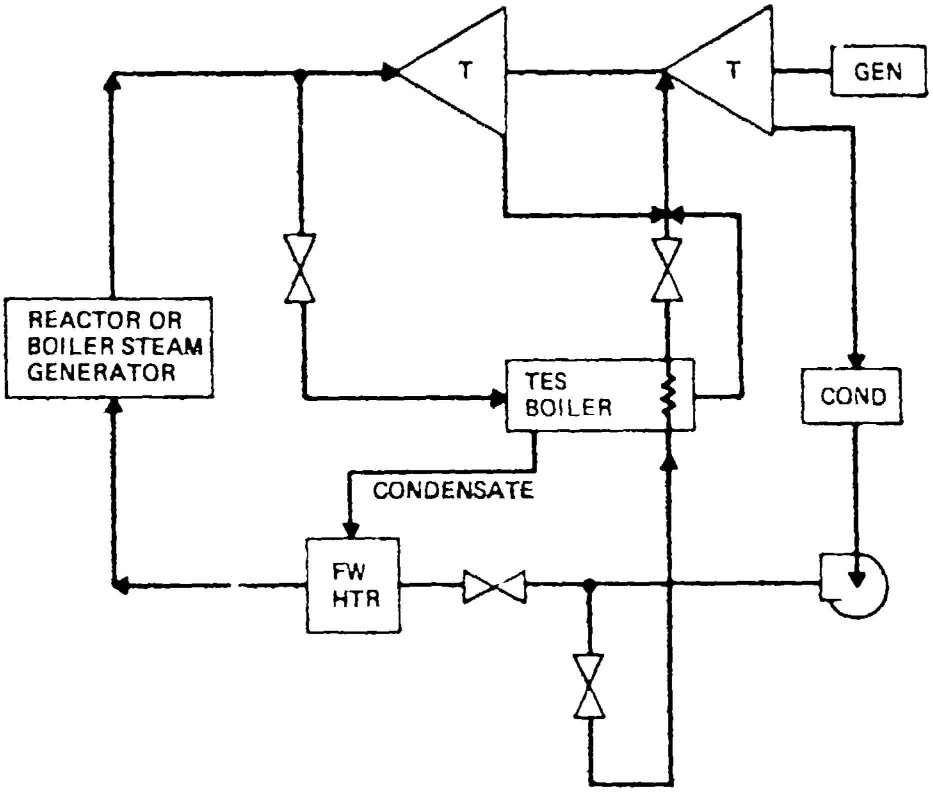

Generating Station		Evaluation of TES Location
Plt. Name	Matrix ID	
Cooper	A6	TES location not recommended a) TES boiler requires nuclear shielding as it would handle radioactive condensate b) NRC licensing problems
TMI	B6	TES location is feasible subject to flow limitations [illegible] LP turbine.
Fort Martin	C6	TES location not recommended, a) IP turbine steam admission state point would be saturated which degrades turbine performance.
Fort St. Vrain	D6	TES location not recommended, see comments for C6.
Roseton	E6	TES location not recommended, see comments for C6.

LOCATION 7 DOUBLE LOOP SEPARATE POWER CONVERSION LOOP – ISOLATED

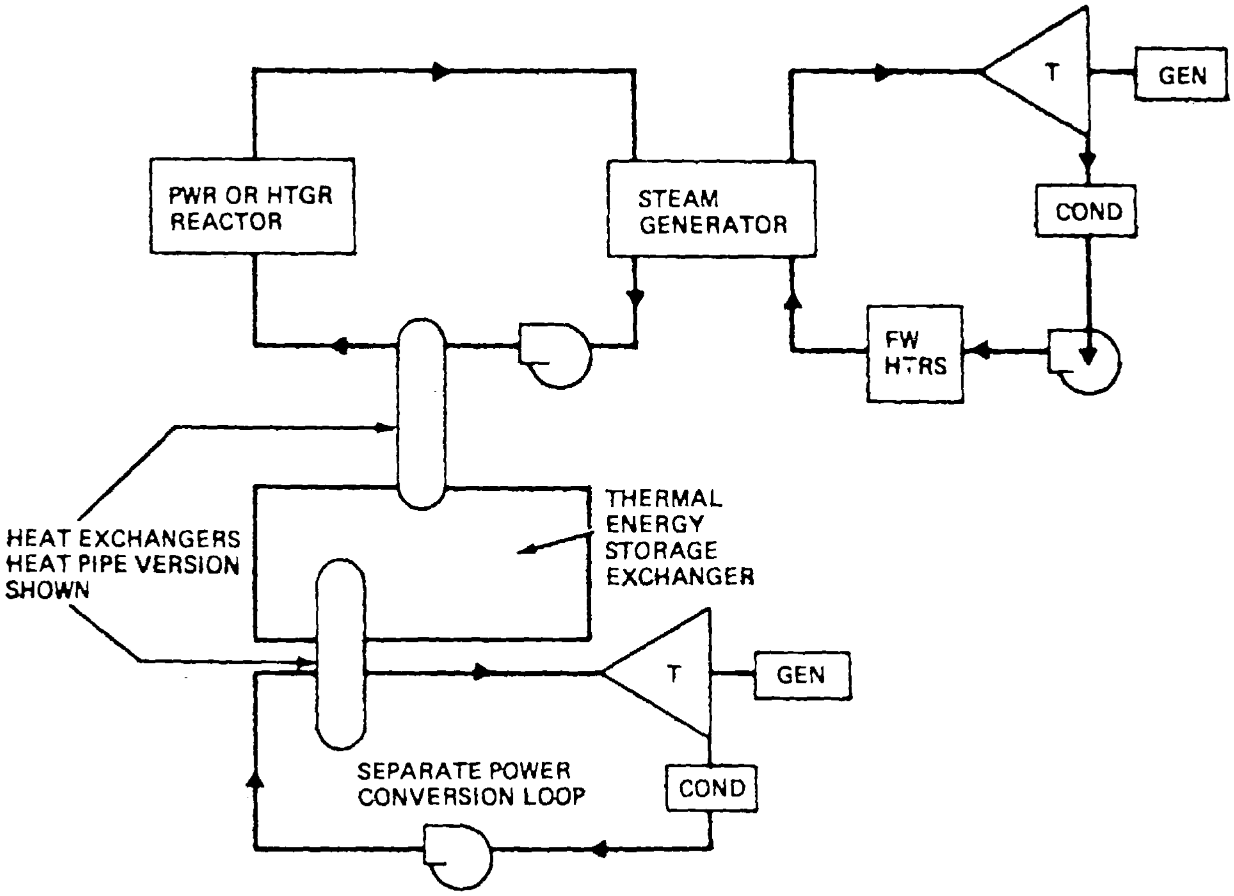

Generating Station		Evaluation of TES Location
Plt. Name	Matrix ID	
Cooper	A7	TES location not applicable for direct cycle BWR.
TMI	B7	TES location not recommended, see comments for B1.
Fort Martin	C7	TES location not applicable for supercritical fossil plt.
Fort St. Vrain	D7	TES location not recommended, see comments for D1.
Roseton	E7	TES location not applicable for high pressure fossil plt.

LOCATION 8 SINGLE LOOP SEPARATE POWER CONVERSION [illegible]

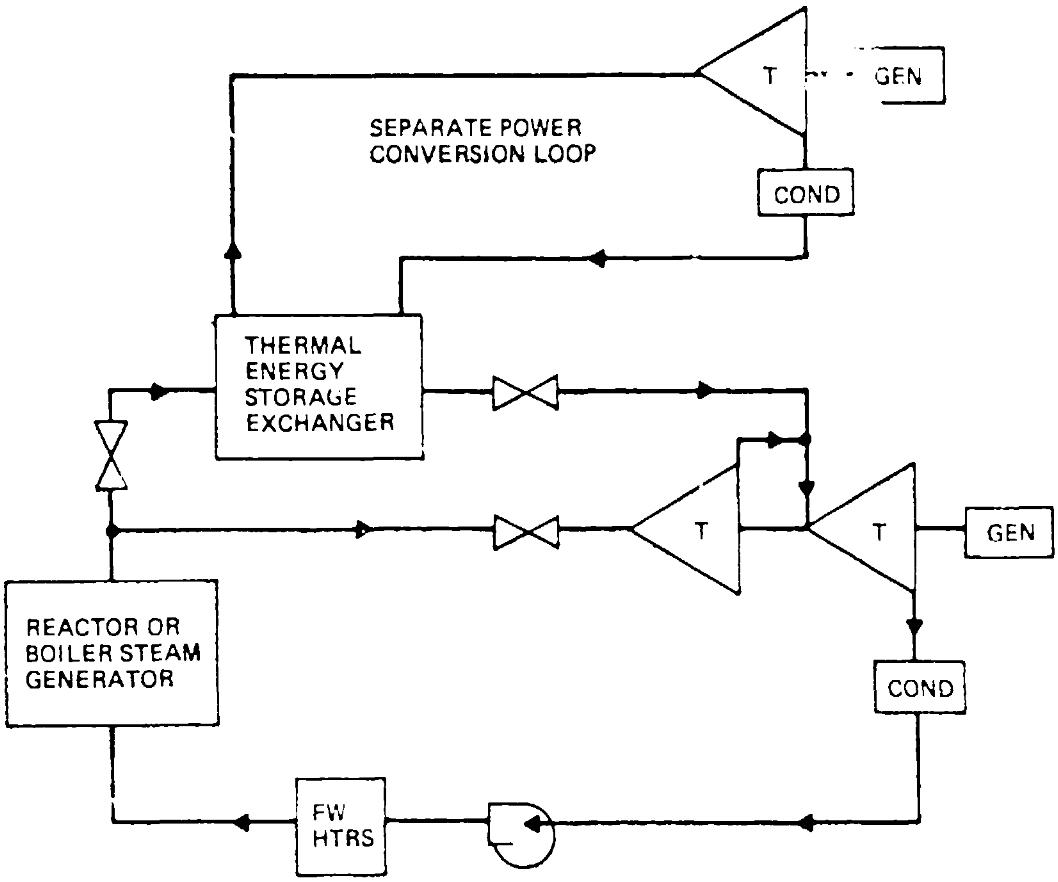

Generating Station		Evaluation of TES Location
Plt. Name	Matrix ID	
Cooper	A8	TES location not recommended a) Throttle steam conditions to TES inadequate b) Steam conditions in secondary power conversion loop poor, net KW output would be low
TMI	B8	TES location not recommended, see comments for A8.
Fort Martin	C8	TES location is candidate for further evaluation.
Fort St. Vrain	D8	TES location is candidate for further evaluation.
Roseton	E8	TES location is candidate for further evaluation.

LOCATION 9 DOUBLE LOOP INTERMEDIATE HEAT EXCHANGE/THERMAL STORAGE

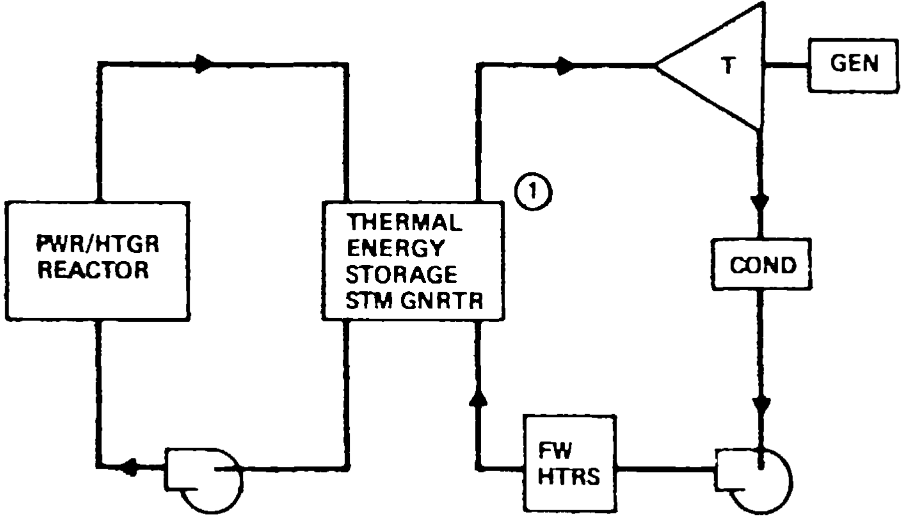

① WOULD INCLUDE SEPARATE TES AND STEAM GENERATING SECTIONS

Generating Station		Evaluation of TES Location
Plt. Name	Matrix ID	
Cooper	A9	TES location not applicable for direct cycle BWR.
TMI	B9	TES location not recommended a) TES steam generator entails extensive development costs b) NRC licensing problems c) Beyond scope of study
Fort Martin	C9	TES location not applicable for supercritical fossil plt.
Fort St. Vrain	D9	TES location not recommended, see comments for B9.
Roseton	E9	TES location not applicable for high pressure fossil plt.

2349-098D

Fig. A-2, Evaluation of Proposed TES Location No. 9

LOCATION 10 SINGLE LOOP INTERMEDIATE EXCHANGER/THERMAL STORAGE (NASA PATENT APPLICATION REF 1)

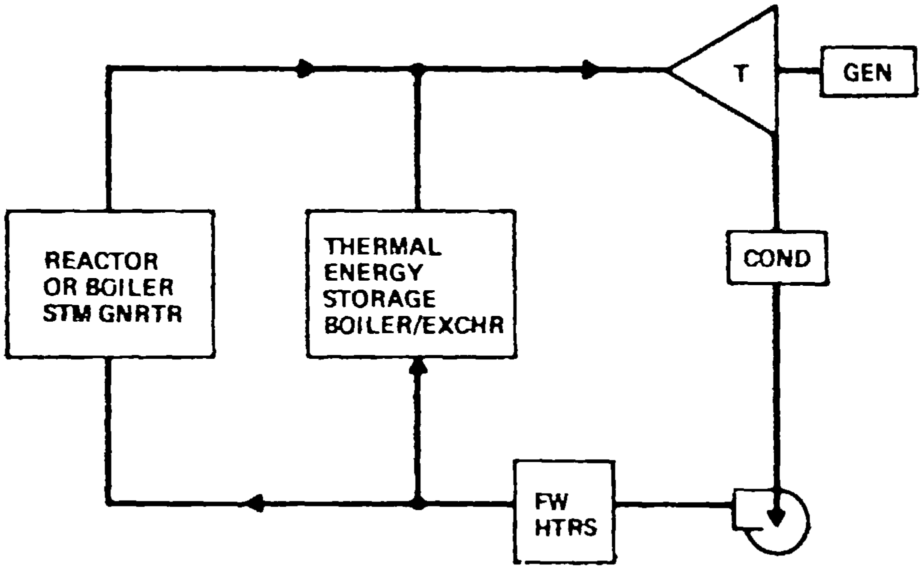

Generating Station		Evaluation of TES Location
Plt. Name	Matrix ID	
Cooper	A10	TES location not recommended, see comments for B9.
TMI	B10	TES location not recommended a) Design entails extensive development b) Beyond scope of study
Fort Martin	C10	TES location not recommended, see comments for B10.
Fort St. Vrain	D10	TES location not recommended, see comments for B10.
Roseton	E10	TES location not recommended, see comments for B10.

2349-021D

Fig. 3-6 Location 8-Single Loop Separate Power Conversion Cycle

APPENDIX B

AVERAGE DAILY DEMAND CURVES

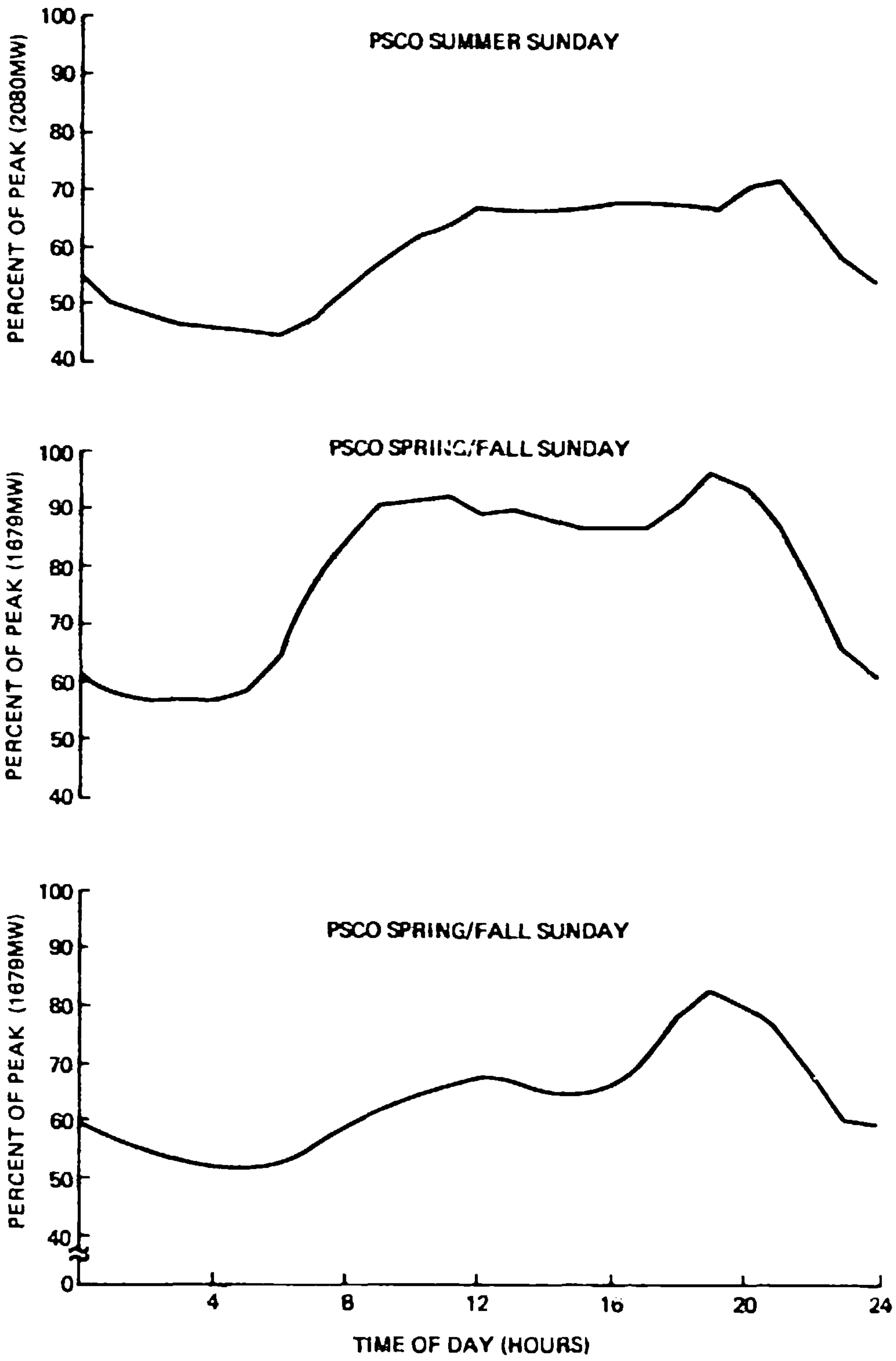

2349-100D

Average Demand, Ft. St. Vrain Unit #1

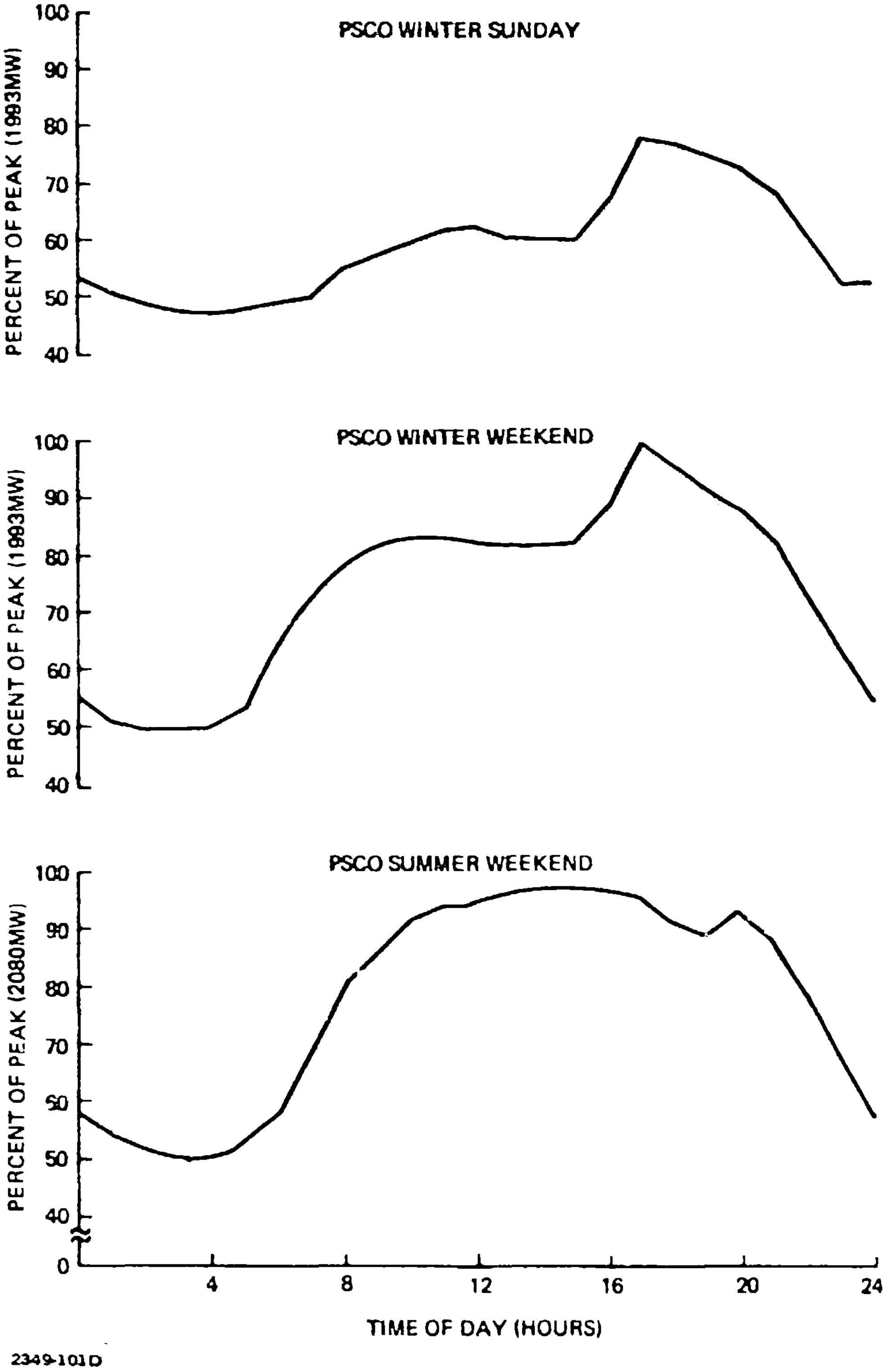

Average Demand, Ft. St. Vrain Unit #1

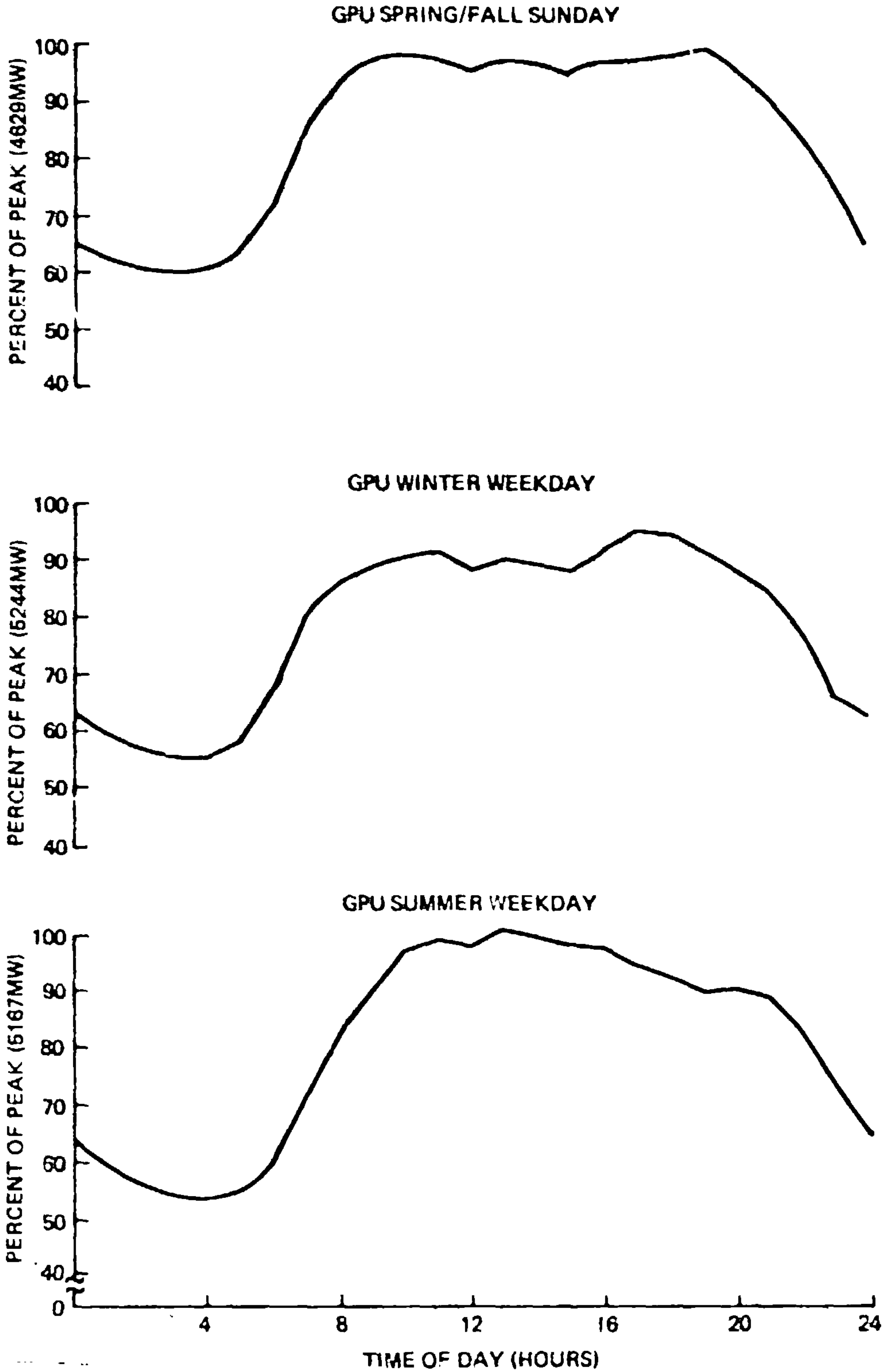

2343-102D

Average Demand, Three Mile Unit #1

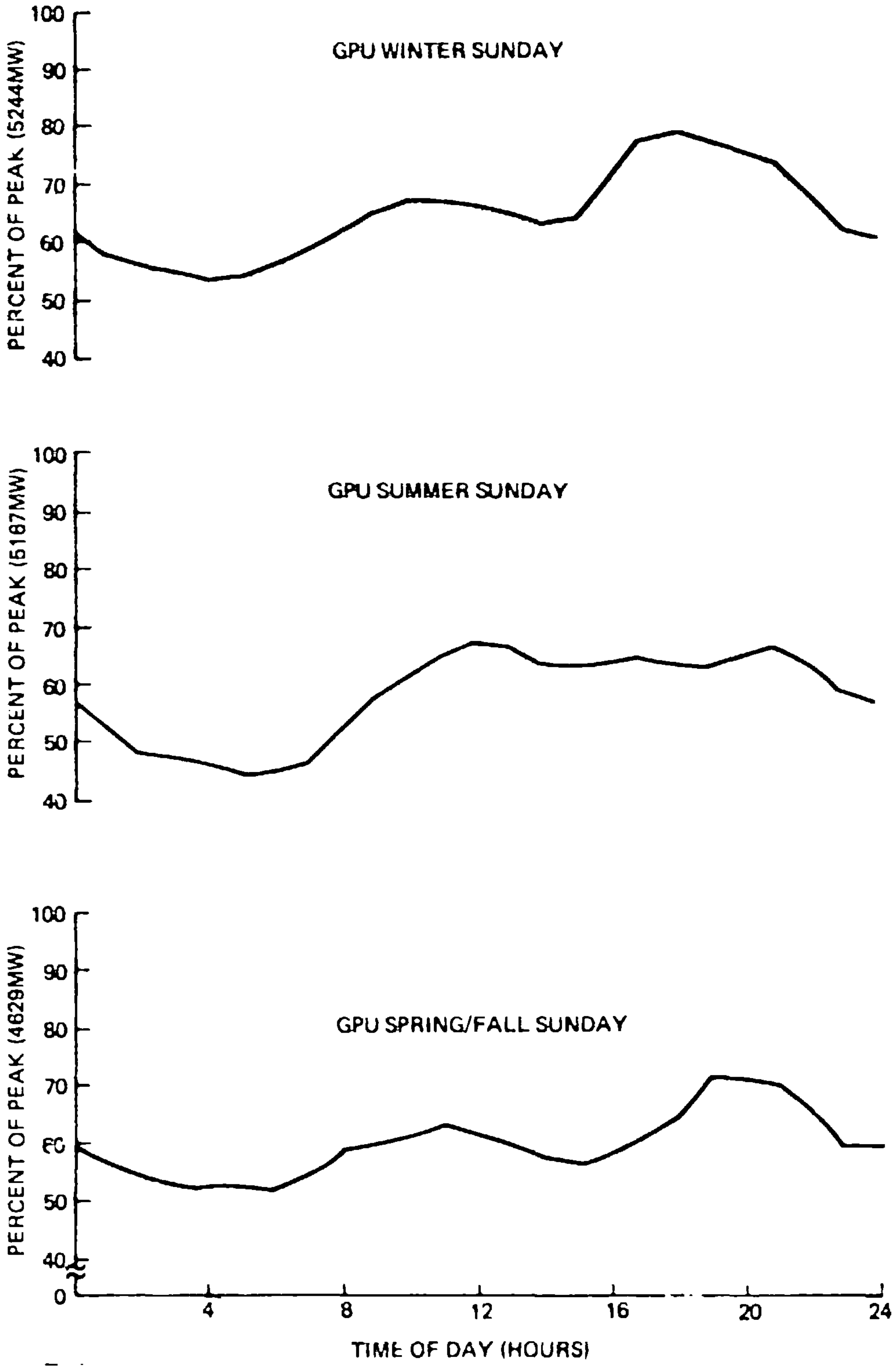

2349-103D

Average Demand, Three Mile Unit #1

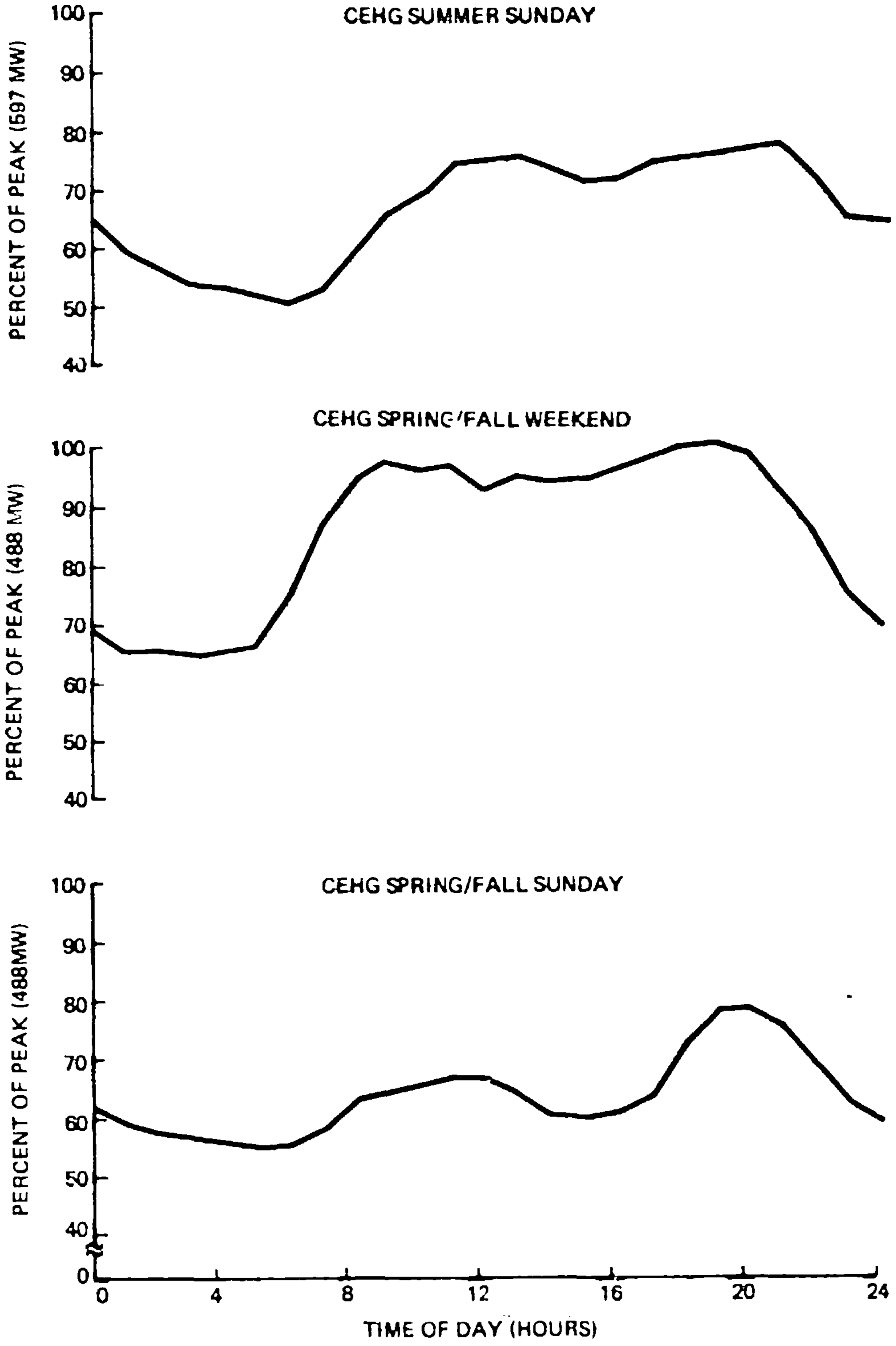

Average Demand, Roseton Unit #1

2349-104D

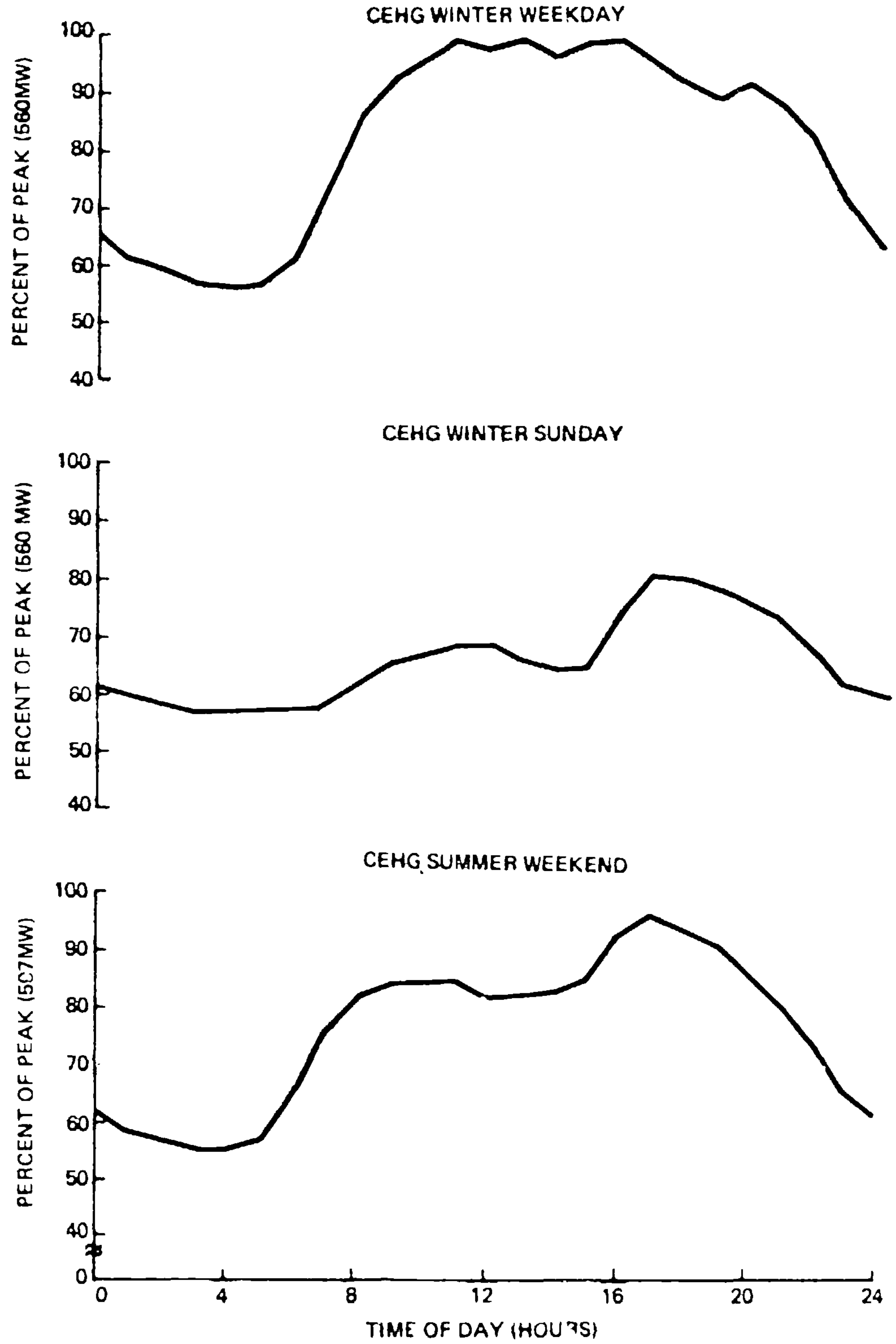

Average Demand, Roseton Unit #1

2349-105D

ALGPS SUMMER WEEKDAY

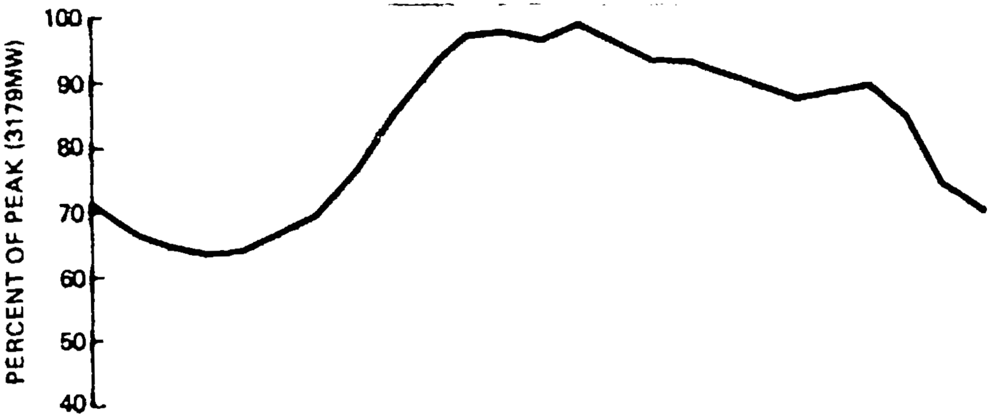

ALGPS WINTER SUNDAY

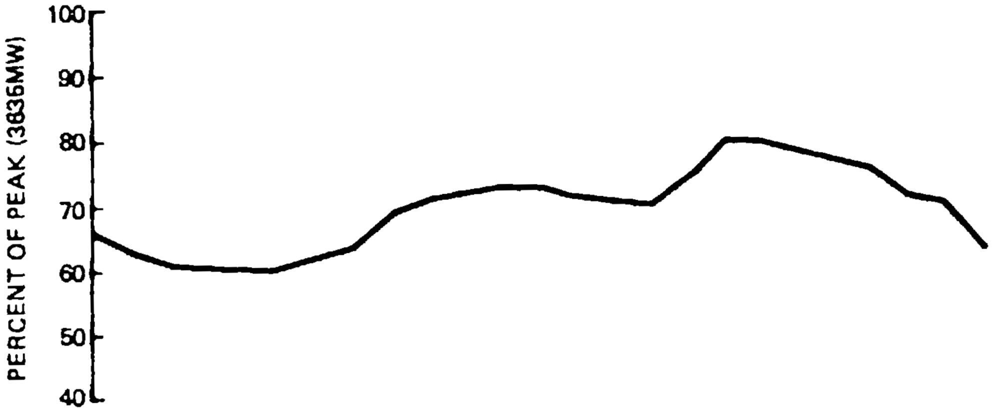

ALGPS WINTER WEEKDAY

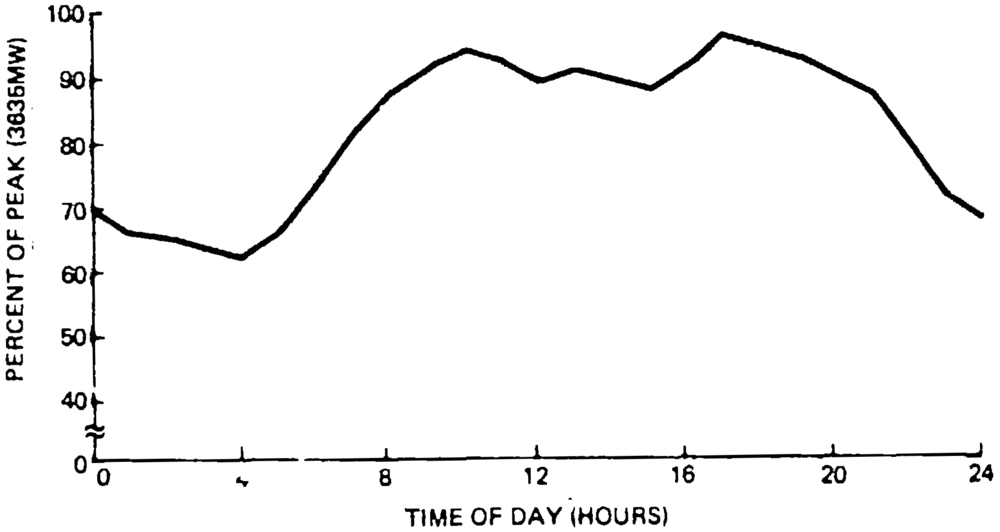

2349-106D

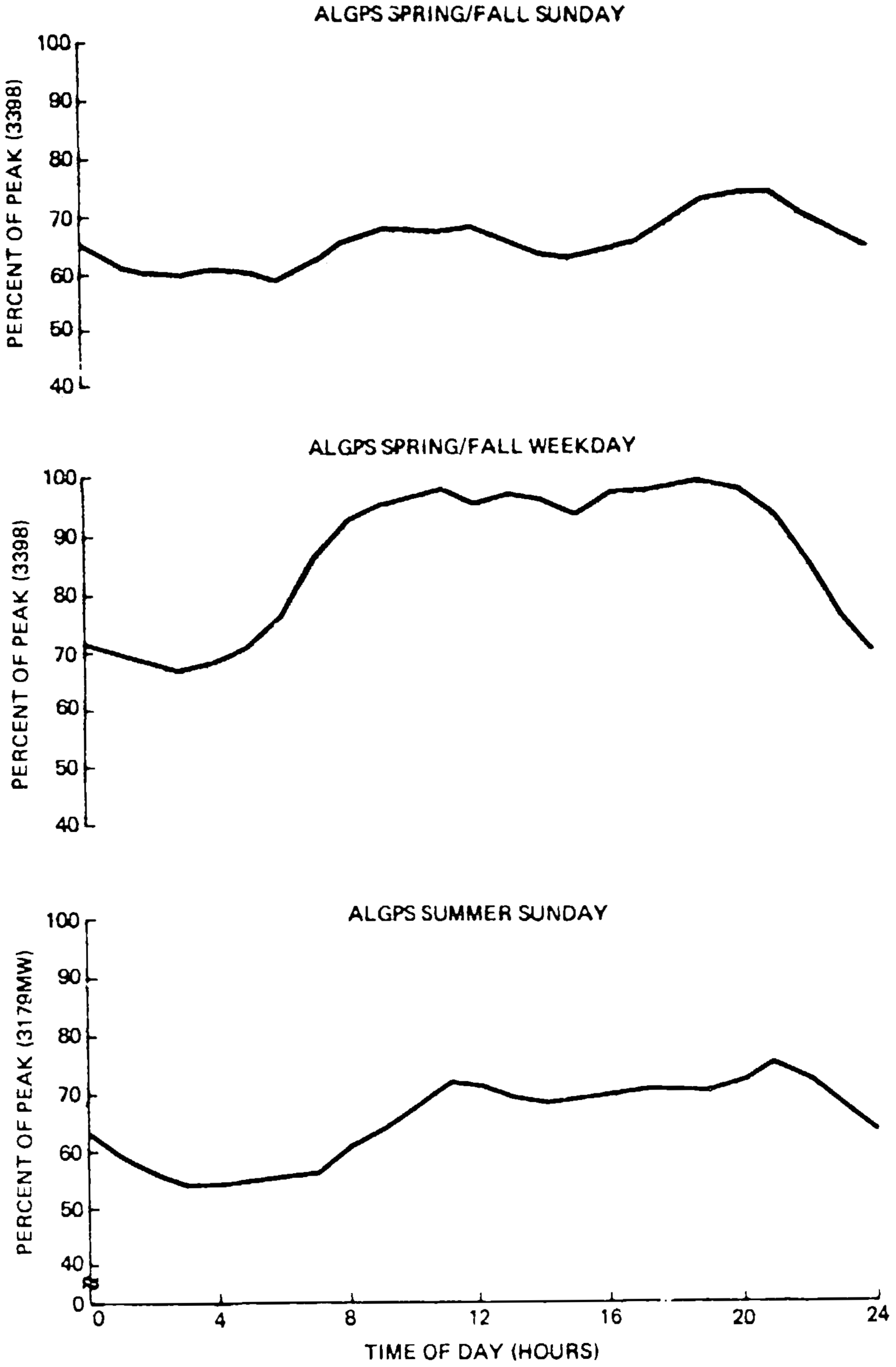
ALGPS SPRING/FALL SUNDAY

ALGPS SPRING/FALL WEEKDAY

ALGPS SUMMER SUNDAY

2349-107D

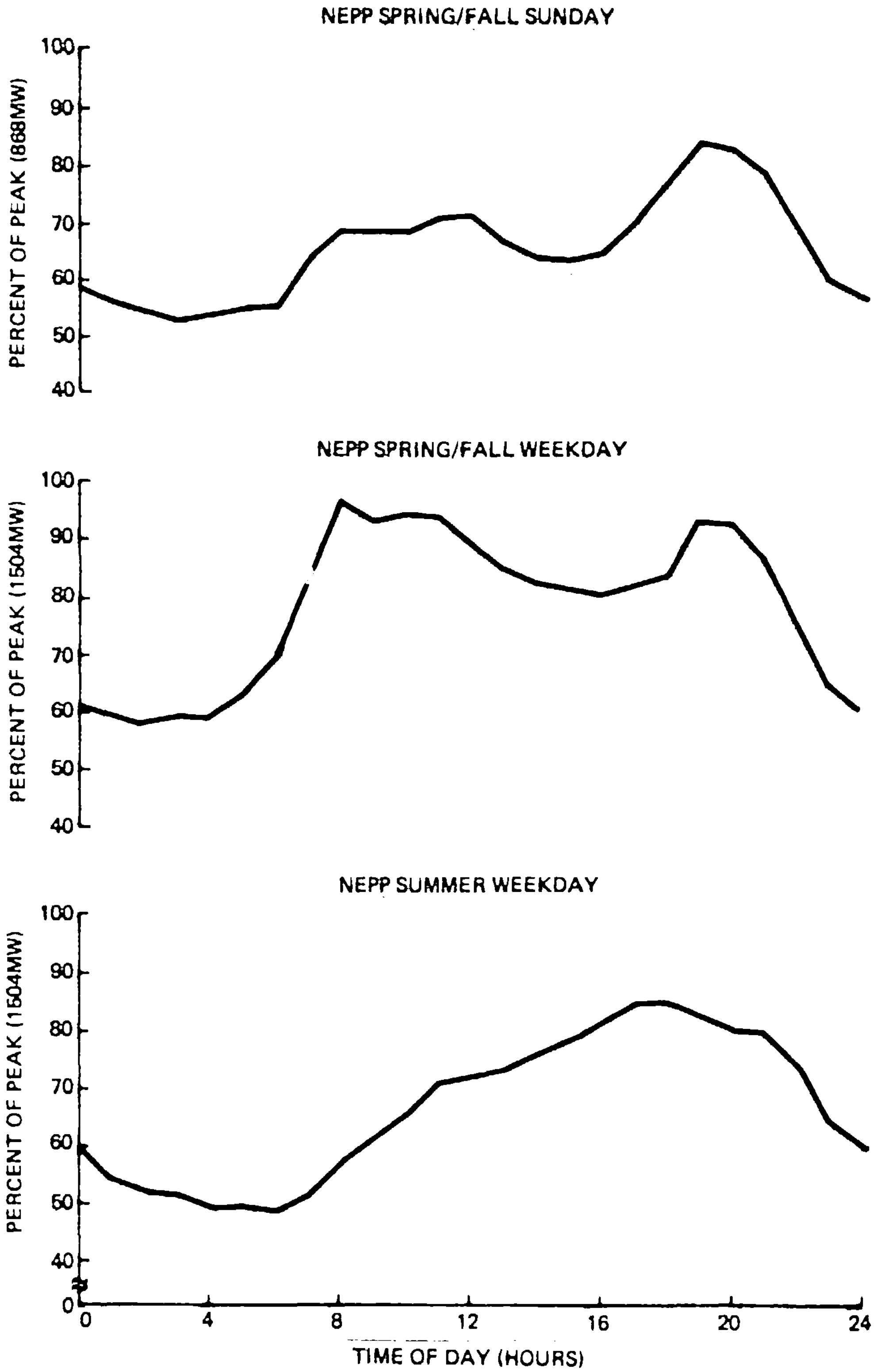

NEPP SPRING/FALL SUNDAY

NEPP SPRING/FALL WEEKDAY

NEPP SUMMER WEEKDAY

2349-108D

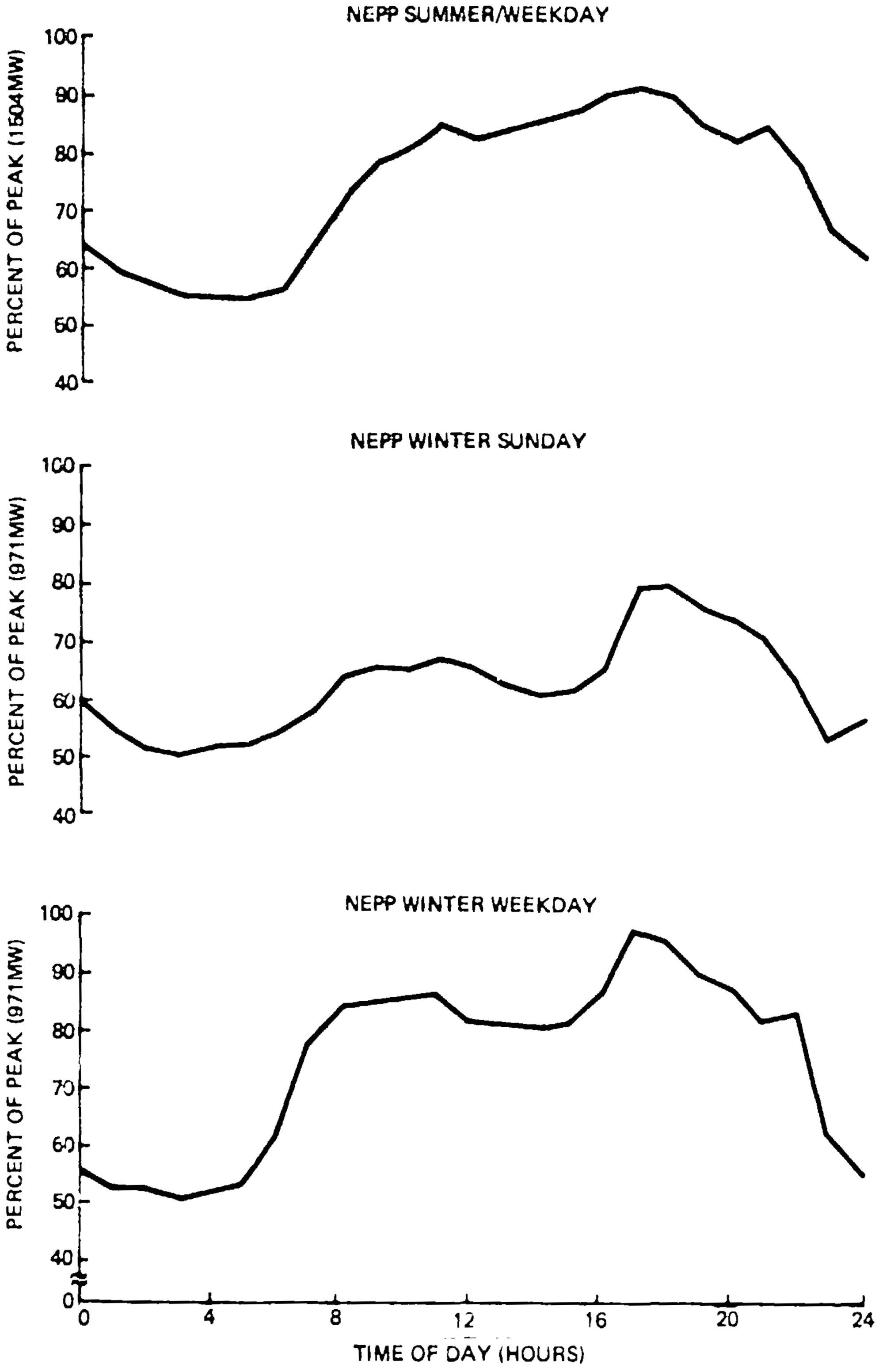
NEPP SUMMER/WEEKDAY
PERCENT OF PEAK (1504MW)
NEPP WINTER SUNDAY
PERCENT OF PEAK (971MW)
NEPP WINTER WEEKDAY
PERCENT OF PEAK (971MW)
100
90
80
70
60
50
40
0
4
8
12
16
20
24
TIME OF DAY (HOURS)

2349-109D

APPENDIX C

COMPILATION OF SALT MATERIALS BASED ON COST

Compilation of Candidate Salt Materials Based on Cost

Source: Chemical Marketing Reporter, 19 July 1976

Salt	Price
Alum Ammonium	$7.90-15.50/100 lb
Alum Potassium	$9.35-16.00/100 lb
Aluminum Chloride	.35/lb
Aluminum Fluoride	.175/lb
Aluminum Hydrate	.65/100 lb
Aluminum Hydroxide	.81/lb
Aluminum Sulfate	114.00/ton
Ammonium Biborate	700.00/ton
Ammonium Bicarbonate	14.15/100 lb
Ammonium Bichromate	.78/lb
Ammonium Bifluoride	.38/lb
Ammonium Bromide	.74/lb
Ammonium Chloride	9.55/100 lb
Ammonium Aimolybdate	1.66/lb
Ammonium Fluorborate	.73/lb
Ammonium Molybdate	1.97/lb
Ammonium Nitrate	9.1/ton
Ammonium Oxalate	.305/lb
Ammonium Pentaborate	603.00/ton
Ammonium Persulfate	.28/lb
Ammonium Silicofluoride	.17/lb
Ammonium Sulfamate	.37/lb
Ammonium Sulfate	.40/lb
Ammonium Sulfide	240.00/ton
Ammonium Thiosulfate	120.50/ton
Antimony Fluoborate	3.02/lb
Antimony Trichloride	.95/lb
Barium Carbonate	215.00/ton
Barium Chloride	310.00/ton
Barium Chlorate	1.04/ton
Barium Hydrate	24.25/lbs
Barium Nitrate	32.50/100 lb
Barium Sulfate	.24/lb
Barium Sulfide	115.00/ton
All Bismuth TOO EXPENSIVE	
Boron trichloride	2.90/lb
Boron Trifluoride	1.43/lb
Cadium Chloride	
Cadium Chloride	2.47/lb
Cadium Fluoborate	2.00/lb
Cadium Nitrate	2.10/lb
Cadium Sulfate	3.05/lb
Calcium Carbide	171.00/ton
Calcium Carbonate	19.00/ton
Calcium Chloride	55.00/ton
Calcium Hydride	2.20/lb
Calcium Hypochlorite	46.00/100 lb
Calcium Hypophospite	1.43/lb
Calcium Phosphate	74.00/ton
Calcium Silicate	.07/lb
Calcium Sulfate	35.00/ton
Chromium Fluoride	.81/lb
Cobalt Carbonate	3.00/lb
Cobalt Chloride	2.00/lb
Cobalt Nitrate	1.34/lb
Cobalt Phosphate	1.35/lb
Cobalt Sulfate	1.50/lb
Copper Bromide	1.34/lb
Copper Carbonate	86.25/100 lb
Copper Chloride	.90/lb
Copper Fluoborate	.72/lb
Copper Nitrate	.435/lb
Copper Sulfate	36.95/190 lb
Ferric Chloride	12.50/100 lb
Ferric Phosphate	1.30/lb
Ferric Sulfate	57.00/ton
Ferrous Fluoborate	.48/lb
Ferrous Sulfate	52.00/ton
Hydrogen Bromide	.65/lb
Hydrogen Chloride	.39/lb
Hydrogen Fluoride	.41/lb
Lead Chloride	.785/lb
Lead Fluorate	.47/lb
Lead Monosilicate	.255/lb
Lead Nitrate	.325/lb
Lead Sulfate	.385/lb
Lead Carbonate	.345/lb
Lithium Bromide	3.00/lb
Lithium Carbonate	.755/lb
Lithium Chloride	1.26/lb
Lithium Fluoride	2.42/lb
Lithium Hypochlorite	.52/lb
Lithium Nitrate	1.14/lb
Lithium Sulfate	1.55/lb
Magnesium Bromide	1.60/lb
Magnesium Carbonate	.221/lb
Magnesium Chloride	.1275/lb
Magnesium Nitrate	.32/lb
Magnesium Phosphate	.75/lb
Magnesium Silicofluoride	.1645/lb
Magnesium Sulfate	7.10/100 lbs
Magnesium Trisilicate	.38/lb
Magnesium Borate	1.68/lb
Magnesium Carbonate	.30/lb
Magnesium Chloride	.31/lb
Magnesium Sulfate	90.00/ton
Nickel Carbonate	2.141/lb
Nickel Chloride	1.04/lb
Nickel Fluoroborate	1.06/lb
Nickel Nitrate	.91/lb
Nickel Sulfate	.76/lb

APPENDIX D

SALT PRICES
AND SPECIFICATIONS

Item D-1, Price Schedule and Specifications Groton Chemical Co., Plainfield, N.J.

PRICE SCHEDULE
EFFECTIVE JANUARY 3, 1977

CALCIUM NITRATE, TECH.

PRICES:

*Truckload (23,000 lbs. min.)	$11.75 per 100 lbs.
10,000 to 22,999 lbs.	12.75 per 100 lbs.
2,000 to 9,999 lbs.	13.75 per 100 lbs.
500 to 1,999 lbs.	15.75 per 100 lbs.

F.O.B.: South Plainfield, New Jersey
*Can be offered for direct shipment from East Coast ports in not less than truckload quantities at a lower price. Call for firm quotation.

PACKING: Poly bags of 100 lbs. net – 101 lbs. gross each.
Bags may be placed on pallets (min. 20 bags per pallet) at a charge of $8.00 per pallet used.

TERMS: Net 30 days – subject to credit approval.

TYPICAL CHEMICAL ANALYSIS:

Calcium (Ca) – 19% min.
Nitrogen (N) – 15.5% min.
insoluble in water – 0.02% max.

Mn – 0.02
Na – 0.015
K – 0.01
Mg – 0.15
Cu – 0.0001
Pb – 0.00005

Fe – 0.001
Al_2 – 0.0001
SO_4 – 0.04
HCOO – 0.3
SiO_2 – 0.005
Urea – 0.1

SCREEN ANALYSIS: pellet form

less than	4	mm	– 0%
	4-2	mm	10%
	2-1	mm	82%
	1-0.5	mm	7%
greater than	0.5	mm	– 0.2%

Minimum invoice for any one shipment to one destination is $100.00

All prices are subject to change without notice.

Item D-1, Price Schedule and Specifications Groton Chemical Co. Plainfield, N.J. (Cont'd)

PRICE SCHEDULE
EFFECTIVE SEPTEMBER 1, 1976

POTASSIUM NITRATE GRANULATED

PRICES:

Truckload (20,000 lbs. min.)	$18.25 per 100 lbs.
10,000 to 19,900 pounds	$19.25 per 100 lbs.
2,000 to 9,900 pounds	$19.75 per 100 lbs.
500 to 1,900 pounds	$20.75 per 100 lbs.

Above can be furnished in a powdered form for an additional charge of $3.00 per 100 lbs. This powder will run 99.9% minimum thru a 60 mesh sieve, and 99.0% minimum thru a 100 mesh sieve.

F.O.B.: South Plainfield, New Jersey

PACKING: Multiwall paper or plastic bags of 100 lbs. or 110 lbs. net each. For 100# drums add $5.00 per 100 lbs; for 300# drums add $3.00 per 100 lbs. Standard pallets will be furnished at no extra charge.

TERMS: Net 30 days from date of shipment – subject to credit approval.

SHIPPING REGULATIONS: Bill of lading must show "Oxidizing material, no label required".

CHEMICAL ANALYSIS: POTASSIUM NITRATE – 99.5% typical

Moisture	0.06%
Insolubles	0.01%
Chlorides as KCl	0.005%
Sodium as oxides	0.20%
Ca & Mg as oxides	0.04%
Ammonium Salts	Nil
Chlorates & Perchlorates Perchlorates	Nil
Fe & Al as oxides	0.01%

Minimum invoice for any one shipment to one destination is $100.00

All prices are subject to change without notice.

Item D-1, Price Schedule and Specifications Groton Chemical Co. Plainfield, N.J. (Cont'd)

PRICE SCHEDULE
EFFECTIVE SEPTEMBER 1, 1976

MURIATE OF POTASH, FIND STD.
(POTASSIUM CHLORIDE)

PRICES:

Truckload (20,000 lbs. min.)	$7.55 per 100 lbs.
10,000 to 19,900 pounds	$7.95 per 100 lbs.
2,000 to 9,900 pounds	$8.50 per 100 lbs.
1,000 to 1,900 pounds	$9.45 per 100 lbs.

F.O.B.: South Plainfield, New Jersey

PACKING: Multiwall paper bags of 50 lbs.

TERMS: Net 30 days – subject to credit approval.

SHIPPING REGULATIONS: None

TYPICAL CHEMICAL ANALYSIS:

Potassium Chloride (KCl)	98.8
Potassium Oxide Equivalent (K_2O)	62.4
Sodium Chloride	0.9
Calcium (Ca)	0.022
Magnesium (Mg)	0.007
Bromide (Br)	0.[illegible]1
Sulphate (SO_4)	0.035
Water Insolubles	0.027
Moisture & Volabiles	0.08
Total Chloride (Cl)	47.53
Other	0.03

TYPICAL SCREEN ANALYSIS:

Retained on 20 mesh	Nil
Retained on 28 mesh	1%
Retained on 35 mesh	2%
Retained on 48 mesh	33%
Retained on 65 mesh	70%
Retained on 80 mesh	81%
Retained on 100 mesh	91%

All prices are subject to change without notice.

Item D-1. Price Schedule and Specifications Groton Chemical Co. Plainfield, N.J. (Cont'd)

PRICE SCHEDULE
EFFECTIVE SEPTEMBER 1, 1976

NITRATE OF SODA, TECH.

PRICES:

	PELLETED	POWDERED	GROUND
packed in	100 lb. bags	300 lb. drums	300 lb. drums
20,000 lbs. or more	$10.95	$14.95	$16.95
10,000 – 19,999 lbs.	$11.45	$15.45	$17.45
2,000 – 9,999 lbs.	$11.95	$15.70	$17.95
500 – 1,999 lbs.	$12.95	$19.45	$21.45

All above prices are per 100 lbs.

F.O.B.: South Plainfield, New Jersey

TERMS: Net 30 days from date of shipment — subject to credit approval.

SHIPPING REGULATIONS: Bill of lading must show "Oxidizing material, no label required".

CHEMICAL ANALYSIS (Typical):	
Sodium Nitrate (Dry Basis)	99.5%
Moisture	0.02%
Sodium Chloride	0.12%
Sulfates as Na_2SO_4	0.09%
Insolubles	0.01%
Mag. and Calcium oxides	0.005%

SIEVE ANALYSIS (Typical):	PELLETED	POWDERED	GROUND
Retained on 40 mesh	80%	—	—
Retained on 60 mesh	—	1%	96%
Retained on 100 mesh	99%	22%	—
Retained on 140 mesh	—	50%	—
Retained on 200 mesh	—	68%	—

Minimum invoice for any one shipment to one destination is $100.00.

All prices are subject to change without notice.

Item D-1, Price Schedule and Specifications Groton Chemical Co. Plainfield, N.J. (Cont'd)

PRICE SCHEDULE
EFFECTIVE JANUARY 1, 1977

SODIUM NITRATE, FLAKE AND GRANULAR

PRICES: Flake and Granular:

6,000 or more pounds	$30.95 per 100 lbs.
2,000 to 5,600 pounds	31.80 per 100 lbs.
800 to 1,600 pounds	33.90 per 100 lbs.
One drum (400 lbs.)	40.50 per 100 lbs.

F.O.B.: South Plainfield, New Jersey

PACKING: 400 lb. fiber drums

TERMS: Net 30 days — subject to credit approval

SHIPPING REGULATIONS: Bill of lading and drums must show "Oxidizing Material".

CHEMICAL ANALYSIS (Typical):

Sodium Nitrite	99.70% min.
Sodium Nitrate	0.16%
Sodium Carbonate	0.03%
Sodium Chloride	0.02%
Moisture	0.06%

All prices subject to change without notice.

Item D-2, Price and Specifications, Dow Chemical Co.

Magnesium Chloride – $MgCl_2$ – Dow
Chemical – $8.50/100 lbs. 99% Flake

$CaCl_2$	MAX	0.5%
NaCl	MAX	1.0%
$Mg(OH)_2$	MAX	0.2%

$CaCl_2$ Calcium Chloride – Dow
$88/Ton

78% Calcium Chloride

20% H_2O

Impurities consisting of Sodium Chloride, Magnesium Chloride

Item D-3, Electromechanical Division, Hooker

Specifications: Potassium Hydroxide – Flake, KOH

Grade:

Mercury Cell, 90% KOH minimum

Price:

$22.00/100 lb.

Element	Minimum	Maximum
KOH	90.00%	91.5%
K_2CO_3		0.8%
NaOH		0.45%
KCl		100 ppm
Fe		10 ppm
SiO_2		40 ppm
$KClO_3$		1 ppm
Ca		5 ppm
K_2SO_4		20 ppm
Hg		0.02 ppm
Mg		5 ppm

Description:

Chalk White in color

Molecular Weight:	56.1
Bulk Density:	Approx. 65 lb./cu. ft.
Melting Point:	90% 219°C Anhydrous 380°C

Item D-3, Electromechanical Division, Hooker (Cont'd)

CAUSTIC SODA (DRY FORMS)

Effective January 1, 1976

	NON-RETURNABLE STEEL DRUMS		PRICE PER 110 POUNDS	
GRADES	NET WEIGHT	GROSS WEIGHT	TRUCKLOADS	LESS TRUCKLOADS
Solid	700 lbs	718 lbs	$14.30	$15.70
Flake, Regular	400 lbs	424 lbs	14.50	16.00
Flake, Regular	100 lbs (See Note 2)	107 lbs	16.50	18.00
Flake, Crystal	450 lbs	474 lbs	$14.50	$16.00

FOB Works, Niagara Falls, New York. Subject to Niagara approval, transportation may be equalized with competitive manufacturers as follows:

SOLID AND ALL GRADES OF FLAKE

Wyandotte, Michigan
Charleston, Tennessee
Houston, Texas
Midland, Michigan
Painesville, Ohio
Wichita, Kansas

SOLID AND REGULAR FLAKE ONLY – Lake Charles Louisiana; Solvay, New York.

TERMS – Net thirty days.

SPECIAL NOTES

1. Minimum order of 2,000 pounds net (1,800 pounds net for 100 lb drums) applies to all less truckload lots.
2. Shipments of 100 pound drums will be made on pallets of 9 drums per pallet with a minimum order of two pallets. Pallet charge is for Buyer's account.
3. On customer pick-up where freight equalization is in excess of $1.25 per hundredweight and prices at schedule approval must be obtained from Seller's Management at Niagara Falls.

Item D-3, Electromechanical Division, Hooker (Cont'd)

Formula NaOH Chemical Name Sodium Hydroxide

DESCRIPTION

Hooker Standard Grade Caustic Soda is available from the Indsutrial Chemicals Division in the East as a solution containing 50% or 73% NaOH by weight and in three flake sizes (regular, fine, crystal) or as a solid cast into drums. Liquid is produced at Niagara Falls, New York, Montague, Michigan, and Taft, Louisiana, dry forms at Niagara Falls only.

For further information on physical properties, analytical methods, handling and storage recommendations, refer to Hooker Caustic Soda Bulletin No. 115.

CHEMICAL SPECIFICATIONS

			50%	73%	Flake & Solid
Sodium Hydroxide	Equiv.	NaOH	49.0-51.0%	70.0-73.0%	97.0 min
Sodium Oxide	Equiv.	Na_2O	38.0-39.5%	54.2-56.6%	75.2% min
Sodium Carbonate		Na_2CO_3	0.20% max	0.25% max	0.70% max
Sodium Chloride		NaCl	1.10% max	1.60% max	2.15% max
Sodium Sulfate		Na_2SO_4	0.020% max	0.030% max	0.10% max
Sodium Chlorate		$NaClO_3$	0.10% max	0.12% max	None
Silicon		Si	0.010% max	0.015% max	0.02% max
Iron		Fe	0.0005% max	0.0007% max	0.0025% max
Calcium		Ca	0.0007% max	0.0010% max	0.0015% max
Magnesium		Mg	0.0010% max	0.0015% max	0.002% max
Aluminum		Al	0.0003% max	0.0005% max	0.001% max
Manganese		Mn	0.00001% max	0.00002% max	0.0005% max
Copper		Cu	0.00007% max	0.0001% max	0.0001% max
Nickel		Ni	0.00007% max	0.0001% max	0.0001% max

PHYSICAL PROPERTIES

Molecular weight	40
Melting point, 50%	55°F
Melting point, 73%	144°F
Melting point	(Anhydrous) 604°F
Boiling point	2534°F
Weight per gallon, 50%	12.8 pounds
Weight per gallon, 73%	14.4 pounds

USES

Caustic soda is used in the manufacture of paper pulp, soap, chemical intermediates, resorcinol, indigo, sodium salts, dyes and pigments, ceramics, pharmaceuticals, cosmetics and in the preparation of boiler water softening and cleaning compounds. It is also used for regenerating water treatment units, reclaiming tin, paper and rubber, bleaching of textiles and paper, mercerizing cotton and dyeing and printing of textiles, in food processing, metal industries, petroleum refineries and many other industries.

Mlt. 11-192

Item D-4, Morton Salt Company 11-66, Industrial Product Data Sheet, Number 105A

A typical average chemical analysis of CULINOX 999, CHEMICAL GRADE would be as follows:

Sodium Chloride	99.98%
Sodium Sulfate	0.02%
Copper	00.00001 (0.1 ppm)
Iron	0.00004 (0.4 ppm)
pH	7.5

CULINOX is an unscreened production with a bulk density of approximately 75 lbs. per cubic foot. A typical average particle size range would be as follows:

U.S. Mesh	30	40	50	70	100	Pan
Per cent Retained	4	30	45	16	4	1

MORTON SALT COMPANY 11-66
Industrial Product Data Sheet
Number 105A

APPENDIX E

SALT REQUIRED FOR SHELL/TUBE HEAT EXCHANGERS

TABLE E-1

SALT REQUIRED FOR SHELL/TUBE AND HEAT PIPE HEAT EXCHANGER – FT. MARTIN C2

Salts 1. NaCl KCl $MgCl_2$ **Melt point:** 725°
2. NaCl $NaNO_3$ **Melt point:** 567°

A) Storage Mode:

Steam in at 1000°F, 3500 psi, h = 1421.7 BTU/lbm

Water out at 705°F, 3200 psi, h = 875.5 BTU/lbm

Temperature range for each salt chosen to provide sufficient ΔT for heat transfer:

Salt 1: 1000° → 800°, 33% total energy
2: 800° → 705°, 67% total energy

	Fluid T, °F	Salt T, °F
Inlet	1000	925
	900	862.5 ($\overline{T}$ salt)
Exhaust	800	725

(a) High Temperature Salt:

Salt 1: $\Delta T = 800^\circ - 725^\circ = 75^\circ F$

Average flow temperature 900°F,

Average Final Salt Temperature $\overline{T} = 900 - 75/2 = 862.5$

so that average sensible component is

$S = C_p \Delta T = .24\ (862.5 - 725) = 33$ BTU/lbm

	Fluid T, °F	Salt T, °F
Inlet	800	662
	752.5	683.5 ($\overline{T}$ salt)
Exhaust	705	567

(b) Low Temperature Salt:

Salt 2: $\Delta T = 705 - 567 = 138$

Average Flow Temperature = 752.5

Average Final Salt Temperature = 752.5 – 138/2 = 683.5

Average Sensible Component is $S = .44\ (683.5 - 567) =$
51.3 BTU/lbm

B) Usage Mode:

Water in at 423°F, h = 404 BTU/lbm

Water out at 514.4°F, h = 504 BTU/lbm

33% – 67% split at 487°F

TABLE E-1 (continued)

B) (continued)

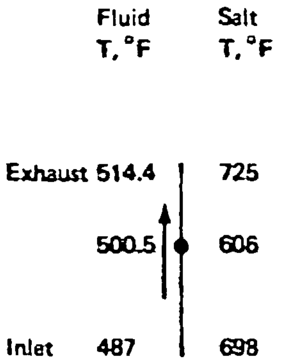

(a) High Temperature Salt

Salt 1: $\Delta T = 725 - 514.4 = 211°F$

Average Flow Temperature 500.5

Average Final Salt Temperature $\bar{T} = 500.5 + 211/2 = 606°F$

Sensible component is .24 (725 − 606) = 29.75 BTU/lbm

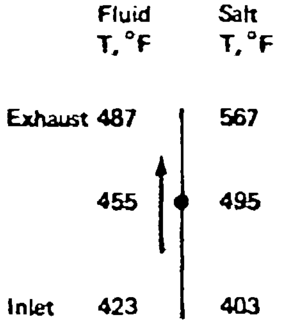

(b) Low Temperature Salt

Salt 2: $\Delta T = 567 - 487 = 80°F$

Average Flow Temperature 455°F

Average Salt Temperature $\bar{T} = 455° + 80/2 = 495°F$

Sensible Component = .24 (567 − 495) = 31 BTU/lbm)

Total Available Energy Storage

Salt 1: Latent + Sensible = $197 + \overbrace{33 + 29.75}^{24\%} = 254.8$ BTU/lbm

Salt 2: Latent + Sensible = $84 + \underbrace{51.3 + 31}_{49\%} = 166.3$ BTU/lbm

C) Salt Masses

Total Q = 1.319×10^9 BTU

33% = 4.35×10^8 BTU

67% = 8.83×10^8 BTU

Salt 1: 1,679,500 lbm

Salt 2: 5,319,300 lbm

TABLE E-2

SALT REQUIRED FOR SHELL/TUBE AND HEAT PIPE TES HEAT EXCHANGER – FT. MARTIN C8

Salts 1: $CaCl_2$ KCl NaCl — Melt Point: 869°F
2: NaCl KCl $MgCl_2$ — Melt Point: 725°F
3: NaCl $NaNO_3$ — Melt Point: 567°F

A) Storage Mode

Steam in at 1000°F, 3500 psi, h = 1421.7 BTU/lbm

Water out at 705°F, 3200 psi, h = 875.5 BTU/lbm

Temperature range for each salt chosen to provide sufficient ΔT for heat transfer:

Salt	Range	Energy
1:	1000° – 890°	16% total energy
2:	890° – 750°	32% total energy
3:	750° – 705°	52% total energy

(a) Highest Temperature Salt

Salt 1: ΔT = 890 – 869 = 21°F

Average Flow Temperature = 945°F

Average Final Salt Temperature = $\bar{T}$ = 945 – 21/2 = 934.5°F

Sensible Component = CP Δ T = .22 (934.5 – 869) = 14.4 BTU/lbm

	Fluid T, °F	Salt T, °F
Inlet	1000	979
	945	934.5
Exhaust	890	869

(b) Middle Temperature Salt

Salt 2: ΔT = 750 – 725 = 25°F

Average Flow Temperature: 820°F

Average Final Salt Temperature: $\bar{T}$ = 820 – 25/2 = 807.5°F

Sensible Component = .24 (807.5 – 725) = 19.8 BTU/lbm

	Fluid T, °F	Salt T, °F
Inlet	890	865
	820	807.5
Exhaust	750	725

(c) Low Temperature Salt

Salt 3: ΔT = 705 – 567 = 138°F

Average Flow Temperature = 732.5°F

Average Final Salt Temperature = 732.5 – 138/2 = 658.5

Sensible = .44 (658.5 – 567) = 40.3 BTU/lbm

	Fluid T, °F	Salt T, °F
Inlet	750	612
	732.5	658.5
Exhaust	705	567

TABLE E-2 (Continued)

B) Usage Mode

Temperature ranges for each salt:

Water in at 294°F, 715 psi, h = 264.8 BTU/lbm

Steam out at 750°F, 615 psi, h = 1379.4 BTU/lbm

Salt 1:	500 – 750	16% total energy
2:	500 – 500	32% total energy
3:	294 – 500	52% total energy

	Fluid T, °F	Salt T, °F
Exhaust	750	869
	625	684.5
Inlet	500	619

(a) Highest Temperature Salt

Salt 1: ΔT = 869 – 750 = 119°F

Average Flow Temperature = 625°F

Average Final Salt Temperature $\bar{T}$ = 625 + 119/2 = 684.5°F

Sensible Component = .22 (869 – 684.5) = 41 BTU/lbm

	Fluid T, °F	Salt T, °F
Exhaust	500	725
Inlet	500	725

(b) Middle Temperature Salt (Boiler)

Salt 2: ΔT = 725 – 500 = 225°F

Average Flow Temperature = 500°F

Average Final Salt Temperature $\bar{T}$ = 500 + 225/8 = 612.5°F

Sensible Component = .24 (725 – 612.5) = 27 BTU/lbm

	Fluid T, °F	Salt T, °F
Exhaust	500	567
	397	430.5
Inlet	294	361

(c) Low Temperature Salt

Salt 3: ΔT = 567 – 500 = 67°F

Average Flow Temperature = 397°F

Average Final Salt Temperature = 397 + 67/2 = 430.5°F

Sensible Component = .44 (567 – 430.5) = 60 BTU/lbm

Total Available Energy Storage

Salt 1: Latent and Sensible = 134 + 14.4 + 41 = 194 BTU/lbm

Salt 2: Latent and Sensible = 197 + 19.8 + 27 = 244

C) Salt 3: Latent and Sensible = 84 + 40.3 + 60 = 184

Salt Masses

Total Q = 1.791 x 10^9 BTU

16% = 2.865 x 10^8 BTU

32% = 5.731 x 10^8 BTU

52% = 9.313 x 10^8 BTU

Salt 1: 1,476,800 lbm

2: 2,348,770 lbm

3: 5,061,500 lbm

TABLE E-3

SALT REQUIRED FOR SHELL/TUBE AND HEAT PIPE TES HEAT EXCHANGER – ROSETON E2

Salt $NaCl \cdot NaNO_3$ Melt Point: 567°F

		Fluid T, °F	Salt T, °F
A) Storage Mode			
Steam in at 1000°F, 2400 psi, h = 1461.3 BTU/lbm	Inlet	1000	917
Water out at 649.5°F, 2200 psi, h = 695.5 BTU/lbm			
ΔT = 649.5 – 567 = 82.5°F		824.7 ↓	783.5
Average Flow Temperature = 824.7°F			
Average Final Salt Temperature			
$\bar{T}$ = 824.7°F – 82.5/2 = 873.5°F	Exhaust	649.5	567
Sensible Component = $C_p \Delta T$ = .44 (783.5 – 567) = 95.3 BTU/lbm			
B) Usage Mode			
Water in at 407.8°F, 3000 psi, h = 386.6 BTU/lbm			
Water out at 479.8°F, 3000 psi, h = 464.7 BTU/lbm	Exhaust	479.8	567
ΔT = 567 – 479.8 = 87.2°F			
Average Flow Temperature = 443.8°F			
Average Final Salt Temperature		443.8 ↑	487.4
$\bar{T}$ = 443.8 + 87.2 = 487.4°F			
Sensible component = .44 (567 – 487.4) = 35.02 BTU/lbm			
Total Available Energy Storage	Inlet	407.8	495.0
Latent + Sensible = 84 + 95.3 + 35.02 = 214.3 BTU/lbm			

C) Salt Mass

Total Q = 1.462×10^9 BTU

Salt = 6,821,450 lbm

TABLE E-4

SALT REQUIRED FOR SHELL/TUBE AND HEAT PIPE TES HEAT EXCHANGER – ROSETON E8

Salts 1: NaCl $BaCl_2$ $MgCl_2$ Melt Point: 784°F

2: $NaNO_3$ Melt Point: 585°F

A) Storage Mode

Steam in at 1000°F, 2400 psi, h = 1461.3 BTU/lbm

Water out at 549.5°F, 2000 psi, h = 695.5 BTU/lbm

Temperature range for each salt chosen to provide sufficient ΔT for heat transfer:

Salt 1: 1000 – 830°F 16% total energy

2: 830 – 649.5°F 84% total energy

(a) High Temperature Salt

Salt 1: ΔT = 830 – 784 = 46°F

Average Flow Temperature = 915°F

Average Final Salt Temperature

$\bar{T}$ = 915 – 46/2 = 892°F

Sensible = .20 (892 – 784) = 21.6 BTU/lbm

	Fluid T, °F	Salt T, °F
Inlet	1000	954
	915	892
Exhaust	830	784

(b) Low Temperature Salt

Salt 2: ΔT = 649.5 – 585 = 64.5

Average Flow Temperature = 739.7°F

Average Final Salt Temperature =

739.7 – 64.5/2 = 707.5°F

Sensible = .44 (707 – 585) = 54 BTU/lbm

	Fluid T, °F	Salt T, °F
Inlet	830	765.5
	739.7	707.5
Exhaust	649.5	585

B) Usage Mode

Water in at 294°F, 717 psi, h = 264.8 BTU/lbm

Steam out at 750°F, 615 psi, h = 1379.4 BTU/lbm

Temperature Range Salt: 1: 500 – 750°F 16% total energy

2: 294 – 500°F 84% total energy

TABLE E-4 (Continued)

B) Continued

(a) High Temperature Salt

Salt 1: $\Delta T = 784 - 750 = 34°F$

Average Flow Temperature = 625°F

Average Final Salt Temperature =

625 + 34/2 = 642°F

Sensible = .20 (784 – 642) = 28 BTU/lbm

	Fluid T, °F	Salt T, °F
Exhaust	750	784
	625	642
Inelt	500	534

(b) Low Temperature Salt

Salt 2: $\Delta T = 585 - 500 = 85°F$

Average Flow Temperature = 397°F

Average Final Salt Temperature = 397 + 85/2 = 439.5

Sensible = .44 (585 – 439.5) = 64 BTU/lbm

Total Available Energy Storage

Latent and Sensible:

Salt 1: 146 + 21.6 + 28 = 196 BTU/lbm

Salt 2: 78 + 54 + 64 = 196

	Fluid T, °F	Salt T, °F
Exhaust	500	585
	397	439.5
Inlet	294	379

C) Salt Masses

Total Q = 1.869×10^9 BTU

16% = 2.990×10^8 BTU

84% = 1.569×10^9 BTU

Salt 1: 1,525,510 lbm

Salt 2: 8,005,102 lbm

REFERENCES

1. Boser, O. "Study of Safety Aspects of High-Temperature Thermal-Energy Storage Systems", PL-54-TE76-1130, NSF, December 1976.
2. Chemical Marketing Reporter, 19 July 1976.
3. Bramlete, T., et al, "Survey of High Temperature Thermal Energy Storage" Sandia Laboratories, March 1976.
4. Eichelberger, J. L., "Investigation of Metal Fluoride Thermal Energy Storage Materials", Progress Report, ERDA, Oct. 1976.
5. Private Communication, letter dated Nov. 9, 1976 from Foote Mineral Co, Exton Pa. to GAC.
6. Janz, G., Consulting report number one to Grumman Aerospace Corporation, Sept. 1976.
7. Borucka, A., Consulting report number two to Grumman Aerospace Corporation, Oct. 1, 1976.
8. Borucka, A., "Survey and Selection of Inorganic Salts for Application to Thermal Energy Storage" ERDA, June 1976.
9. Littlewood, R., "Diagramatic Representation of the Thermodynamics of Metal Fused Chloride Systems", Journal Electrochem Soc. V109, #6, June 1962.
10. Littlewood, R., and Edeleanu, C., "Thermodynamics of Corrosion in Fused Chlorides", Electrochemical Acts, Vol. 3, pp. 195-207, 1960.
11. Koger, J. "Chromium Depletion and Void Formation in Iron-Nickel-Chromium Alloys" Chem. Eng. Prog. Vol 56, No. 3, March 1960,
12. Susskind, H., et al, "Combating Corrosion in Molten Extraction Processes", Chemical Engineering Progress, Vol. 56, No. 3, March 1960.
13. DeVan, J., Molten Salt Reactor Group ORNL Personal Communication 29, October 1976.
14. Chubb, T., "Development of a Heat of Fusion Energy Storage-Boiler Tank", ERDA, Sept. 1976.

REFERENCES (Cont)

15. Maru, H.C., et al, "Molten Salt Thermal Energy Storage Systems: Salt Selection", ERDA, August 1976.

16. Comstock and Wescott Inc., Report on Contract 87-5030 ERDA, August 1976.

17. Borucka, A., Consulting Report Number Four to Grumman Aerospace Corporation, Feb. 10, 1977.

18. Kirst, W.E., et al, "A New Heat Transfer Medium for High Temperatures", JACS Meeting, May 1940.

19. Technical Bulletin J-9, Park Chemical Company, Detroit MI., 1976.

20. Salt Price Sheets, Croton Chemical Company, South Plainfield, New Jersey, January 1977.

21. Carslow, H.S., & Jaeger, J.C., "Conduction of Heat in Solids", Oxford, Univ. Press, Gt. Britain, 1959, 2nd edition.

22. U.S. Patent No. 4019571: Gravity Assisted Wick System for Condensers, Evaporators and Heat Pipes, R. Kosson, Grumman Aerospace Corp.

23. McAdams, W.H., "Heat Transmission", McGraw Hill Book Co., Inc., N.Y., 1954, 3rd Edition.

24. Rohsenow, W. & Choi, H., "Heat, Mass and Momentum Transfer", Prentice-Hall, 1961, N.J.

25. Parmelee, G.V. and Aubele, W.W., "Radiant Energy Emission of Atmosphere and Ground", Heating, Piping and Air Conditioning, Nov. 1951.

26. "Climatic Atlas of the U.S.", Department of Commerce, Washington, D.C., June 1968.